Vanadium and Iron Complexes for Catalytic Oxidation

Alette Ligtenbarg

Cover picture: The goddess Vanadis, provided by prof. dr. L. Pettersson, Umeå University, Sweden.

This research project was financially supported by the Unilever Research Laboratory, Vlaardingen.

RIJKSUNIVERSITEIT GRONINGEN

Vanadium and Iron Complexes for Catalytic Oxidation

PROEFSCHRIFT

ter verkrijging van het doctoraat in de
Wiskunde en Natuurwetenschappen
aan de Rijksuniversiteit Groningen
op gezag van de
Rector Magnificus, dr. D.F.J. Bosscher,
in het openbaar te verdedigen op
vrijdag 1 juni 2001
om 16.00 uur

door

Alette Gerda Jeannet Ligtenbarg

geboren op 19 maart 1974
te Groningen

Promotor: Prof. dr. B.L. Feringa
Referent: Dr. R. Hage

Beoordelingscommissie:
Prof. dr. J.G. de Vries
Prof. dr. A.M. van Leusen
Prof. dr. A.W. Gal

ISBN 90-367-1413-3

Voorwoord

Een groot aantal mensen heeft in meer of mindere mate een bijdrage geleverd aan de totstandkoming van dit proefschrift. In dit voorwoord wil ik dan ook al die personen hartelijk bedanken. Een aantal van hen wil ik echter met name noemen.

Allereerst wil ik mijn promotor prof. dr. Ben Feringa bedanken voor de mogelijkheid om in zijn groep dit promotieonderzoek uit te voeren, voor de vrijheid die ik heb gekregen en voor het in mij gestelde vertrouwen. Dr. Ronald Hage van Unilever Research wil ik niet alleen bedanken voor het schrijven van dit onderzoeksvoorstel, maar ook voor zijn ontelbare waardevolle suggesties, hulp en enthousiasme.

De leden van de beoordelingscommissie, prof. dr. J.G. de Vries, prof. dr. A.M. van Leusen, en prof. dr. A.W. Gal wil ik bedanken voor de kritische correctie van het manuscript. Ook dr. Adri Minnaard, die als extra lid van de beoordelingscommissie fungeerde, ben ik veel dank verschuldigd voor de zeer vlotte en grondige correctie van de hoofdstukken.

De (ex-)leden van de oxidatiesubgroep ben ik erkentelijk voor de vele nuttige discussies. Vooral aan Gerard Roelfes en René La Crois heb ik heel veel te danken. Zij stonden altijd voor mij klaar met tips en adviezen en waren zeer royaal met het ‘uitlenen’ van hun liganden. Hartelijk dank hiervoor!

Dr. František Hartl en Taasje Mahabiersing (Universiteit van Amsterdam) hebben mij de mogelijkheid geboden in hun groep cyclovoltammetrische en spectro-elektrochemische metingen te doen. Ik wil hen hierbij bedanken voor hun hulp en gastvrijheid. Dr. E. Bill, dr. E. Bothe and especially dr. T. Weyhermüller (Max-Planck Institut für Strahlenchemie in Mülheim (Ruhr), Germany) are kindly acknowledged for performing the EPR, magnetic susceptibility, coulometry, and spectro-electrochemical measurements described in chapter 7. Prof. dr. J.G. Vos (Dublin University, Ierland) wil ik bedanken voor het beschikbaar stellen van een triazoolligand, dat geschikt bleek voor complexatie met vanadium (zie hoofdstuk 6). Peter Oosting ben ik zeer erkentelijk voor zijn bijdragen aan hoofdstuk 8. Zijn hoofdvakonderzoek heeft als uitgangspunt gediend voor de verdere bestudering van μ-oxo-ijzer(III)-verbindingen. Maaike de Loos wil ik hartelijk bedanken voor de prettige samenwerking op het gebied van de triureumverbindingen beschreven in hoofdstuk 4.

Margot Jeronimus-Strating en dr. Andries Bruins hebben in de loop der jaren vele elektrospray-massaspectra voor mij opgenomen en helpen interpreteren. Ik wil hen dan ook hartelijk bedanken voor hun inspanningen. Dit geldt ook voor Marc van Gelder en Marinus Suijkerbuijck, die hebben geassisteerd bij de vele GC-analyses. Jan Ebels, Harm Draaijer en Jannes Hommes wil ik bedanken voor de elementanalyses, en Albert Kievit voor het opnemen van massaspectra. Dr. Martin Lutz, dr. Ton Spek (Universiteit van Utrecht) en met name Auke Meetsma ben ik zeer erkentelijk voor het opheldern van de kristalstructuren beschreven in dit proefschrift. Wim Kruizinga, Jan Herrema en Peter Witte waren altijd erg behulpzaam bij het opnemen van ^{51}V-NMR spectra.

Op het gebied van de vanadiumchemie heb ik veel geleerd van dr. Isabel Arends (Universiteit van Delft). Onze gezamenlijke reis naar een vanadiumsymposium in Mexico was niet alleen leerzaam maar ook erg gezellig. Bedankt hiervoor!

I would like to thank prof. dr. D.C. Crans (Colorado State University, Fort Collins, USA) and prof. dr. L. Pettersson (Umeå University, Sweden) cordially for their efforts to provide me with the picture of the goddess Vanadis.

Alle C-poters en andere OMAC'ers die hebben bijgedragen aan de plezierige werksfeer wil ik bijzonder bedanken. In dit kader wil ik met name noemen mijn (ex-)zaalgenoten Marten Klopstra, Fokke van der Berg, Rob Hoen en Maartje Verdouw-de Vries. Hanneke van der Deen en René La Crois wil ik bedanken voor de gezelligheid op het lab en voor de zeer prettige samenwerking bij het organiseren van de werkweek naar Arnhem.

Tenslotte wil ik mijn ouders, Carsten Jan en Robert bedanken. Hun belangstelling voor het onderzoek en hun steun hebben heel veel voor mij betekend.

Contents

Chapter 3 A Vanadium Diamidate Complex as Model System for Vanadium Bromoperoxidase

Chapter 4 Development of New Ligand Systems for Vanadium

Chapter 5 Vanadium(V) Complexes Based on a Bis(pyridine)-imine Ligand

Chapter 6 Triazole Ligands for the Formation of Vanadium(V) Complexes

Chapter 7 Chiral Ligands for Vanadium and Manganese

Chapter 8 Non-heme Iron Complexes for Catalytic Oxidation

Chapter 9 Conclusions and Future Prospects

Chapter 1

Introduction

1.1 History and occurrence of vanadium

In 1802, the mineralogist Andres Manuel del Rio (1764-1849) believed that he discovered a new metal similar to chromium and uranium in a brown lead mineral from Mexico.[1,2] He first named it *panchromium*, because of the varied colours of its salts, but changed the name later on in *erythronium* ('red') as a reference to the red colour of its salts when treated with acids.[2] However, soon he withdrew his discovery, since a French chemist incorrectly declared that this new element was only impure chromium. Vanadium was rediscovered in 1831 by the Swedish chemist Nils Gabriel Sefström (1787-1845) in remnants of iron ore quarried at the Taberg in Småland. He named the element *vanadin*, after the goddess of beauty, youth and love, Vanadis, referring to the beautiful multicoloured compounds.[3] Vanadis is a common name for Freyja according to the Northern Germanic tribes. After Sefström announced the discovery of vanadium, the brown lead ore from Mexico was reanalysed and it was shown that it really contained vanadium instead of chromium.

Natural vanadium is a mixture of two isotopes, ^{51}V (99.76%) and ^{50}V (0.24%), the latter being slightly radioactive with a half-life of $>3.9 \times 10^{17}$ years. Important sources of the metal are the minerals *carnotite* [$K_2(UO_2)_2(VO_4)_2$] and *vanadinite* [$Pb(VO_4)_3Cl$]. It is also present in some crude oils in the form of organic complexes.

Vanadium occurs with an abundance of 0.014% in the earth's crust and is widespread.[4] The element is the second most abundant transition metal in the oceans (50 nM).[4] Some aquatic organisms are known to accumulate vanadium. For instance, members of an order of tunicates (*Ascidiacea*) concentrate vanadium to 0.15 M in specialised blood cells.[5] However, the actual function of vanadium and the nature of the vanadium compounds present in these organisms remains unclear.[1] In 1983, a naturally occurring vanadium-containing enzyme, vanadium bromoperoxidase (V-BrPO), was discovered in the marine brown alga *Ascophyllum nodosum*.[6] Since then, several vanadium haloperoxidases (*vide infra*) have been isolated and studied.[7,8] Many of these enzymes have been detected in brown and red seaweeds.[9] However, the accumulation of vanadium is not restricted to marine organisms, since vanadium containing haloperoxidases have also been isolated from terrestrial fungi[10] and a vanadium compound of low molecular weight (amavadin) has been isolated from the toadstool *Amanita muscaria*.[11]

Vanadium can exist in eight oxidation states ranging from –3 to +5, but with the exception of –2.[12] Only the three highest, *i.e.* +3, +4 and +5, are important in biological systems.[13,14,15,16] Under ordinary conditions, the +4 and +5 oxidation states are the most stable ones.[12] The majority of vanadium(IV) compounds contains the VO^{2+} unit (vanadyl ion). These complexes typically have square planar pyrimidal or bipyrimidal geometries with an axial oxo ligand.

The coordination chemistry of vanadium(V) compounds is dominated by oxo complexes, containing the VO^{3+} or the VO_2^+ moiety. V^{4+} and V^{5+} ions are very small with radii of 0.61 Å and 0.59 Å, respectively.[17] Therefore these ions are even smaller than lithium (the radius of a Li^+ ion is 0.78 Å).[17]

Due to the d^1 configuration of V(IV) ions, vanadium(IV) species are easily identified by EPR spectroscopy. Typical eight-line patterns are observed due to hyperfine interaction of the ^{51}V nucleus (I = 7/2).[18] V(V) is EPR silent due to its d^0 state. Vanadium(V) complexes are therefore diamagnetic, which makes them appropriate for NMR analyses.[18] Especially ^{51}V NMR is a useful tool in the characterisation of vanadium(V) complexes, since the chemical shifts are very sensitive to the nature of the coordination sphere of the metal.[19]

1.2 Vanadium containing enzymes

Haloperoxidases are enzymes that catalyse the oxidation of halides to the corresponding hypohalous acids (or to a related two-electron oxidised halogenating intermediate such as OX^-, X_3^- and X^+) using hydrogen peroxide as the oxidant. In the presence of suitable nucleophilic acceptors, halogenated compounds are formed.

$$H_2O_2 + X^- + H^+ \longrightarrow H_2O + HOX$$

$$HOX + \text{Org-H} \longrightarrow \text{Org-X} + H_2O$$

The nomenclature of these enzymes is based on the most electronegative halide which can be oxidised by the enzyme. Thus iodoperoxidase merely catalyses the oxidation of iodide, bromoperoxidase catalyses the oxidation of bromide, and iodide, while chloroperoxidase catalyses the oxidation of chloride, bromide and iodide. The function of these haloperoxidases *in vivo* is the generation of a diversity of halogenated organic compounds.[20,21] These products probably are formed because of the biocidal effects of HOBr and some of the organohalogens. Presumably, these compounds are part of the host defence system, because they may prevent fouling by microorganisms or act as an antifeeding system.[22]

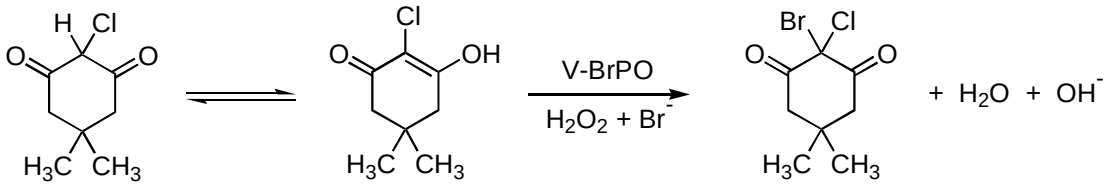

Scheme 1.1 *Bromination of MCD, the standard substrate in haloperoxidase activity determinations.*

Vanadium peroxidases have been shown to catalyse the bromination of various organic substrates[23] including monochlorodimedone (MCD, 2-chloro-5,5-dimethyl-1,3-cyclohexane-

dione), the standard substrate for the determination of haloperoxidase activity,[24] using H_2O_2 as the oxidant (Scheme 1.1). In the absence of a nucleophilic acceptor, however, a second equivalent of hydrogen peroxide reduces the brominating intermediate resulting in the formation of bromide and singlet oxygen.[25] This disproportionation reaction of hydrogen peroxide is a bromide-mediated reaction, *i.e.* V-BrPO does not catalyse the formation of singlet oxygen in the absence of bromide. At pH 6.5, the enzyme functions with a turnover rate of 4.7 x 10^5 mol of brominated product per mol of enzyme per hour.[26] A common intermediate (' Br^+ ') is likely to exist of which the formation is rate determining and which is responsible for both the generation of singlet dioxygen and brominated products (see Scheme 1.2). Nevertheless, the exact nature of this halogenating intermediate still is a matter of debate.

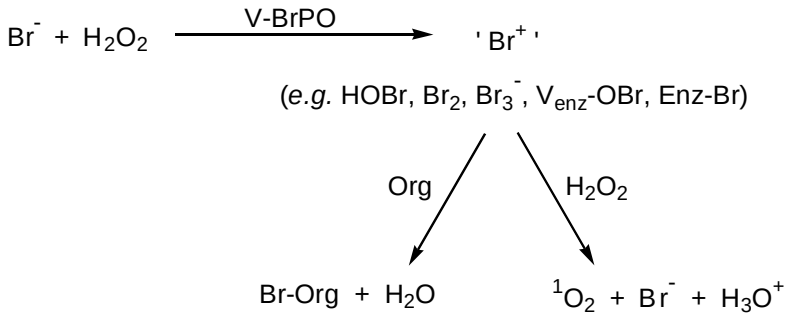

Scheme 1.2 *Proposed mechanism of bromoperoxidase activity catalysed by V-BrPO.*

To get a better understanding of the working mechanism of the enzyme and to determine the role of vanadium, many functional mimics of V-BrPO have been developed.[27] Furthermore, many spectroscopic studies have been carried out in order to reveal the nature of the active site.[28] In 1996, the crystal structure of an azide containing vanadium chloroperoxidase (V-ClPO) isolated from the fungus *Curvularia inaequalis* was determined by Messerschmidt and Wever.[29] In 1997, the X-ray structure of the peroxide form of the chloroperoxidase enzyme was published.[30] In the native state, a five-coordinated trigonal bipyrimidal V(v) moiety is present which is coordinated by three nonprotein oxo groups in the equatorial plane and one histidine and a hydroxy group at the axial positions (Figure 1.1). The oxygens are hydrogen bonded to several amino acid residues of the protein chain. In the peroxo state, the peroxide ligand is bound in an η^2-manner in the equatorial plane. The coordination geometry around the vanadium centre is a distorted tetragonal pyramid with the two peroxo oxygens, one oxygen and the nitrogen in the basal plane and one oxygen in the apical position. A proposed mechanism for the catalytic cycle of V-ClPO is discussed in Chapter 3. A partial amino acid sequence comparison of this chloroperoxidase with a vanadium bromoperoxidase showed a close similarity between the enzymes.[29]

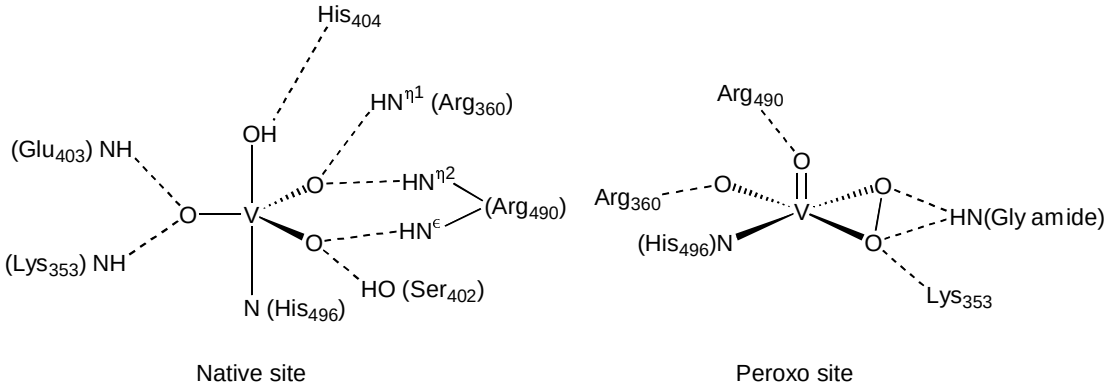

Figure 1.1 *The native and peroxo vanadium site in V-ClPO.*[29,30]

A second class of enzymes that contain vanadium are the vanadium nitrogenases.[22] Nitrogenases are multicomponent metalloenzyme complexes that are capable of reducing dinitrogen to ammonia:[31]

$$N_2 + 12\,e^- + 12\,H^+ \longrightarrow 2\,NH_3 + 3\,H_2$$

Many nitrogenases consist of an Fe-S cluster and a molybdenum-dependent component.[13] The first vanadium containing nitrogenase, *i.e.* a VFe-protein (Figure 1.2), was isolated and purified in 1986 from certain nitrogen-fixing bacteria.[1,32]

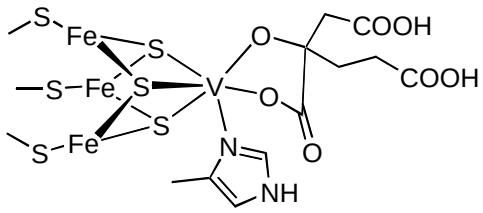

Figure 1.2 *Proposed vanadium environment in vanadium nitrogenase.*[1]

Vanadium(II) hydroxide, $V(OH)_2$, has been found to reduce dinitrogen to ammonia in a stoichiometric reaction.[33] Several VFe_3S_4-clusters have been studied as models for vanadium nitrogenase as well.[1,33] None of them have been reported to reduce dinitrogen, although, for instance, $[(DMF)_3VFe_3S_4Cl_3]^-$ (Figure 1.3) catalyses the conversion of hydrazine to ammonia and is active in the reduction of phenylhydrazine to aniline and ammonia.[1]

To gain more insight into the coordination properties of sulfur containing ligands, many thiovanadium complexes have been studied in recent years and their redox activity examined.[1,34] The oxidation state of vanadium in these compounds range from +2 to +5.

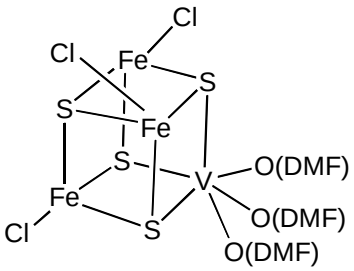

Figure 1.3 *Schematic representation of the $[VFe_3S_4Cl_3(DMF)_3]^-$ cluster.*[1]

1.3 Vanadium complexes for oxidation chemistry

As a consequense of their low radius/charge ratio, vanadium(V) centres are usually strong Lewis acids, which makes them suitable for the activation of peroxidic reagents.[35] Accordingly, vanadium(V) complexes have been found to act as catalyst precursors in various oxidation reactions like bromination reactions, epoxidations of alkenes and allylic alcohols, oxidations of sulfides to sulfoxides and sulfones, hydroxylations of alkanes and arenes, and oxidations of primary and secondary alcohols to the corresponding aldehydes and ketones (Figure 1.4).[36] Examples of these types of oxidations will be discussed below. The active species has been identified in stoichiometric reactions as mononuclear oxoperoxovanadium(V) complexes, some of which have been structurally characterised.[37] In all cases the peroxide is bound in an η^2–manner in the equatorial plane relative to the axial oxo ligand. Vanadium(IV) complexes can also be used as precursors in these oxidation reactions. In the presence of excess peroxide, they are readily converted to the oxoperoxovanadium(V) complexes.[36]

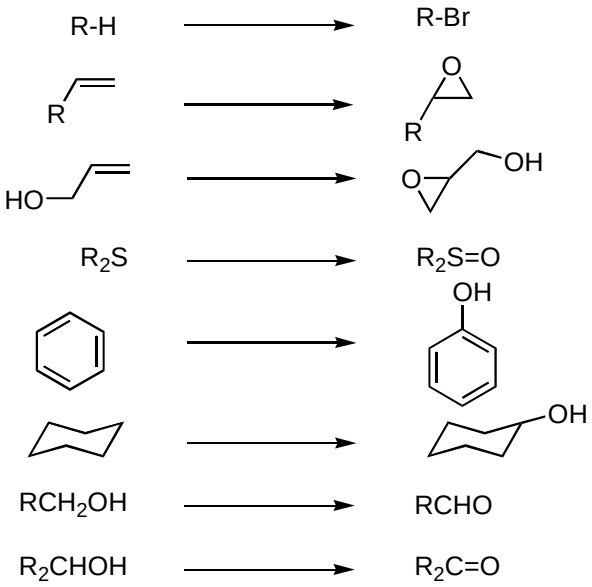

Figure 1.4 *Examples of the reaction types mediated by peroxovanadium(V) complexes.*

Simple vanadium complexes, *e.g.* vanadyl acetylacetonate [$VO(acac)_2$], are useful catalysts in the epoxidation of allylic alcohols.[38] The actual oxoperoxo catalyst is formed *in situ* by oxidation of V(IV) to V(V) with excess of alkylhydroperoxide, yielding an alkylhydroperoxo vanadium(V) complex.[39] An excellent example of high regioselectivity is the epoxidation of geraniol catalysed by a $VO(acac)_2$–TBHP (tert-butylhydroperoxide) system. The allylic double bond is selectively oxidised, whereas peracids preferentially epoxidise the isolated double bond (Scheme 1.3).[40,41]

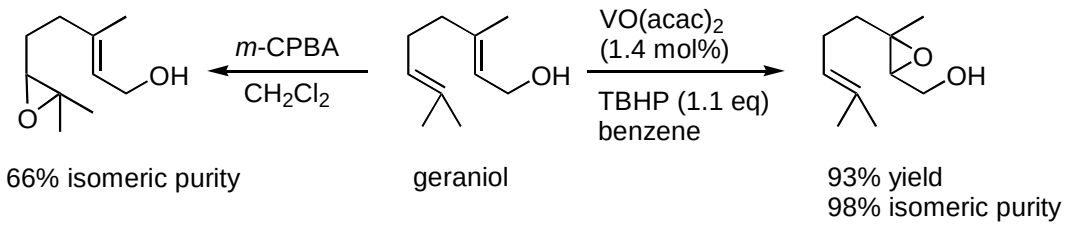

Scheme 1.3 *Epoxidation of geraniol catalysed by $VO(acac)_2$ and TBHP or m-CPBA.*

Several vanadium complexes are known to catalyse the oxidation of unfunctionalised olefins.[37,42] It was proposed that when a vacant site on the vanadium centre is present, the olefins are able to coordinate to the vanadium centre, leading to the formation of epoxides with high selectivity.[37b] However, when coordination of the olefin is not possible, one-electron oxidation processes often play a role, which proceed in a non-stereoselective manner.[43]

Simple vanadium(V) peroxide complexes also are efficient and selective catalysts in the oxidation of prochiral dialkyl, arylalkyl or diaryl sulfides to the corresponding sulfoxides. These complexes are usually generated *in situ* from vanadium salts such as $VO(acac)_2$, sodium *meta*-vanadate ($NaVO_3$), or vanadium pentoxide (V_2O_5) and H_2O_2. The reactions are often nearly quantitative with respect to the peroxide. Two mechanisms may occur, dependent on the nature of the ligand.[44] The reaction pathway proceeds either *via* heterolytic or homolytic cleavage of the peroxidic oxygen-oxygen bond.

For example, $VO(O_2)(OCH_3)$ oxidises di-*n*-butyl sulfide as well as methyl phenyl sulfide in a bimolecular, electrophilic reaction. In the proposed mechanism the sulfide does not coordinate to the metal centre, but undergoes nucleophilic addition to the peroxide oxygen, *i.e.* the oxygen is electrophilic in nature. This mechanistic route is common for peroxometal complexes such as Ti(IV) and Mo(VI) derivatives.[42]

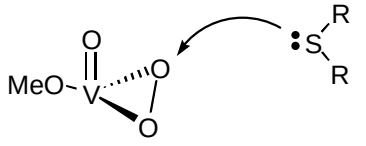

Figure 1.5 *Nucleophilic addition of a sulfide to the peroxide oxygen of $VO(O_2)(OCH_3)$.*

The electrophilic or nucleophilic character of the peroxide oxygen transfered to the sulfide can be established by using thianthrene 5-oxide (SSO) as a mechanistic probe (Scheme 1.4).[45] This compound has both a sulfide and a sulfoxide site. The sulfide sulfur atom, being electron rich, is expected to undergo preferably electrophilic oxidation giving SOSO, whereas the more electron deficient sulfoxide sulfur is expected to undergo nucleophilic oxidation yielding SSO_2. Consequently, those oxidants that give high amounts of SOSO product are electrophilic in their reactivity, while high yields of sulfone point to a nucleophilic oxidant.

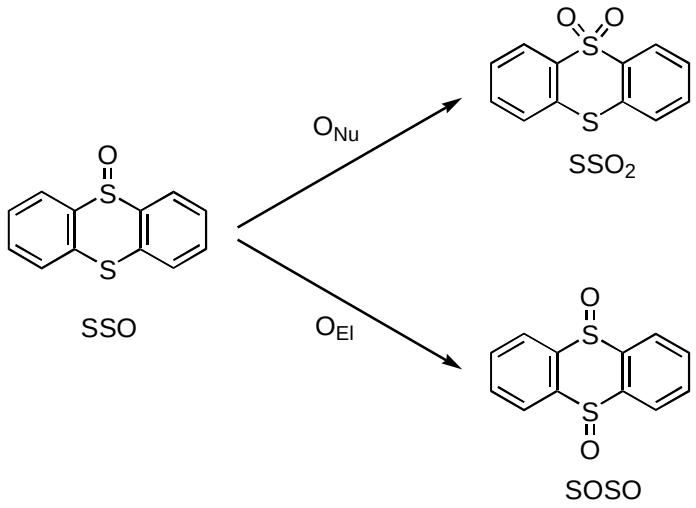

Scheme 1.4 *Reaction of thianthrene 5-oxide (SSO) with nucleophilic and electrophilic peroxide species.*

Given the electrophilic nature of the $VO(O_2)(OCH_3)$ catalyst, the preference for sulfide oxidation over sulfoxide oxidation is obvious. This explains the quantitative yields of sulfoxide found in sulfide oxidation reactions. However, a peroxovanadium(V) complex of picolinic acid (L^1), for example, shows low selectivity in sulfide oxidation leading to mixtures of sulfoxides and sulfones. It was proposed that the ligand suppresses the rate of the heterolytic reaction by reducing the electrophilicity of the peroxo oxygen. Here, a competitive homolytic pathway is likely to occur *via* one-electron transfer of the bound sulfide, forming a radical cation- radical anion pair (Scheme 1.5).[46]

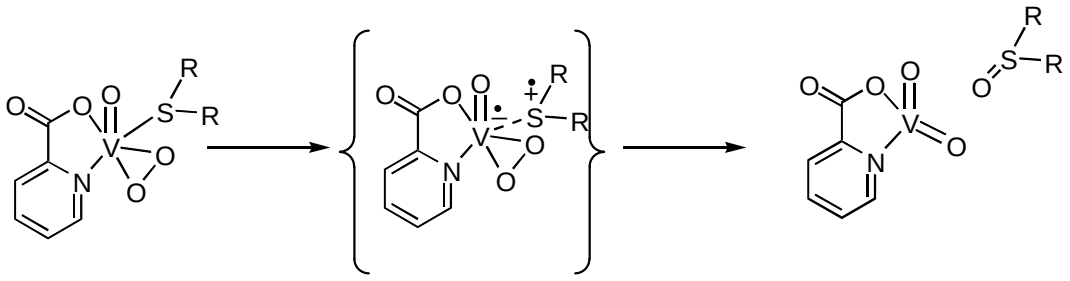

Scheme 1.5 *Radical mechanism for the sulfide oxidation catalysed by $VO(O_2)(L^1)$.*

The hydroxylation of aromatic hydrocarbons to the corresponding phenolic compounds forms another type of reaction that peroxovanadium(V) complexes are able to catalyse.[37a,47] Aliphatic hydrocarbons are also hydroxylated, though less easily than arenes, giving alcohols and ketones as the reaction products.[48,49]

Finally, vanadium(V) peroxo complexes are known to catalyse the oxidation of primary and secondary alcohols to aldehydes and ketones.[50] For instance, vanadium(V) oxytriisopropoxide, $VO(O^iPr)_3$, catalyses the oxidation of 2-propanol by H_2O_2 to acetone. Similarly, ethanol is oxidised to acetaldehyde.[51]

1.4 History and occurrence of iron

Iron is the most abundant transition metal after aluminum and the fourth most abundant element in the earth's crust (6.2%).[17,52] Iron has been known since prehistoric times. Its name is Anglo-Saxon in origin (*iren*) and the symbol 'Fe' is derived from the Latin word *ferrum*, iron.[53] The chief ores are *haematite* (Fe_2O_3), *magnetite* (Fe_3O_4), *limolite* ($\sim 2Fe_2O_3 \cdot 3H_2O$) and *siderite* ($FeCO_3$).[52] Chemically pure iron can be obtained *e.g.* by reduction with H_2 of iron oxide, which is formed by thermal decomposition of iron(II) oxalate, carbonate, or nitrate.

The common oxidation states of iron are +2 (the ferrous form) and +3 (the ferric form). There is a strong tendency for Fe(II) complexes to achieve six-coordination by the adoption of two axial ligands (usually nitrogen donors) and to become low-spin.[54] Therefore, most Fe(II) complexes have an octahedral geometry, although there are examples of four-, five- and even eight-coordination. Most iron(III) complexes are also octahedral and they are often high-spin. However, also four-, five-, and seven-coordination is well-known.[54] Iron(III) centres have a strong affinity for oxygen ligands and they readily form oxo-bridged complexes.[55]

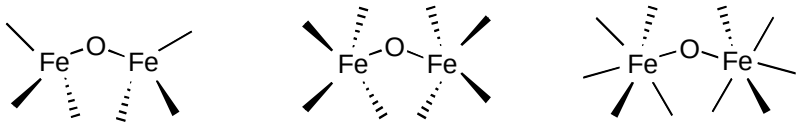

Figure 1.6 *Schematic bridging structures of μ-oxo diiron complexes.*[55]

In nature, many iron containing enzymes[56] are known which are capable of binding, transport, and activation of dioxygen.[57] Some of them contain a heme group, *i.e.* a porphyrin group with an iron(III) centre. Others are so-called non-heme proteins which are either mononuclear[58] or binuclear.[59] Examples of proteins capable of dioxygen binding and transport are hemoglobin, myoglobin, and hemerythrin.[60,61,62]

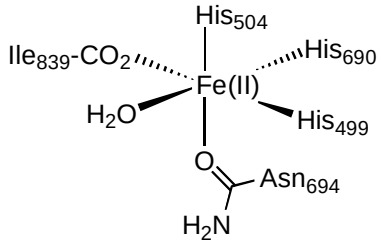

Figure 1.7 *Active site of the iron containing enzyme lipoxygenase.*[58]

Oxygen-activating enzymes include catechol dioxygenases and Rieske dioxygenases, which are involved in the degradation of aromatic molecules in the environment, lipoxygenase, which catalyses the oxidation of unsaturated fatty acids and oxygenases like methane monooxygenase,[62] and cytochrome P-450.[60,63] Purple acid phosphates are responsible for the hydrolysis of phosphate esters.[64]

Investigations concerning these enzymes are frequently facilitated by using model systems, because they can provide insight in the nature of the active site, the reactivity, and reaction mechanisms. In recent years, these type of studies have afforded valuable structural, spectroscopic, and magnetic information.[65] Based on these models various iron oxidation catalysts have been developed.[66]

1.5 History and occurrence of manganese

Metallic manganese was first isolated in 1774 by the Swedish chemist J.G. Gahn, after the discovery of C.W. Scheele that *pyrolusite* (MnO_2) contained a new element.[17,53] The element was named manganese, derived from the Latin word *magnes* (magnet), from the magnetic properties of *pyrolusite*.[3] Manganese is relatively abundant, constituting about 0.085% of the earth's crust.[52] Among the heavy metals, only iron is more abundant. Besides *pyrolusite*, *rhodochrosite* ($MnCO_3$) is a common ore.[52] The metal is obtained by reduction of the oxide with sodium, magnesium, aluminum, or by electrolysis.[3]

Mn^{2+} is the common and most stable oxidation state and the majority of the Mn(II) compounds are high-spin.[54] The highest possible oxidation state of Mn is its +7 state, which only occurs in oxo compounds like $NaMnO_4$, Mn_2O_7, and MnO_3F.[52] Many Mn(III) and Mn(IV) compounds are also well-known, just like some Mn(V) and Mn(VI) species.[54]

There are many redox enzymes known which contain one or more manganese ions in their active sites.[67] They catalyse a variety of reactions, like water oxidation (photosystem II), hydrogen peroxide decomposition (catalases), polyunsaturated fatty acid oxidation (lipoxygenase), superoxide decomposition (superoxide dismutase), and reduction of ribonucleotides in DNA synthesis (ribonucleotide reductase).[68]

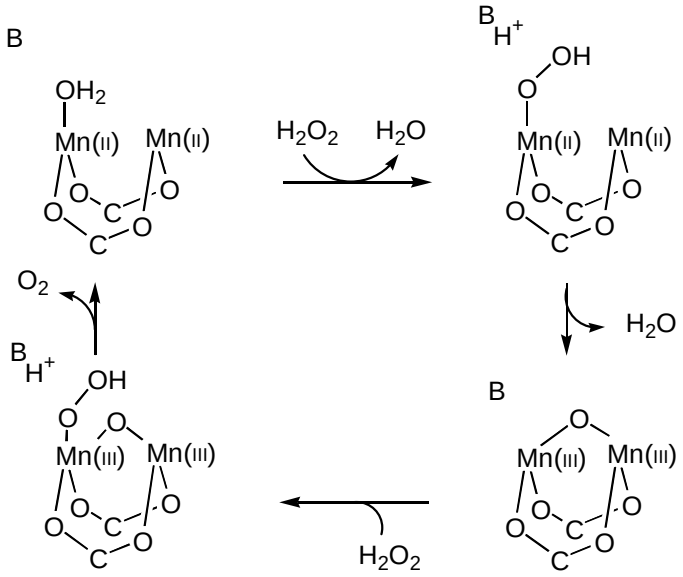

Scheme 1.6 *Proposed mechanism for Mn-catalase: two molecules of H_2O_2 are converted into two molecules of H_2O and dioxygen.*[68]

To gain insight in the working mechanisms of these enzymes, many mimics for the active sites have been developed.[68] For example, Dismukes *et al.* explored the catalase activity of a dinuclear Mn(II) complex based on ligand L^2 (Figure 1.8) and Wieghardt *et al.* reported a catalase model system based on 1,4,7-trimethyl-1,4,7-triazacyclononane (Me_3tacn, L^3) and 2,2'-bipyridine ligands.[69] Furthermore, various manganese oxidation catalysts have evolved out of these models.[70]

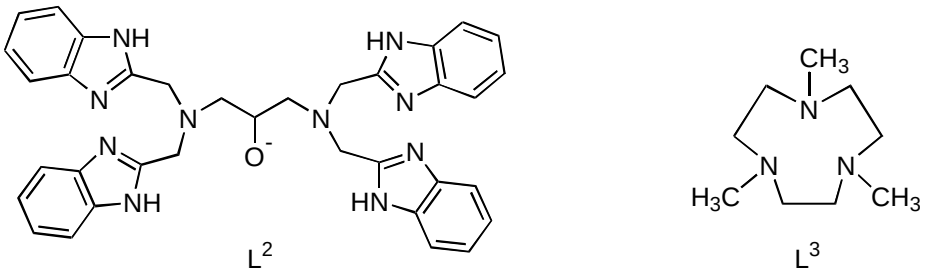

Figure 1.8 *Ligands used in manganese catalase mimics.*[69]

1.6 Research objectives and outline of this thesis

The aim of this research project was to synthesise and characterise novel vanadium complexes and to explore their catalytic properties in a variety of oxidation reactions, like *e.g.* biomimetic bromination reactions and epoxidations. The synthesis and characterisation of all kinds of vanadium complexes are already reported in the literature, but only a few of

them were employed as oxidation catalysts.[27,71] Furthermore, the fact that vanadium(V) species are known to act as catalysts in a large variety of oxidation reactions[36] stimulated us to concentrate on this subject.

The research described in this thesis has mainly been focussed on the development of a number of high-valent oxovanadium and dioxovanadium complexes, which were structurally characterised and tested as catalysts in bromination reactions and epoxidations using either H_2O_2 or TBHP (*tert*-butylhydroperoxide) as stoichiometric oxidants. Furthermore, new chiral ligands based on pyridine *N*-oxide groups have been synthesised and attempts have been made to prepare the corresponding chiral vanadium complexes, which *e.g.* could be used in asymmetric epoxidations and sulfide oxidations. A pyridine *N*-oxide salen-like ligand proved to be suitable for the incorporation of manganese and a dinuclear Mn(II) complex has been obtained.

The second part of this research has been aimed at the development of iron complexes based on N4Py[72,73] derived ligands and the investigation of their catalytic properties in oxidation reactions of alcohols, alkenes and alkanes.

The outline of this thesis is described below.

In Chapter 2 the synthesis of an imine (*N*-(2-carboxyphenyl)salicylidenimine), whose corresponding vanadium complex has been reported in literature as a functional mimic for vanadium bromoperoxidase, is described. The unexpected hydrogen bonding properties of this compound in the solid state as well as in solution are elaborated.

Chapter 3 describes the synthesis and characterisation of an oxovanadium(IV) diamidate complex and the bromination experiments with this complex as the catalyst. The results are compared with literature data.

Chapter 4 deals with the development of new ligand systems for vanadium. New dinucleating ligands were synthesised and routes towards the corresponding dinuclear vanadium complexes are shown. Furthermore, tris-urea ligands were prepared for the incorporation of vanadate, which might serve as a structural model for vanadium bromoperoxidase.

In Chapter 5 the synthesis and characterisation of two novel dioxovanadium(V) complexes based on a bis(pyridine)-imine ligand is discussed. An unexpected vanadium-mediated oxidative ligand cyclisation reaction was observed and details of this process will be given.

In Chapter 6, triazole ligands are used for the formation of vanadium(V) complexes. The synthesis and detailed characterisation of the vanadium-triazole complexes will be described. An overview of the catalytic oxidation studies will be given.

Chapter 7 deals with the design and synthesis of chiral ligands based on pyridine *N*-oxides for vanadium and manganese. Complexation studies with vanadium were performed and a novel manganese complex based on a salen-like pyridine *N*-oxide ligand was obtained. Spectroelectrochemical measurements with this manganese complex are described.

In Chapter 8 the synthesis of several non-heme iron complexes is shown, which were tested as oxidation catalysts. A μ-oxo Fe(III) dinuclear complex proved to be capable of selective oxidation of primary and secondary alcohols in the presence of H_2O_2. Spectro-

electrochemical measurements on three related μ-oxo Fe(III) dinuclear complexes are described.

In Chapter 9 some general conclusions on the vanadium and iron oxidation chemistry will be drawn. Future prospects for the use of vanadium complexes as oxidation catalysts will be discussed.

1.7 References

1 Rehder, D. *Coord. Chem. Rev.* **1999**, *182*, 297.

2 Nriagu, J.O. in *Vanadium in the Environment, Part One: Chemistry and Biochemisty*, Nriagu, J.O., Ed.; John Wiley & Sons, New York, 1998, Chapter 1.

3 *Handbook of Chemistry and Physics*, Lide, D.R., Ed.; 72nd Edition, 1991-1992.

4 Rehder, D. *Angew. Chem., Int. Ed. Engl.* **1991**, *30*, 148.

5 Oltz, E.M.; Brüning, R.C.; Smith, M.J.; Kustin, K.; Nakanishi, K. *J. Am. Chem. Soc.* **1988**, *110*, 6162.

6 Vilter, H. *Phytochemistry* **1984**, *23*, 1387.

7 Vilter, H. *Met. Ions Biol. Syst.* **1995**, *31*, 325.

8 See for instance (a) Căsný, M.; Rehder, D.; Schmidt, H.; Vilter, H.; Conte, V. *J. Inorg. Biochem.* **2000**, *80*, 157. (b) Rao, A.V.S.; Ravishankar, H.N.; Ramasarma, T. *Arch. Biochem. Biophys.* **1996**, *334*, 121. (c) Weyand, M.; Hecht, H.-J.; Vilter, H.; Schomburg, D. *Acta Cryst.* **1996**, *D52*, 864. (d) Soedjak, H.S.; Walker, J.V.; Butler, A. *Biochem.* **1995**, *34*, 12689. (e) Tschirret-Guth, R.A., Butler, A. *J. Am. Chem. Soc.* **1994**, *116*, 411. (f) Coughlin, P.; Roberts, S.; Rush, C.; Willetts, A. *Biotechnol. Lett.* **1993**, *15*, 907. (g) Van Schijndel, J.W.P.M.; Vollenbroek, E.G.M.; Wever, R. *Biochim. Biophys. Acta* **1993**, *1161*, 249. (h) Knüttel, K.; Müller, A.; Rehder, D.; Vilter, H.; Wittneben, V. *FEBS Lett.* **1992**, *302*, 11. (i) Soedjak, H.S.; Butler, A. *Biochim. Biophys. Acta* **1991**, *1079*, 1. (j) Soedjak, H.S.; Butler, A. *Biochem.* **1990**, *29*, 7974. (k) Everett, R.R.; Soedjak, H.S.; Butler, A. *J. Biol. Chem.* **1990**, *265*, 15671. (l) Everett, R.R.; Kanofsky, J.R.; Butler, A. *J. Biol. Chem.* **1990**, *265*, 4909. (m) Tromp, M.G.M.; 'Olafsson, G.; Krenn, B.E.; Wever, R. *Biochim. Biophys. Acta* **1990**, *1040*, 192. (n) Everett, R.R.; Butler, A. *Inorg. Chem.* **1989**, *28*, 395. (o) Krenn, B.E.; Tromp, M.G.M.; Wever, R. *J. Biol. Chem.* **1989**, *264*, 19287. (p) Plat, H.; Krenn, B.E.; Wever, R. *Biochem. J.* **1987**, *248*, 277. (q) De Boer. E.; Plat, H.; Tromp, M.G.M.; Wever, R.; Franssen, M.C.R.; Van der Plas, H.C.; Meijer, E.M.; Schoemaker, H.E. *Biotechnol. Bioeng.* **1987**, *30*, 607.

9 (a) Butler, A. in *Bioinorganic Catalysis*, Reedijk, J., Ed., Marcel Dekker, New York, 1993, Chapter 13. (b) Wever, R.; Hemrika, W. in *Vanadium in the Environment, Part One: Chemistry and Biochemistry*, Nriagu, J.O., Ed., John Wiley & Sons, New York, **1998**, Chapter 12.

10 Van Schijndel, J.W.P.M.; Vollenbroek, E.G.M.; Wever, R. *Biochim. Biophys. Acta* **1993**, *1161*, 249.

11 Kneifel, H.; Bayer, E. *Angew. Chem., Int. Ed. Engl.* **1973**, *12*, 508.

12 *Comprehensive Coordination Chemistry*, Wilkinson, G., Ed.; Pergamon Press, Oxford, 1987, *3*, 454.

13 Butler, A.; Carrano, C.J. *Coord. Chem. Rev.* **1991**, *109*, 61.

14 *Vanadium in Biological Systems: Physiology and Biochemistry*, Chasteen, N.D., Ed.; Kluwer Academic Publishers, Dordrecht, 1990.

15 Crans, D.C.; Amin, S.S.; Keramidas, A.D. in *Vanadium in the Environment, Part One: Chemistry and Biochemisty*, Nriagu, J.O., Ed.; John Wiley & Sons, New York, 1998, Chapter 4.

16 Page, E.M. *Coord. Chem. Rev.* **1998**, *172*, 111.

17 Emsley, J. *The Elements*, Clarendon Press, Oxford, 1989.

18 Micera, G.; Sanna, D. in *Vanadium in the Environment, Part One: Chemistry and Biochemisty*, Nriagu, J.O., Ed.; John Wiley & Sons, New York, 1998, Chapter 7.

19 (a) Conte, V.; Di Furia, F.; Moro, S. *J. Mol. Cat. A* **1995**, *104*, 159. (b) Rehder, D.; Weidemann, C.; Duch, A.; Priebsch, W. *Inorg. Chem.* **1988**, *27*, 584. (c) Heath, E.; Howarth, O.W. *J. Chem. Soc., Dalton Trans.* **1981**, 1105.

20 Geschwend, P.M.; MacFarlane, J.K.; Newman, K.A. *Science*, **1985**, *227*, 1033.

21 Gribble, G.W. *Chem. Soc. Rev.* **1999**, *28*, 335.

22 Wever, R.; Hemrika, W. in *Vanadium in the Environment, Part One: Chemistry and Biochemisty*, Nriagu, J.O., Ed.; John Wiley & Sons, New York, 1998, Chapter 12.

23 (a) Butler, A. *Coord. Chem. Rev.* **1999**, *187*, 17. (b) Franssen, M.C.R.; Jansma, J.D.; Plas, H.C. van der; Boer, E. de; Wever, R. *Bioorg. Chem.* **1988**, *16*, 352.

24 Hager, L.P.; Morris, D.R.; Brown, F.S.; Eberwein, H. *J. Biol. Chem.* **1966**, *241*, 1768.

25 Everett, R.R.; Kanofsky, J.R.; Butler, A. *J. Biol. Chem.* **1990**, *265*, 4908.

26 Butler, A. in *Bioinorganic Catalysis*, Reedijk, J., Ed.; Marcel Dekker, New York, 1993, 425.

27 See Chapter 3.

28 See Chapter 4.

29 Messerschmidt, A.; Wever, R. *Proc. Natl. Acad. Sci. USA* **1996**, *93*, 392.

30 Messerschmidt, A.; Prade, L.; Wever, R. *Biol. Chem.* **1997**, *378*, 309.

31 Holm, R.H.; Kennepohl, P.; Solomon, E.I. *Chem. Rev.* **1996**, *96*, 2239.

32 (a) Hales, B.J.; Case, E.E.; Morningstar, J.E.; Dzeda, M.F.; Mauterer, L.A. *Biochemistry* **1986**, *25*, 7251. (b) Robson, R.L.; Eady, R.R.; Richardson, T.H.; Miller, R.W.; Hawkins, M.; Postgaste, J.R. *Nature* **1986**, *332*, 388.

33 Clague, M.J.; Butler, A. in *Advanced Inorganic Biochemistry, Part 9: Models in Inorganic Chemistry*, Eichhorn, G.L.; Marzilli, L.G., Eds.; PTR Prentice-Hall, New Jersey, **1994**, Chapter 6.

34 (a) Farahbakhsh, M.; Nekola, H.; Schmidt, H.; Rehder, D. *Chem. Ber./ Recueil* **1997**, *130*, 1129. (b) Cornman, C.R.; Stauffer, T.C.; Boyle, P.D. *J. Am. Chem. Soc.* **1997**, *119*, 5986. (c) Klich, P.K.; Daniher, A.T.; Challen, P.R.; McConville, D.B.; Youngs, P.R. *Inorg. Chem.* **1996**, *35*, 347.

35 Conte, V.; Di Furia, F.; Moro, S. *J. Phys. Org. Chem.* **1996**, *9*, 329.

36 Butler, A.; Clague, M.J.; Meister, G.E. *Chem. Rev.* **1994**, *94*, 625.
37 (a) Mimoun, H.; Saussine, L.; Daire, E.; Postel, M. Fischer, J.; Weiss, R. *J. Am. Chem. Soc.* **1983**, *105*, 3101. (b) Mimoun, H.; Chaumette, P.; Mignard, M.; Saussine, L.; Fischer, J.; Weiss, R. *Nouv. J. Chim.* **1983**, *7*, 467.
38 (a) *Organic Syntheses by Oxidation with Metal Compounds*, Mijs, W.J.; Jonge, C.R.H.I. de, Eds.; Plenum Press, New York, 1986, 6. (b) Sharpless, K.B.; Michaelson, R.C. *J. Am. Chem. Soc.* **1973**, *95*, 6136.
39 Sams, C.K.; Jorgensen, K.A. *Acta Chem. Scand.* **1995**, *49*, 839.
40 Itoh, T.; Jitsukawa, K.; Kaneda, K.; Teranishi, S. *J. Am. Chem. Soc.* **1979**, *101*, 159.
41 Sharpless, K.B. *ChemTech* **1985**, 692.
42 Mimoun, H.; Mignard, M.; Brechot, P.; Saussine, L. *J. Am. Chem. Soc.* **1986**, *108*, 3711.
43 See also Chapter 6.
44 Bonchio, M.; Conte, V.; Di Furia, F.; Modena, G. *Res. Chem. Intermed.* **1989**, *12*, 111.
45 Adam, W.; Golsch, D. *Chem. Ber.* **1994**, *127*, 1111.
46 Ballistreri, F.; Tomaselli, G.A.; Toscano, R.M.; Conte, V.; Di Furia, F. *J. Am. Chem. Soc.* **1991**, *113*, 6209.
47 Bianchi, M.; Bonchio, M.; Conte, V.; Coppa, F.; Di Furia, F.; Modena, G.; Moro, S.; Standen, S. *J. Mol. Catal.* **1993**, *83*, 107.
48 Shul'pin, G.B.; Attanasio, D.; Suber, L. *J. Catal.* **1993**, *142*, 147.
49 Moiseev, I.I.; Gekhman, A.E.; Shishkin, D.I. *New. J. Chem.* **1989**, *13*, 683.
50 Bortolini, O.; Conte, V.; Di Furia, F.; Modena, G. *Nouv. J. Chim.* **1985**, *9*, 147.
51 Conte, V.; Di Furia, F.; Modena, G. *J. Org. Chem.* **1988**, *53*, 1665.
52 Cotton, F.A.; Wilkinson, G. *Advanced Inorganic Chemistry*, Fifth Ed., John Wiley & Sons, New York, 1988.
53 Greenwood, N.N.; Earnshaw, A. *Chemistry of the Elements*, Pergamon Press, Oxford, 1984.
54 *Comprehensive Coordination Chemistry*, Wilkinson, G., Ed.; Pergamon Press, Oxford, 1987, *4*.
55 Kurtz, D.M., Jr. *Chem. Rev.* **1990**, *90*, 585.
56 Solomon, E.I.; Brunold, T.C.; Davis, M.I.; Kemsley, J.N.; Lee, S.-K.; Lehnert, N.; Neese, F.; Skulan, A.J.; Yang, Y.-S.; Zhou, J. *Chem. Rev.* **2000**, *100*, 235.
57 (a) Sono, M.; Roach, M.P.; Coulter, E.D.; Dawson, J.H. *Chem. Rev.* **1996**, *96*, 2841. (b) Que, L., Jr. in *Bioinorganic Catalysis*, Reedijk, J.; Bouwman, E., Eds.; Second Edition, Marcel Dekker, New York, 1999, 269.
58 Que, L., Jr.; Ho, R.Y.N. *Chem. Rev.* **1996**, *96*, 2607.
59 Wallar, B.J.; Lipscomb, J.D. *Chem. Rev.* **1996**, *96*, 2625.
60 Roelfes, G. 'Models for Non-Heme Iron Containing Oxidation Enzymes', PhD Thesis, Groningen, 2000.
61 Lubben, M. 'Model Systems for Iron and Copper Containing Oxygenases', PhD Thesis, Groningen, 1994.
62 See Chapter 8.

63 (a) Mansuy, D.; Battioni, P. in *Bioinorganic Catalysis*, Reedijk, J.; Bouwman, E., Eds.; Second Edition, Marcel Dekker, New York, 1999, 323. (b) Sono, M.; Roach, M.P.; Coulter, E.D.; Dawson, J. H. *Chem. Rev.* **1996**, *96*, 2841.

64 Wilcox, D.E. *Chem. Rev.* **1996**, *96*, 2435.

65 See for instance: (a) Chen, K.; Que, L., Jr. *Angew. Chem. Int. Ed.* **1999**, *38*, 2227. (b) Ito, M.; Que, L., Jr. *Angew. Chem., Int. Ed. Engl.* **1997**, *36*, 1342. (c) Ménage, S.; Vincent, J.-M.; Lambeaux, C; Fontecave, M. *J. Mol. Cat. A* **1996**, *113*, 61. (d) Bossek, U.; Hummel, H.; Weyhermüller, T.; Bill, E.; Wieghardt, K. *Angew. Chem., Int. Ed. Engl.* **1995**, *34*, 2642. (e) Yan, S.; Que, L., Jr. *J. Am. Chem. Soc.* **1988**, *110*, 5222.

66 Bartos, M.J.; Gordon-Wylie, S.W.; Fox, B.G.; Wright, L.J.; Weintraub, S.T.; Kauffmann, K.E.; Münck, E.; Kostka, K.L.; Uffelman, E.S.; Rickard, C.E.F.; Noon, K.R.; Collins, T.J. *Coord. Chem. Rev.* **1998**, *174*, 361.

67 (a) Law, N.A.; Caudle, M.T.; Pecoraro, V.L. *Adv. Inorg. Chem.* **1999**, *46*, 305. (b) Wilkaira, J.; Gorun, S.M. in *Bioinorganic Catalysis*, Reedijk, J.; Bouwman, E., Eds.; Second Edition, Marcel Dekker, New York, 1999, 355.

68 Hage, R. *Recl. Trav. Chim. Pays-Bas* **1996**, *115*, 385.

69 (a) Bossek, U.; Saher, M.; Weyhermüller, T.; Wieghardt, K. *J. Chem. Soc., Chem. Commun.* **1992**, 1780. (b) Mathur, P.; Crowder, M.; Dismukes, G.C. *J. Am. Chem. Soc.* **1987**, *109*, 5227.

70 (a) La Crois, R.M. 'Manganese Complexes as Catalysts in Epoxidation Reactions', PhD Thesis, Groningen, 2000. (b) Hoogenraad, M. 'Manganese Complexes as Catalysts for Homogeneous Oxidation Reactions', PhD Thesis, Leiden, 2000, and references cited therein.

71 See Chapter 7.

72 N4Py = *N*,*N*-bis(2-pyridylmethyl)-*N*-bis(2-pyridyl)methylamine.

73 (a) Roelfes, G.; Lubben, M.; Hage, R.; Que, L., Jr.; Feringa, B.L. *Chem. Eur. J.* **2000**, *6*, 2152. (b) Ho, R.Y.N.; Roelfes, G.; Feringa, B.L.; Que, L., Jr. *J. Am. Chem. Soc.* **1999**, *121*, 264. (c) Roelfes, G.; Lubben, M.; Chen, K.; Ho, R.Y.N.; Meetsma, A.; Genseberger, S.; Hermant, R.M.; Hage, R.; Mandal, S.K.; Young, V.G., Jr.; Zang, Y.; Kooijman, H.; Spek, A.L.; Que, L., Jr.; Feringa, B.L. *Inorg. Chem.* **1999**, *38*, 1926. (d) Lubben, M.; Meetsma, A.; Wilkinson, E.C.; Feringa, B.; Que, L., Jr. *Angew. Chem., Int. Ed. Engl.* **1995**, *34*, 1512.

Chapter 2

Hydrogen Bonding Properties and Intermediate Structure of *N*-(2-Carboxyphenyl)salicylidenimine[1]

2.1 Introduction

Schiff base compounds are often used as ligands in coordination chemistry because they are generally known for their metal binding ability. In particular salicylaldimines are useful for the synthesis of transition metal complexes. Noteworthy examples include copper,[2] iron,[3] manganese,[4] and vanadium[5] complexes. For instance, Butler *et al.* synthesised *N*-(2-carboxyphenyl)salicylidenimine **2.1** as tridentate ligand for the formation of an oxovanadium(V) complex[6] and used it as a biomimic of vanadium bromoperoxidase (V-BrPO) (Scheme 2.1).[7,8]

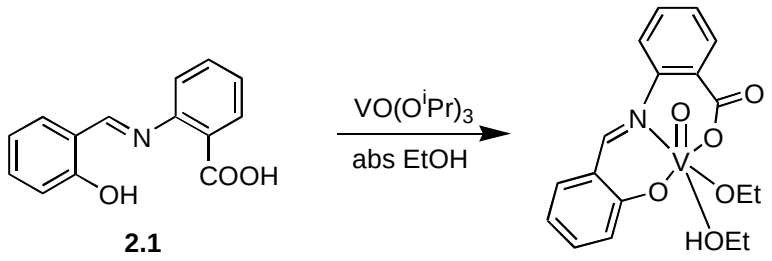

Scheme 2.1 *Synthesis of the V(V)O^{3+} complex of N-(2-carboxyphenyl)salicylidenimine **2.1**.*

To allow comparison of the halogenating properties of the vanadium(IV) complex described in Chapter 3 (complex **3.1**) with the best V-BrPO biomimics known to date,[6,7,8] ligand **2.1** and the corresponding VO^{3+} complex were prepared. Analysis of **2.1** uncovered that this compound adopts an interesting dimeric structure in the solid state. Therefore we decided to study this compound in more detail. It turned out that **2.1** exists as an unusual intermediate form between a phenol-imine (**I**) and a quinoid structure (**II**) (Figure 2.1).

In recent years a number of studies have been reported concerning the reversible solid-state photochromic or thermochromic reaction[9] of this type of *N*-salicylideneaniline ('anil') compounds.[10,11] Organisation of bistable organic molecules in the solid state is of great current interest in the context of molecular data storage.[12,13] The reversible changes in colour of the anil crystals upon illumination or heating are accompanied by a transition that takes place between two tautomeric structures due to an intramolecular proton transfer. These tautomers, a phenol-imine structure **I** and a quinoid structure **II**, are shown in Figure 2.1. This behaviour of *e.g. N*-(2-hydroxybenzylidene)aniline and its derivatives has been extensively studied by UV, IR, X-ray diffraction, Raman, and NMR spectroscopy. Various

studies were carried out with these systems in order to establish the existence of intramolecular hydrogen bonding, stabilising one of the tautomeric forms.[10]

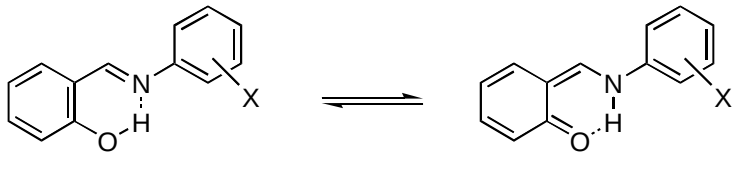

I II

Figure 2.1 *Intramolecular hydrogen transfer in N-salicylideneaniline compounds.*

Until now, most of the X-ray structures known for this class of compounds are referred to as phenol-imine tautomers.[14] However, a few quinoid structures[15] have been established as well, *e.g. N*-salicylidene-2-hydroxyaniline (measured at 123 K)[15b] and *α*-(2-hydroxymethyl)-phenyl-2,3-dihydroxybenzenemethanimine (at 300 K).[15d]

2.2 Synthesis and characterisation of 2.1

2.2.1 X-ray analysis

Compound **2.1** was prepared according to a literature procedure[16] as described in the Experimental Part. Crystals suitable for X-ray analysis were obtained from a concentrated methanolic solution of **2.1** by slow evaporation of the solvent.

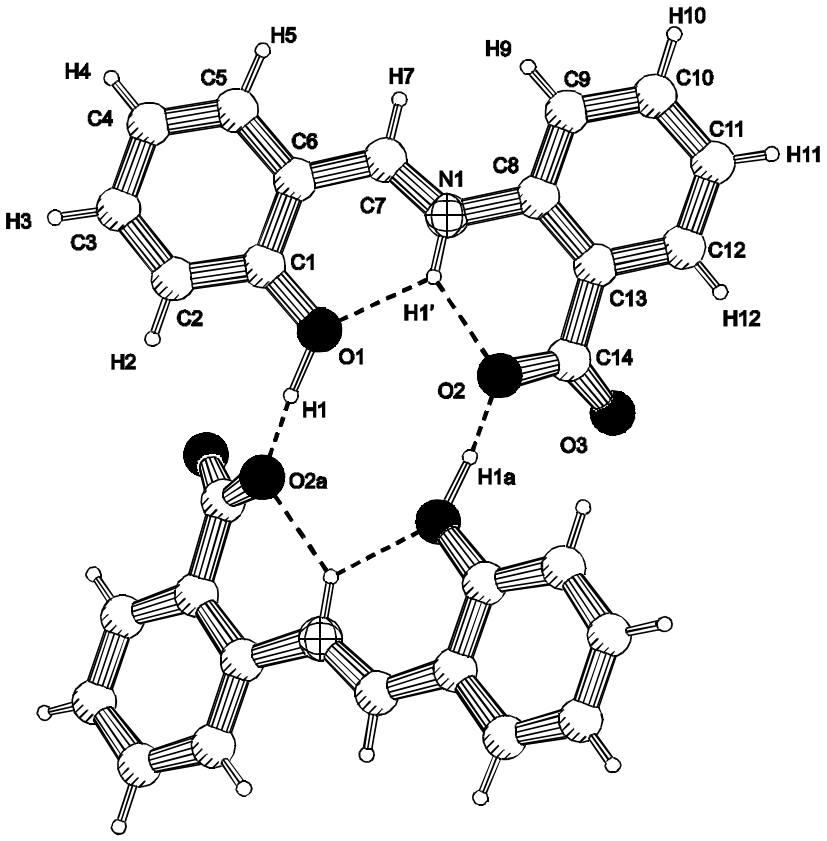

Figure 2.2 *A PLUTON representation of the structure of **2.1** at 295 K.*

The compound partially decomposed during crystallisation due to sensitivity of the molecule towards methanol. Crystallisation from other organic solvents, however, yielded crystals of inferior quality. The molecular structure (measured at 295 K) and the adopted atom numbering are presented in Figure 2.2. Bond distances and angles are listed in Table 2.1.

Table 2.1 *Selected bond distances(Å), angles (°) and torsion angle (°) of **2.1** with estimated standard deviations (esd's) in parentheses measured at 130 K and 295 K, respectively.*

Bond distances					
	130 K	**295 K**		**130 K**	**295 K**
O(1)-C(1)	1.3192(16)	1.3165(15)	C(5)-C(6)	1.414(2)	1.4102(18)
O(2)-C(14)	1.2809(17)	1.2744(16)	C(6)-C(7)	1.4250(1)	1.4190(16)
O(3)-C(14)	1.2296(18)	1.2229(18)	C(8)-C(9)	1.3923(19)	1.3917(18)
N(1)-C(7)	1.3022(18)	1.2999(16)	C(8)-C(13)	1.4004(19)	1.3970(17)
N(1)-C(8)	1.4264(16)	1.4250(15)	C(9)-C(10)	1.3808(19)	1.376(2)
C(1)-C(2)	1.4070(19)	1.4050(18)	C(10)-C(11)	1.384(2)	1.369(2)
C(1)-C(6)	1.4198(19)	1.4183(17)	C(11)-C(12)	1.383(2)	1.381(2)
C(2)-C(3)	1.375(2)	1.372(2)	C(12)-C(13)	1.3896(19)	1.3847(18)
C(3)-C(4)	1.399(2)	1.391(2)	C(13)-C(14)	1.5150(19)	1.5117(17)
C(4)-C(5)	1.3725(19)	1.363(2)			
Bond angles and torsion angle					
O(1)-C(1)-C(6)	118.57(12)	118.65(10)	N(1)-C(8)-C(13)	118.47(11)	118.66(10)
C(7)-N(1)-C(8)	125.99(12)	126.07(10)	C(8)-C(13)-C(14)	123.21(12)	123.32(10)
O(3)-C(14)-C(13)	119.23(12)	119.34(11)	O(2)-C(14)-O(3)	126.01(13)	125.81(12)
C(2)-C(14)-C(13)	114.75(11)	114.84(11)	C(1)-C(6)-C(7)	122.88(12)	122.82(11)
C(8)-C(13)-C(14)-O(2)	-31.70(19)	-30.90(18)			

The monoclinic *I*-centred unit cell contains eight molecules. In the crystal lattice two molecules are coupled by two strong intermolecular O-H···O bridges [O(1)···O(2a) = 2.455(1) Å (at 295 K)] resulting in the formation of dimers[17] which have a crystallographic imposed twofold axis. Weaker C-H···O interactions link them to infinite one-dimensional chains along the [100] vector (Table 2.2).

Another interesting feature of this structure is the presence of two intramolecular N-H···O hydrogen bonds which stabilise this conformation [N(1)-H(1')···O(1) = 2.654(1) and N(1)-H(1')···O(2) = 2.663(1) Å]. Proton H(1') is hydrogen-bonded to the imine-nitrogen atom forming a six-membered ring, whereas this proton is also hydrogen-bonded to the oxygen atom of the phenolic moiety. In this manner an eight-membered pseudocycle is created. Distances between hydrogen-bonded atoms are listed in Table 2.2. A comparable dimer formation is known for α-(2-hydroxymethyl)phenyl-2,3-dihydroxy-benzenemethanimine, but in this case the hydrogen bonds connecting the dimers are significantly longer [A···D = 2.879(4) Å].[15d]

Table 2.2 *Hydrogen bonds observed for **2.1** measured at 130 K and 295 K, respectively.*

D-H···A / Å	D-A / Å at 130 K; 298 K	D-H / Å at 130 K; 298 K	H···A / Å at 130 K; 298 K	D-H···A / ° at 130 K; 298 K
O(1)-H(1)···O(2a)	2.453(1); 2.455(1)	1.10(2); 1.12(2)	1.36(2); 1.34(2)	173(2); 173(2)
N(1)-H(1')···O(1)	2.656(2); 2.654(1)	0.95(2); 0.97(2)	1.94(2); 1.96(2)	131(2); 126(1)
N(1)-H(1')···O(2)	2.667(2); 2.663(1)	0.95(2); 0.97(2)	1.95(2); 1.90(2)	131(2); 133(1)
C(7)-H(7)···O(3)	3.232(2); 3.253(2)	1.00(2); 0.97(1)	2.26(2); 2.30(2)	166(1); 166(1)
C(9)-H(9)···O(3)	3.237(2); 3.246(2)	0.93(2); 0.93(2)	2.39(2); 2.42(2)	148(2); 148(2)

Bond distances were compared with the mean values for similar structures referred to as phenol-imine tautomers[14] from the Cambridge Structural Database and a number of unusual features are observed (Table 2.3). For instance, C(6)-C(7) is considerably shortened in comparison with the observed bond length in phenol-imine structures [1.4190(16) Å instead of 1.445 Å]. C(1)-O(1) is also shortened [from 1.349 to 1.3165(15) Å], while the value of C(7)-N(1) is slightly increased [from 1.287 to 1.2999(16) Å]. The shortening of C(6)-C(7) and C(1)-O(1) bonds and lengthening of C(7)-N(1) can be explained as follows. The hydrogen of the hydroxy group attached to C(1) is placed between atoms O(1) and O(2a) forming strong O(1)-H(1)···O(2a) intermolecular hydrogen bonds [O(1)-H(1) = 1.12(2); H(1)···O(2a) = 1.34(2) Å], thereby introducing partial tautomerisation with appreciable keto character to the C(1)-O(1) bond and partial double bond character to the C(6)-C(7) bond. This causes an increase in C(7)-N(1) bond length. However, comparing these distances with those found for quinoid structures,[15] it is obvious that **2.1** can neither be referred to as being completely in the quinoid tautomeric state. For instance C(1)-O(1) and C(6)-C(7) bonds are too long [1.3165(15) instead of 1.294 Å and 1.4190(16) instead of 1.407 Å, respectively], whereas C(7)-N(1) possesses too much double bond character [1.2999(16) instead of 1.327 Å].

The conformation of the molecule is nearly planar. The deviation (at 295 K) of the atoms O(1), C(1)-C(10), N(1), C(13) and C(14) from the least squares plane does not exceed 0.0558(16) Å. O(2) deviates 0.6245(11) Å from that plane, whereas C(11) and C(12) lie 0.1297(19) and 0.1402(16) Å out of the plane, respectively.

Table 2.3 *Bond distances (at 295 K) of **2.1** (Å) with esd's in parentheses compared with mean distances (determined at various temperatures) for related quinoid[15a-d] and phenolic[14a-t] structures (Å). Minimum and maximum values are given in parentheses.*

Bond	Distances for 2.1	Quinone	Phenol
C(7)-N(1)	1.2999(16)	1.327 (1.302; 1.347)	1.287 (1.266; 1.317)
C(1)-O(1)	1.3165(15)	1.294 (1.279; 1.301)	1.349 (1.323; 1.399)
N(1)-H(1')	0.97(2)	1.053 (0.903; 1.204)	1.818 (1.388; 3.536)
O(1)-H(1)	1.12(2)	1.644 (1.414; 1.836)	0.970 (0.789; 1.250)
C(6)-C(7)	1.4190(16)	1.407 (1.399; 1.413)	1.445 (1.426; 1.457)

We concluded that **2.1** exists at 295 K in the solid state as an intermediate form between tautomers **I** and **II** (Figure 2.4). However, it could also be that the crystal contains 50% of each tautomer, providing an average structure which would be visible in large anisotropic thermal displacement parameters. To clarify this problem, the crystal structure was also determined at low temperature (130 K). The ORTEP plot is shown in Figure 2.3. Bond distances and angles are listed in Table 2.1.

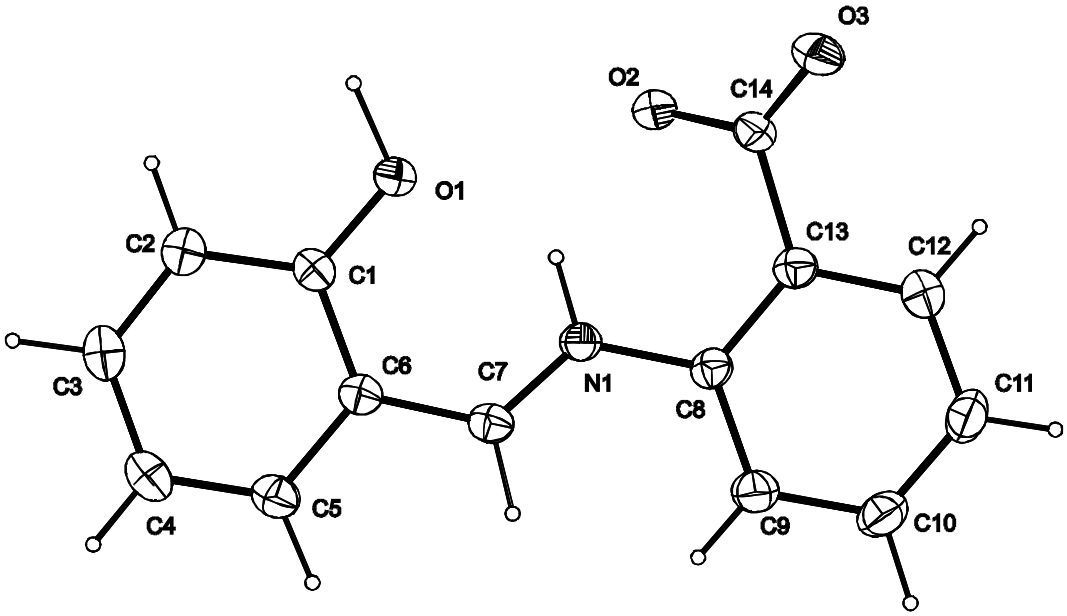

Figure 2.3 *An ORTEP plot of **2.1** measured at 130 K (50% probability level).*

The anisotropic thermal displacement parameters turned out not to be substantial and also the rigid body analysis[18] is within the range of standard deviations. The ratios of the main axes for example, are below 3.0 and for most atoms even below 2.0. Bond distances of **2.1** recorded at 298 K are slightly shorter than those found at 130 K (Table 2.1 and Table 2.2), but this was to be expected due to the thermic motion model. From these results it can be concluded that **2.1** indeed is an intermediate structure between phenolic and quinoid tautomers (both at 298 and 130 K) and does not exist as two limiting structures (type **I** and **II**, Figure 2.4).

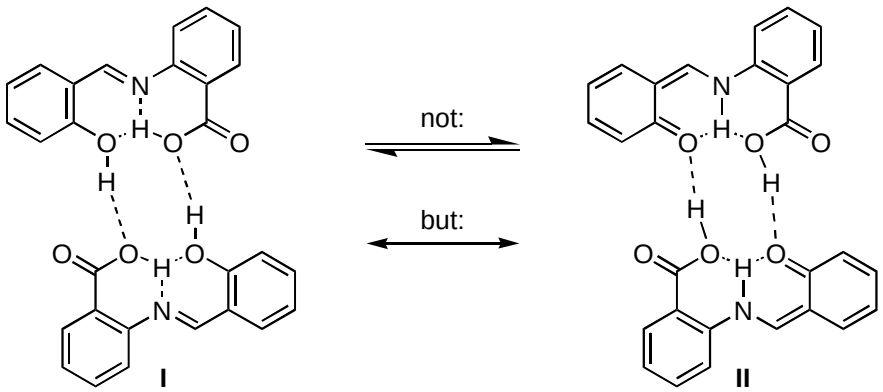

Figure 2.4 *Schematic representation of phenol-imine and quinoid tautomeric structures of **2.1**.*

2.2.2 Infrared spectroscopy

The infrared spectrum of solid **2.1** recorded using a KBr disk shows an absorption at 1691 cm^{-1}, which is attributed to a C=O stretching vibration.[19] A broad O-H stretching vibration is observed at about 3450 cm^{-1}. This is an indication for hydrogen bonding, because the normal position for free O-H is in the range of 3730-3520 cm^{-1}.[19] A strong C=N stretching vibration band is observed at 1618 cm^{-1}. It is known that if the nitrogen atom of the C=N bond is substituted in such a way that it has a more polar character, the absorption can be found in the region 1659-1510 cm^{-1} (whereas normal C=N is expected in the range of 1680-1650 cm^{-1}).[19] In this case the hydrogen atom of the acid functionality located on the nitrogen causes this shift. An absorption band at 1582 cm^{-1} may be assigned to C=C stretching vibration.[19]

The IR-spectra of solid samples and solutions are clearly different. Although in acetonitrile the absorption of the C=N bond is observed at 1620 cm^{-1} (1618 cm^{-1} for the solid sample), a shift is observed for the C=O stretching vibration from 1691 to 1727 cm^{-1}. Varying the concentration of **2.1** does not influence the spectrum. This is an indication for the absence of the intermolecular hydrogen bonds. Apparently, in solution the hydrogen of the acid moiety is still hydrogen bonded to the imine nitrogen, but hydrogen bonding to the phenol functionality of a second monomer does not occur. Therefore it can be concluded that while the solid-state structure shows a dimeric entity, in solution it appears to be monomeric. However, the degree and nature of dimerisation in solution is often a sensitive function of the donor and acceptor properties and the dryness of the solvent. Therefore, the compound was further investigated by ^{1}H NMR spectroscopy.

2.2.3 ^{1}H NMR analysis

To further support the occurrence of monomeric species of compound **2.1** in solution, additional NMR analyses were carried out. ^{1}H NMR spectra of aggregates in a hydrogen-bonding solvent such as DMSO-d_6 in general only show fully dissociated components.[20] A typical ^{1}H NMR spectrum of monomeric **2.1** in DMSO-d_6 is shown in Figure 2.5. The spectrum of **2.1** in acetonitrile-d_3 is similar to the spectrum recorded in DMSO-d_6, which indicates the existence of a monomeric phenol-imine tautomeric form in acetonitrile. These observations are in agreement with the IR-spectra (*vide supra*).

^{1}H NMR spectra of **2.1** in methanol-d_4 were difficult to interpret because the compound is not stable in methanol solution. Most likely, the molecule is attacked by methanol at the imine N(1)-C(7) bond, forming eventually, among other products, an acetal from salicylaldehyde [5.56 ppm (s, acetal proton)], 2-aminobenzoic acid [6.73-6.64 (m, 2H)] and salicylaldehyde [9.86 ppm (s, CHO)]. Although full analysis of these spectra was very complicated, dimer formation does not occur under the conditions employed, because no concentration dependent shifts were observed.[21]

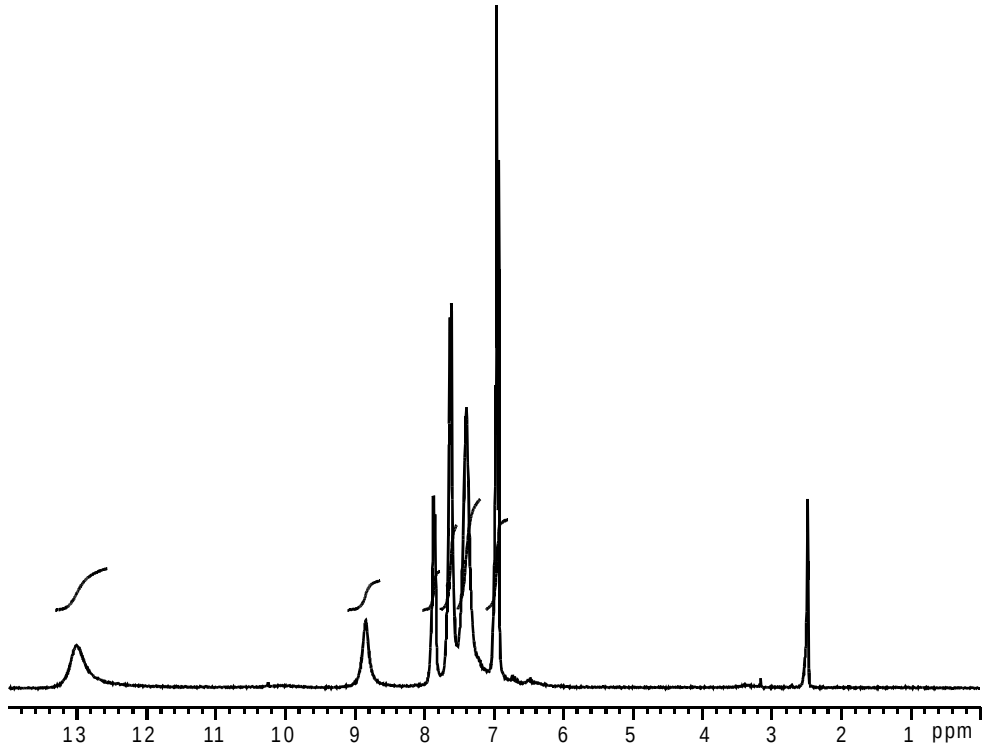

Figure 2.5 *^{1}H NMR spectrum of **2.1** in DMSO-d^6*

2.2.4 Electrospray mass measurements

Additional experiments were performed using electrospray mass spectrometry (ES/MS).[22] Varying the concentration of **2.1** in methanol starting from 1 x 10^{-6} to 1 x 10^{-3} M reveals a continuing increase of a mass peak of 483, which corresponds to ($2M$ + H^+). These results differ from the observations made with ^{1}H NMR in methanol (*vide supra*). However, it is known to be difficult with ES/MS to distinguish between dimers in solution and cluster formation inside the mass spectrometer.[23] Samples measured at higher concentrations (10^{-5} M and above) can give association of two molecules held together by a H^+ or a Na^+. A lot of degradation products were also found, which is in agreement with the NMR studies. When acetonitrile was used as solvent, no significant dimer formation was observed at the same concentrations, which is also in agreement with the NMR data. The mass spectra and NMR experiments both showed greater stability of **2.1** in acetonitrile than in methanol.

2.2.5 UV spectroscopy

The UV-spectrum of **2.1** recorded in acetonitrile exhibits four bands at 214, 274, 336, and 429 nm. The band at 214 nm (ε = 26.1 x 10^3 M^{-1} cm^{-1}) is considered to arise from electronic π-π^* transitions in the aromatic rings.[15d] The band at 274 nm (ε = 10.6 x 10^3 M^{-1} cm^{-1}) can be

assigned to π-π* transitions involving one aromatic ring and the imine functionality.[15d] The band at even longer wavelength, 336 nm (ε = 9.5 x 10^3 M^{-1} cm^{-1}), probably arises from an intramolecular charge transfer interaction.[24] Strong intramolecular hydrogen bonding between the carboxylic hydrogen and the imino-nitrogen forces planarity, which facilitates the charge transfer to take place. The band at 429 nm (ε = 0.3 x 10^3 M^{-1} cm^{-1}) is assigned to a n-π* transition confirming that **2.1** possesses partial *ortho*-quinoid character.[25]

2.3 Synthesis and structural analysis of related salicylidenimine 2.3

To further study the ability of these compounds in forming hydrogen-bonded aggregates in solution, alkyl-substituted derivative **2.3** was synthesised. Compound **2.3** was expected to show higher solubility in chloroform. In this solvent, salicylidenimine **2.1** is insoluble. If dimerisation in solution would be possible with these type of compounds, we expected it to occur in chloroform.[20]

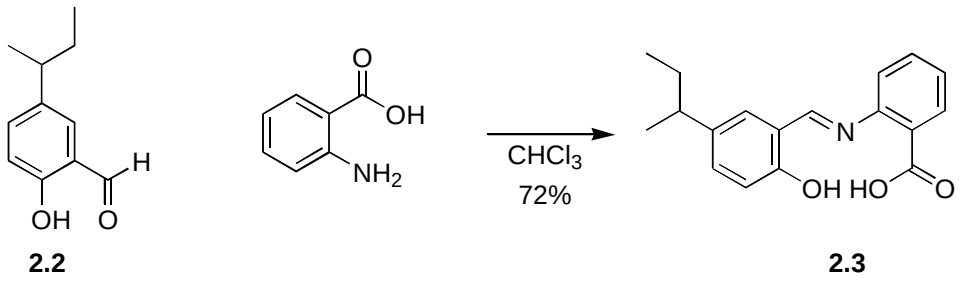

2.2 **2.3**

Scheme 2.2 *Synthesis of compound **2.3**.*

The Schiff base 2-[2-Hydroxy-5-(2-methylbutyl)benzylidene aminomethyl]benzoic acid **2.3** was synthesised reaction of 2-hydroxy-5-(1-methylpropyl)benzaldehyde **2.2** and 2-aminobenzoic acid in chloroform (Scheme 2.2). Compound **2.2** was prepared earlier *via* a Reimer-Tiemann reaction,[26] but only in 30% yield. Therefore, a route was developed analogously to a literature procedure[27] in which *o*-hydroxyaryl aldehydes are formed by treating aryloxymagnesium bromides with paraformaldehyde in the presence of triethylamine. In this way, **2.2** was obtained in 63% yield.

Again, electrospray mass spectrometry (ES/MS) was used to examine possible dimer formation of **2.3**. In chloroform, a significant amount of a dimer with a mass of 595 ($2M$ + H^+) was observed besides the mass of the monomer (298 corresponds to M + H^+). Molecular weight determinations in chloroform at 38 °C of 0.015 (M = 271), 0.04 (M = 275), 0.07 (M = 281) and 0.09 M (M = 272) solutions, however, indicated that dimerisation does not occur. Concentration dependent ^{1}H NMR measurements in deuterated chloroform are consistent with a monomeric phenol-imine tautomeric structure as well. Thus, cluster formation seems

to occur inside the mass spectrometer. Experiments in acetonitrile show comparable results as discussed earlier for imine **2.1** *i.e.* no dimerisation was observed according to ES/MS as well as to ^{1}H NMR. Schiff base **2.3** is not stable in methanol solution as well. In the mass spectra as well as in the ^{1}H NMR spectra several degradation products are observed.

The UV-spectrum recorded in chloroform resembles that of **2.1** recorded in acetonitrile. Also in this case four bands are observed, at 242 (ε = 18.7 x 10^3 M^{-1} cm^{-1}), 279 (ε = 11.1 x 10^3 M^{-1} cm^{-1}), 312 (ε = 9.4 x 10^3 M^{-1} cm^{-1}) and 438 nm (ε = 1.4 x 10^3 M^{-1} cm^{-1}). The latter one shows that **2.3** also possesses partial *ortho*-quinoid character as was observed for **2.1**.

The infrared spectra of **2.3** in the solid state as well as in solution are very similar to those of **2.1**. The absorptions in the solid state are found at 1693 (C=O), 1622 (C=N) and 1568 cm^{-1} (C=C). Around 3450 cm^{-1} a broad O-H band is observed. In chloroform solution the C=O stretching vibration band shifts towards 1727 cm^{-1} and the C=N stretching vibration band is located at 1627 cm^{-1}.

2.4 Conclusions

A dimeric structure was obtained for **2.1** in the solid state, showing short intermolecular hydrogen bonds giving rise to the formation of an eight-membered pseudocycle. Variable temperature X-ray analyses show that its structure can best be described as intermediate between phenol-imine and quinoid tautomeric forms and not as an average of the two limiting structures. It was shown, using ^{1}H NMR, UV, and IR measurements, that in solution the compound exists as a monomer. In addition, a related salicylidenimine **2.3**, soluble in chloroform, was investigated. This Schiff base showed similar properties compared to **2.1**. Most probably, **2.3** also exists as a dimer in the solid state, since for instance IR-spectra in solid samples and in solutions are very similar in the O-H region as well as in the carbonyl and imine region, indicating comparable dimerisation behaviour for both compounds.

2.5 Experimental section

2.5.1 General information

^{1}H and ^{13}C NMR spectra were recorded on a Varian VXR-300 spectrometer (at 300 MHz and 75.4 MHz, respectively). Chemical shifts are reported in δ units (ppm) relative to the residual deuterated solvent signals of $CHCl_3$ (^{1}H: δ 7.24 ppm, ^{13}C: δ 77.0 ppm), CH_3OH (^{1}H: δ 3.30 ppm, ^{13}C: δ 49.0 ppm), DMSO (^{1}H: δ 2.49 ppm, ^{13}C: δ 39.5 ppm) or CH_3CN (^{1}H: δ 1.93 ppm, ^{13}C: δ 117.8 ppm). All solvents used for NMR experiments were dried on molecular sieves (4Å), degassed and stored under an atmosphere of argon. High-resolution mass spectra were obtained on an AEI MS-902 spectrometer by electron impact (EI) and were performed

by A. Kiewit. Electrospray mass (ES/MS) spectra were recorded on a NERMAG mass spectrometer by M. Jeronimus-Strating. Infrared spectra were recorded on a Perkin-Elmer 841 spectrometer. UV-Vis spectra were recorded on a HP-8453 spectrophotometer. Melting points (uncorrected) were determined on a Mettler FP-1 melting point apparatus, equipped with a Mettler FP-52 microscope. Elemental analyses and molecular weight determinations were performed by H. Draaijer, J. Ebels and J. Hommes. X-ray structures were determined by Drs. A. Meetsma.

2.5.2 X-ray crystallography of 2.1

An orange-red coloured block-shaped crystal of **2.1** having approximate dimensions of 0.15 x 0.15 x 0.40 mm mounted on top of a glass fiber was used for the X-ray study.

Crystal data. $C_{14}H_{11}NO_3$, M = 241.25, monoclinic, space group $I2/a$, T = 295 K, a = 14.840(1), b = 6.813(1), c = 22.680(1) Å, β = 97.796(6)°, V = 2271.9(4) Å^3, Z = 8, D_x = 1.411 g cm^{-3}, μ(MoKα) = 1.0 cm^{-1}, F(000) = 1008; T = 130 K, a = 14.831(1), b = 6.718(1), c = 22.660(5) Å, β = 97.61(1)°, V = 2237.8(6) Å^3, Z = 8, D_x = 1.432 g cm^{-3}, μ(MoKα) = 1.0 cm^{-1}, F(000) = 1008.

Data collection, structure analysis and refinement. The intensity data were collected on an Enraf-Nonius CAD-4*F* diffractometer with graphite monochromated MoKα radiation (λ = 0.71073 Å) using $\omega/2\theta$ mode with ω scan width = 0.85 + 0.34 tan θ at 295 K and 0.80 + 0.34 tan θ at 130 K, respectively. Intensity data were corrected for Lorentz and polarisation effects, scale variation, but not for absorption and reduced to F_0^2. The structure was solved by direct methods with *SHELXS*86.[28] Refinement on F^2 was carried out by full-matrix least-squares techniques: observance criterion $F^2 \geq 0$ was applied during refinement. A subsequent difference Fourier synthesis resulted in the location of all the hydrogen atoms, which coordinates and isotropic thermal displacement parameters were refined. The crystal (at 295 K) exhibited some secondary extinction for which the F_c values were corrected by refinement of an empirical isotropic extinction parameter. Final refinement on F^2 carried out by full-matrix least-squares techniques converged at wR(F^2) = 0.1148 for 2364 reflections with $F_0^2 \geq 0$ and $R(F)$ = 0.0388 for 1967 reflections obeying $F_0 \geq 4.0\ \sigma(F_0)$ criterion and 208 parameters. A final difference Fourier map did not show residual peaks outside the range ±0.22(4) e/Å^3. Final refinement on F^2 (at 130 K) converged at wR(F^2) = 0.1001 for 2192 reflections with $F_0^2 \geq 0$ and $R(F)$ = 0.0359 for 1783 reflections obeying $F_0 \geq 4.0\ \sigma(F_0)$ criterion and 207 parameters. A final difference Fourier map did not show residual peaks outside the range ±0.21(5) e/Å^3.

2.5.3 Syntheses

_N_-(2-Carboxyphenyl)salicylidenimine (2.1)

To a hot solution of *o*-aminophenol (3.43 g, 0.025 mol) in absolute ethanol (15 ml) was added a solution of salicylaldehyde (3.05 g, 0.025 mol) in absolute ethanol (5 ml). The orange

reaction mixture was heated for 5 min and then cooled in an ice bath. Filtration of the orange precipitate yielded **2.1** (5.47 g, 0.023 mmol, 91%). Crystals suitable for X-ray analysis were obtained from a concentrated solution of **2.1** in methanol by slow evaporation of the solvent (yield 20-40%). ^{1}H NMR (DMSO-d_6) 13.00 (br, 2H, H^1 + $H^{1'}$, see Figure 2.2 for the numbering scheme), 8.83 (br, 1H, H^7), 7.84 (d, 1H, J = 7.0 Hz, H^{12}), 7.62-7.60 (m, 2H, H^{11} + H^5), 7.45-7.30 (m, 3H, H^{10} + H^9 + H^3), 6.96-6.91 (m, 2H, H^2 + H^4); ^{1}H NMR (CD_3CN) 8.70 (br, 1H, H^7), 7.94 (d, 1H, J = 7.7 Hz, H^{12}), 7.65-7.58 (m, 1H, H^{11}), 7.55-7.52 (m, 1H, H^5), 7.40-7.33 (m, 3H, H^{10} + H^9 + H^3), 6.98-6.93 (m, 2H, H^2 + H^4); ES / MS (CH_3CN) *m/z* 242 (M + H^+); ES / MS (MeOH) *m/z* 242 (M + H^+), 264 (M + Na^+), 301, 360, 483 (2M + H^+), 585 (2M + Na^+); HRMS calcd for $C_{14}H_{11}NO_3$: 241.074, found: 241.074; mp 209-210 °C; Anal. calcd. for $C_{14}H_{11}NO_3$: C 69.70; H 4.60; N 5.81%, found: C 69.63; H 4.75; N 5.70%; λ_{max}(CH_3CN) 214 nm (ε = 26.1 x 10^3 M^{-1} cm^{-1}), 274 (ε = 10.6 x 10^3 M^{-1}), 336 (ε = 9.5 x 10^3 M^{-1}), 429 (ε = 0.3 x 10^3 M^{-1}).

2-Hydroxy-5-(1-methylpropyl)benzaldehyde (**2.2)**

Compound **2.2** was obtained analogously to a literature procedure[27] as a slightly yellow oil after Kugelrohr distillation (97 °C at 0.4 mmHg) in 63% yield. ^{1}H NMR ($CDCl_3$) 10.86 (s, 1H, CHO), 9.87 (s, 1H, OH), 7.38-7.33 (m, 2H), 6.92 (d, 1H, J = 8.1 Hz), 2.60 (heptet, 1H, J = 7.0 Hz, CH), 1.65-1.50 (m, 2H, CH_2), 1.23 (d, 3H, J = 6.8 Hz, CH_3), 0.81 (t, 3H, J = 7.5 Hz, CH_3); ^{13}C NMR ($CDCl_3$) 196.6 (CHO), 159.6 (C), 138.9 (C), 135.9 (CH), 131.4 (CH), 120.2 (C), 117.2 (CH), 40.4 (CH), 30.9 (CH_2), 21.5 (CH_3), 11.9 (CH_3); HRMS calcd for $C_{11}H_{14}O_2$: 178.099, found: 178.100.

2-[2-Hydroxy-5-(2-methyl-butyl)benzylidene aminomethyl]benzoic acid (2.3)

To a solution of *sec*-butylsalicylaldehyde **2.2** (0.200 g, 1.12 mmol) in chloroform (10 ml) was added 2-aminobenzoic acid (0.155 g, 1.12 mmol) in chloroform (10 ml). The reaction mixture was stirred for 2 h. Sodium sulfate was added and the yellow solution was stirred for an additional 30 min. After filtration and slow evaporation of the solvent **2.3** was obtained as a yellow powder (0.24 g, 0.81 mmol, 72%). ^{1}H NMR ($CDCl_3$) 11.15 (br, 2H, H^1 + $H^{1'}$, numbering scheme analogously to **2.1** as shown in Figure 2.2), 8.44 (s, 1H, H^7), 8.07 (d, 1H, J = 7.9 Hz, H^{12}), 7.54-7.49 (m, 1H, H^{11}), 7.27 (t, 1H, J = 7.7 Hz, H^5), 7.17-7.11 (m, 3H, H^{10} + H^9 + H^3), 6.98 (d, 1H, J = 8.4 Hz, H^2), 2.51-2.44 (m, 1H, CH), 1.53-1.43 (m, 2H, CH_2), 1.13 (d, 3H, J = 6.6 Hz, CH_3), 0.73 (t, 3H, J = 7.3 Hz, CH_3); ES / MS ($CHCl_3$) *m/z* 298 (M + H^+) and 595 (2M + H^+); ES / MS (CH_3CN) *m/z* 298 (M + H^+); ES / MS (MeOH) *m/z* 138 (*o*-aminophenol + H^+), 178 (*sec*-butylsalicylaldehyde + H^+), 193, 247, 298 (M + H^+), 595 (2M + H^+); HRMS calc for $C_{18}H_{19}NO_3$: 297.136, found: 297.139; mp 169-170 °C; Anal. calcd. for $C_{14}H_{11}NO_3$ C 72.71; H 6.44; N 4.71%, found: C 72.19; H 6.35; N 4.68%; λ_{max}($CHCl_3$) 242 nm (ε = 18.7 x 10^3 M^{-1} cm^{-1}), 279 (ε = 11.1 x 10^3 M^{-1} cm^{-1}), 312 (ε = 9.4 x 10^3 M^{-1} cm^{-1}), 438 (ε = 1.4 x 10^3 M^{-1} cm^{-1}).

2.6 References

1 Ligtenbarg, A.G.J.; Hage, R.; Meetsma, A.; Feringa, B.L. *J. Chem. Soc., Perkin Trans. 2* **1999**, 807.

2 (a) Sorell, T.N. *Tetrahedron*, **1989**, *45*, 3. (b) Gelling, O.J.; Feringa, B.L. *J. Am. Chem. Soc.* **1990**, *112*, 7599.

3 (a) Dutta, S.K.; Ensling, J.; Werner, R.; Flörke, U.; Haasse, W.; Gütlich, P.; Nag, K. *Angew. Chem., Int. Ed. Engl.* **1997**, *36*, 152. (b) Pyrz, J.W.; Pan, X.; Britton, D.; Que, L., Jr. *Inorg. Chem.* **1991**, *30*, 3461.

4 (a) Jacobsen, E.N. *Catalytic Asymmetric Synthesis*, I. Ojima, Ed.; VCH, New York, 1993. (b) Connors, J.; McAuliffe, C.A.; Tames, J. *Rev. Inorg. Chem.* **1982**, *3*, 257.

5 (a) Farahbakhsh, M.; Nekola, H.; Schmidt, H.; Rehder, D. *Chem. Ber./Recueil* **1997**, *130*, 1129. (b) Nakajima, K.; Kojima, M.; Azuma, S.; Kasahara, R.; Tsuchimoto, M.; Kubozono, Y.; Maeda, H.; Kashino, S.; Ohba, S.; Yoshikawa, Y.; Fujita, J. *Bull. Chem. Soc. Jpn.* **1996**, *69*, 3207. (c) Root, C.A.; Hoeschele, J.D.; Cornman, C.R.; Kampf, J.W.; Pecoraro, V.L. *Inorg. Chem.* **1993**, *32*, 3855.

6 Clague, M.J.; Keder, N.L.; Butler, A. *Inorg. Chem.* **1993**, *32*, 4754.

7 See Chapter 3.

8 Later on it was reported that the ligand described in ref. 6, dissociates from the vanadium ion upon addition of H_2O_2. These revised results can be found in: Butler, A.; Baldwin, A.H. *Structure and Bonding* **1997**, *89*, 109.

9 Cohen, M.D.; Flavian, S. *J. Chem. Soc. B* **1967**, 334 and references therein.

10 See, *e.g.* Hadjoudis E. in *Photochromism, Molecules and Systems*, H. Dürr, H. Bouas-Laurent, Ed.; Elsevier Science Publishers, B.V., Amsterdam, 1990, Chapter 17.

11 (a) Ogawa, K.; Harada, J.; Tamura, I.; Noda, Y. *Chem. Lett.* **2000**, 528. (b) Suzuki, T.; Kaneko, Y.; Arai, T. *Chem. Lett.* **2000**, 756. (c) Ogawa, K.; Fujiwara, T. *Chem. Lett.* **1999**, 657. (d) Harada, J.; Uekusa, H.; Ohashi, Y. *J. Am. Chem. Soc.* **1999**, *121*, 5809. (e) Kawato, T.; Kanatomi, H.; Amimoto, K.; Koyama, H.; Shigemizu, H. *Chem. Lett.* **1999**, 47. (f) Ogawa, K.; Kasahara, Y.; Ohtani, Y.; Harada, J. *J. Am. Chem. Soc.* **1998**, *120*, 7107.

12 Nakatani, K.; Delaire, J.A. *Chem. Mater.* **1997**, *9*, 2682.

13 Irie, M.; Uchida, K.; Eriguchi, T.; Tsuzuki, H. *Chem. Lett.* **1995**, 899.

14 (a) Lindeman, S.V.; Andrianov, V.G.; Kravcheni, S.G.; Potapov, V.M.; Potekhin, K.A.; Struchkov, Yu. T. *Zh. Strukt. Khim.* **1981**, *22*, 123. (b) Filipenko, O.S.; Ponomarev, V.I.; Bolotin, B.M.; Atovmyan, L.O. *Kristallografiya*, **1983**, *28*, 889. (c) Aldoshin, S.M.; Atovmyan, L.O.; Ponomarev, V.I. *Khim. Fiz. (Sov. J. Chem. Phys.)* **1984**, *3*, 787. (d) Bregman, L. Leiserowitz, K. Osaki, *J. Chem. Soc.* **1964**, 2086. (e) Aldoshin, S.M.; Knyazhanskii, M.I.; Tymyanskii, Ya.R.; Atovmyan, L.O.; D'Yachenko, O.A. *Khim. Fiz. (Sov. J. Chem. Phys.)* **1982**, 1015. (f) Obodovskaya, A.E.; Starikova, Z.A.; Bolotin, B.M.; Safonova, T.N.; Etingen, N.B. *Zh. Strukt. Khim.* **1985**, *26*, 111. (g) Filipenko, O.S.; Atovmyan, L.O.; Tarnopol'skii, B.L.; Safina, Z.Sh. *Zh. Strukt. Khim.* **1979**, *20*, 80. (h) Ondracek, J.; Kovarova, Z.; Maixner, J.; Jursik, F. *Acta Cryst.* **1993**, *C49*, 1948. (i) Mansilla-Koblavi, F.; Toure, S.; Lapasset, J.; Carles, M.; Bodot, H. *Acta Cryst.* **1989**, *C45*,

451. (j) Inabe, T.; Hoshino, N.; Mitani, T.; Maruyama, Y. *Bull. Chem. Soc. Jpn.* **1989**, *62*, 2245. (k) Moloney, G.P.; Gable, R.W.; Iskander, M.N.; Craik, D.J.; Mackay, M.F. *Aust. J. Chem.* **1990**, *43*, 99. (l) Inabe, T.; Gautier-Luneau, I.; Hoshino, N.; Okaniwa, K.; Okamoto, H.; Mitani, T.; Nagashima, U.; Maruyama, Y. *Bull. Chem. Soc. Jpn.* **1991**, *64*, 801. (m) Sergienko, V.S.; Mistryukov, A.E.; Litvinov, V.V.; Knyazhanskii, M.I.; Garnovskii, A.D.; Porai-Koshits, M.A. *Koord. Khim.* **1990**, *16*, 168. (n) Yeap, G.-Y.; Gan, C.-L.; Fun, H.-K.; Shawkataly, O.B.; Teoh, S.-G. *Acta Cryst.* **1992**, *C48*, 1143. (o) Wozniak, K.; He, H.; Klinowski, J.; Jones, W.; Dziembowska, T.; Grech, E. *J. Chem. Soc., Faraday Trans.* **1995**, *91*, 77. (p) Kwiatkowski, M.; Kwiatkowski, E.; Olechnowicz, A.; Kosciuszko-Panek, B.; Ho, D.M. *Pol. J. Chem.* **1994**, *68*, 85. (q) Mansilla-Koblavi, F.; Tenon, J.A.; Toure, S.; Ebby, N.; Lapasset, J.; Carles, M. *Acta Cryst.* **1995**, *C51*, 1595. (r) Fernández-G., J.M.; Rodríguez-Romero, A.; Panneerselvam, K.; Soriano-García, M. *Acta Cryst.* **1995**, *C51*, 1643. (s) Elerman, Y.; Elmali, A.; Atakol, O.; Svoboda, I. *Acta Cryst.* **1995**, *C51*, 2344. (t) Tenon, J.A.; Carles, M.; Aycard, J.-P. *Acta Cryst.* **1995**, *C51*, 2603.

15 (a) Tafeenko, V.A.; Popov, S.I.; Medvedev, S.V. *Zh. Strukt. Khim.* **1991**, *32*, 106. (b) Lindeman, S.V.; Antipin, M.Yu.; Struchkov, Yu.T. *Sov. Phys. Crystallogr.* **1988**, *33*, 215. (c) Tafeenko, V.A.; Bogdan, T.V.; Medvedev, S.V.; Kozyrev, A.A.; Popov, S.I. *Zh. Strukt. Khim.* **1991**, *32*, 169. (d) Puranik, V.G.; Tavale, S.S.; Kumbhar, A.S.; Yerande, R.G.; Padhye, S.B.; Butcher, R.J. *J. Cryst. Spectrosc. Res.* **1992**, *22*, 725.

16 Westland, A.D.; Tarafder, M.T.H. *Inorg. Chem.* **1981**, *20*, 3992.

17 (a) Sartorius, J.; Schneider, H.-J. *Chem. Eur. J.* **1996**, *2*, 1446. (b) Beijer, F.H.; Kooijman, H.; Spek, A.L.; Sijbesma, R.P.; Meijer, E.W. *Angew. Chem. Int. Ed.* **1998**, *37*, 75.

18 Hirshfeld, F.L. *Acta Cryst.* **1976**, *A32*, 239.

19 Bellamy, L.J. *The Infra-red Spectra of Complex Molecules*, Third Ed., Chapman and Hall Ltd., London, 1975.

20 Mammen, M.; Simanek, E.E.; Whitesides, G.M. *J. Am. Chem. Soc.* **1996**, *118*, 12614.

21 Pimentel, G.C.; McClellan, A.L. *The Hydrogen Bond*, W.H. Freeman and company, San Francisco, 1960, Chapter 4 (Part I).

22 (a) Cheng, X.; Gao, Q.; Smith, R.D.; Simanek, E.E.; Mammen, M.; Whitesides, G.M. *J. Org. Chem.* **1996**, *61*, 2204. (b) Russell, K.C.; Leize, E.; Dorsselaer, A.V.; Lehn, J.M. *Angew. Chem., Int. Ed. Engl.* **1995**, *34*, 209.

23 Meng, C.K.; Fenn, J.B. *Org. Mass Spectrom.* **1991**, *26*, 542.

24 Mahmoud, M.R.; El-Samahy, A.A.; El-Gyar, S.A. *Bull. Soc. Chim. Fr.* **1981**, I-424.

25 Salman, S.R.; Kanber, S.K.; Arsalan, L.K. *Spectroscopy Lett.* **1991**, *24*, 1153.

26 Ansar, M.; Al Akoum Ebrik, S.; Mouhoub, R.; Berthelot, P.; Vaccher, C.; Vaccher, M.P.; Flouquet, N.; Caignard, D.H.; Renard, P.; Pirard, B.; Rettori, M.C.; Evrard, G.; Durant, F.; Debaert, M. *Eur. J. Med. Chem.* **1996**, *31*, 449.

27 Wang, R.X.; You, X.Z.; Meng, Q.J.; Mintz, E.A.; Bu, X.R. *Synth. Commun.* **1994**, *24*, 1757.

28 Sheldrick, G.M. *Acta Cryst.* **1990**, *A46*, 467.

Chapter 3

A Vanadium Diamidate Complex as Model System for Vanadium Bromoperoxidase

3.1 Vanadium haloperoxidases

As was described in Chapter 1, haloperoxidases are enzymes that catalyse the oxidation of halides using hydrogen peroxide.[1,2] Although the majority of these enzymes in terrestrial systems contain the FeHeme unit, haloperoxidases which contain vanadate in their active site predominate in marine algae systems. Since the discovery in 1983 by Vilter[3] of the first vanadium containing bromoperoxidase (V-BrPO) isolated from the marine brown alga *Ascophyllum nodosum*, several vanadium haloperoxidases have been isolated and studied.[4,5] Many of these enzymes have been detected in brown and red seaweeds,[6] whereas some of them have been found in terrestrial fungi.[5k] Investigations concerning the coordination environment around vanadium were performed on the native enzyme as well as on the reduced V(IV) form *e.g.* using X-ray absorption measurements, EPR spectroscopy, and ^{51}V NMR spectroscopy.[7] Furthermore, to get a better understanding of the working mechanism of the enzyme and to determine the role of vanadium, many functional mimics for V-BrPO were developed.[8]

3.2 Functional mimics for V-BrPO

The first reported fully functional mimic of V-BrPO is *cis*-dioxovanadium(V) (VO_2^+) in acidic aqueous solution (Figure 3.1).[9]

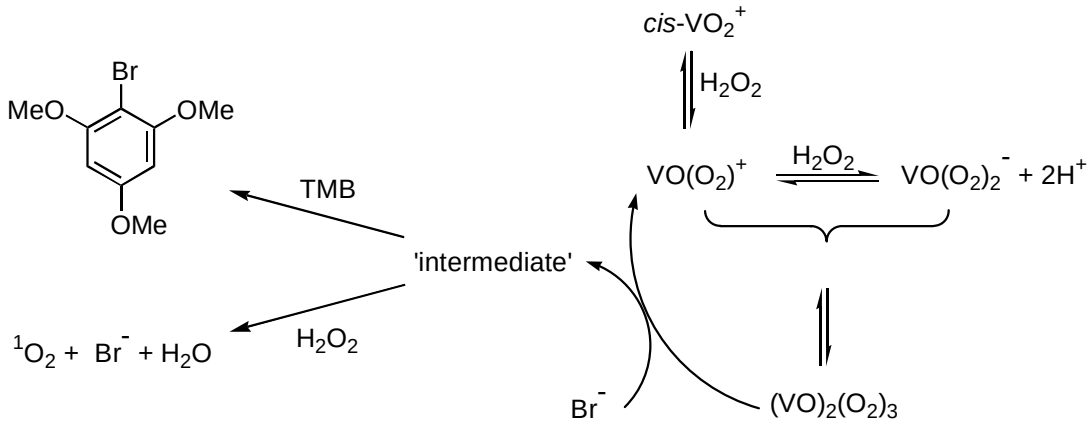

Scheme 3.1 *Bromination activity of the V-BrPO mimic cis-dioxovanadium(V).*[9]

Cis-dioxovanadium(V) is shown to catalyse the bromination of 1,3,5-trimethoxybenzene (TMB) as well as the bromide-mediated disproportionation of H_2O_2.[10] In a first step, H_2O_2 is complexed giving red oxoperoxo [$VO(O_2)^+$] and yellow oxodiperoxo [$VO(O_2)_2^-$] complexes.[11] The ratio between these two species depends on the H_2O_2 concentration and the pH. In a second step these complexes combine, yielding dioxotriperoxodivanadium(V) [$(VO)_2(O_2)_3$], which is considered to be the actual oxidant. Contrary to natural haloperoxidases, *cis*-dioxovanadium(V) only functions at low pH (2 or less), because at lower acid concentrations the amount of monoperoxovanadate is insufficient for dimerisation to occur to [$(VO)_2(O_2)_3$]. Another difference with the enzyme is the low rate of catalysis[9] indicating the importance of the protein environment around the active site. Therefore, in recent years several vanadium complexes of multidentate ligands containing O and N donor sites (depicted in Figure 3.1) were tested for catalysis of bromide oxidation.[8]

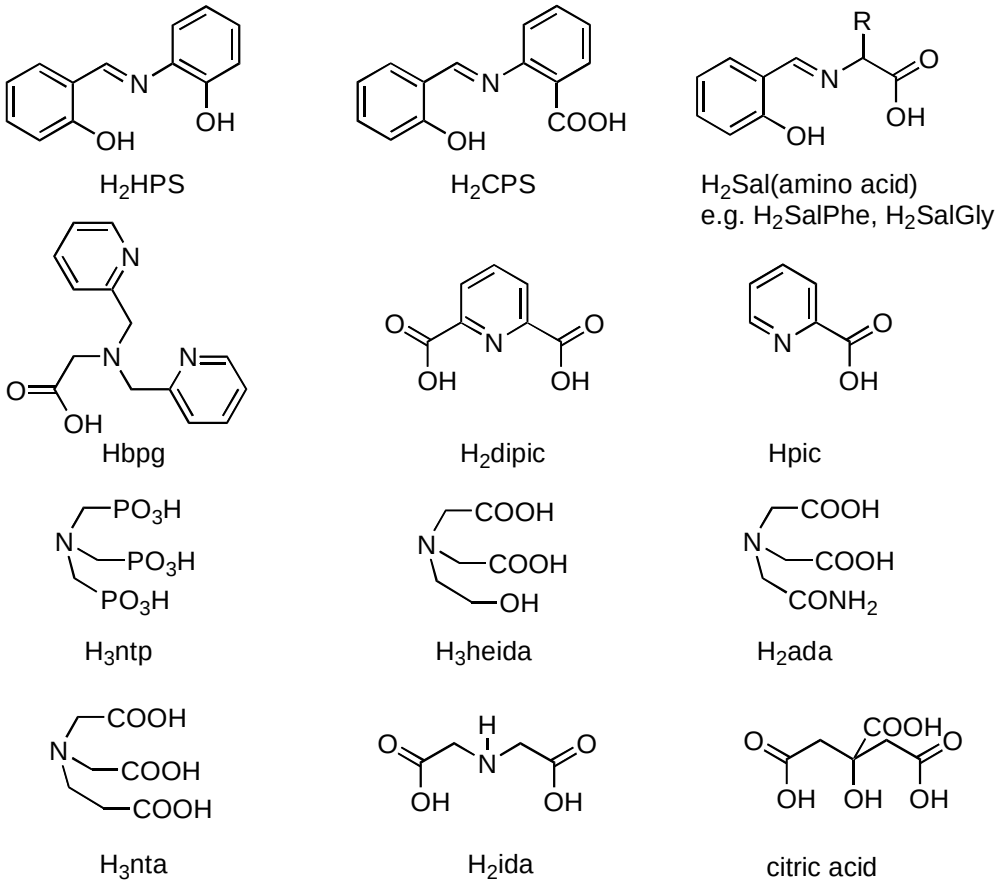

Figure 3.1 *Ligands whose V(V) complexes have been tested for catalysis of bromide oxidation.*[8]

The complexes tested in the biomimetic bromination reaction can be divided into three classes: (i) active catalysts in which the ligand remains coordinated to vanadium.

(ii) complexes with a ligand which effectively stabilises the formed peroxo intermediate, leading to inactive compounds.

(iii) complexes which lose their ligand by reaction with H_2O_2 under the applied conditions.

Ligands that yield active functional model systems for V-BrPO include Schiff base ligands derived from salicylideneamino acid (H_2SalPhe, H_2SalGly)[12], an imine of salicylaldehyde (H_2HPS)[13], iminodiacetic acid (H_2ida)[14], nitrilotriacetic acid (H_3nta) [14], citric acid,[8c] and a few tripodal amine ligands (H_3heida, H_2ada, Hbpg).[14] However, for instance pyridine-2,6-dicarboxylic acid (H_2dipic) stabilises the peroxo adduct of the corresponding vanadium(V) compound. Therefore, no oxidation of bromide is observed. Examples of complexes that are not stable under the applied reaction conditions are the corresponding vanadium(V) compounds of carboxyphenylsalicylideneamine (H_2CPS)[8], pyridine-2-carboxylic acid (Hpic),[8b] and nitrilotriphosphoric acid (H_3ntp).[8c] These ligands dissociate from the metal ion in the presence of acid and H_2O_2.

The best studied V-BrPO mimic is the oxovanadium(V) complex of hydroxyphenyl-salicylideneamine [(HPS)VO(OEt)(EtOH)] (Scheme 3.2).[13]

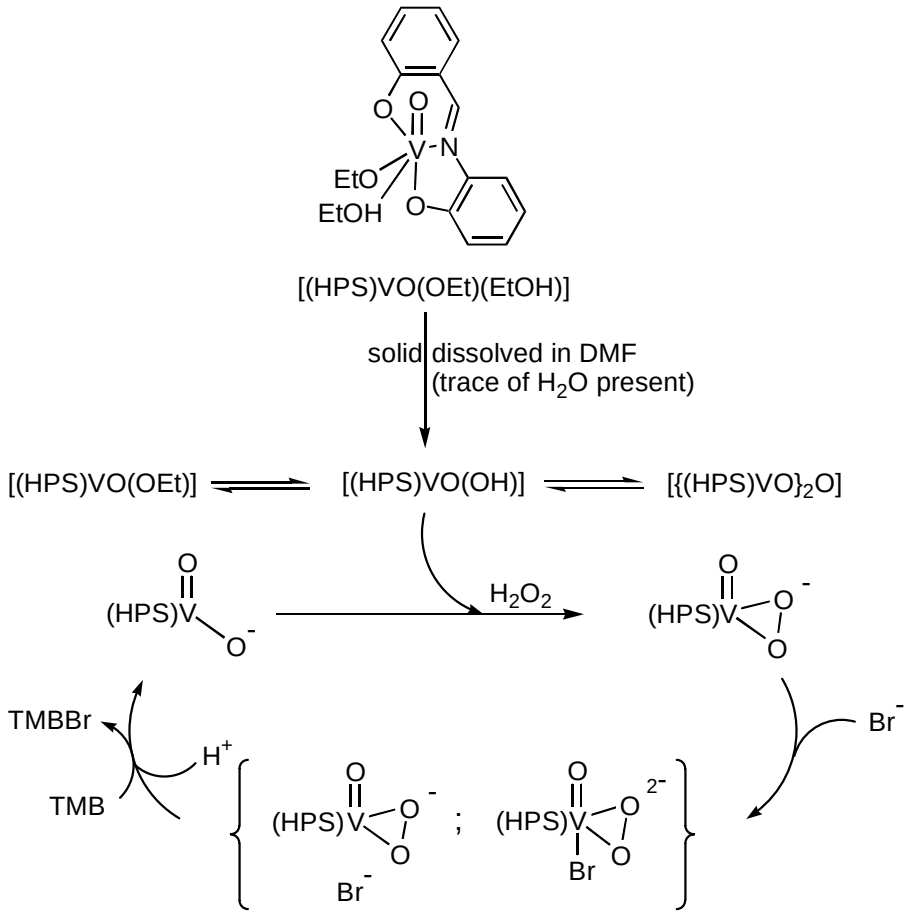

Scheme 3.2 *Proposed mechanism for bromide oxidation by H_2O_2 catalysed by (HPS)VO(OH).*

The bromination experiments with [(HPS)VO(OEt)(EtOH)] are performed in DMF solution. Several vanadium species are formed as was identified by ^{51}V NMR spectroscopy.[8,13] Upon addition of H_2O_2, a single oxoperoxovanadium(V) complex [(HPS)VO(O_2)$^-$] is formed. Subsequently addition of bromide affords one turnover towards

a two-electron oxidised form (*e.g.* HOBr, Br_2, Br_3^-, or V-OBr), which in the presence of trimethoxybenzene (TMB) yields one equivalent of the brominated product TMBBr (2-bromo-1,3,5-trimethoxybenzene). It is still not clear whether the Br^- is bound directly to vanadium, which is then followed by oxidation by the vanadium peroxo complex, or that there is a nucleophilic attack by Br^- on the coordinated peroxide, giving rise to bound ^-OBr. The formed intermediate, however, is subject to rapid equilibration with HOBr, Br_2, and Br_3^-, since the presence of Br_3^- was spectroscopically established. The brominiation reaction becomes catalytic when acid is used in at least stoichiometric quantities with respect to H_2O_2.

Other examples of well-studied V-BrPO mimics are several vanadyl [$V(IV)O^{2+}$] complexes with oxalate, glutarate, succinate, malonate, and acetate ligands by Sakurai and Tsuchiya.[15] The mechanism they propose includes the formation of a V(IV) intermediate, which is distinct from the mechanism proposed for vanadium haloperoxidases. The V(IV) state for the enzyme could not be detected using EPR spectroscopy and therefore it was assumed that this type of intermediate does not play a role in the catalytic cycle of the enzyme.[5f,16,17]

3.3 Vanadium chloroperoxidase

In 1996, the crystal structure of an azide containing vanadium chloroperoxidase (V-ClPO) isolated from the fungus *Curvularia inaequalis* was reported by Messerschmidt and Wever and based on this analysis some of the unresolved questions were answered at once.[18] For instance, the vanadate moiety proved to be five-coordinated rather than six-coordinated as was originally proposed.[19] In 1997, the X-ray structure of the peroxide form of the chloroperoxidase enzyme was published.[20] Schematic representations of the active sites of the native form as well as the peroxide form are given in Chapter 4. The proposed catalytic mechanism is depicted in Scheme 3.3.[20]

The apical hydroxy unit is hydrogen bonded to a histidine residu (His_{404}) in a protein environment. This hydrogen bond makes the ^-OH group more nucleophilic. When a peroxide molecule approaches the active site, the ^-OH unit is protonated and ^-OOH is generated. The weakly ligated water molecule dissociates from the vanadium ion and a side-on bound peroxide intermediate is formed after the departure of another water molecule. Subsequently, attack of a chloride ion at one of the peroxo atoms and the uptake of a proton from a surrounding water molecule leads to the generation of hypochlorous acid (HOCl) and restoration of the native state.

At higher acid concentrations, the halogenation activity was inhibited. It was assumed that this is due to protonation of His_{404}.[20] As a result, the formation of the peroxide form does not occur, since it is now impossible for the histidine residue to form a hydrogen bond to the apical OH group. As a consequence, this hydroxy unit loses its ability to activate the H_2O_2 by deprotonation and therefore the peroxide can not be bound to the vanadium ion.

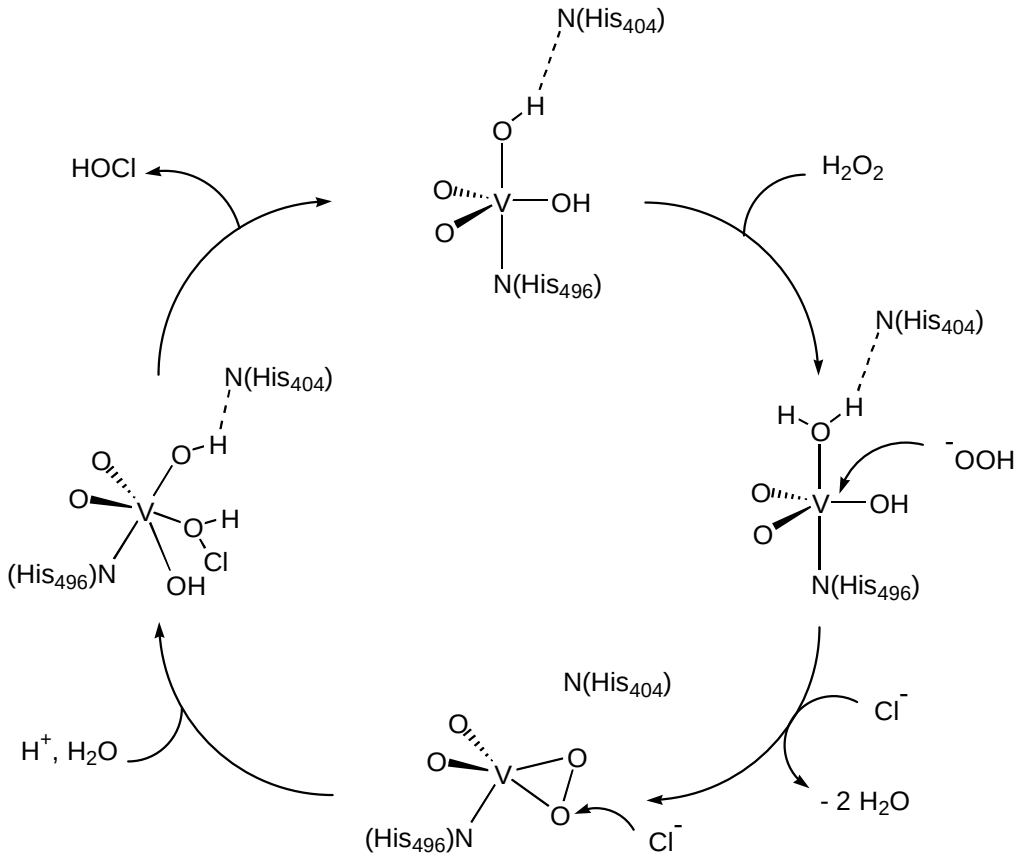

Scheme 3.3 *Proposed catalytic mechanism of V-ClPO.*[20]

3.4 Synthesis of a vanadium(IV) diamidate complex

In the literature, several vanadium complexes with amidate ligands are known which are used as model systems to study vanadium-protein interactions.[21,22] However, these type of compounds were never tested as mimics for V-BrPO. Therefore, we prepared vanadium(IV) diamidate complex **3.1** according to a literature procedure[21] and used it as a catalyst in the bromination reaction of trimethoxybenzene.

Ligand H_4hybeb (1,2-bis(2-hydroxybenzamido)benzene)[21] for the synthesis of **3.1** was obtained by condensation of 1,2-phenylenediamine with acetylsalicyloyl chloride in dioxane solution (Scheme 3.4). Deprotection of the acetyl groups was achieved by adding a small amount of concentrated HCl to a dioxane solution of the ligand. The oxovanadium(IV) complex of **3.1** was easily obtained by refluxing a methanol solution of H_4hybeb and vanadyl acetylacetonate [$VO(acac)_2$] in the presence of two equivalents of sodium hydroxide under an argon atmosphere.[21] The product was obtained by crystallisation from a MeOH-Et_2O mixture as green crystals.

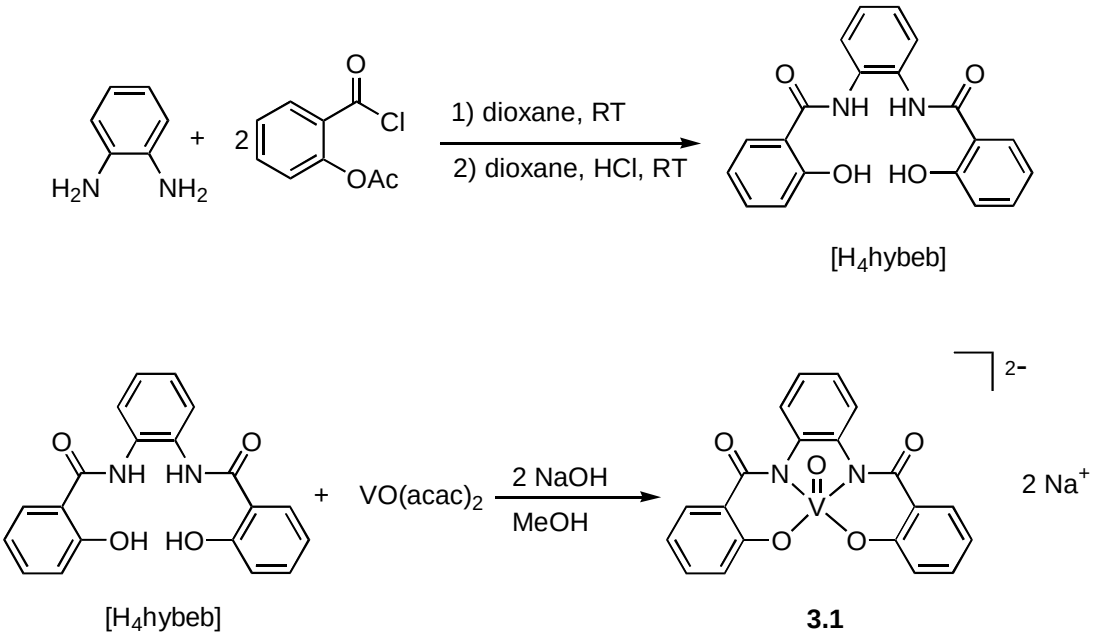

Scheme 3.4 *Synthesis of the vanadium(IV) bisamide complex **3.1**.*[21]

The negative electrospray mass (ES / MS) spectrum[23] of **3.1** recorded in acetonitrile showed peaks at *m* / *z* 206, 412, and 434, which correspond to {[(hybeb)V(IV)O]$^{2-}$}, {[(hybeb)V(IV)O]$^{2-}$ + 1H^{+}} and {[(hybeb)V(IV)O]$^{2-}$ + 1Na^{+}}, respectively. However, the positive ion spectrum recorded in MeOH showed major peaks at *m* / *z* 457, 480, and 413 which are attributed to {[(hybeb)V(V)O]$^{-}$ + 2Na^{+}}, {[(hybeb)V(IV)O]$^{2-}$ + 3Na^{+}} and {[(hybeb)V(V)O]$^{-}$ + 2H^{+}}. Obviously, the vanadium(IV) ion is oxidised to V(V) under these conditions. Indeed, this oxovanadium(V) complex could be easily prepared by oxidation of **3.1** using silver nitrate in acetonitrile.[21] $NaNO_3$ and Ag which precipitated from the reaction mixture were filtered off and the vanadium(V) complex **3.2** was obtained as a dark blue powder after addition of Et_2O. In the ES / MS spectrum of **3.2** recorded in acetonitrile, one parent peak at *m* / *z* 411 was present which can be assigned to {[(hybeb)V(V)O]$^{-}$}. Also the ^{1}H NMR spectrum recorded in dimethylformamide-d_7 is in agreement with this assignment, since no phenolic or amidate hydrogens were observed. The ^{51}V NMR spectrum (in DMF-d_7) showed a single resonance at -472 ppm (band width, b.w. = 197 Hz).

The UV spectrum of the green complex **3.1** recorded in DMF displays bands at 266 nm (ε = 1.7 x 10^{4} M^{-1} cm^{-1}) and at 320 nm ((ε = 1.6 x 10^{4} M^{-1} cm^{-1}), whereas the blue complex **3.2** shows one band at 592 nm (ε = 7.6 x 10^{3} M^{-1} cm^{-1}).

The stability of complex **3.1** in the presence of H_2O_2 was investigated using ^{51}V NMR measurements. Because **3.1** is paramagnetic due to the +4 oxidation state of the vanadium ion, no signal was observed, but after addition of H_2O_2, one peak at –726 ppm (b.w. = 258 Hz) appeared (CD_3CN was used as the solvent). This signal was attributed to a peroxodiamidatevanadium(V) species, since it is known that often a signal for (diperoxo)vanadium(V) arises at –585 ppm when the ligand dissociates from the metal.[8c]

Even after 30 min, the formation of dissociation products was not detected. Therefore it was assumed that the complex remains intact under the applied reaction conditions.

3.5 Bromination reactions

In order to examine halide oxidation catalysed by **3.1**, the complex was tested in the bromination reaction of TMB, which is frequently used as a model substrate (Scheme 3.5).[8,9,13] Hydrogen peroxide (30% in water) was used as the oxidant and tetrabutylammonium bromide (Bu_4NBr) as the bromide source. Dimethylformamide was used as the solvent, since we found that in that case only 2-bromo-1,3,5-trimethoxybenzene [TMBBr] was obtained. When *e.g.* a mixture of EtOAc and DMF was used, dibrominated 2,4-bromo-1,3,5-trimethoxybenzene [$TMBBr_2$] was formed as well. In a typical experiment, 10 mM of TMB and 50 mM of Bu_4NBr were used. The reactions were performed under an argon atmosphere because it is known that the complex is hydrolysed when both water and air are present.[21] The progress of the reaction was monitored by GC. The addition of acid (HCl) was necessary for the reaction to proceed (*vide infra*). No chlorination products were observed. The results are summarised in Table 3.1.

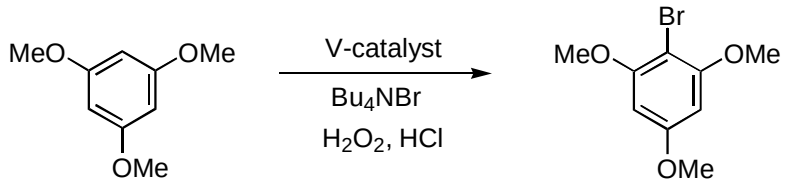

Scheme 3.5 *Vanadium catalysed bromination of 1,3,5-trimethoxybenzene.*

Table 3.1 *Catalytic oxidation experiments using TMB. Reactions were performed using 10 mM TMB and 50 mM Bu_4NBr. Amounts of product (determined with GC) are given in mM.*

	[H_2O_2]	**[H^+]**	**[cat]**	**[TMBBr] 1h**	**[TMBBr] 3h**	**t.o.n.**[a]
a	4	0	0.25	0	0	0
b	10	0	0.25	0	0	0
c	4	2	0	0	0.7	-
d	10	8	0	1.8	3.5	-
e	4	2	0.25	1.6	1.7	7
f	6	4	0.25	3.3	3.4	14
g[b]	8	6	0.25	4.7	4.9	20
h[b]	10	8	0.25	6.2	6.4	26
i	6	4	0.025	1.9	3.7	148
j	10	8	0.025	2.4	4.9	196

(a) t.o.n. = mol product / mol catalyst. (b) After 2h, an additional 0.05 ml of H_2O_2 was added.

From entries *a* and *b* in Table 3.1 it is clear that no product was obtained in the absence of acid in contrast to the stoichiometric reaction found for [(HPS)VO(OEt)(EtOH)].[13] Furthermore, it must be emphasised that the blank reaction (entry *d*) is already fast when 8 mM of HCl is applied (3.5 mM of brominated product is generated after 3 hours). The best result was obtained with 10 mM of TMB and 8 mM HCl where 62% conversion towards TMBBr (*i.e.* 6.2 mM) was reached after one hour (with a blank reaction of 18%). Since the reactions as described in entries *g* and *h* show no further conversion after 90 min, an additional amount of H_2O_2 (0.05 ml) was added after two hours. However, no significant increase in conversion was observed, indicating that the catalyst is no longer active.

3.6 Comparison

Because unligated vanadium(v) already is an effective catalyst in the bromination reaction (Scheme 3.5),[24] the results obtained for **3.1** were compared with those of commercially available $VO(acac)_2$. This reagent was chosen for this purpose because it is readily soluble in DMF. Other reagents like sodium vanadate or ammonium vanadate are only soluble in wet DMF. The best model system known to date, [(HPS)VO(OEt)(EtOH)], was also tested for comparison under the same reaction conditions. Table 3.2 summarises the results using 0.025 mM and 0.25 mM of catalyst, 10 mM TMB, 10 mM H_2O_2, 8 mM HCl, and 50 mM Bu_4NBr.

Table 3.2 *Comparison of **3.1** with [(HPS)VO(OEt)(EtOH)] and $VO(acac)_2$ in the bromination of TMB using 10 mM TMB, 10 mM H_2O_2, 8 mM HCl, and 50 mM Bu_4NBr.*

	[Catalyst] (mM)	[TMBBr] 0.5h	[TMBBr] 1h	[TMBBr] 2h	[TMBBr] 3h	[TMBBr] 4h
3.1	0.025	1.5	2.4	4.0	5.2	6.2
(HPS)VO(OEt)(EtOH)	0.025	1.8	2.6	4.4	5.7	6.8
$VO(acac)_2$	0.025	1.7	2.5	4.3	5.6	6.7
3.1	0.25	4.8	6.2	6.2	6.4[a]	6.4
(HPS)VO(OEt)(EtOH)	0.25	5.1	7.7	7.9	8.1[a]	8.2
$VO(acac)_2$	0.25	3.6	3.7	3.8	4.5[a]	4.6

(a) After 2h, an additional 0.05 ml of H_2O_2 was added.

In all cases, the only observed product was 2-bromo-1,3,5-trimethoxybenzene (TMBBr). When 0.025 mM of catalyst was used, no significant difference in activity was observed between $VO(acac)_2$ and [(HPS)VO(OEt)(EtOH)], whereas complex **3.1** is only slightly less active. When on the other hand 0.25 mM of catalyst was applied, $VO(acac)_2$ proved to be inferior to the other two catalysts, in particular at the beginning of the reaction. When after two hours an additional amount of H_2O_2 was added, the conversion increased from 3.8 mM

to 4.5 mM TMBBr, whereas in the other cases the amount of product remained nearly the same. Complex **3.1** is not quite as active as [(HPS)VO(OEt)(EtOH)] when 0.25 mM of the catalyst is used, although the two catalysts, as already mentioned, are almost equally active at a concentration of 0.025 mM. Preliminary experiments using **3.2** as the catalyst show similar results as for **3.1**.

3.7 Discussion and conclusions

Since it was not indisputably proven by the ^{51}V NMR experiments described in Chapter 3.4 that the ligand of **3.1** remains coordinated to the metal centre during the reaction and that the bromination is not catalysed by a small amount of unligated vanadium(V), the reaction was followed by UV-Vis spectroscopy. It was shown that the ligand only very slowly dissociates from the metal ion in the presence of H_2O_2 (after 24 h complete dissociation had occurred). A vanadium species with an absorption maximum around 590 nm is then generated (Figure 3.2). After addition of acid to a solution of **3.1** and H_2O_2 in DMF, however, the absorptions for the ligand [H_4hybeb] were instantly observed.

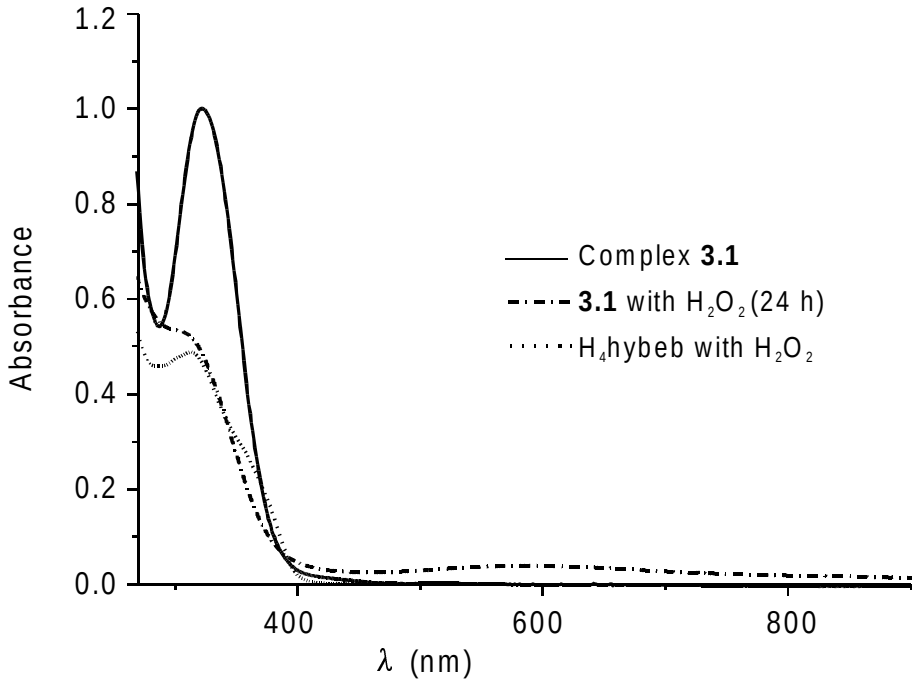

Figure 3.2 *UV-Vis spectrum recorded in DMF of **3.1** and **3.1** 24 h after the addition of H_2O_2, compared to the spectrum of the ligand (H_4hybeb) in the presence of H_2O_2.*

Upon dissociation of the complex, the ligand $[hybeb]^{4-}$ probably becomes protonated to form H_4hybeb, which supposedly can not bind to the vanadium centre. Therefore, the observed catalysis is presumably accomplished by the generated bare vanadium(V) species.

The nature of this vanadium(V) species was not investigated. However, preliminary ^{51}V NMR measurements with **3.2** in the presence of excess H_2O_2 in CD_3CN suggest that $[(VO)_2(O_2)_3]$ may be responsible for the catalytic activity, because a resonance at -670 ppm (b.w. = 361 Hz) is observed after a few minutes. This signal was attributed to the binuclear oxovanadium(V) triperoxo species $[(VO)_2(O_2)_3]$ by comparison with literature data.[8b,25] The bromination activity using **3.1** or **3.2** as the catalyst is identical, which suggests that the catalysis is achieved by the same vanadium species. Although this signal was not observed in the ^{51}V NMR spectrum of **3.1** and H_2O_2 (*vide supra*), it is highly conceivable that after addition of acid also in this case the triperoxo species is formed.

For [(HPS)VO(OEt)(EtOH)] an extensive study on the stability of the complex in the presence of H_2O_2 and acid ($HClO_4$) is described in literature.[13] UV-Vis and ^{51}V NMR spectroscopy experiments show that in this case the ligand $[HPS]^{2-}$ remains bound to the vanadium(V) centre under the applied conditions.

Although the experiments with **3.1** show that the ligand (H_4hybeb) probably does not play a role and that the catalysis is accomplished by an unligatedvanadium(V) species, a few conclusions can be drawn from this work and the literature data described above. It appears that unligated vanadium reagents are often almost as active or even more active than ligated complexes. Furthermore, because of the acid dependency of the bromination reaction, already a fairly fast blank reaction has to be overcome. Moreover, these harsh reaction conditions may easily cause the dissociation of the ligand. It appears that only ligands containing two or three donor oxygen atoms yield vanadium complexes which are likely to be stable under the reaction conditions. However, although *e.g.* **3.1** and $[H_2CPS]$[8,13] fulfill these requirements, they dissociate upon addition of H_2O_2 and acid. On the other hand, the tripodal amine ligand [Hbpg][14] which contains two pyridine nitrogen donors and only one oxygen donor atom, proved to be an active functional bromoperoxidase mimic. Therefore it can be concluded that the search for a ligand system that provides a robust catalyst capable of approaching the enzyme in reaction rate and selectivity remains a difficult task.

3.8 Experimental section

3.8.1 General information

For general information see Chapter 2. GC analyses were performed on a Hewlett Packard 6890 Gas Chromatograph using a HP-1 dimethylpolysiloxane column. Calibration was performed using authentic samples of 1,3,5-trimethoxybenzene (TMB), 2-bromo-1,3,5-trimethoxybenzene (TMBBr),[26] and 2,4-dibromo-1,3,5-trimethoxybenzene ($TMBBr_2$)[26] and independent samples of further byproducts. Conversions and yields were determined using hexadecane as internal standard, and calculated using the Chemstation software. $VO(acac)_2$ was obtained from Aldrich and was used as received. Methanol was distilled over magnesium methoxide, acetonitrile and dimethylformamide were distilled over calcium hydride, diethyl ether was distilled from phosphorus pentoxide and 1,4-dioxane was dried over molecular sieves. Ligand H_4hybeb[21] and the complexes **3.1**[21], **3.2**,[21] and

[(HPS)VO(OEt)(EtOH)][13] were prepared using exactly the same procedures as described in the literature. Synthesis of the complexes was performed under an atmosphere of argon using standard Schlenk techniques. ^{51}V-NMR spectra were recorded on a Varian VXR-300 spectrometer (relative to $\delta(VOCl_3) = 0$ ppm).

3.8.2 Catalytic oxidations

The bromination reactions were performed in dimethylformamide as solvent, under an argon atmosphere at room temperature. Typical procedure: to 2 ml of a stock solution in DMF of TMB (40 mM), Bu_4NBr (0.2 M) and a known amount of hexadecane were consecutively added the required amounts (see Table 3.1) of a stock solution of H_2O_2 (16 mM), DMF in order to attain a total reaction volume of 8 ml (when all the ingredients are added) and a stock solution of HCl (16 mM). The stock solutions of H_2O_2 and HCl were prepared by dilution of respectively 30% and 37% aqueous solutions with DMF to 16 mM. Immediately after addition of the acid, 1 ml of a stock solution of the catalyst (2 mM or 0.2 mM) was added. The reaction was monitored by GC.

3.8.3 Syntheses

[V(IV)O(hybeb)][Na$_2$] (3.1) The complex was prepared according to a literature procedure.[21] ES / MS (CH_3CN) *m/z* 206 ($M - 2Na^+$), 412 ($M - 2Na^+ + 1H^+$), 434 ($M - 1Na^+$); ES / MS (CH_3OH) *m/z* 457 ([(hybeb)V(V)O]$^-$ + $2Na^+$), 480 ([(hybeb)V(IV)O]$^{2-}$ + $3Na^+$), 413 ([(hybeb)V(V)O]$^-$ + $2H^+$); λ_{max}(DMF) 266 nm ($\varepsilon = 1.7 \times 10^4$ M^{-1} cm^{-1}), 320 ($\varepsilon = 1.6 \times 10^4$ M^{-1} cm^{-1}).

[V(V)O(hybeb)][Na] (3.2) The complex was prepared according to a literature procedure.[21] ^{1}H NMR (DMF-d_7) 8.31-8.11 (m, 4H), 7.59-7.54 (m, 2H), 7.16-7.10 (m, 4H), 6.98 (d, 2H, J = 8.4 Hz; ^{51}V NMR (DMF-d_7) –472 (b.w. = 197 Hz) ES / MS (CH_3CN) *m/z* 411 ([V(V)O(hybeb)]$^-$); λ_{max}(DMF) 592 nm ($\varepsilon = 7.6 \times 10^3$ M^{-1} cm^{-1}).

3.9 References

1 Butler, A. *Coord. Chem. Rev.* **1999**, *187*, 17.

2 Butler, A.; Walker, J.V. *Chem. Rev.* **1993**, *93*, 1937.

3 Vilter, H. *Phytochemistry* **1984**, *23*, 1387.

4 Vilter, H. *Met. Ions Biol. Syst.* **1995**, *31*, 325.

5 See for instance (a) De Boer. E.; Plat, H.; Tromp, M.G.M.; Wever, R.; Franssen, M.C.R.; Van der Plas, H.C.; Meijer, E.M.; Schoemaker, H.E. *Biotechnol. Bioeng.* **1987**, *30*, 607. (b)

Plat, H.; Krenn, B.E.; Wever, R. *Biochem. J.* **1987**, *248*, 277. (c) Krenn, B.E.; Tromp, M.G.M.; Wever, R. *J. Biol. Chem.* **1989**, *264*, 19287. (d) Everett, R.R.; Butler, A. *Inorg. Chem.* **1989**, *28*, 395. (e) Everett, R.R.; Kanofsky, J.R.; Butler, A. *J. Biol. Chem.* **1990**, *265*, 4909. (f) Tromp, M.G.M.; 'Olafsson, G.; Krenn, B.E.; Wever, R. *Biochim. Biophys. Acta* **1990**, *1040*, 192. (g) Everett, R.R.; Soedjak, H.S.; Butler, A. *J. Biol. Chem.* **1990**, *265*, 15671. (h) Soedjak, H.S.; Butler, A. *Biochem.* **1990**, *29*, 7974. (i) Soedjak, H.S.; Butler, A. *Biochim. Biophys. Acta* **1991**, *1079*, 1. (j) Knüttel, K.; Müller, A.; Rehder, D.; Vilter, H.; Wittneben, V. *FEBS Lett.* **1992**, *302*, 11. (k) Van Schijndel, J.W.P.M.; Vollenbroek, E.G.M.; Wever, R. *Biochim. Biophys. Acta* **1993**, *1161*, 249. (l) Tschirret-Guth, R.A., Butler, A. *J. Am. Chem. Soc.* **1994**, *116*, 411. (m) Coughlin, P.; Roberts, S.; Rush, C.; Willetts, A. *Biotechnol. Lett.* **1993**, *15*, 907. (n) Soedjak, H.S.; Walker, J.V.; Butler, A. *Biochem.* **1995**, *34*, 12689. (o) Weyand, M.; Hecht, H.-J.; Vilter, H.; Schomburg, D. *Acta Cryst.* **1996**, *D52*, 864. (p) Rao, A.V.S.; Ravishankar, H.N.; Ramasarma, T. *Arch. Biochem. Biophys.* **1996**, *334*, 121. (q) Căsný, M.; Rehder, D.; Schmidt, H.; Vilter, H.; Conte, V. *J. Inorg. Biochem.* **2000**, *80*, 157.

6 (a) Butler, A. in *Bioinorganic Catalysis*, Reedijk, J. Ed., Marcel Dekker, New York, **1993**, chapter 13. (b) Wever, R.; Hemrika, W. in *Vanadium in the Environment, Part One: Chemistry and Biochemistry*, Nriagu, J.O., Ed., John Wiley & Sons, New York, **1998**, Chapter 12.

7 Clague, M.J.; Butler, A. in *Advanced Inorganic Biochemistry, Part Nine: Models in Inorganic Chemistry*, Eichhorn, G.L.; Marzilli, L.G., Eds., PTR Prentice-Hall, Inc., New Jersey, **1994**, Chapter 6.

8 (a) Butler, A. in *Bioinorganic Catalysis*, Second Ed.; Reedijk, J.; Bouwman, E., Eds.; Marcel Dekker, Inc., New York, **1999**, Chapter 5. (b) Butler, A.; Baldwin, A.H. *Structure and Bonding*, Sadler, P.; Hill, H.A.O.; Thompson, A., Eds., **1997**, *89*, 109. (c) Butler, A.; Clague, M.J. *Adv. Chem. Ser.* **1995**, *246* (*Mechanistic Bioinorganic Chemisty*, Thorp, H.H.; Pecoraro, V.L., Eds.), 329.

9 De la Rosa, R.; Clague, M.J.; Butler, A. *J. Am. Chem. Soc.*, **1992**, *114*, 760.

10 See Chapter 1.

11 Campbell, N.J.; Dengel, A.C.; Griffith, W.P. *Polyhedron* **1989**, *8*, 1379.

12 (a) Perrin, C.L.; Dwyer, T.J. *Chem. Rev.* **1990**, *90*, 935. (b) Crans, D.C.; Holst, H.; Rehder, D. *Inorg. Chem.* **1995**, *34*, 2524.

13 Clague, M.J.; Keder, N.L.; Butler, A. *Inorg. Chem.* **1993**, *32*, 4754.

14 (a) Colpas, G.J.; Hamstra, B.J.; Kampf, J.W.; Pecoraro, V.L. *J. Am. Chem. Soc.* **1996**, *118*, 3469. (b) Colpas, G.J.; Hamstra, B.J.; Kampf, J.W.; Pecoraro, V.L. *J. Am. Chem. Soc.* **1994**, *116*, 3627.

15 Sakurai, H.; Tsuchiya, K. *FEBS Lett.* **1990**, *260*, 109.

16 Butler, A.; Carrano, C.J. *Coord. Chem. Rev.* **1991**, *109*, 61.

17 Küsthardt, U.; Hedman, B.; Hodgson, K.O.; Hahn, R.; Vilter, H. *FEBS Lett.* **1993**, *329*, 5.

18 Messerschmidt, A.; Wever, R. *Proc. Natl. Acad. Sci. USA* **1996**, *93*, 392.

19 (a) Carrano, C.J.; Mohan, M.; Holmes, S.M.; De la Rosa, R.; Butler, A.; Charnock, J.M.; Garner, C.D. *Inorg. Chem.* **1994**, *33*, 646. (b) Arber, J.M.; De Boer, E.; Garner, C.D.; Hasnain, S.S.; Wever, R. *Biochem.* **1989**, *28*, 7968.

20 Messerschmidt, A.; Prade, L.; Wever, R. *Biol. Chem.* **1997**, *378*, 309.

21 Keramidas, A.D.; Papaioannou, A.B.; Vlahos, A.; Kabanos, T.A.; Bonas, G.; Makriyannis, A.; Rapropoulou, C.P.; Terzis, A. *Inorg. Chem.* **1996**, *35*, 357.

22 (a) Vlahos, A.T.; Tolis, E.I.; Raptopoulou, C.P.; Tsohos, A.; Sigalas, M.P.; Terzis, A.; Kabanos, T.A. *Inorg. Chem.* **2000**, *39*, 2977. (b) Cornman, C.R.; Zovinka, E.P.; Boyajian, Y.D.; Geiser-Bush, K.M.; Boyle, P.D.; Singh, P. *Inorg. Chem.* **1995**, *34*, 4213. (c) Vlahos, A.T.; Kabanos, T.A.; Raptopoulou, C.P.; Terzis, A. *Chem. Commun.* **1997**, 269. (d) Kabanos, T.A.; Keramidas, A.D.; Papaioannou, A.B.; Terzis, A. *J. Chem. Soc., Chem. Commun.* **1993**, 643.

23 In the literature (ref 21) only the elemental analyses of **3.1** and **3.2** were reported.

24 Crans, D.C.; Willging, E.M.; Butler, S.K. *J. Am. Chem. Soc.* **1990**, *112*, 427.

25 Clague, M.J.; Butler, A. *J. Am. Chem. Soc.* **1995**, *117*, 3475.

26 Vogel's Textbook of Practical Organic Chemistry, Fourth Edition, Longman Inc., New York, 1978, p. 725.

Chapter 4

Development of New Ligand Systems for Vanadium

4.1 Dinuclear vanadium compounds

Besides the development of functional mimics for vanadium haloperoxidases as described in the previous chapter, the synthesis of new oxidation catalysts is of current interest. In the design of new catalytically active complexes, the choice of the ligand is of major importance. The coordination environment determines the nature of the metal ions which can be incorporated, and the electronic properties of the metal centre. Furthermore, the ligand must provide a well-defined environment in which the metal is readily incorporated.

In recent years, dinuclear metal complexes have attracted considerable attention. This interest stems from biochemistry, where several metalloenzymes and metalloproteins that contain two metal ions in their active site show high catalytic activity.[1,2] Due to cooperation of the two metal ions in the catalytic reaction, a higher activity and selectivity can be achieved. Prominent examples of these kind of enzymes include the non-heme diiron containing enzyme methane monooxygenase (MMO), which selectively oxidises methane to methanol using dioxygen,[3] and manganese catalase,[4] a dinuclear manganese containing enzyme which decomposes hydrogen peroxide. Another example is the dinuclear copper enzyme tyrosinase[5] which uses dioxygen in the hydroxylation of monophenols to *o*-diphenols and for the two-electron oxidation of *o*-diphenols to *o*-quinones. Many model systems for these enzymes have been developed and the synthesis of new dinuclear complexes has become popular as well. For this purpose a variety of new polydentate ligands capable of simultaneously binding two metal ions, so-called dinucleating ligands, have been designed.[6,7] Since 1970, the research towards these ligands and their related complexes have increased significantly, and several review articles have been published on this subject.[1,8] An excellent example of a dinuclear catalyst which exhibits higher regioselectivity and reactivity then the related mononuclear system by bimetallic cooperation is the dirhodium complex as developed by Stanley *et al.* for the hydroformylation of *a*-olefins.[9]

Also several dinuclear vanadium complexes have been prepared and characterised.[10] Two examples are depicted in Scheme 4.1. In the first one, a dinuclear vanadium(III) complex was synthesised from a heptadentate ligand (dpot, 2-oxo-1,3-diaminopropane-*N*,*N*,*N'*,*N'*-tetraacetate) containing a bridging alkoxo group using VCl_3.[11] The metal centres adopt a distorted octahedral structure and the carboxylato group of *m*-hydroxybenzoate (*m*-hbza) bridges between the vanadium ions. Variable-temperature susceptibility measurements show that the two vanadium(III) centres are ferromagnetically coupled. In the second example dinucleating tetraaminodiphenol macrocyclic ligand [tadp] was used and a dinuclear oxovanadium(IV) complex was obtained after treatment with $VO(SO_4)\cdot xH_2O$ and

Et_3N in boiling methanol solution (Scheme 4.1).[12] The two octahedral vanadium centres are bridged by sulfate and have *syn* oxo configuration. The two metal centres exhibit a fairly strong antiferromagnetic exchange interaction.

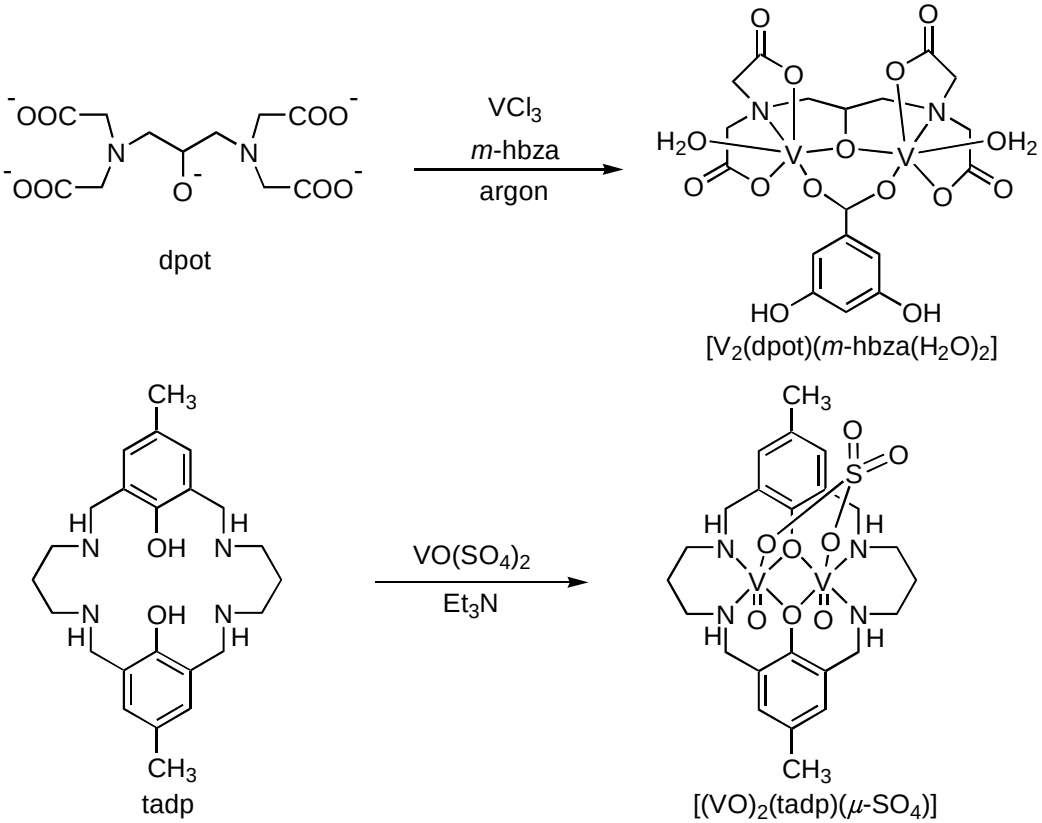

Scheme 4.1 *Synthesis of some dinuclear vanadium complexes.*

However, no examples were found in the literature of dinuclear vanadium complexes which catalytic properties in the presence of H_2O_2 have been explored. Therefore, the aim was to synthesise new dinuclear vanadium compounds and to study the relation between their structure and catalytic activity.

4.2 Multidentate O/N-ligands: design and synthesis

As discussed in the previous section, when designing dinuclear metal complexes the choice of the ligand system is of prime importance. It should be capable of incorporating two metal ions. Furthermore, it must provide well-defined dinuclear structures. Ligands which afford complexes with the metal ions sharing at least one donor atom (the so-called compartimental ligands)[7] seem appropiate for this purpose.

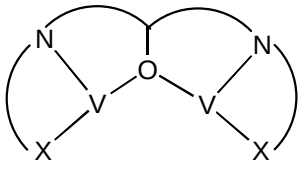

Figure 4.1 *Schematic representation of a complex based on a compartimental dinucleating ligand.*

In our group successful studies on dinuclear copper and nickel complexes of aminomethylated phenol ligands have been performed.[13] Furthermore, non-symmetric dinucleating diaminomethylated phenols were synthesised for the formation of dicopper complexes.[14] In the literature, also several diiron[15] and dinuclear zinc[16] complexes are known based on the diaminomethylated phenol skeleton which provide models for iron-oxo proteins and dimetallic aminopeptidases, respectively. Also the dinickel site of urease as well as dimanganese sites[17] were modelled with this type of dinucleating ligands.[18]

Imino nitrogen atoms are often suitable donor atoms for the coordination of transition metal ions and many Schiff base ligands have been used for the synthesis of vanadium complexes. For example, several tridentate N_2O and NO_2 ligands based on salicylaldehyde and its derivatives have been used[19] as well as many N_2O_2, salen-like ligands.[20] Also a few dinuclear structures based on Schiff base chelates are known.[21] For instance, a dinuclear vanadium(IV) complex based on this concept has been published (Scheme 4.2).[22] Ligand L^1 was prepared from 2,6-bis(aminomethyl)-4-methylphenol dihydrochloride and salicyl-aldehyde.[24b] The complex was characterised by X-ray analysis, infrared spectroscopy, and by temperature dependent magnetic susceptibility measurements. The two vanadium ions are bridged by a methoxo group and a dimethyl sulfoxide solvent molecule and are in an octahedral coordination environment. The oxo groups adopt a *syn* configuration. However, the catalytic activity of this complex in oxidation chemistry was not explored.

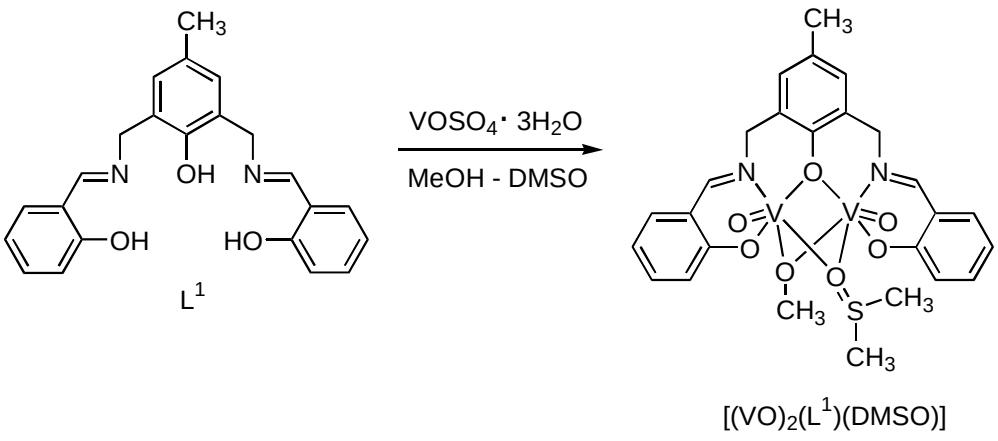

Scheme 4.2 *Synthesis of dinuclear complex [$(VO)_2(L^1)$(DMSO)] according to ref 22.*

In our case, 2-hydroxy-5-methylisophthalaldehyde[23] L^2 (Scheme 4.3) was chosen as the starting compound for the preparation of the ligands. Reaction of this dialdehyde with several amines should provide a class of Schiff base ligands which contain adjacent coordination sites and a central donor atom which acts as a bridge. The compound was prepared following a literature procedure[23] starting from *p*-cresol. After reaction of the dialdehyde with *o*-aminophenol in absolute ethanol under reflux conditions, dinucleating ligand L^3 was formed in 67% yield upon crystallisation from a dichloromethane / hexane mixture (Scheme 4.3).

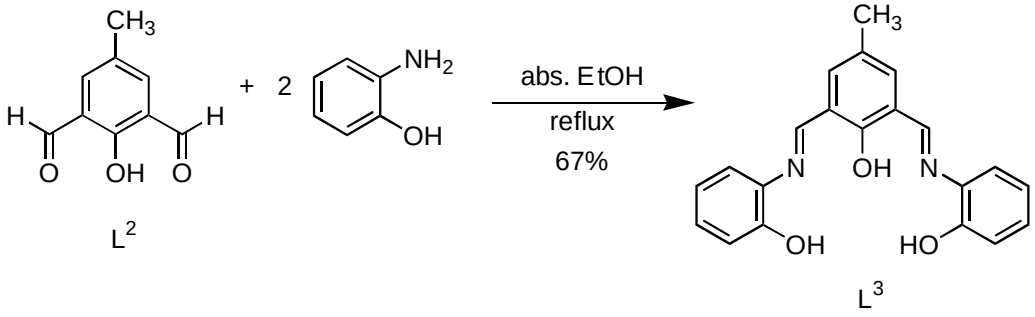

Scheme 4.3 *Synthesis of dinucleating ligand L³.*

For the synthesis of diimine ligand L^4 (Scheme 4.4), the dialdehyde was reacted with two equivalents of 2-aminoethylpyridine in dichloromethane at room temperature. After purification by crystallisation from dichloromethane / pentane, the ligand was obtained in 57% yield.

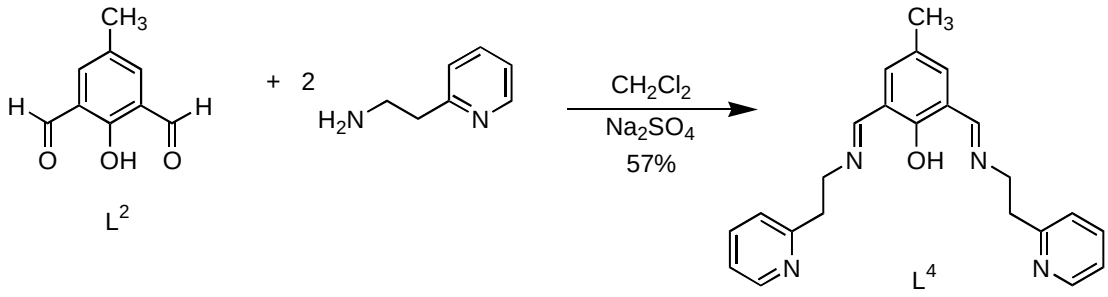

Scheme 4.4 *Synthesis of dinucleating ligand L⁴.*

Ligand L^4 was used earlier for the synthesis of a dinuclear copper complex of which the redox behaviour was investigated in relation to that of dinuclear copper containing proteins.[24] In that case, the ligand was not isolated and characterised, but prepared *in situ* before complexation with copper.[24a]

For ligand L^5, the dialdehyde was condensed with two equivalents of freshly distilled aminoethanol in refluxing absolute ethanol (Scheme 4.5). In this case, besides the bridging phenolic oxygen, an additional oxygen donor atom is present for coordination to the metal centre, instead of the two pyridine moieties in L^4. The diimine crystallised directly from the reaction mixture in 90% yield and further purification was unnecessary.

The described Schiff base ligands L^3, L^4, and L^5 are easily accessible and imino nitrogen atoms are suitable donors for the formation of metal complexes. However, under the applied reaction conditions in catalytic oxidation procedures using H_2O_2 (30% in water) they might easily be hydrolysed.[25] Secondary amines, on the other hand, are anticipated to be less prone to hydrolysis under these reaction conditions. Therefore diimine ligand L^5 was reduced to the corresponding diamine ligand L^6. This was achieved by simple hydrogenation using palladium on carbon (10%) in a methanol solution. The compound was obtained pure in 79% yield after crystallisation from chloroform.

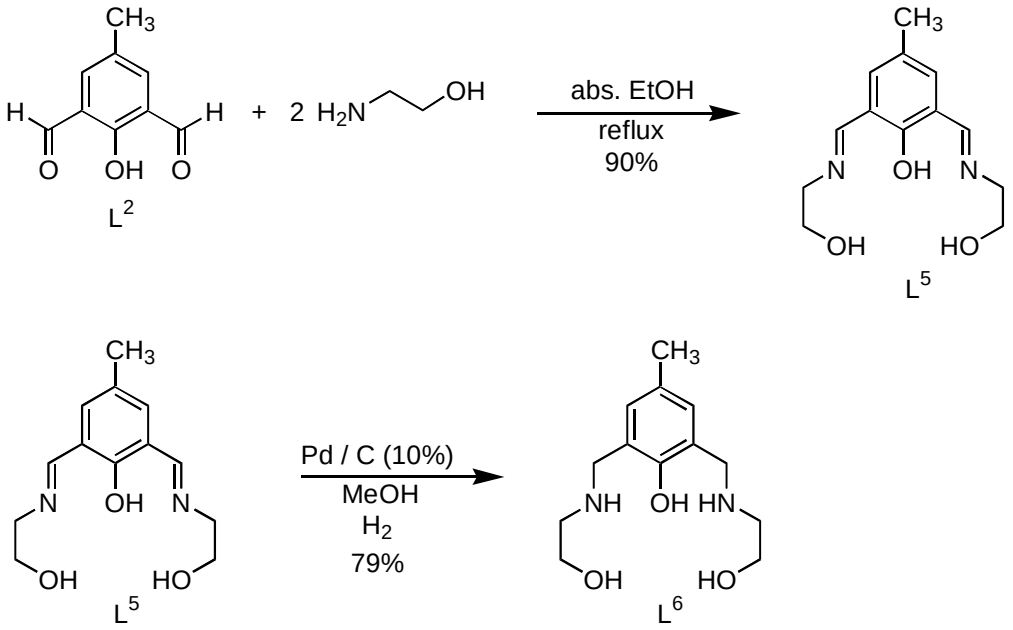

Scheme 4.5 *Synthesis of dinucleating ligands L^5 and L^6.*

The related dinucleating ligands L^7 and L^8 are Schiff bases derived from on 1,3-diamino-2-propanol (Figure 4.2).[26] Ligand L^7 was obtained by reaction of two equivalents of salicylaldehyde, whereas for L^8 the diamine was condensed with acetylacetone.[26] Both ligands L^7 and L^8 proved to be appropriate for the synthesis of dinuclear copper complexes[26,27] containing an additional (external) carboxylate bridge. A diiron complex of L^7 is also known.[28] However, in this case two ligands are coordinated to the metal centres forming a dinuclear bridged complex of the type $[Fe_2(L^7)_2]$.

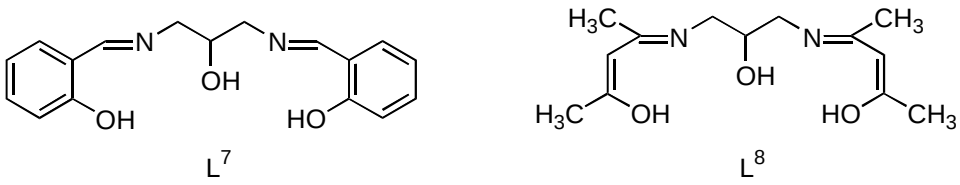

Figure 4.2 *Dinucleating ligands L[7] and L[8].*

Ligands resembling L^7 and L^8 exhibit increased flexibility compared to the class of ligands based on dialdehyde L^2, due to the presence of the flexible backbone derived from 1,3-diamino-2-propanol. As a result, the distance and orientation of two incorporated metal ions is also more flexible, which may lead to improved catalytic activity.

4.3 Complexation studies with vanadium using dinucleating ligands

The dinucleating ligands described in Chapter 4.2, were prepared for the synthesis of vanadium complexes. It was intented to explore the catalytic properties of these complexes in oxidation reactions like epoxidations, brominations or hydroxylation reactions. Some of the prepared ligands are known to be capable of incorporating metal ions like copper or iron and ligand L^1 was found to afford a dinuclear vanadium(IV) complex. Therefore it was anticipated that these systems can act as suitable ligands for vanadium. Various attempts were made to isolate vanadium complexes from L^4, L^5, L^6, L^7, and L^8 but unfortunately, no well defined products were obtained. A few illustrative examples of these attempts will be discussed here. Vanadium reagents like $VO(O^iPr)_3$, $VO(acac)_2$, $VOCl_3$, $VOSO_4$, NH_4VO_3, $NaVO_3$, and $[(VO_2Cl_2)PPh_4]$[29] were used. Often sodium acetate and sodium benzoate were added as additional bridging ligands. Sodium hydroxide, potassium *tert*-butoxide, and triethylamine were used as base and the majority of the reactions were performed under an argon atmosphere. Isolated products were characterised using ^1H and ^{51}V NMR spectroscopy, electrospray (ES / MS) mass spectrometry and IR spectroscopy.

In an attempt to synthesise a dinuclear vanadium(V) complex of L^5, the ligand was allowed to react with triisopropoxyvanadium(V) oxide $[VO(O^iPr)_3]$ in absolute ethanol (Scheme 4.6). After slow evaporation of ether into the resulting solution, a golden-coloured powder was obtained. However, the ^{51}V NMR spectrum in methanol-d_4 showed three major resonances at -535.6 ppm (band width, b.w. = 161 Hz), -539 ppm (b.w. = 45 Hz) and -550 (b.w. = 184 Hz). Furthermore, some minor impurities were observed. Attempts to purify the product by recrystallisation in the presence of sodium tetraphenylborate from a water-acetonitrile mixture were unsuccessful. Although again a yellow solid was obtained, infrared spectroscopy experiments revealed that the ligand was no longer present in the isolated product. Strong absorptions were observed at 1662, 1643, 1528, 736, and 707 cm^{-1}, but these are attributable to sodium tetraphenylborate.[30]

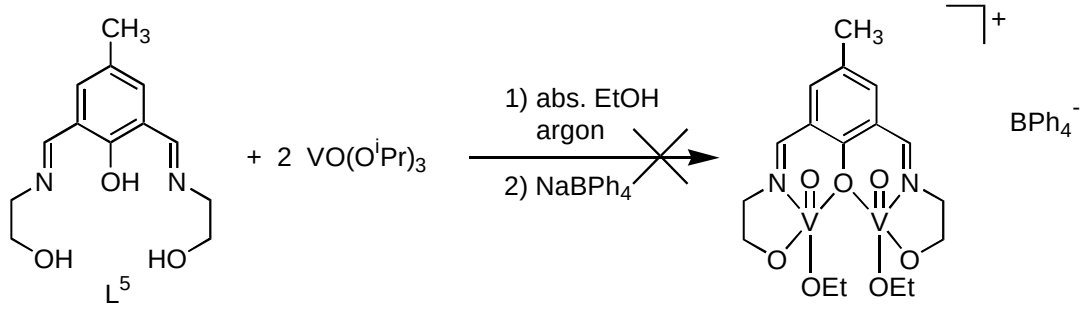

Scheme 4.6 *Attempted synthesis of a dinuclear vanadium(V) complex of L5.*

In order to synthesise a dinuclear vanadium(IV) complex of L^5, the ligand was reacted with two equivalents of vanadyl acetylacetonate [$VO(acac)_2$] in the presence of three equivalents of triethylamine in a methanol solution at room temperature (Scheme 4.7). Sodium acetate (one equiv.), which can act as a bridging ligand between the two incorporated vanadium ions, was added. Upon workup a yellow solid was isolated. Unfortunately, the ES/MS spectrum only shows a peak at *m/z* 251, which corresponds to {ligand L^5 + $1H^+$}.

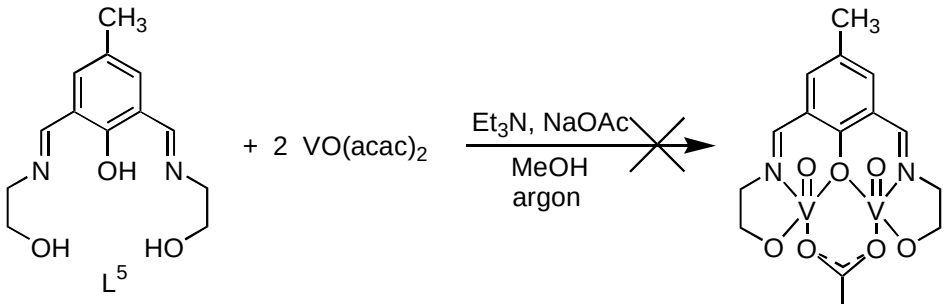

Scheme 4.7 *Attempted synthesis of a dinuclear vanadium(IV) complex of L5.*

In another attempt to synthesise a dinuclear vanadium complex of L^5, a procedure analogously to the published synthesis[22] of [$(VO)_2(L^1)$(DMSO)] was used. To a methanol-DMSO (1 : 1) solution of L^5 was added $VOSO_4 \cdot 3H_2O$. After filtration, a few drops of triethylamine were added and the resulting dark brown solution was left at 5 °C for a few days. However, no product could be isolated.

Various attempts were performed to obtain dinuclear vanadium complexes of ligands L^7 and L^8 as well. An example is given in Scheme 4.8. Ligand L^7 was allowed to react with two equivalents of vanadyl acetylacetonate in methanol under an argon atmosphere. Again

triethylamine was added as a base, as well as one equivalent of sodium benzoate. After stirring for one hour, a yellow ochre coloured precipitate was collected, which was insoluble in common organic solvents like acetonitrile, diethylether, toluene, dichloromethane, or dimethylsulfoxide. The product was therefore not further characterised.

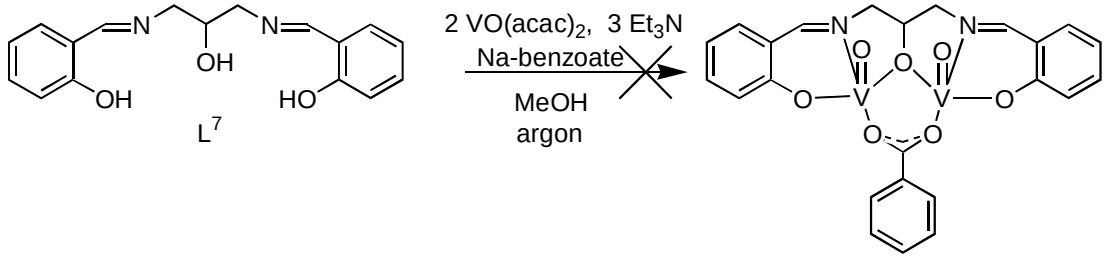

Scheme 4.8 *Attempted synthesis of a dinuclear vanadium(IV) complex of L7.*

In summary, it can be concluded that the prepared dinucleating ligands are inappropriate for the synthesis of dinuclear oxovanadium(IV) or oxovanadium(V) complexes, since no well-defined complexes were isolated. The fact that ligand L^1 is capable of providing a stable dinuclear vanadium(IV) complex is probably due to the presence of an additional carbon atom in the arms attached to the central *p*-cresol part. As a result, upon binding of a metal ion a six-membered cycle is formed, whereas in our ligands a less favourable five-membered cycle is created. Using modified procedures, there were indications that vanadium ions were coordinated to the ligand systems, but mixtures of products were obtained that were difficult to characterise. After a few attempts to purify the products, only starting materials were isolated. Therefore, no more efforts were undertaken to synthesise these type of dinuclear vanadium complexes.

4.4 Design of a structural mimic for vanadium haloperoxidases

4.4.1 Structure of the vanadium haloperoxidases

As described in Chapters 1 and 3, several vanadium haloperoxidases have been isolated from seaweeds and fungi. They catalyse the oxidation of halides (*i.e.* chlorides, bromides, and iodides) by H_2O_2 to the corresponding hypohalous acids (HOX). When a suitable nucleophilic acceptor is present, a reaction will take place with HOX to form a variety of halogenated products. This class of enzymes has been studied in detail using *e.g.* extended X-ray absorption fine structure and spin echo envelope modulation.[31] In 1996, the crystal structure of vanadium chloroperoxidase (V-ClPO), isolated from *Curvularia inaequalis*, has been elucidated by Messerschmidt and Wever to 2.03 Å resolution.[32] The active site

incorporates the vanadate (VO_3^-) unit. It is coordinated at the top of one of the two four-helix bundles in a broad channel, which is lined on one half with predominantly polar residues and several main-chain carbonyl oxygens. The other half of the channel is hydrophobic, containing Pro-47, Pro-211, Trp-350, Phe-393, Pro-395, Pro-396; and Phe-397 (see Figure 4.3).

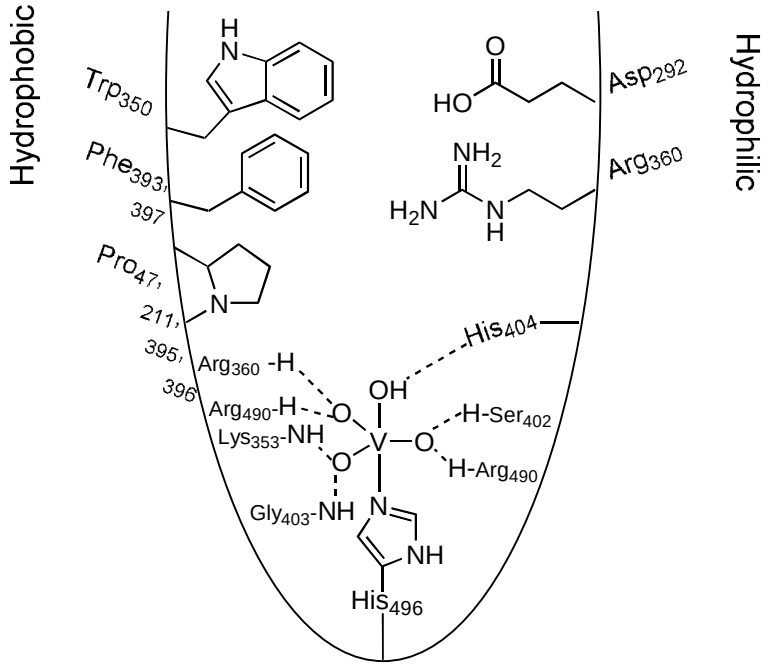

Figure 4.3 *Active site of vanadium chloroperoxidase (V-ClPO) according to ref. 33.*

The V(v) ion is in a trigonal-bipyrimidal environment and in the axial position the metal is covalently attached to a histidyl side-chain through the imidazole N^{ε}, whereas in the opposite axial position it is linked to a hydroxo group which is in hydrogen-bonding contact with water molecules and an additional histidine.[33] The negative charge of the VO_3 group is compensated by hydrogen bonds to several positively charged protein side chains and the main chain amide nitrogen of Gly-403. One of the three oxygen atoms in the equatorial plane forms hydrogen bonds to nitrogens of Arg-360 (2.94 Å) and Arg-490 (2.93 Å), another oxygen to nitrogens of Lys-353 (2.72 Å) and Gly-403 (2.99 Å) and the third oxygen to the oxygen atom of Ser-402 (2.71 Å) and the nitrogen of Arg-490 (3.04 Å).

Besides the X-ray structure of the native enzyme, the structure of the peroxide intermediate in V-ClPO was also determined to 2.1 Å resolution.[34] The trigonal-bipyrimidal arrangement is converted to tetragonal-pyrimidal upon addition of H_2O_2 (Figure 4.4). The oxo group is now placed in the apical position, whereas the peroxo ligand is located in the tetragonal plane. Also in the peroxide form an extensive hydrogen-bonding pattern is

present. One oxygen of the peroxo group is hydrogen-bonded to the nitrogen of Lys-353 and to the amide nitrogen of Gly-403. The second peroxo oxygen is also linked to this glycine nitrogen. The other oxygens form hydrogen bonds to Ser-402 and Arg-490, respectively, and to the arginine residues Arg-360 and Arg-490, respectively. A catalytic mechanism has been proposed by Messerschmidt and Wever[34] which is discussed in detail in Chapter 3.

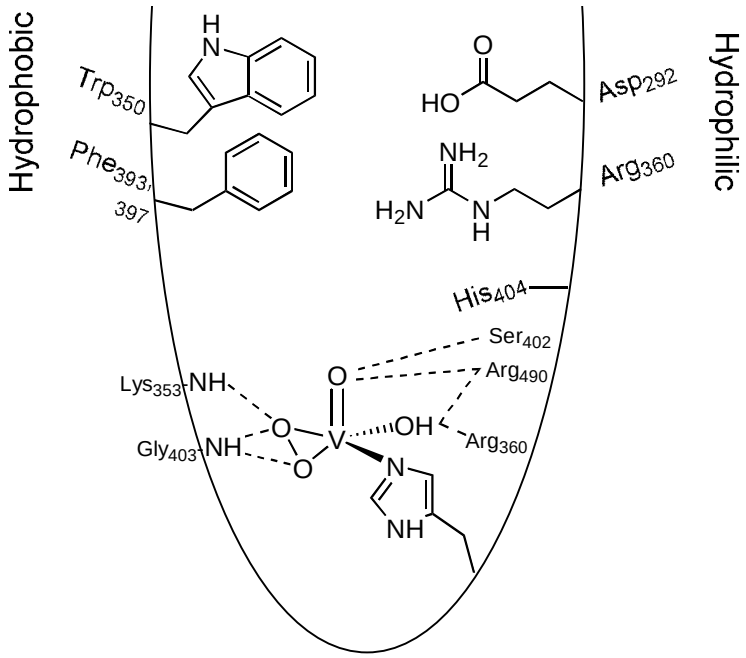

Figure 4.4 *The peroxo-vanadium site in V-ClPO.*[37]

4.4.2 Structural models for vanadium-dependent haloperoxidases

As already described in the previous chapter, many functional models for V-BrPO have been developed since their discovery in 1983 by Vilter.[35] In spite of spectroscopic studies carried out on the native enzyme, the coordination environment around the vanadium(v) centre was unknown initially. Therefore, functional mimics were developed to obtain more insight in the structural and electronic aspects of the enzyme.[36] Later on, model systems were also designed examine which structural features are important for the catalytic properties of these enzymes, and a variety of structural models for the vanadium-dependent haloperoxidases were developed.[37,38] The latter complexes were designed to mimic the coordination environment of the vanadium centre in the active site of the enzyme regardless of their activity in the presence of H_2O_2. A selection of these compounds is depicted in Figure 4.5.

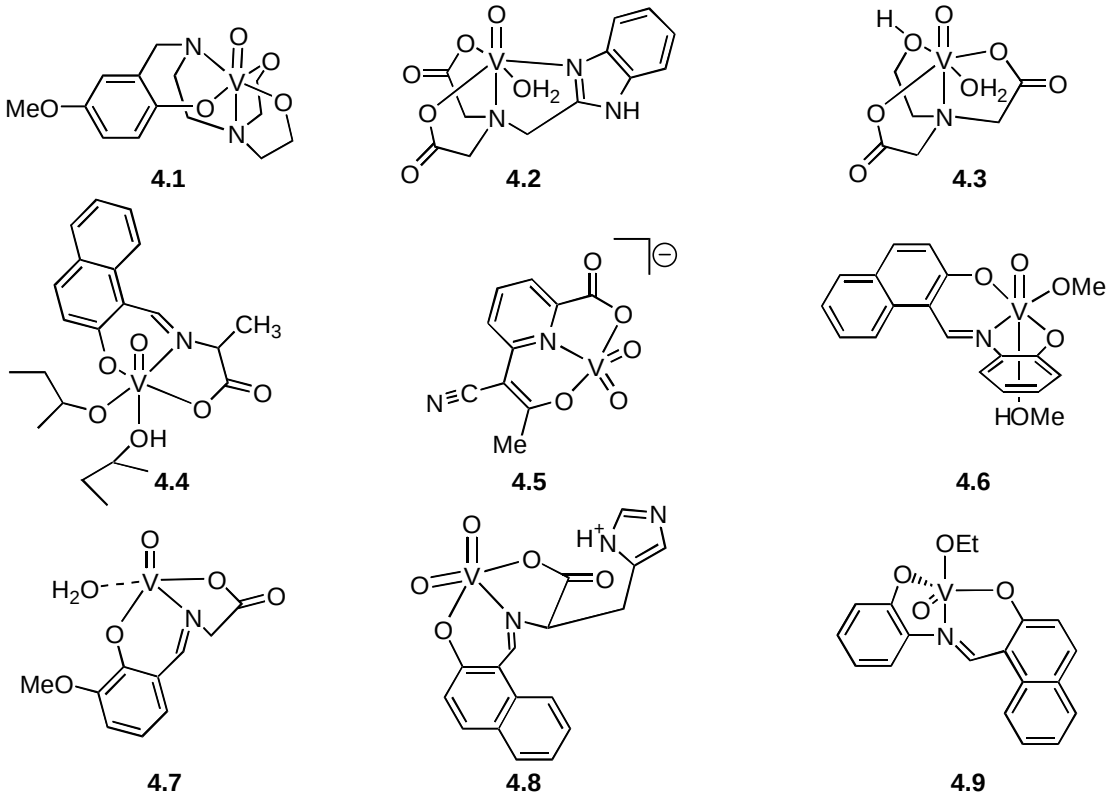

Figure 4.5 *Structural models for the active site of vanadate-dependent haloperoxidases.*[37]

Vanadium is either in the +4 oxidation state (**4.2**[45], **4.3**,[39] and **4.7**[43]) or the +5 state (**4.1**[40], **4.4**[41], **4.5**[42], **4.6**[43], **4.8**[44], **4.9**[43]). All ligands consist of oxygen donor sites and often one or two oxo groups are present at the vanadium centre. The non-oxo oxygens stem from alkoxide and phenolate moieties or from a water molecule. Compound **4.2** exists of an benzimidazol unit incorporated in the ligand system, thus providing a model for the coordination of histidine in the enzyme.[45] In some of the complexes, one of the vanadium-to-oxygen linkages is a weak bond, for instance when water (**4.3** and **4.7**) or an alcohol (**4.4** and **4.6**) coordinate to the metal. These bonds may easily be broken to provide an additional coordination site for a substrate.

4.4.3 Design of the ligand[46]

As becomes clear from Figure 4.5 in the previous section, the structural models known to date mimic the oxygen-rich coordination environment of the metal and the binding of histidine in the presence of oxo groups, phenolate and alkoxide moieties, and one nitrogen donor unit. However, none of these structures display the characteristic hydrogen bonding pattern of the oxo groups on vanadium to other residues present in the ligand. Therefore, the design of a structural mimic in which the vanadate (VO_3^-) moiety is coordinated to a

nitrogen donor atom and stabilised *via* hydrogen bonds to other parts of the ligand, remained a real challenge. In the course of this work, the synthesis of a polyamine receptor ligand containing two guanidinium units and an imidazole ligand as a template suitable to bind vanadate *via* hydrogen bridges was reported (Figure 4.6).[47] This ligand was designed according to the structural properties known from the X-ray crystal structure from vanadium chloroperoxidase. The bisguanidinium moieties were chosen taking into account the well-established recognition of phosphate by these type of receptors. The structure of the corresponding vanadate complex is not published yet.

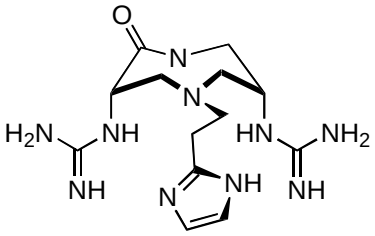

Figure 4.6 *Bisguanidinium receptor ligand for the incorporation of vanadate.*[47]

Recently, Borovik and coworkers developed a cobalt[48] and a manganese[49] complex where they use a ligand that can provide up to three intramolecular hydrogen bonds to an external ligand coordinated to the metal centre. This tripodal urea-based ligand affords a cavity structure that incorporates the metal and the additional hydroxo or oxo group on the metal is stabilised by the hydrogen bonds. The synthesis of the cobalt complex is depicted in Scheme 4.9.

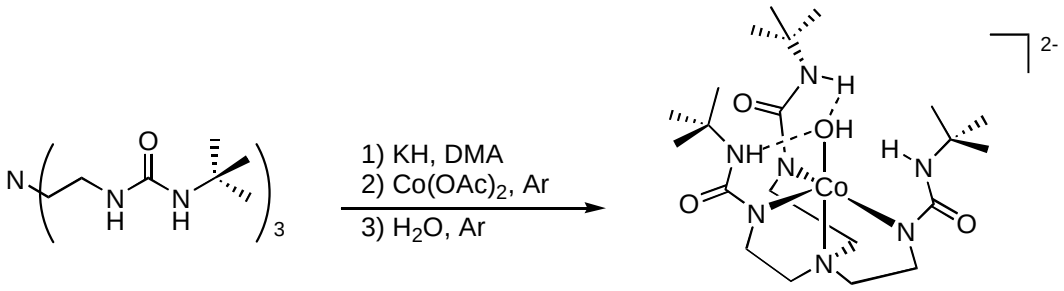

Scheme 4.9 *Synthesis of a Co-OH complex using intramolecular hydrogen bonds to stabilise the metal-ligand adduct.*[48]

In our research group, the intermolecular hydrogen bond forming properties of urea groups were explored by studying the gelation of organic solvents by several bis-urea compounds as well.[46,50] Furthermore, tripodal urea compound L[9] has been reported as a receptor for phosphate.[51] An association constant (K_{ass}) of 1.1 x 10^4 M^{-1} was obtained with

tris(tetra-methylammonium)phosphate in DMSO-d_6 (Figure 4.7). Since physiological effects of vanadium are mainly attributed to the similarity of vanadate(V) ions and phosphate ions[52] and because it was recently discovered that the active sites of vanadate containing haloperoxidases and of families of acid phosphatases are very similar,[53] it was envisaged that this tripodal ligand is also capable of coordination of vanadate.

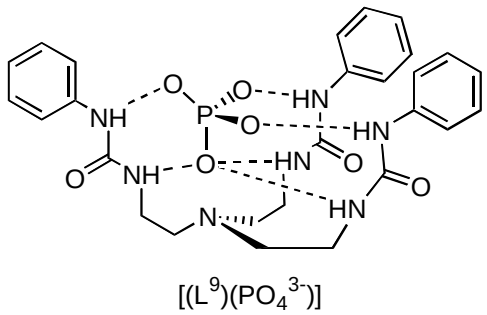

Figure 4.7 *Proposed phosphate-receptor complex based on ligand L^9 according to ref 51.*

To study the possibilities of these types of tripodal urea-based compounds as ligands for vanadate, five derivatives were synthesised. Reaction of tris(2-aminoethyl)amine with phenyl, butyl, or benzyl isocyanate in chloroform afforded L^9, L^{10} and L^{11}, respectively, in good yields (Scheme 4.10). Although tris(2-aminoethyl)amine appeared to be a suitable spacer for a phosphate receptor, also two ligands based on the C3-spacer tris(3-aminopropyl)amine were prepared for the purpose of comparison (L^{12} and L^{13}).

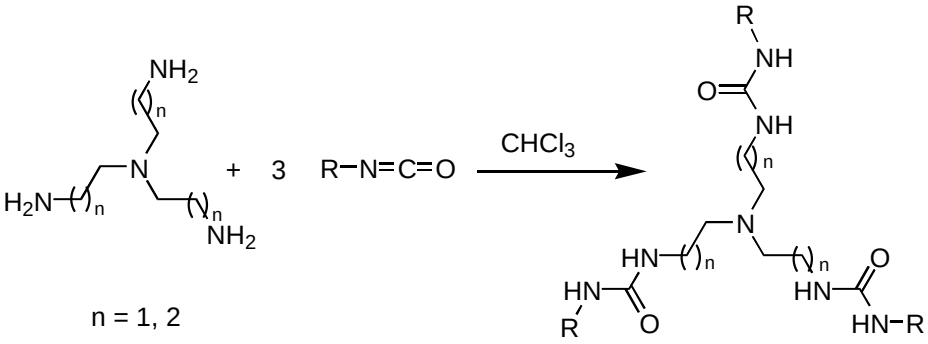

Scheme 4.10 *Synthesis of tripodal ligands.*

Compound	Spacer	R	Yield (%)
L^9	C_2	phenyl	96
L^{10}	C_2	butyl	75
L^{11}	C_2	benzyl	71
L^{12}	C_3	butyl	82
L^{13}	C_3	benzyl	91

4.4.4 Complexation studies with vanadium

In order to achieve incorporation of the vanadate ion into the ligand cavity, tetra-*n*-butylammonium vanadate **4.10** was used, which was prepared *via* a slightly modified literature procedure from vanadium pentoxide (V_2O_5) and a 0.4 M solution of [(*n*-Bu)$_4$N]OH in water.[54] The target structure based on ligands L^{12} or L^{13} is depicted in Scheme 4.11.

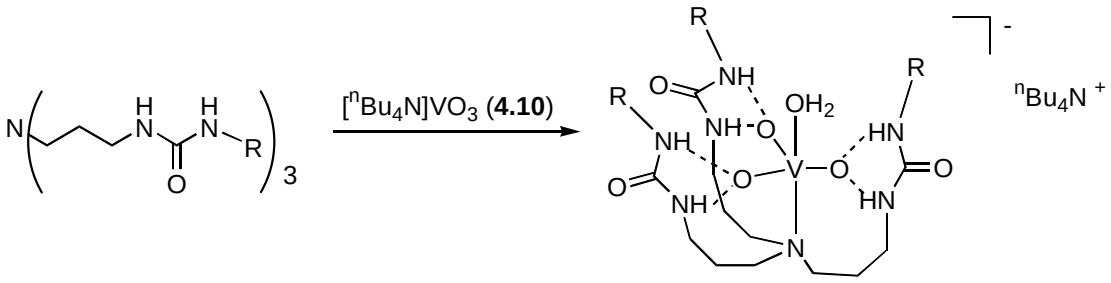

Scheme 4.11 *Target structural model system of vanadium bromoperoxidase using tripodal ligand L^{12} or L^{13}.*

In the first attempts to synthesise the target molecule, ligands L^9, L^{10}, L^{11}, L^{12}, or L^{13} were mixed with [(^{n}Bu$_4$N)VO$_3$] (**4.10**) in a 1 : 1 ratio using DMA (*N*,*N*-dimethylacetamide) as the solvent. After slow diffusion of diethyl ether into the solution, purple crystals were obtained in all cases. However, ^{1}H NMR revealed that the ligands were absent in the compound. According to the elemental analysis, probably a tetra-*n*-butylammonium hydrogen divanadate complex [(^{n}Bu$_4$N)HV$_2$O$_6$] was formed.[55] Also addition of ethylacetate, benzene and diisopropylether yielded these purple crystals. Unfortunately, the crystal quality was too poor for determination of the X-ray structure.

When the reaction was performed in octanol, only starting material (the ligand or the vanadium reagent) could be isolated after slow addition of diethyl ether or evaporation of the solvent.

The association constant (K_{ass}) of ligand L^9 with phosphate was determined in DMSO-d$_6$.[51] Accordingly, concentration dependent ^{51}V NMR experiments were performed in this solvent using ligand L^{12} and **4.10** in a 1 : 1 ratio. The vanadium reagent exhibits a signal at –570 ppm and addition of the ligand had no influence on this value. Subsequently dilution of the sample also did not produce a concentration dependent shift, indicating that coordination of the vanadate moiety does not occur.

Since the tripodal ligands, insoluble in acetone, readily dissolve by addition of excess [(^{n}Bu$_4$N)VO$_3$], it was assumed that in acetone perhaps coordination of the vanadate moiety to the urea groups occurs. Therefore, ^{51}V NMR studies in acetone-d$_6$ were performed using the vanadium reagent and ligand L^{12}. A single resonance at –564 ppm was detected for [(^{n}Bu$_4$N)VO$_3$]. Unfortunately, this remained the same after addition of the ligand, which implies that incorporation of vanadate into the triurea compound *via* hydrogen bonding does not occur. Perhaps, the tetrabutylammonium cations bind to the triurea compound instead, thus inhibiting the coordination of vanadate.

From the results described above it can be concluded that although *e.g.* tripodal ligand L^9 is a suitable ligand for the incorporation of a phosphate unit, we were unable to establishe that it is also capable of complexing the vanadate moiety. Efforts made to crystallise the target structure were also unsuccessful. These attempts were further complicated by the limited solubility of the ligands in many organic solvents.

4.5 Experimental section

4.5.1 General information

For general information, see Chapter 2. Tris(2-aminoethyl)amine was obtained from Aldrich and tris(3-aminopropyl)amine was purchased from TCI, Tokyo Kasei. $[(VO_2Cl_2)PPh_4]$ was prepared following a literature procedure.[29] Triisopropoxyvanadium(V) oxide $[VO(O^iPr)_3]$, vanadyl acetylacetonate $[VO(acac)_2]$, vanadium(V)oxytrichloride $[VOCl_3]$, ammonium metavanadate $[NH_4VO_3]$, and sodium metavanadate $[NaVO_3]$ were purchased from Aldrich, whereas vanadyl sulfate hydrate $[VOSO_4 \cdot xH_2O]$, and tetrabutylammonium hydroxide (40 wt% solution in water) were obtained from Acros. Phenyl isocyanate, benzyl isocyanate, and *n*-butyl isocyanate were purchased from Aldrich and used without purification. ^{51}V-NMR spectra were recorded on a Varian Unity 500 spectrometer (relative to $\delta(VOCl_3) = 0$ ppm).

4.5.2 Syntheses

2-Hydroxy-5-methylisophthalaldehyde (L^2) The dialdehyde was prepared following a literature procedure.[23]

2,6-Bis{[2-(hydroxyphenyl)imino]methyl}-4-methylphenol (L^3) To a hot solution of hydroxy-5-methylisophthalaldehyde L^2 (0.50 g, 3.05 mmol) in absolute EtOH (15 ml) was added slowly a hot solution of *o*-aminophenol (0.66 g, 6.09 mmol, 2.0 equiv.) in absolute EtOH (15 ml). The dark red solution was heated under reflux for 2 h. After removal of the solvent, the product was crystallised from a two-layer system of CH_2Cl_2 / hexane. Ligand L^3 was obtained as a dark red powder (0.71 g, 2.05 mmol, 67%). ^{1}H NMR ($CDCl_3$) 8.98(s, 2H), 7.74 (s, 2H), 7.30-7.18 (m, 4H), 7.05-6.91 (m, 4H), 2.41 (s, 3H); ^{13}C NMR (DMSO-d_6) 182.95 (C), 157.33 (CH), 151.20 (C), 133.67 (CH), 127.88 (CH), 126.87 (C), 121.56 (C), 119.66 (CH), 119.19 (CH), 116.31 (CH), 98.10 (C), 19.97 (CH_3); HRMS calcd for $C_{21}H_{18}N_2O_3$: 346.132, found: 346.133; mp 192-193 °C.

4-Methyl-2,6-bis({[2-(2-pyridinyl)ethyl]amino}methyl)phenol (L^4) 2-Hydroxy-5-methylisophthalaldehyde L^2 (0.20 g, 1.22 mmol) was dissolved in CH_2Cl_2 (20 ml). Freshly distilled aminoethylpyridine (0.30 g, 2.44 mmol, 2.0 equiv.) was added dropwise. The resulting orange solution was stirred for 30 min. Subsequently, Na_2SO_4 was added and the reaction

mixture was stirred for an additional 30 min. After filtration and evaporation of the solvent, the crude product was crystallised from a CH_2Cl_2 / pentane mixture, yielding L^4 as yellow-orange crystals (0.26 g, 0.70 mmol, 57%). ^{1}H NMR ($CDCl_3$) 13.70 (br, 1H), 8.53 (d, 2H, *J* = 8.5 Hz), 8.45 (s, 2H), 7.55 (t, 2H, *J* = 7.7 Hz), 7.38 (br, 2H), 7.16-7.07 (m, 4H), 3.99 (t, 4H, *J* = 7.1 Hz), 3.15 (t, 4H, *J* = 7.1), 2.24 (s, 3H); ^{13}C NMR ($CDCl_3$) 159.28 (2x C), 158.89 (C), 149.25 (CH, 2x), 136.16 (CH), 127.24 (C), 123.45 (CH), 121.22 (CH, 2x), 39.49 (2x CH_2), 20.06 (CH_3); HRMS calcd for $C_{23}H_{24}N_4O$: 372.195, found: 372.196.

2-{[(2-Hydroxyethyl)imino]methyl}-4-methyl-6-[(propylimino)methyl]phenol (L^5) 2-Hydroxy-5-methylisophthalaldehyde L^2 (0.75 g, 4.57 mmol) was dissolved in absolute EtOH (6 ml). Aminoethanol, freshly distilled by Kugelrohr distillation (0.57 g, 9.23 mmol, 2.0 equiv.) was added followed by an additional amount of absolute EtOH (1 ml). The reaction mixture was heated under reflux for 90 min. Slow cooling in cotton wool and finally in an ice-bath yielded L^5 as yellow fluffy needles (1.03 g, 4.13 mmol, 90%).^{1}H NMR (DMSO-d_6) 14.3 (br, 1H, OH), 8.55 (s, 2H), 7.51 (s, 2H), 4.69 (br, 2H, OH); ^{13}C NMR (DMSO-d_6) 161.49 (CH), 160.15 (C), 132.26 (CH), 126.02 (C), 120.93 (C), 61.90 (CH_2), 60.63 (CH_2), 60.54 (CH_2), 19.87 (CH_3); HRMS calcd for $C_{13}H_{18}N_2O_3$: 250.132, found: 250.132; mp 167 °C; Anal. calcd. for $C_{13}H_{18}N_2O_3$: C 62.24; H 7.25; N 11.19%, found: C 62.00; H 7.30; N 11.10%.

2-{[(2-Hydroxyethyl)amino]methyl}-4-methyl-6-[(propylamino)methyl]phenol (L^6) The diimine ligand L^5 (0.25 g, 0.10 mmol), was dissolved in MeOH (25 ml). A microspatula of Pd / C (10%) was added and the mixture was stirred for 18 h under a hydrogen atmosphere. The reaction mixture was filtered over Celite and the solvent was evaporated. The remaining white solid was recrystallised from $CHCl_3$. Ligand L^6 was isolated as a white fluffy powder (0.20 g, 0.79 mmol, 79%). ^{1}H NMR ($CDCl_3$) 6.82 (s, 2H), 3.83 (s, 4H), 3.69 (t, 4H, *J* = 5.1 Hz), 2.77 (t, 4H, *J* = 5.1 Hz), 3.83-3.38 (br, 3H, OH), 2.23 (s, 3H); ^{13}C NMR ($CDCl_3$) 154.15 (C), 128.90 (CH), 127.72 (C), 124.21 (C), 60.91 (CH_2), 50.62 (CH_2), 50.46 (CH_2), 20.41 (CH_3); CI / MS *m* / *z* 255 {M + 1H$^+$}; mp 118-119 °C; Anal. calcd. for $C_{13}H_{22}N_2O_3$: C 61.39; H 8.72; N 11.01%, found: C 60.91; H 8.75; N 10.85%.

2-{[(2-Hydroxy-3-{[(2-hydroxyphenyl)methylidene]amino}propyl)imino]methyl}phenol (L^7)[26] To a solution of 1,3-diamino-2-propanol (2.00 g, 22.2 mmol) in $CHCl_3$ (200 ml) was added salicylaldehyde (5.42 g, 44.4 mmol, 2.0 equiv.). The resulting bright yellow solution was stirred for 30 min. Na_2SO_4 was added and the reaction mixture stirred for an additional 30 min. After filtration, the Schiff base was obtained as a yellow powder by distilling of the solvent (6.21 g, 20.8 mmol, 94%). Crystallisation from EtOAc yielded analytically pure L^7. ^{1}H NMR ($CDCl_3$) 8.26 (s, 2H), 7.23-7.12 (m, 4H), 6.86-6.74 (m, 4H), 4.15-4.11 (m, 1H), 3.76-3.71 (m, 2H), 3.61-3.55 (m, 2H); ^{13}C NMR ($CDCl_3$) 167.25 (CH), 160.98 (C), 132.48 (CH), 131.48 (CH), 118.63 (CH), 118.48 (C), 116.91 (CH), 70.29 (CH), 63.01 (CH_2); Anal. calcd. for $C_{17}H_{18}N_2O_3$: C 68.44; H 6.08; N 9.39%, found: C 68.36; H 6.11; N 9.35%.

4-[(2-Hydroxy-3-{[3-hydroxy-1-methyl-2-butenylidene]amino}propyl)imino]-2-penten-2-ol (L^8) According to a literature procedure,[26] acetylacetone and 1,3-diaminopropan-2-ol were mixed in absolute EtOH and refluxed for 2 h. Ligand L^8 was obtained after removal of the solvent as a pale yellow powder in quantitative yield. ^{1}H NMR (DMSO-d_6) 11.11 (br, OH), 5.32 (s, 2H), 4.05-4.02 (m, 1H), 3.73-3.51 (m, 4H), 2.28 (s, 3H), 2.24 (s, 3H); ^{13}C NMR (DMSO-d_6) 192.93 (C), 162.96 (C), 94.93 (CH), 68.82 (CH), 46.04 (CH_2), 28.59 (CH_3), 18.70 (CH_3).

Attempted synthesis of a dinuclear vanadium(v) complex of L^5 To a hot solution of ligand L^5 (0.20 g, 0.81 mmol) in absolute EtOH (3 ml) was added by syringe $VO(O^iPr)_3$ (0.4 ml, 1.70 mmol, 2.1 equiv.). After stirring of the clear red-brown solution under an argon atmosphere for 2 h, diethyl ether was allowed to slowly evaporate into the reaction mixture using a double schlenk vessel. After a few days a golden-coloured precipitate was formed with was collected and washed with diethyl ether. ^{51}V NMR (CD_3OD), -536 (b.w. = 161 Hz), -539 (45 Hz), -550 (184 Hz). To purify the compound by crystallisation, the ligand was dissolved in water and a solution of an excess of sodium tetraphenylborate ($NaBPh_4$) was added. Acetonitrile was added to dissolve the resulting yellow precipitate. Slow evaporation of the solvent through cotton wool, resulted in precipitation of a yellow solid. IR (KBr) 1662, 1643, 1528, 736, 707 cm^{-1}, attributable to $NaBPh_4$.

Attempted synthesis of a dinuclear vanadium(iv) complex of L^5 To a suspension of L^5 (150 mg, 0.60 mmol) in MeOH (3 ml) was subsequently added Et_3N (0.25 ml, 1.80 mmol, 3 equiv.) and $VO(acac)_2$ (0.32 g, 1.20 mmol). The colour of the reaction mixture rapidly changed from green to dark brown. Sodium acetate (49 mg, 0.60 mmol, 1 equiv.) was added and an additional 1 ml of MeOH was added as well. After stirring at room temperature for 4 h, the dark brown reaction mixture was filtered over cotton wool. The solution was concentrated *in vacuo* until a reaction volume of about 2.5 ml is reached. Next, diethylether (3 ml) was added and after a few days a yellow precipitate was obtained. ES/MS *m*/*z* 251 {ligand L^5 + $1H^+$}.

Attempted synthesis of dinuclear vanadium(iv) complex of L^5 Analogously to a literature procedure[22] $VOSO_4 \cdot 3H_2O$ (266 mg, 1.14 mmol) was added with stirring to a methanol-dimethyl sulfoxide (1 : 1) solution (10 ml) of L^5 (95 mg, 0.38 mmol). The resulting solution was filtered and a few drops of Et_3N were added to the filtrate. The solution was left to stand at 4 °C for several days, but no precipitate was formed. Even when only 5 ml of solvent (MeOH-DMSO, 1 : 1 mixture) was used, no product could be isolated.

Attempted synthesis of a dinuclear vanadium(iv) complex of L^7 To a solution of the ligand L^7 (106 mg, 0.36 mmol) in MeOH (6 ml) was added $VO(acac)_2$ (191 mg, 0.72 mmol), sodium benzoate (52 mg, 0.36 mmol) and a few drops of triethylamine. The reaction mixture was stirred under an argon atmosphere for 1 h. The resulting yellow ochre coloured precipitate was collected by filtration and washed with methanol. Further purification was impossible

due to insolubility of the product in acetonitrile, diethyl ether, toluene, dichloromethane and dimethyl sulfoxide.

***N*-[2-(Bis{2-[(anilinocarbonyl)amino]ethyl}amino)ethyl]-*N*'-phenylurea (L^{9})** Phenyl isocyanate (2.69 g, 22.6 mmol, 3.3 equiv.) was dissolved in $CHCl_3$ (75 ml) and added in portions to a solution of tris(2-aminoethylamine) (1.00 g, 6.84 mmol) in $CHCl_3$ (75 ml). After stirring for 2 h, the white solid was collected, washed with Et_2O and dried in vacuo. Yield 3.30 g (6.55 mmol, 96%). ^{1}H NMR (DMSO-d_6) 8.50 (s, 3H, NH), 7.36 (d, 6H, *J* = 7.7 Hz), 7.18 (t, 6H, *J* = 7.9 Hz), 6.86 (t, 3H, *J* = 7.3 Hz), 6.16 (m, 3H, NH), 3.17 (m, 6H), 2.58 (t, 6H, *J* = 6.4 Hz); ^{13}C NMR (DMSO-d_6) 155.28 (C), 140.42 (C), 128.56 (CH), 120.97 (CH), 117.70 (CH), 53.92 (CH_2), 37.50 (CH_2); CI / MS *m* / *z* 504 {*M* + 1H$^+$}, mp 201-202 °C.

***N*-{2-Bis(2-{[(butylamino)carbonyl]amino}ethyl)amino}ethyl-*N*'-butylurea (L^{10})** ^{n}Butyl isocyanate (1.00 g, 10.1 mmol, 3.0 equiv.) was dissolved in $CHCl_3$ (50 ml) and added in portions to a solution of tris(2-aminoethyl)amine (0.45 g, 3.06 mmol) in $CHCl_3$ (25 ml). After stirring for 2 h, the solvent was evaporated and the white solid crystallised from $CHCl_3$ providing small white needles. Yield: 1.12 g (2.50 mmol, 75%). ^{1}H NMR ($CDCl_3$) 6.18 (br, 3H, NH), 5.62 (br, 3H, NH), 3.13-3.07 (m, 12H), 2.48 (m, 6H), 1.48-1.28 (m, 12H), 0.89 (t, 9H, *J* = 7.1 Hz); ^{13}C NMR ($CDCl_3$) 159.68 (C), 55.06 (CH_2), 39.99 (CH_2), 38.37 (CH_2), 32.48 (CH_2), 20.09 (CH_2), 13.79 (CH_3); CI / MS *m* / *z* 444 {*M* + 1H$^+$}; mp 160-163 °C; Anal. calcd. for $C_{21}H_{45}N_7O_3$: C 56.86; H 10.22; N 22.10%, found: C 56.78; H 10.17; N 22.10%.

***N*-Benzyl-*N*'-{2-[bis(2-{[(benzylamino)carbonyl]amino}ethyl)amino]ethyl}urea (L^{11})** Benzyl isocyanate (2.50 g, 18.0 mmol, 2.9 equiv.) in $CHCl_3$ (50 ml) was added in portions to a solution of tris(2-aminoethyl)amine (0.95 g, 6.47 mmol). The reaction mixture was stirred for 1 h. The resulting white precipitate was collected and stirred in Et_2O for 15 min. Filtration yielded 2.49 g (4.57 mmol, 71%) of a white solid. ^{1}H NMR (DMSO-d_6) 7.32-7.18 (m, 15H), 6.44 (t, 3H, NH, *J* = 5.9 Hz), 6.02 (m, 3H, NH), 4.19 (d, 6H, *J* = 5.5 Hz), 3.08 (d, 6H, *J* = 5.5 Hz), 2.49 (d, 6H, *J* = 6.2 Hz); ^{13}C NMR (DMSO-d_6) 158.16 (C), 140.82 (C), 128.14 (CH), 126.92 (CH), 126.45 (CH), 54.31 (CH_2), 42.90 (CH_2), 37.78 (CH_2); CI / MS *m* / *z* 546 {*M* + 1H$^+$}; mp 194-195 °C; Anal. calcd. for $C_{30}H_{39}N_7O_3$: C 66.03; H 7.20; N 17.97%, found: C 65.90; H 7.23; N 18.02%.

***N*-(3-Bis(3-{[(butylamino)carbonyl]aminopropyl}amino)propyl)-*N*'-butylurea (L^{12})** ^{n}Butyl isocyanate (1.74 g, 17.5 mmol, 3.3 equiv.), was dissolved in $CHCl_3$ (15 ml) and added in portions to a solution of tris(3-aminopropyl)amine (1.00 g, 5.31 mmol) in $CHCl_3$. After stirring at room temperature for 3 h, the white precipitate was collected, washed with Et_2O and dried in vacuo. L^{12} was obtained as a white solid. Yield: 2.12 g (4.36 mmol, 82%). ^{1}H NMR (DMSO-d_6) 5.87-5.81 (m, 6H, NH), 2.97-2.91 (m, 12H), 2.26 (t, 6H, *J* = 6.2 Hz), 1.45-1.41 (m, 6H), 1.33-1.19 (m, 12H), 0.83 (t, 9H, *J* = 7.0 Hz); ^{13}C NMR (DMSO-d_6) 158.20 (C), 50.61 (CH_2), 38.89 (CH_2), 37.45 (CH_2), 32.15 (CH_2), 27.34 (CH_2), 19.49 (CH_2), 13.63 (CH_3); CI / MS *m* / *z* 486 {*M* + 1H$^+$}; mp 172 °C; Anal. calcd. for $C_{24}H_{51}N_7O_3$: C 59.35; H 10.58; N 20.19%, found: C 59.47; H 10.83; N 20.20%.

***N*-Benzyl-*N*'-(3-bis(3-{[(benzylamino)carbonyl]amino}propyl)amino)propylurea (L^{13})** Benzyl isocyanate (1.50 g, 11.3 mmol, 3.3 equiv.) was dissolved in $CHCl_3$ (15 ml) and added in portions to a solution of tris(3-aminopropyl)amine (0.64 g, 3.40 mmol) in $CHCl_3$. After stirring for 3 h, the white precipitate was collected, washed thoroughly with Et_2O and dried in vacuo. L^{13} was obtained as a white solid. Yield: 1.81 g (3.08 mmol, 91%). ^{1}H NMR (DMSO-d_6) 7.29-7.24 (m, 6H), 7.20-7.17 (m, 9H), 6.37-6.33 (br, 3H, NH), 6.04 (br, 3H, NH), 4.13 (d, 6H, *J* = 5.5 Hz), 3.03-3.01 (m, 6H), 2.30 (t, 6H, *J* = 6.2 Hz), 1.48 (t, 6H, *J* = 6.2 Hz); ^{13}C NMR (DMSO-d_6) 158.20 (C), 140.90 (C), 128.14 (CH), 126.88 (CH), 126.46 (CH), 50.69 (CH_2), 42.86 (CH_2), 37.61 (CH_2), 27.35 (CH_2); CI/MS *m*/*z* 588 {*M* + 1H$^+$}; mp 194-196 °C; Anal. calcd. for $C_{33}H_{45}N_7O_3$: C 67.44; H 7.72; N 16.68%, found: C 67.26; H 7.76; N 16.53%.

Tetra-*n*-butylammonium vanadate (4.10) [^{n}Bu$_4$N]VO_3 was prepared according to a slightly modified literature procedure.[54] To a 40 % aqueous solution of [^{n}Bu$_4$N]OH (27.2 g, 0.042 mol) was added enough H_2O until a reaction volume of 100 ml was reached. Subsequenly, V_2O_5 (3.8 g, 0.021 mol) was added and the reaction mixture was stirred for 18 h. After removal of a small amount of insoluble material, the solution was evaporated to complete dryness. A pure sample was obtained by dissolving the crude off-white product (1.0 g) in acetone (4 ml), precipitating by adding diethylether (8 ml) and washing. ^{51}V NMR (DMSO-d_6) –570. ^{51}V NMR (acetone-d_6) –563.

4.6 References

1 *Bioinorganic Catalysis*, Second Edition, Reedijk, J.; Bouwman, E., Eds.; Marcel Dekker, New York, 1999.

2 Holm, R.H.; Kennepohl, P.; Solomon, E.I. *Chem. Rev.* **1996**, *96*, 2239.

3 Wallar, B.J.; Lipscomb, J.D. *Chem. Rev.* **1996**, *96*, 2625.

4 See Chapters 1 and 7.

5 (a) Solomon, E.I.; Sundaram, U.M.; Machonkin, T.E. *Chem. Rev.* **1996**, *96*, 2563. (b) Decker, H.; Dillinger, R.; Tuczek, F. *Angew. Chem. Int. Ed.* **2000**, *39*, 1591.

6 (a) Robson, R. *Inorg. Nucl. Chem. Lett.* **1970**, *6*, 125. (b) Robson, R. *Austr. J. Chem.* **1970**, *23*, 2217.

7 Fenton, D.E.; Okawa, H. *Chem. Ber./Recueil* **1997**, *130*, 433.

8 (a) Van den Beuken, E.K.; Feringa, B.L. *Tetrahedron* **1998**, *54*, 12985. (b) Fenton, D.E.; Casellato, U.; Vigato, P.A.; Vidali, M. *Inorg. Chim. Acta* **1984**, *95*, 187. (c) Fenton, D.E.; Casellato, U.; Vigato, P.A.; Vidali, M. *ibid.* **1982**, *62*, 57.

9 Broussard, M.E.; Juma, B.; Train, S.G.; Peng, W.J.; Lanerman, S.A.; Stanley, G.G. *Science* **1993**, *260*, 1784.

10 (a) Copeland, E.P.; Kahwa, I.A.; Mague, J.T.; McPherson, G.L. *J. Chem. Soc., Dalton Trans.* **1997**, 2849. (b) Kruger, P.E.; Moubaraki, B.; Murray, K.S. *J. Chem. Soc., Dalton*

Trans. **1996**, 1223. (c) Kanamori, K.; Okayasu, T.; Okamoto, K.-I. *Chem. Lett.* **1995**, 105. (d) Neves, A.; Vencato, I.; Hörner, M.; Fenner, H. *Acta Cryst.* **1995**, C51, 809. (e) Kanamori, K.; Yamamoto, K.; Okamoto, K.-I. *Chem. Lett.* **1993**, 1253.

11 Kanamori, K.; Yamamoto, K.; Okayasu, T.; Matsui, N.; Okamoto, K.-I.; Mori, W. *Bull. Chem. Soc. Jpn.* **1997**, *70*, 3040.

12 Das, R.; Nanda, K.K.; Mukherjee, A.K.; Mukherjee, M.; Helliwell, M.; Nag, K. *J. Chem. Soc., Dalton Trans.* **1993**, 2241.

13 (a) Gelling, O.J.; Feringa, B.L. *J. Am. Chem. Soc.* **1990**, *112*, 7599. (b) Gelling, O.J. 'Bimetallic Oxidation Catalysts', PhD Thesis, Groningen, 1990. (c) Rispens, M.T. 'Enantioselective Oxidation Using Transition Metal Catalysts', PhD Thesis, Groningen, 1996.

14 (a) Lubben, M; Hage, R.; Meetsma, A.; Bijma, K.; Feringa, B.L. *Inorg. Chem.* **1995**, *34*, 2217. (b) Lubben, M. 'Model Systems for Iron and Copper Containing Oxygenases', PhD Thesis, Groningen, 1994. (c) Lubben, M.; Feringa, B.L. *J. Org. Chem.* **1994**, *59*, 2227.

15 (a) Nie, H.; Aubin, S.M.J.; Mashuta, M.S.; Wu, C.-C.; Richardson, J.F.; Hendrickson, D.N.; Buchanan, R.M. *Inorg. Chem.* **1995**, *34*, 2382. (b) Neves, A.; Aires de Brito, M.; Drago, V.; Griesar, K.; Haase, W. *Inorg. Chim. Acta* **1995**, *237*, 131. (c) Krebs, B.; Schepers, K.; Bremer, B.; Henkel, G.; Althaus, E.; Müller-Warmuth, W.; Griesar, K.; Haase, W. *Inorg. Chem.* **1994**, *33*, 1907. (d) Neves, A.; Erthal, S.M.D.; Drago, V.; Griesar, K.; Haase, W. *Inorg. Chim. Acta* **1992**, *197*, 121. (e) Mashuta, M.S.; Webb, R.J.; McCusker, J.K.; Schmitt, E.A.; Oberhausen, K.J.; Richardson, J.F.; Buchanan, R.M.; Hendrickson, D.N. *J. Am. Chem. Soc.* **1992**, *114*, 3815. (f) Borovik, A.S.; Papaefthymiou, V.; Taylor, L.F.; Anderson, O.P.; Que, L., Jr. *J. Am. Chem. Soc.* **1989**, *111*, 6183.

16 Erxleben, A.; Hermann, J. *J. Chem. Soc., Dalton Trans.* **2000**, 569, and references cited therein.

17 Hage, R. *Recl. Trav. Chim. Pays-Bas* **1996**, *115*, 385.

18 (a) Koga, T.; Furutachi, H.; Nakamura, T.; Fukita, N.; Ohba, M.; Takahashi, K.; Okawa, H. *Inorg. Chem.* **1998**, *37*, 989. (b) Sakiyama, H.; Tamaki, H.; Kodera, M.; Matsumoto, N.; Okawa, H. *J. Chem. Soc., Dalton Trans.* **1993**, 591.

19 (a) Page, E.M. *Coord. Chem. Rev.* **1998**, *172*, 111. (b) Vetter, A.H.; Berkessel, A. *Tetrahedron Lett.* **1998**, *39*, 1741. (c) Modal, S.; Ghosh, P.; Chakravorty, A. *Inorg. Chem.* **1997**, *36*, 59. (d) Asgedom, G.; Sreedhara, A.; Kivikoski, J.; Kolehmainen, E.; Rao, C.P. *J. Chem. Soc., Dalton Trans.* **1996**, 93. (e) Cavaco, I.; Costa Pessoa, J.; Costa, D.; Duarte, M.T.; Gillard, R.D.; Matias, P. *J. Chem. Soc., Dalton Trans.* **1994**, 149. (f) Li, X.; Soo Lah, M.; Pecoraro, V.L. *Inorg. Chem.* **1988**, *27*, 4657.

20 (a) Choudhary, N.F.; Connelly, N.G.; Hitchcock, P.B.; Leigh, G.J. *J. Chem. Soc., Dalton Trans.* **1999**, 4437. (b) Hoshina, G.; Ohba, S.; Nakajima, K.; Ishida, H.; Kojima, M.; Tsuchimoto, M. *Bull. Chem. Soc. Jpn.* **1999**, *72*, 1037. (c) Bunce, S.; Cross, R.J.; Farrugia, L.J.; Kunchandy, S.; Meason, L.L.; Muir, K.W.; O'Donnell, M.; Peacock, R.D.; Stirling,

D.; Teat, S.J. *Polyhedron* **1998**, *17*, 4179. (d) Hughes, D.L.; Kleinkes, U.; Leigh, G.J.; Maiwald, M.; Sanders, J.R.; Sudbrake, C. *J. Chem. Soc., Dalton Trans.* **1994**, 2457.

21 (a) Copeland, E.P.; Kahwa, I.A.; Mague, J.T.; McPherson, G.L. *J. Chem. Soc., Dalton Trans.* **1997**, 2849. (b) Duncan, C.A.; Copeland, E.P.; Kahwa, I.A.; Quick, A.; Williams, D.J. *J. Chem. Soc., Dalton Trans.* **1997**, 917. (c) Kruger, P.E.; Moubaraki, B.; Murray, K.S. *J. Chem. Soc., Dalton Trans.* **1996**, 1223.

22 Mikuriya, M.; Fukuya, M. *Bull. Chem. Soc. Jpn.* **1996**, *69*, 679.

23 Gagné, R.R.; Spiro, C.L.; Smith, T.J.; Hamann, C.A.; Thies, W.R.; Shiemke, A.K. *J. Am. Chem. Soc.* **1981**, *103*, 4073.

24 (a) Gagné, R.R.; Kreh, R.P.; Dodge, J.A. *J. Am. Chem. Soc.* **1979**, *101*, 6917. (b) Mazurek, W.; Bond, A.M.; Murray, K.S.; O'Connor, M.J.; Wedd, A.G. *Inorg. Chem.* **1985**, *24*, 2484.

25 La Crois, R.M. 'Manganese Complexes as Catalysts in Epoxidation Reactions', PhD Thesis, Groningen, 2000, Chapter 4.

26 Nishida, Y.; Kida, S. *J. Chem. Soc., Dalton Trans.* **1986**, 2633.

27 Geetha, K.; Tiwary, S.K.; Chakravarty, A.R.; Ananthakrishna, G. *J. Chem. Soc., Dalton Trans.* **1999**, 4463.

28 Aneetha, H.; Panneerselvam, K.; Liao, T.-F.; Lu, T.-H.; Chung, C.-S. *J. Chem. Soc., Dalton Trans.* **1999**, 2689.

29 Ahlborn, E.; Diemann, E.; Müller, A. *Z. Anorg. Allg. Chem.* **1972**, *394*, 1.

30 The Aldrich Library of Infrared Spectra, Third Edition; Pouchert, C.J.; Aldrich Chemical Company Inc., Milwaukee, 1981, p. 1552.

31 (a) Butler, A. in *Bioinorganic Catalysis*, Reedijk, J., Ed.; Marcel Dekker, New York, 1993, 425-445. (b) Arber, J.M.; Boer, E. de; Garner, C.D.; Hasnain, S.S.; Wever, R. *Biochemistry*, **1989**, *28*, 7968. (c) Boer, E. de; Boon, K.; Wever, R. *Biochemistry*, **1988**, *27*, 1629. (d) Hormes, J.; Kuetgens, U.; Chauvistre, R.; Schreiber, W.; Anders, N.; Vilter, H.; Rehder, D.; Weidemann, C. *Biochim. Biophys. Acta* **1988**, *956*, 293. (e) Vilter, H.; Rehder, D. *Inorg. Chim. Acta* **1987**, *136*, L7. (f) Rehder, D.; Vilter, H.; Duch, A.; Priebsch, W.; Weidemann, C. *Recl. Trav. Chim. Pays-Bas* **1987**, *106*, 408.

32 Messersmidt, A.; Wever, R. *Proc. Natl. Acad. Sci.* **1996**, *93*, 392.

33 Butler, A., In *Bioinorganic Catalysis*, Second Edition, Reedijk, J.; Bouwman, E., Eds.; Marcel Dekker, New York, 1999, Chapter 5.

34 Messerschmidt, A.; Prade, L.; Wever, R. *Biol. Chem.* **1997**, *378*, 309.

35 Vilter, H. *Phytochem.* **1984**, *23*, 1387.

36 For examples of functional model systems for vanadium bromoperoxidase, see Chapter 3.

37 Rehder, D. *Coord. Chem. Rev.* **1999**, *182*, 297.

38 Rehder, D.; Schulzke, C.; Dau, H.; Meinke, C.; Hanss, J.; Epple, M. *J. Inorg. Biochem.* **2000**, *80*, 115.

39 Mahroof-Tahir, M.; Keramidas, A.D.; Goldfarb, R.B.; Anderson, O.P.; Miller, M.M.; Crans, D.C. *Inorg. Chem.* **1997**, *36*, 1657.

40 Plass, W. *Z. Anorg. Allg. Chem.* **1997**, *623*, 461.
41 Fulwood, R.; Schmidt, H.; Rehder, D. *J. Chem. Soc., Chem. Commun.* **1995**, 1443.
42 Julien-Cailhol, N; Rose, E.; Vaisserman, J.; Rehder, D. *J. Chem. Soc., Dalton Trans.* **1996**, 2111.
43 Bashirpoor, M.; Schmidt, H.; Schulzke, C.; Rehder, D. *Chem. Ber./Recueil* **1997**, 651.
44 Vergopoulos, V.; Priebsch, W.; Fritzsche, M.; Rehder, D. **1993**, *32*, 1844.
45 Crans, D.C.; Keramidas, A.D.; Amin, S.S.; Anderson, O.P.; Miller, S.M. *J. Chem. Soc., Dalton Trans.* **1997**, 2799.
46 Loos, M. de; Ligtenbarg, A.G.J.; Esch, J. van; Kooijman, H.; Spek, A.L.; Hage, R.; Kellogg, R.M.; Feringa, B.L. *Eur. J. Org. Chem.* **2000**, 3675.
47 Martinez-Perez, J.A.; Pickel, M.A.; Caroff, E.; Woggon, W.-D. *Synlett* **1999**, *12*, 1875.
48 Hammes, B.S.; Young, V.G., Jr.; Borovik, A.S. *Angew. Chem. Int. Ed.* **1999**, *38*, 666.
49 Shirin, Z.; Hammes, B.S.; Young, V.G., Jr.; Borovik, A.S. *J. Am. Chem. Soc.* **2000**, *122*, 1836.
50 Esch, J. van; Schoonbeek, F.; Loos, M. de; Kooijman, H.; Spek, A.L.; Kellogg, R.M.; Feringa, B.L. *Chem. Eur. J.* **1999**, *5*, 937.
51 Raposo, C.; Almaraz, M.; Martín, M.; Weinrich, V.; Mussóns, M.L.; Alcázar, V. *Chem. Lett.* **1995**, 759.
52 Plass, W. *Angew. Chem. Int. Ed.* **1999**, *38*, 909.
53 Hemrika, W.; Renirie, R.; Dekker, H.L.; Barnett, P.; Wever, R. *Proc. Natl. Acad. Sci. USA*, **1997**, *94*, 2145.
54 Day, V.W.; Klemperer, W.G.; Yagasaki, A. *Chem. Lett.* **1990**, 1267.
55 Anal. Calcd. for $[(^{n}Bu_4N)HV_2O_6]$, $\{C_{16}H_{37}NO_6V_2\}$ C 43.52; H 8.45; N 3.17; V 23.10%. Found: C 43.31; H: 8.14; N 3.21; V 20-25%.

Chapter 5
Vanadium(v) Complexes Based on a Bis(pyridine)-imine Ligand[1]

5.1 Introduction

A dominant structural unit in the coordination chemistry of vanadium in the pentavalent state is the dioxo VO_2^+ moiety.[2] Dioxovanadium(v) complexes $[VO_2L]$ all show a *cis* geometry of the two oxo groups in a five- or six-coordination environment.[3,4] They are protonated on addition of acid to give first $[VO(OH)L]^+$ and then $[V(OH)_2L]^{2+}$, which is probably better formulated as $[VOL]^{2+} + H_2O$.[5] Upon addition of H_2O_2 these compounds are converted into the corresponding oxoperoxovanadium complexes which are known for their oxidising properties.[6] Recent investigations on the reactivity of dioxovanadium(v) complexes with H_2O_2 by Pecoraro *et al.*[7] suggest that peroxide binds either to a protonated form of the vanadium complex or to the complex itself (Scheme 5.1). Subsequently, loss of a bound hydroxide or water molecule in a rate-determining step and rapid rearrangement result in the formation of the oxoperoxovanadium complex.

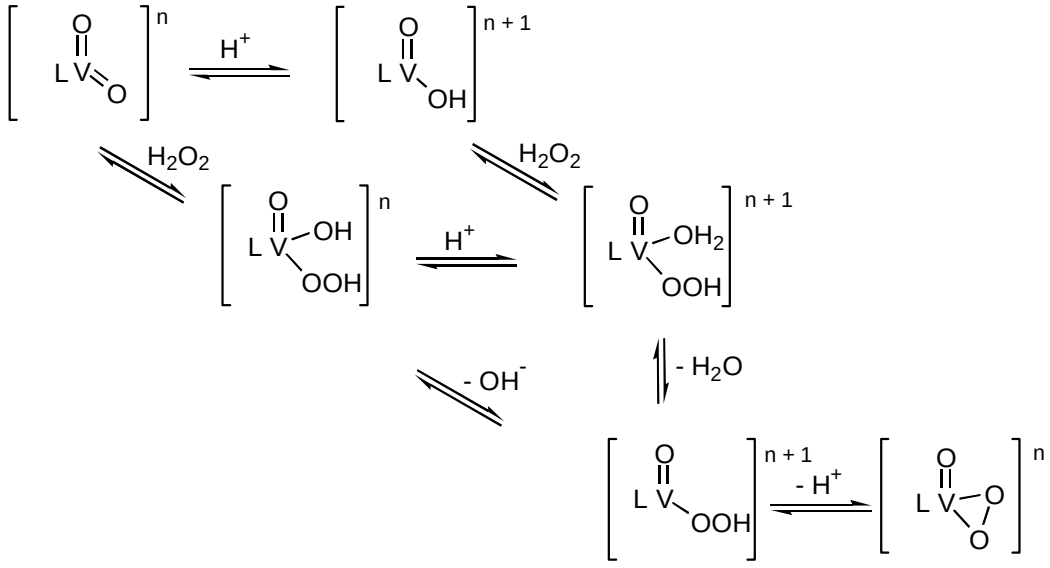

Scheme 5.1 *Proposed mechanism for the formation of oxoperoxovanadium complexes from dioxovanadium(v) compounds and H_2O_2 by Pecoraro et al.*[7]

In our laboratory, a tetradentate Schiff-base ligand (HL) was designed containing two pyridines and one phenol moiety (Scheme 5.2).[8] Good results were obtained in manganese

catalysed epoxidation reactions in the presence of this ligand.[9] In the previous chapter some multidentate O/N-ligands for the formation of vanadium complexes were described, including similar Schiff-base ligands as HL. Therefore this ligand seemed suitable for the synthesis of a dioxovanadium(V) complex, which would be potentially interesting as oxidation catalyst.

5.2 Synthesis and characterisation of 5.1

(2-Hydroxybenzylidene)di(2-pyridin-2-yl)methylamine (HL) was prepared starting from dipyridin-2-yl-methylamine[10] and salicylaldehyde in 93% yield according to a literature procedure.[1,8] HL was subsequently treated with triisopropoxyvanadium(V) oxide [$VO(O^iPr)_3$] in MeOH in the presence of air under reflux conditions for 5 min. An unexpected oxidative cyclisation of the Schiff base ligand L led to the formation of an imidazo[1,5-*a*]pyridine[11] type of ligand (L') and dioxovanadium(V) complex **5.1** [VO_2L'] was obtained in 39% yield.[12,13]

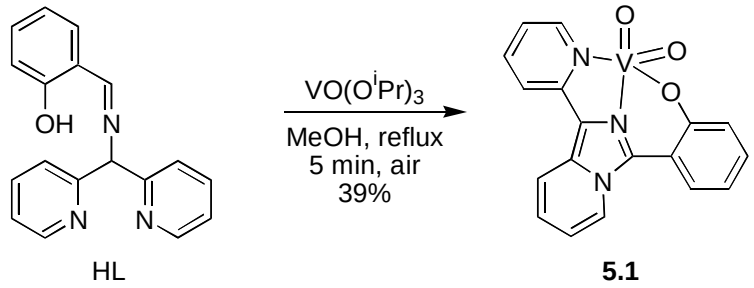

HL **5.1**

Scheme 5.2 *Synthesis of complex **5.1**.*

A related iron mediated oxidative cyclisation of a poly-pyridine ligand has been published by Meunier *et al.*[14] However, in that case the obtained cyclised product was released from the metal, whereas **5.1** was isolated and completely characterised.

Yellow crystals of **5.1** suitable for X-ray analysis were obtained by evaporation of a MeOH/EtOH solution (1:1). An ORTEP plot is shown in Figure 5.1. The compound indeed contains a dioxovanadium(V) moiety. The vanadium centre is pentacoordinated by two nitrogen atoms [2.173(3) and 2.090(3) Å with a bond angle between N(1)-V(1)-N(3) of 72.87(12)°], one oxygen atom of the deprotonated phenolic moiety [1.888(3) Å and a bond angle between N(1)-V(1)-O(1) of 81.44°] and two oxo groups [1.610(4), 1.632(4) Å]. The V=O distances are nearly equal and typical for dioxovanadium(V) complexes in which the oxygens are not involved in hydrogen bonding.[15] The bond angle between the oxo groups and the vanadium centre is 109.02(16)°.

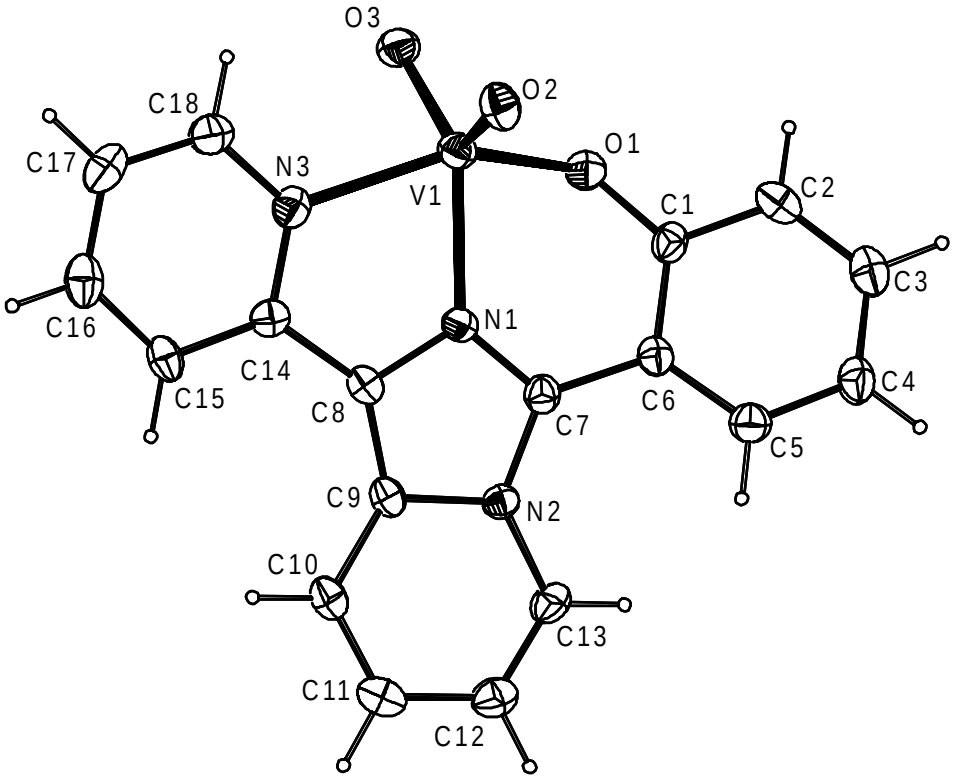

Figure 5.1 *An ORTEP plot of complex **5.1** (50% probability level).*

Table 5.1 *Selected bond distances (Å) and angles (°) of **5.1** with estimated standard deviations (esd's) in parentheses.*

Bond distances			
V(1)-O(1)	1.888(3)	N(1)-C(7)	1.328(2)
V(1)-O(2)	1.610(4)	N(1)-C(8)	1.368(5)
V(1)-O(3)	1.632(4)	N(2)-C(7)	1.381(5)
V(1)-N(1)	2.090(3)	N(2)-C(9)	1.413(4)
V(1)-N(3)	2.173(3)	O(1)-C(1)	1.336(5)
Bond angles			
O(1)-V(1)-O(2)	106.70(14)	O(3)-V(1)-N(3)	88.10(14)
O(1)-V(1)-O(3)	99.68(15)	N(1)-V(1)-N(3)	72.87(12)
O(1)-V(1)-N(1)	81.44(12)	V(1)-O(1)-C(1)	129.8(3)
O(1)-V(1)-N(3)	148.28(13)	V(1)-N(1)-C(7)	129.9(2)
O(2)-V(1)-O(3)	109.02(16)	V(1)-N(1)-C(8)	120.8(2)
O(2)-V(1)-N(3)	99.50(15)	V(1)-N(3)-C(14)	119.5(2)

Electrospray mass (ES / MS) spectra of **5.1** in acetonitrile show peaks at *m/z* 369.8 and 739.3 which are attributed to {VO_2L' + $1H^+$} and {$2VO_2L'$ + $1H^+$}, respectively. In addition, electron ionisation mass spectrometry (EI / MS) measurements show, besides the parent peak at *m/z* 369, a peak at *m/z* 287, which corresponds to the mass of free HL'.

The infrared spectrum of solid **5.1** recorded using a KBr disk, reveals two V=O absorptions. The bands are found at 926 and 949 cm^{-1}, and are assigned to symmetrical ν(O=V=O) and asymmetrical ν(O=V=O) stretching absorptions, respectively.[4i] These observations correspond to the data known from the literature for stretching frequencies of V=O in similar compounds.[4i,4g]

The UV-spectrum of complex **5.1** in acetonitrile exhibits three bands at 212 (ε = 0.89 x 10^4 M^{-1} cm^{-1}), 304 (ε = 0.25 x 10^4 M^{-1} cm^{-1}), 343(ε = 0.36 x 10^4 M^{-1} cm^{-1}), and 417 nm (ε = 0.24 x 10^4 M^{-1} cm^{-1}). This spectrum probably closely resembles the one of the free ligand.[5] Vanadium(v) is a d^0 species and therefore no *d-d* transitions are observed. LMCT bands may be expected due to the high oxidation state of the metal centre, but this is not the case for VO_2^+ species since the *d* orbital energy is raised due to a decrease in net positive charge at the metal centre.[16] In fact, all complexes reported until now containing the VO_2^+ moiety are yellow.[5] On the other hand, complexes with the VO^{3+} or bare V^{5+} bound to phenolic or catecholate groups all show intense absorption bands in the visible region from 550 to 800 nm and these can be assigned to LMCT transitions from the phenolate oxygens to empty *d* orbitals on the vanadium.[17]

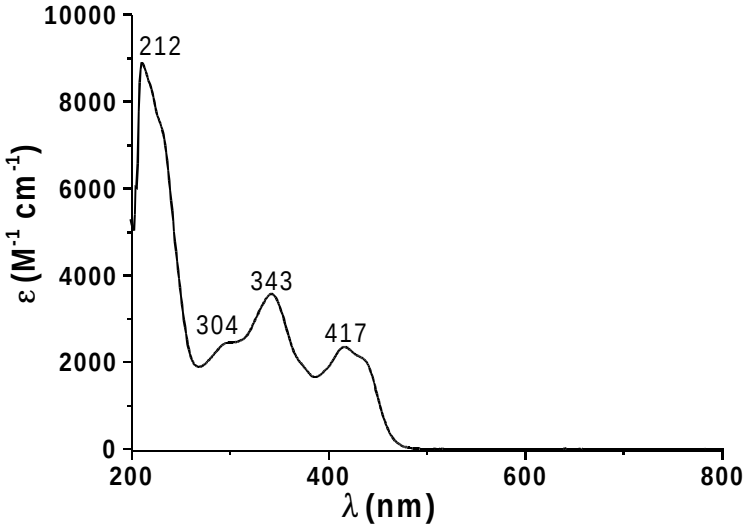

Figure 5.2 *UV-Vis spectrum of **5.1** recorded in acetonitrile.*

5.3 Synthesis and characterisation of 5.2

It was assumed that initially, upon addition of $VO(O^iPr)_3$ to a solution of HL in MeOH complex **5.2** is formed. This complex could then act as a precursor in the formation of **5.1**. In

fact, complex **5.2** was isolated when Schiff base ligand HL was allowed to react with $VO(O^iPr)_3$ under an argon atmosphere at 0 °C in EtOH in 60% yield (Scheme 5.3). Unfortunately, no crystals suitable for X-ray analysis were obtained.

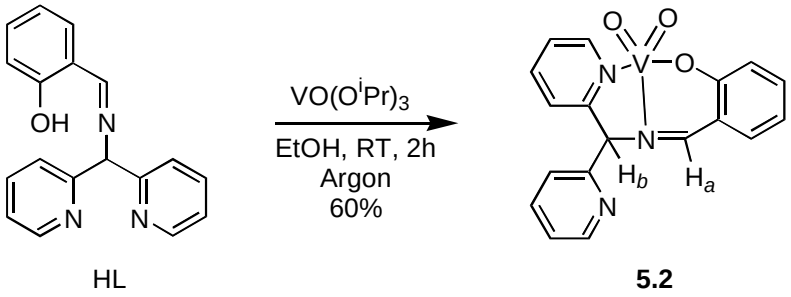

HL **5.2**

Scheme 5.3 *Synthesis of complex **5.2**.*

Complex **5.2** was characterised using electrospray mass spectrometry, UV-Vis, IR, ^1H and ^{51}V NMR measurements. In the ES/MS spectrum of **5.2** in acetonitrile peaks were observed at *m/z* 372.0 $\{VO_2L + 1H^+\}$ and 743.4 $\{2VO_2L + 1H^+\}$. The UV-spectrum of **5.2** in acetonitrile exhibits three bands at 212 nm (ε = 1.89 x 10^4 M^{-1} cm^{-1}), 266 (ε = 1.23 x 10^4 M^{-1} cm^{-1}) and 384 (ε = 0.23 x 10^4 M^{-1} cm^{-1}). As expected, the spectrum resembles the one recorded in acetonitrile of free HL [213 nm (ε = 3.64 x 10^4 M^{-1} cm^{-1}), 262 (ε = 1.95 x 10^4 M^{-1} cm^{-1}) and 319 (ε = 0.45 x 10^4 M^{-1} cm^{-1})], but is clearly distinct from the one for **5.1**.

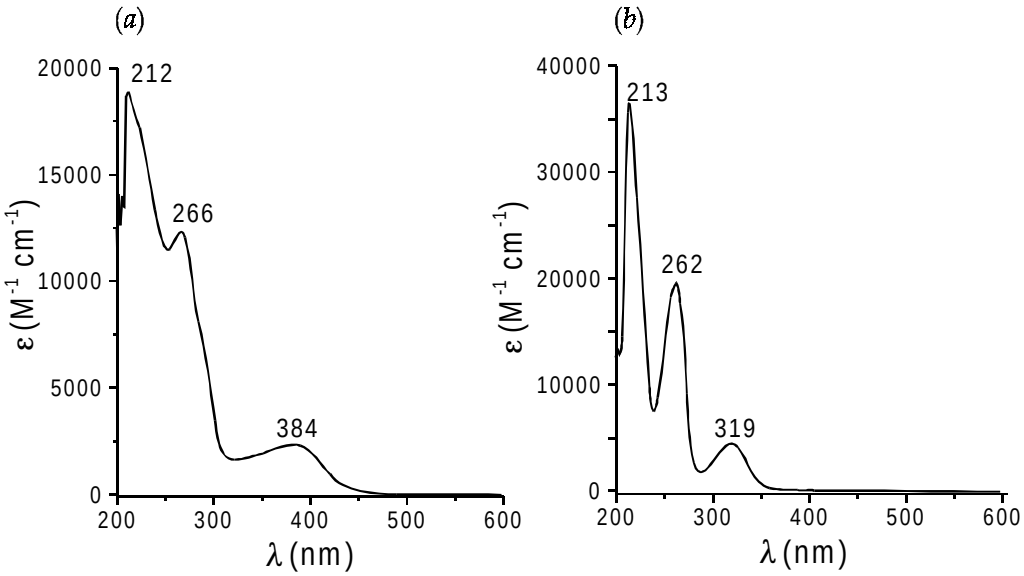

Figure 5.3 *UV-Vis spectra of **5.2** (a) and of HL (b) recorded in acetonitrile.*

The ^{1}H NMR spectra also indicate the difference between the two ligand systems in the vanadium(V) complexes. Complex **5.1** lacks two protons compared with **5.2**, *i.e.* the characteristic imine hydrogen signal (H_a, Scheme 5.3) has disappeared, as well as the signal for the double benzylic proton (H_b). ^{51}V NMR spectra of these two complexes, however, look very similar. Complex **5.1** dissolved in DMSO-d_6 displays a single resonance at –543 ppm (band width, b.w. = 1303 Hz), whereas **5.2** shows a single resonance at –540 ppm (b.w. = 965 Hz). This is a strong indication that the coordination sphere around the vanadium(V) centre is quite similar in both structures,[18] suggesting that in the case of **5.2** the vanadium ion is surrounded by one pyridine nitrogen, the imine nitrogen, the deprotonated phenolic oxygen, and two oxo groups, as depicted in Scheme 5.3. As a result, the second pyridine entity is expected to be non-coordinating.

In the infrared spectrum of solid **5.2** two V=O absorptions are observed as well, at 918 and 953 cm^{-1}. These data support the assumption that one group is not bound to the vanadium ion, since it is known that ν(V=O) modes fall below 900 cm^{-1} for hexacoordinate species and these values shift to higher wave numbers in pentacoordinate complexes.[19]

5.4 Proposed mechanism for the formation of 5.1

It is known for some imines of di(2-pyridyl)methylamine that they cyclise spontaneously to imidazo[1,5-*a*]pyridines by air oxidation.[20] But in our case the vanadium(V) ion is likely to play an active role in the cyclisation process, because HL remained intact even after refluxing in MeOH solution in the air for 3 h. Furthermore, heating a solution of **5.2** in air in MeOH resulted in the formation of **5.1** as was shown by ^{1}H NMR measurements. Based on these results, a reaction mechanism is proposed for the ligand cyclisation reaction resulting in the formation of **5.1** starting from **5.2** (Scheme 5.4).[21]

First the Schiff base ligand is oxidised by vanadium(V) giving a vanadium(IV) species containing one oxo ligand and one hydroxy group (**A** and **B**). This hydroxy moiety can be partially exchanged by a methoxy group originating from the solvent. The radical centre in resonance structure **B** then attacks the non-coordinating pyridine nitrogen resulting in the formation of **C**, which is subsequently oxidised by air to form **5.1**. The involvement of a vanadium(IV) species is supported by results of EPR experiments in DMF with crude **5.1**. An EPR signal was observed at g = 1.97, which was attributed to a mononuclear vanadium(IV) species by comparison with literature data.[22,23] A typical eight-line pattern is observed due to hyperfine interaction between the vanadium nucleus (I = 7/2 and natural abundance = 99.75%) and the unpaired electron.[16] Although the lines were not equally spaced, an isotropic hyperfine coupling parameter A_o of approximately 70 G was determined, which is comparable with values known in the literature for vanadium(IV) compounds.[24]

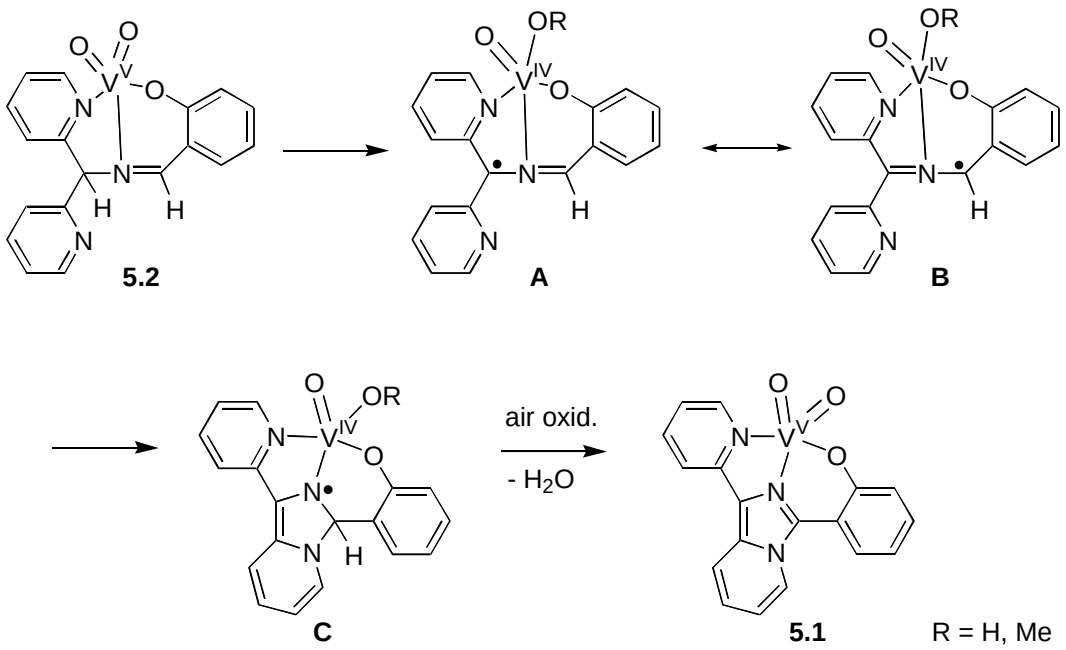

Scheme 5.4 *Proposed mechanism for the formation of complex **5.1**.*

5.5 Reactivity of 5.1

The ^{51}V NMR spectrum of **5.1** dissolved in DMF-d_7 has one resonance at –537 ppm (b.w. = 455 Hz). Addition of a small excess of H_2O_2 converts the vanadium complex to a major species with resonance at –602 (b.w. = 478 Hz). Two small resonances at –578 and –636 ppm also appear (Figure 5.4). The major species was attributed to a peroxo adduct of **5.1**. The observed upfield shift is consistent with the observations of Tracey *et al.*[25] who examined the aqueous formation of complexes of the type $[LVO(O_2)_n]$ in which L is an amino acid ligand. In this case too, shifts to higher field were observed upon coordination of peroxide. The appearance of the two minor species remains unclear. Possibly, these signals may be attributed to the formation of vanadate oligomers, due to decomposition of the peroxo species of **5.1**.

Because it was shown that **5.1** reacts with H_2O_2 in DMF solution presumably resulting in the formation of an oxoperoxovanadium(v) species, this complex was tested as catalyst in the biomimetic bromination reaction of trimethoxybenzene in the presence of H_2O_2 and HCl in DMF as described in Chapter 3. Unfortunately, no catalytic activity was observed. Perhaps, the ligand stabilises the formed peroxo intermediate yielding an inactive peroxo complex.[26] A preliminary oxidation study with **5.2** as the catalyst was not successful either and therefore this was not further elaborated.

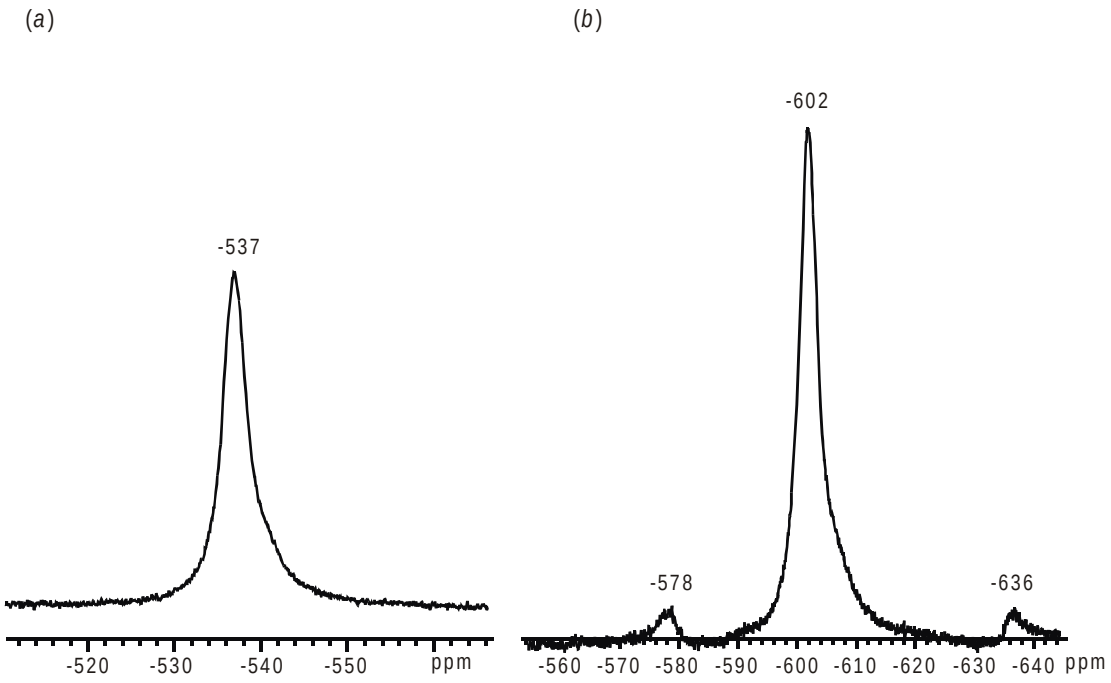

Figure 5.4 *^{51}V NMR spectra in DMF-d_7 of (a) complex **5.1** and (b) **5.1** in the presence of H_2O_2.*

5.6 Conclusions

Schiff base ligand HL was found to be effective in the formation of dioxovanadium(V) complex **5.2** at 0 °C and under an argon atmosphere. However, when HL is heated in the air in the presence of vanadium(V), imidazo-pyridine ligand L' is formed due to an oxidative cyclisation reaction leading to the formation of complex **5.1**. The latter complex proved to be catalytically inactive, although it reacts with H_2O_2 as suggested by the ^{51}V NMR data.

5.7 Experimental section

5.7.1 General information

For general information, see Chapter 2. Ligand HL was prepared as previously reported.[1,8] Triisopropoxyvanadium(V) oxide [VO(O^iPr)$_3$] was purchased from Aldrich and used as received. MeOH and EtOH were distilled from Mg, and Et_2O over Na/benzophenone, under an atmosphere of N_2. ^{51}V-NMR spectra were recorded on a Varian VXR-300

spectrometer (relative to $\delta(VOCl_3) = 0$ ppm). The X-ray structure was determined by Dr. A. L. Spek (University of Utrecht).

5.7.2 X-ray crystal determination of 5.1

A yellow coloured needle-shaped crystal of **5.1** having approximate dimensions of 0.10 x 0.12 x 0.43 mm was used for the X-ray study.

Crystal data. $C_{18}H_{12}N_3O_3V$, M_r = 369.25, monoclinic, space group $P2_1/c$ (no. 14) with a = 7.0787(16), b = 16.833(5), c = 13.573(5) Å, β = 115.21(2)°, V = 1463.3(8) Å^3, Z = 4, D_c = 1.676 g cm^{-3}, μ(MoKα) = 7.0 cm^{-1}, 6346 reflections measured, 3006 independent, R(int) = 0.106, F(000) = 752 , θ_{max} = 26.5°, ω scan, T = 150 K.

Data collection, structure analysis, and refinement. The intensity data were collected on an Enraf-Nonius CAD4T on a rotating anode with graphite monochromated Mo-Kα radiation (λ = 0.71073 Å). Data were corrected for absorption (PLATON / DELABS). The structure was solved by direct methods (SHELXS86) and refined on F^2 using SHELXL97. Hydrogen atoms were taken into account at calculated positions. Convergence was reached at R = 0.0579 for 1984 reflections with $I > 2\sigma(I)$ and 226 parameters.

5.7.3 Syntheses

[L'VO_2] (5.1)[12] To a hot solution of HL (50 mg, 1.73 mmol) in MeOH (5 ml) was added $VO(O^iPr)_3$ (0.5 ml, 0.21 mmol) by syringe. The resulting dark red solution was heated under reflux in the presence of air for 5 min. After slow cooling down to RT, **5.1** was obtained as a dark yellow powder (25 mg, 39%). Crystals suitable for X-ray analysis were obtained by slow evaporation of a MeOH / EtOH solution (1:1) of **5.1**. ^{1}H NMR (DMSO-d_6) 9.24 (m, 1H), 9.05 (m, 1H), 8.49 (m, 2H), 8.28(m, 2H), 7.54 (m, 3H), 7.27 (m, 1H), 7.09 (m, 2H); ^{51}V NMR (DMSO-d_6) –543 (b.w. = 1303 Hz) and (DMF-d_7) –537 (b.w. = 455 Hz); ES / MS (CH_3CN) m/z 369.8 {VO_2L' + 1H$^+$}, 739.3 {2VO_2L' + 1H$^+$}; λ_{max} (CH_3CN) 212 nm (ε = 0.89 x 10^4 M^{-1} cm^{-1}), 304 (ε = 0.25 x 10^4 M^{-1} cm^{-1}), 343 (ε = 0.36 x 10^4 M^{-1} cm^{-1}), 417 (ε = 0.24 x 10^4 M^{-1} cm^{-1}).

[LVO_2] (5.2) A suspension of HL (101 mg, 0.35 mmol) in 3 ml of EtOH was stirred at 0 °C under an atmosphere of argon. $VO(O^iPr)_3$ (91 mg, 0.37 mmol) was added slowly by syringe. The reaction mixture was stirred for 2h at 0 °C. The solvent was decanted, the slightly yellow precipitate washed with Et_2O (4 x 5 ml) and dried in vacuo (78 mg, 60%). ^{1}H NMR (DMSO-d_6) 9.22 (s, 1H), 8.86 (s, 2H), 8.06 (m, 2H), 7.70 (m, 3H), 7.57 (m, 3H), 6.93 (m, 3H); 7.09 (m, 2H); ^{51}V NMR (DMSO-d_6) –540 (b.w. = 965 Hz); ES / MS (CH_3CN) m/z 372.0 {VO_2L + 1H$^+$}, 743.4 {2VO_2L + 1H$^+$}; λ_{max} (CH_3CN) 212 nm (ε = 1.89 x 10^4 M^{-1} cm^{-1}), 266 (ε = 1.23 x 10^4 M^{-1} cm^{-1}), 384 (ε = 0.23 x 10^4 M^{-1} cm^{-1}).

5.8 References

1 Part of this chapter has been described in: Ligtenbarg, A.G.J.; Spek, A.L.; Hage, R.; Feringa, B.L. *J. Chem. Soc., Dalton Trans.* **1999**, 659.

2 See Chapter 1.

3 *Comprehensive Coordination Chemistry*, Wilkinson, G., Ed.; Pergamon Press, Oxford, 1987, *3*, 501.

4 See *e.g.* (a) Plass, W.; Pohlmann, A.; Yozgatli, H.-P. *J. Inorg. Biochem.* **2000**, *80*, 181. (b) Süss-Fink, G.; Stanislas, S.; Shul'pin, G.B.; Nizova, G.V.; Stoeckli-Evans, H.; Neels, A.; Bobillier, C.; Claude, S. *J. Chem. Soc., Dalton Trans.* **1999**, 3169. (c) Yamaki, R.T.; Paniago, E.B.; Carvalho, S.; Lula, I.S. *J. Chem. Soc., Dalton Trans.* **1999**, 4407. (d) Lee, M.-H.; Nam, H.H.; Hayashi, S. *Polyhedron* **1998**, *17*, 55. (e) Asgedom, G.; Sreedhara, A.; Kivikoski, J.; Valkonen, J.; Kolehmainen, E.; Rao, C.P. *Inorg. Chem.* **1996**, *35*, 5674. (f) Asgedom, G.; Sreedhara, A.; Kivikoski, J.; Kolehmainen, E.; Rao, C.P. *J. Chem. Soc., Dalton Trans.* **1996**, 93. (g) Asgedom, G.; Sreedhara, A.; Kivikoski, J.; Valkonen, J.; Rao, C. *J. Chem. Soc., Dalton Trans.* **1995**, 2459. (h) Schulz, D.; Weyhermüller, T.; Wieghardt, K.; Nuber, B. *Inorg. Chim. Acta* **1995**, *240*, 217. (i) Liu, H.-X.; Wang, W.; Wang, X.; Tan, M.Y. *J. Coord. Chem.* **1994**, *33*, 347. (j) Vergopoulos, V.; Priebsch, W.; Fritzsche, M.; Rehder, D. *Inorg. Chem.* **1993**, *32*, 1844.

5 Butler, A.; Carrano, C.J. *Coord. Chem. Rev.* **1991**, *109*, 61.

6 Butler, A.; Clague, M.J.; Meister, G.E. *Chem. Rev.* **1994**, *94*, 625.

7 Hamstra, B.J.; Colpas, G.J.; Pecoraro, V.L. *Inorg. Chem.* **1998**, *37*, 949.

8 La Crois, R.M. 'Manganese Complexes as Catalysts in Epoxidation Reactions', PhD Thesis, Groningen, 2000, Chapter 2.

9 Ref 8, Chapter 4.

10 Niemers, E.; Hiltmann, R. *Synthesis* **1976**, 593.

11 Davey, D.D. *J. Org. Chem.* **1987**, *52*, 1863.

12 Complex **5.1** was stable for at least several weeks when stored under an atmosphere of dry argon.

13 Dr. M. Döring (University of Jena) informed us about a copper mediated cyclisation of ligand HL. An abstract was recently published: Döring, M.; Ciesielski, M.; Görls, H. *J. Inorg. Biochem.* **1999**, *74*, 117.

14 Renz, M.; Hemmert, C.; Donnadieu, B.; Meunier, B. *Chem. Commun.* **1998**, 1635.

15 Root, C.A.; Hoeschele, J.D.; Cornman, C.R.; Kampf, J.W., Pecoraro, V.L. *Inorg. Chem.* **1993**, *32*, 3855.

16 Micera, G.; Sanna, D. in *Vanadium in the Environment, Part One: Chemistry and Biochemistry*, Nriagu, J.O., Ed.; John Wiley & Sons, New York, **1998**, Chapter 7.

17 Bonadies, J.S.; Carrano, C.J. *J. Am. Chem. Soc.* **1986**, *108*, 4088.

18 Conte, V.; Di Furia, F.; Moro, S. *J. Mol. Catal. A* **1995**, *104*, 159.

19 Crans, D.C.; Shin, P.K. *J. Am. Chem. Soc.* **1994**, *116*, 1305.

20 (a) Krapcho, A.P.; Powell, J.R. *Tetrahedron Lett.* **1986**, *27*, 3713. (b) Edgar, M.T.; Pettit, G.R.; Krupa, T.S. *J. Org. Chem.* **1979**, *44*, 396. (c) Grigg, R.; Kennewell, P.; Savic, V.; Sridharan, V. *Tetrahedron* **1992**, *48*, 10423.

21 (a) Fossey, J.; Lefort, D.; Sorba, J. *Free Radicals in Organic Chemistry*, John Wiley & Sons, New York, 1995. (b) Fukuda, T.; Sakamoto, F.; Sato, M.; Nakano, Y., Tan, X.S.; Fujii, Y. *Chem. Commun.* **1998**, 1391.

22 Bonchio, M.; Conte, V.; Di Furia, F.; Modena, G.; Moro, S.; Edwards, J.O. *Inorg. Chem.* **1994**, *33*, 1631.

23 (a) Hagen, H.; Barbon, A.; Van Faassen, E.E.; Lutz B.T.G.; Boersma, J.; Spek, A.L.; Van Koten, G. *Inorg. Chem.* **1999**, *38*, 4079. (b) Chakravarty, J.; Dutta, S.; Dey, A.; Chakravorty, A. *J. Chem. Soc., Dalton Trans.* **1994**, 557. (c) Cavaco, I.; Pessoa, J.C.; Costa, D.; Duarte, M.T.; Gillard, R.D.; Matias, P. *J. Chem. Soc., Dalton Trans.* **1994**, 149. (d) Chakravarty, J.; Dutta, S.; Kumar Chandra, S.; Basu, P.; Chakravorty, A. *Inorg. Chem.* **1993**, *32*, 4249.

24 Klich, P.R.; Daniher, A.T.; Challen, P.R.; McConville, D.B.; Youngs, W.J. *Inorg. Chem.* **1996**, *35*, 347.

25 Tracey, A.S.; Jaswal, J.S. *J. Am. Chem. Soc.* **1992**, *114*, 3835.

26 See Chapter 4.

Chapter 6

Triazole Ligands for the Formation of Vanadium(v) Complexes

6.1 Introduction

In the previous chapter the synthesis and X-ray structure of a dioxovanadium(v) complex with an imidazo[1,5-*a*]pyridine type of ligand (HL' in Figure 6.1) was described. However, preliminary catalytic studies showed that this complex was inactive in the biomimetic bromination reaction. Also, the complex could not easily be obtained in large quantities, which complicated further reactivity studies. Therefore it would be interesting to synthesise a similar but more readily accessible and air stable complex which would, as a consequence, be more useful in investigations towards catalytic oxidation. For this purpose, 1,2,4-triazole based ligand H_2L^1 was chosen (Figure 6.1).[1,2] A phenol substituent and a pyridine moiety attached to this triazole unit could provide a comparable coordination environment around the vanadium ion as in complex **5.1**.

It is known in the literature that 1,2,4-triazole derivatives are very suitable as ligands for transition metals.[3] The triazole unit can coordinate to the metal ion in two possible ways: in an imidazole (*via* N4) or in a pyrazole geometry (*via* N1). It can also act as a bridging unit between two metal centres, which usually involves metal coordination to N1 and N2. Although *e.g.* Cu, Ni, Ag, Pt, Ru, Os, Co, Zn, Mn, and Fe complexes based on these type of compounds are known,[3] no examples of vanadium–1,2,4-triazole complexes are found in the literature.

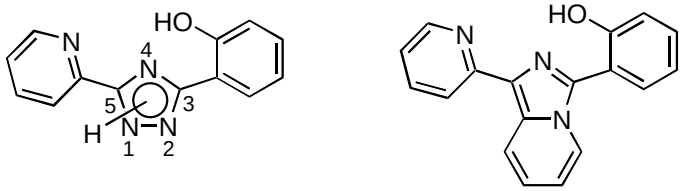

H_2L^1 HL'

Figure 6.1 *3-(2-Hydroxyphenyl)-5-(pyridin-2-yl)-1,2,4-triazole (H_2L^1)* [1,2] *and ligand L' (see complex **5.1**).*

6.2 Synthesis and characterisation of complex 6.1

Triazole ligand H_2L^1 (Figure 6.1)[1,2] was treated with sodium metavanadate ($NaVO_3$) in MeOH under an argon atmosphere. The resulting air stable dioxovanadium(v) complex

$[VO_2L^1](NH_4)\cdot CH_3CN$, **6.1**, was obtained upon crystallisation from $MeOH/Et_2O$ in the presence of an excess of NH_4PF_6 as yellow needles in 44% yield (Scheme 6.1). In this way, crystals suitable for X-ray analysis were obtained.

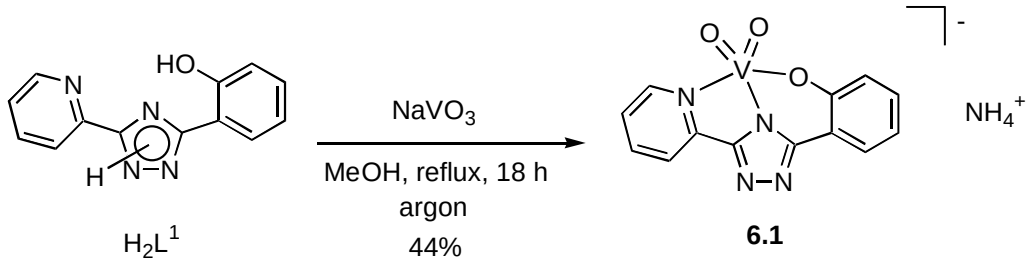

Scheme 6.1 *Synthesis of complex **6.1**.*

An ORTEP plot of the anion of **6.1** is shown in Figure 6.2. The ammonium ion which acts as the counter ion is omitted for clarity. Selected bond distances and angles are shown in Figure 6.1. The vanadium ion is pentacoordinated by the pyridine nitrogen atom [2.170(3) Å], the phenolate oxygen [1.910(3) Å], a nitrogen of the triazole unit [2.031 Å] and two oxo groups [1.625(3) and 1.629(3) Å]. The triazole unit is deprotonated and coordination to the vanadium occurs in an imidazole binding geometry (N1). The bond angle between the oxo groups and the vanadium centre is 109.02(16). The triazole unit and the pyridine moiety of the ligand in **6.1** are nearly planar (*e.g.* the torsion angle between N4-C9-C8-N1 is 0.20°). However, the phenol unit is slightly twisted compared to the nitrogen heterocycles (the torsion angle between O1-C1-N4-C9 is 174.40°) as shown in Figure 6.3*b*. In the crystal lattice one solvent molecule (MeOH) is incorporated per molecule of **6.1** as illustrated in Figure 6.3*a*.

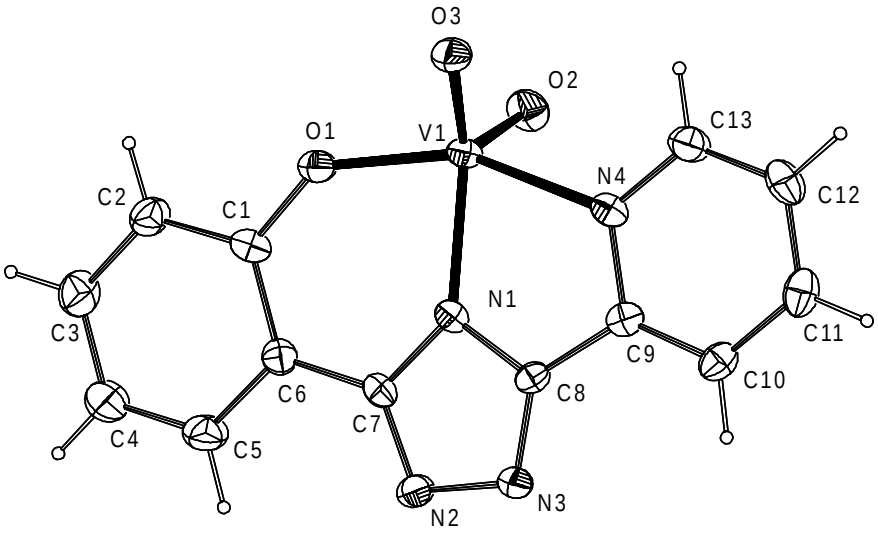

Figure 6.2 *ORTEP plot of the anion of **6.1** (50% probability level).*

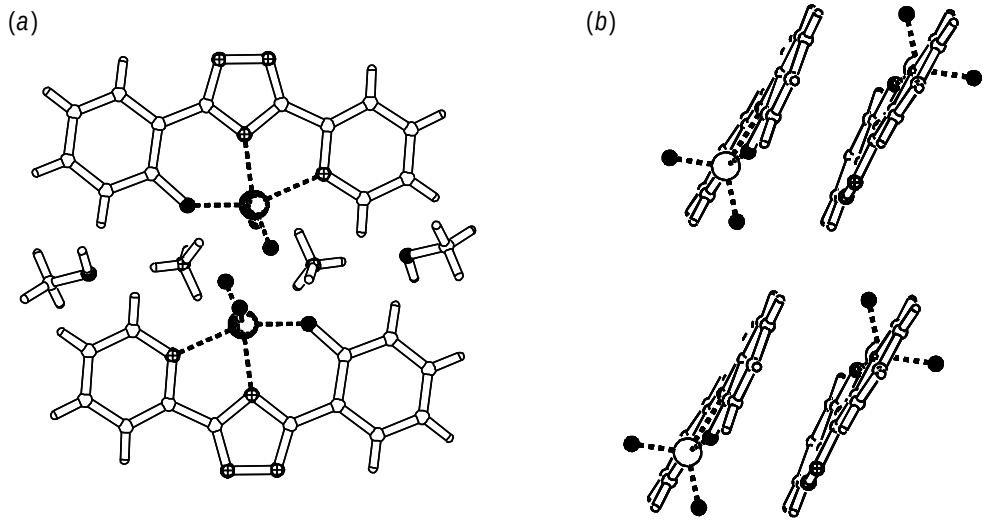

Figure 6.3 *PLUTON plots of **6.1**: (a) Two residues including the ammonium cations and two MeOH solvent molecules, (b) Spacial arrangement of **6.1** residues in the unit cell.*

Table 6.1 *Selected bond distances (Å) and angles (°) of **6.1** with estimated standard deviations (esd's) in parentheses.*

Bond distances			
V-O(1)	1.910(3)	N(2)-N(3)	1.388(5)
V-O(2)	1.629(3)	N(1)-C(8)	1.350(5)
V-O(3)	1.625(3)	N(3)-C(8)	1.327(5)
V-N(1)	2.031(4)	N(1)-C(7)	1.364(6)
V-N(4)	2.170(3)	N(2)-C(7)	1.336(5)
O(1)-C(1)	1.355(5)		
Bond angles			
O(1)-V-O(2)	104.69(14)	O(3)-V-N(1)	134.08(14)
O(2)-V-O(3)	109.85(15)	N(1)-V-N(4)	73.31(14)
O(1)-V-O(3)	99.02(14)	V-N(1)-C(7)	134.4(3)
O(1)-V-N(4)	153.06(13)	V-N(1)-C(8)	121.5(3)
O(1)-V-N(1)	81.78(13)	V-O(1)-C(1)	137.2(3)
O(2)-V-N(4)	94.95(14)	V-N(4)-C(9)	118.7(3)
O(2)-V-N(1)	114.29(15)		

The bond lengths and angles of **6.1** closely resemble those found in complex **5.1** (Chapter 5). Accordingly, the coordination environment around the vanadium centres is as expected very similar, although in the latter case only one negatively-charged donor atom (the

phenolate) is bound to the metal centre, whereas in **6.1** the triazole unit is also negatively charged. This is reflected in the shorter V(1)-N(1) distance [2.031(4) Å] compared to V(1)-N(1) in **5.1** [2.090(3) Å]. However, these distances fall well within the range found for V-N distances in similar complexes.[4,5] Also the V-O bond distances are normal.[5,6,7,8] The shortest intermolecular V-V distances in **6.1** are 6.2981(18) and 6.3508(18) Å.

Complex **6.1** was further characterised using electrospray mass (ES/MS) spectrometry, IR and UV-Vis spectroscopy, and ^{1}H and ^{51}V NMR measurements. The negative ES/MS spectrum for **6.1** recorded in MeOH shows a parent peak at m/z 318.9, which corresponds to $\{VO_2L^1 - NH_4^+\}$. In the infrared spectrum of solid **6.1** using a KBr disk, two V=O absorptions were observed at 921 and 930 cm^{-1}, which can be assigned to symmetrical ν(O=V=O) and asymmetrical ν(O=V=O) stretching vibrations, respectively.[5,9] These are well within the range expected for dioxovanadium(V) compounds.[5,10,11]

The ^{51}V NMR spectrum was recorded in DMF solution and a single resonance was observed at -541 ppm (b.w. = 849 Hz), which is similar to the value found for **5.1** (at -537 ppm). Addition of a small amount of H_2O_2 converts the vanadium complex into two species with resonances at -569 (b.w. = 538 Hz) and -597 ppm (b.w. = 335 Hz). The latter value is similar to the major resonance observed for **5.1** in the presence of H_2O_2 at -602 ppm.[12] These values are within the expected range for vanadium-peroxo adducts.[13]

As already mentioned in Chapter 5, VO_2^+ compounds do not display intense ligand to metal charge transfer (LMCT) bands.[14] Even no visible charge transfer bands are observed when VO_2^+ is coordinated to phenolate groups. This is due to raising of the *d* orbital energy as a consequence of the decrease in net positive charge at the vanadium centre.[15] The UV spectrum recorded in DMF therefore exhibits only one band at 296 nm (ε = 4.3 x 10^4 M^{-1} cm^{-1}) and a small shoulder at 370 nm (ε = 1.6 x 10^4 M^{-1} cm^{-1}), which closely resembles the spectrum of the free ligand (306 nm (ε = 9.68 x 10^4 M^{-1} cm^{-1})).

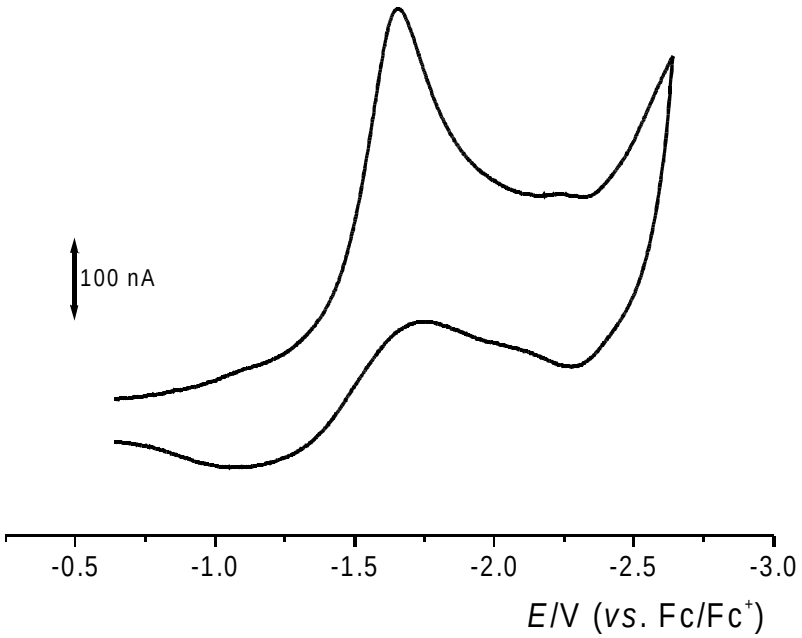

Figure 6.4 *Cyclic voltammogram of **6.1** in DMF at RT. Scan rate 100 mV s^{-1}.*

The redox properties of **6.1** in DMF have been examined using cyclic voltammetry measurements.[16] The cyclic voltammogram of **6.1** displays an irreversible reduction peak at $E_{1/2}$ = -1.65 V (relative to the Fc/Fc^+ couple), indicating the degradation of the formed vanadium species (Figure 6.4).

6.3 Synthesis of the ligands H_3L^2 and HL^3

To examine the influence of ligand variations on the stability and reactivity of the vanadium complex, two analogues of H_2L^1 were synthesised. In one ligand the pyridine part was replaced by a phenol unit yielding 3,5-bis(*o*-hydroxyphenyl)-1,2,4-triazole (H_3L^2, Scheme 6.2). The synthesis was carried out as reported in the literature.[17] Heating of phenylsalicylate (salol) and salicylamide yielded *o*-salicylsalicylamide, which was rearranged quantitatively to disalicylamide by boiling with water. Subsequently, treatment with $HClO_4$ in acetic anhydride yielded the cyclised perchlorate product, which was converted to the triazole compound by reaction with hydrazine monohydrate.

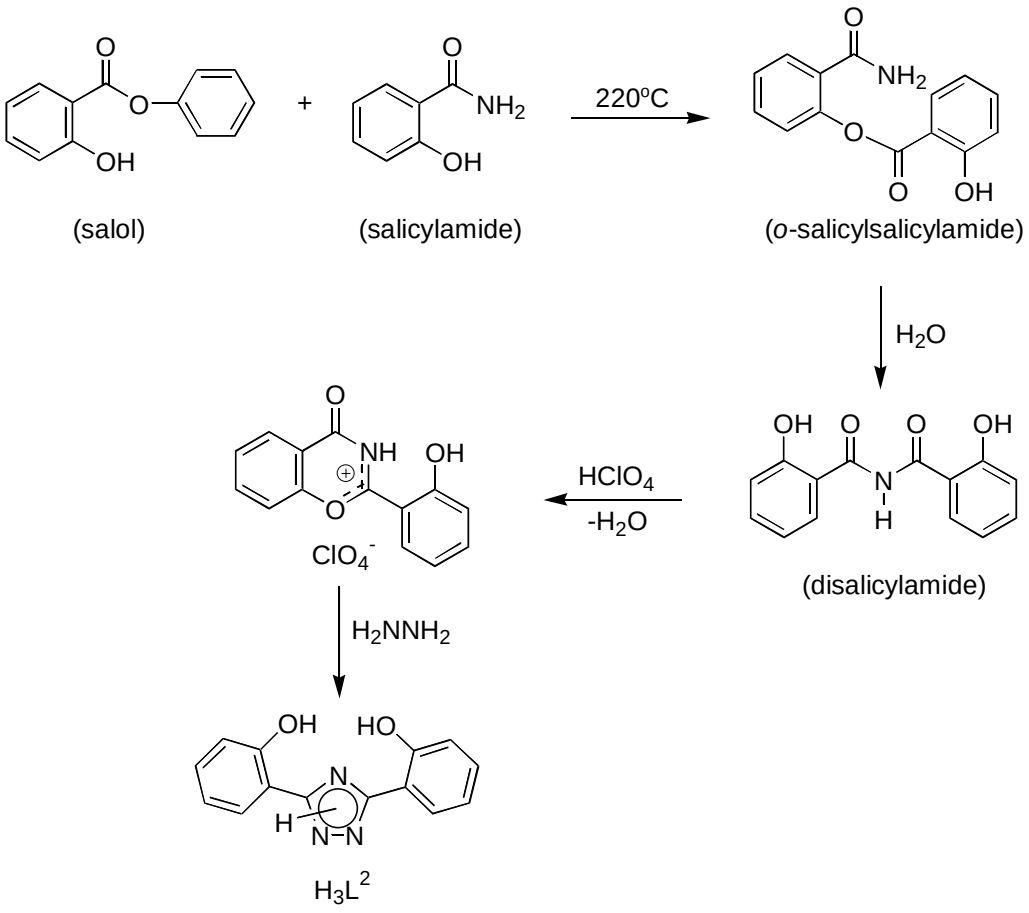

Scheme 6.2 *Synthesis of ligand H_3L^2.[17]*

In the second ligand, 3,5-bis(pyridin-2-yl)-1,2,4-triazole HL^3, two pyridine units are present (Figure 6.5). It was synthesised following a literature procedure[18] by heating 2-cyanopyridine and hydrazine monohydrate under reflux. The resulting 3,6-di(2-pyridyl)-1,2-dihydro-1,2,4,5-tetrazine was rearranged to 3,5-di(2-pyridyl)-4-amino-1,2,4-triazole by addition of nitric acid (5 M). Treatment of this product with nitrous acid afforded the desired triazole ligand HL^3.

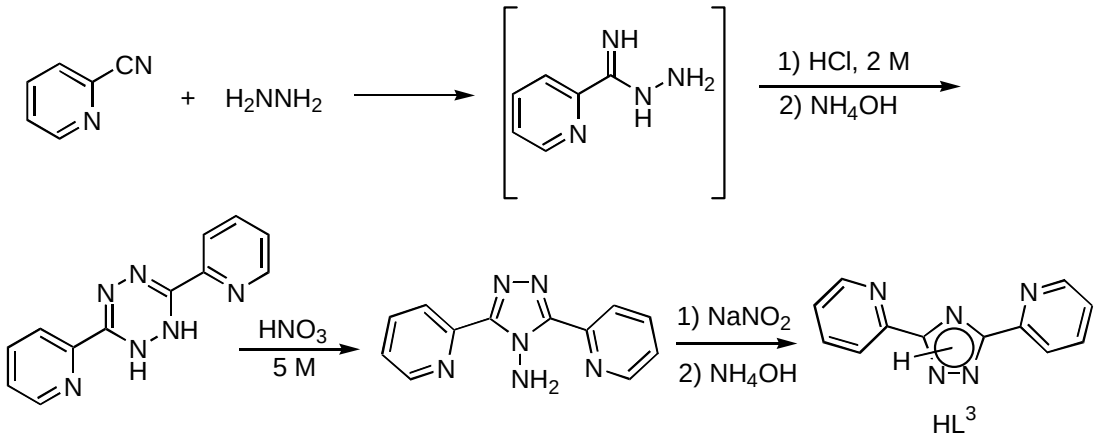

Figure 6.5 *Synthesis of ligand HL^3.*[18]

6.4 Synthesis and characterisation of complex 6.2

The corresponding vanadium complex of H_3L^2, was synthesised using triisopropoxy-vanadium(V)oxide [$VO(O^iPr)_3$] in a 1 : 1 mixture of CH_3CN and MeOH as solvent. Dinuclear complex **6.2** was formed in 77% yield (Scheme 6.3). Dark green crystals suitable for X-ray analysis were obtained by slow evaporation of a $MeOH/CH_3CN$ solution of the complex. An ORTEP plot of **6.2** is shown in Figure 6.6.

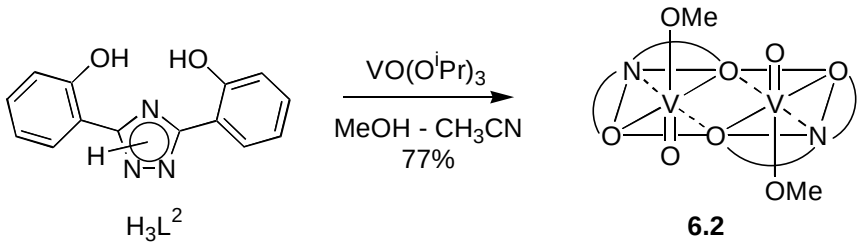

Scheme 6.3 *Synthesis of complex **6.2**.*

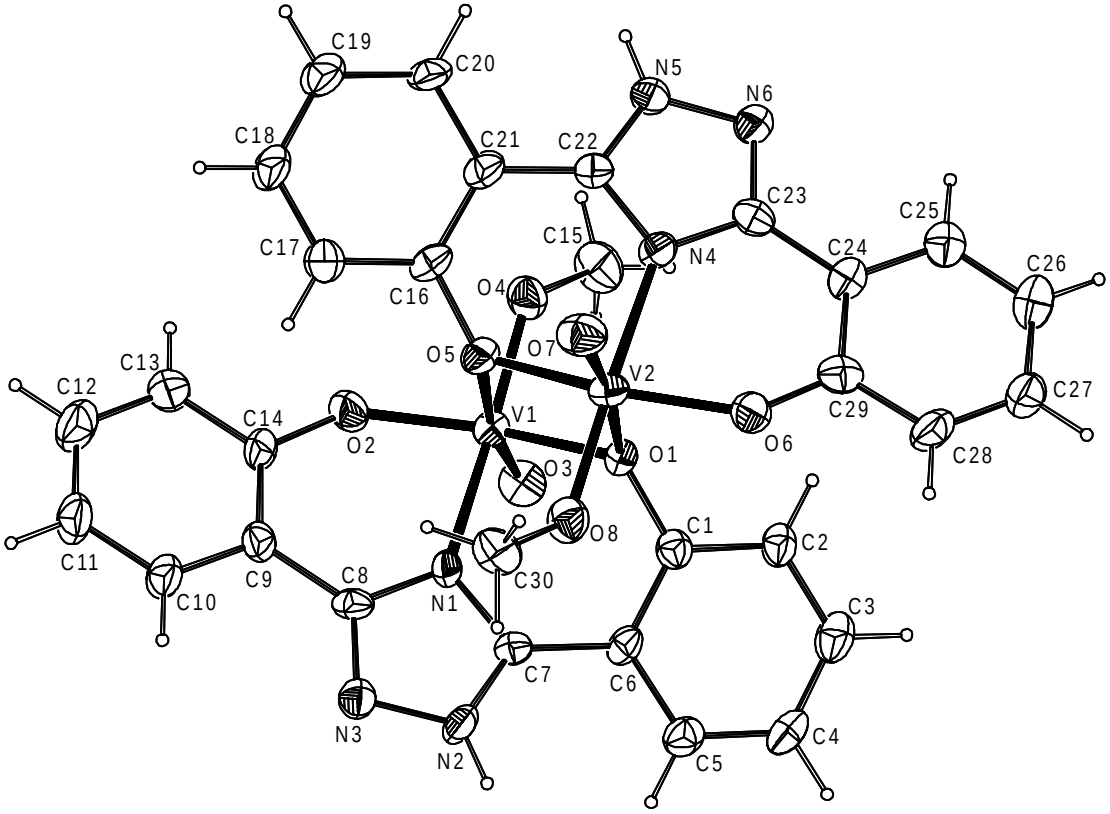

Figure 6.6 *ORTEP plot of **6.2** (50% probability level).*

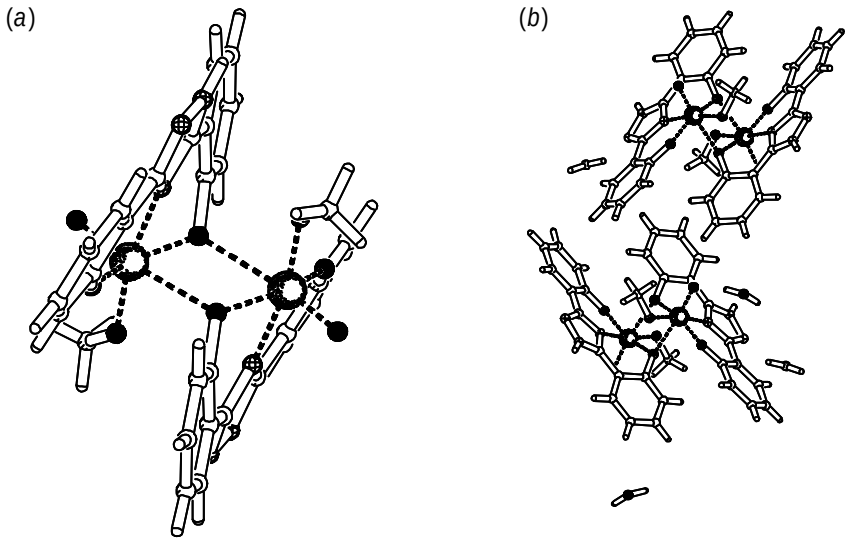

Figure 6.7 *PLUTON plots of **6.2** (a) Side-view of the dinuclear complex and (b) Spacial arrangement of **6.2** in the unit cell including the incorporated H_2O molecules.*

In the dimeric complex, each vanadium ion is located in a slightly distorted octahedral environment. In the equatorial plane, two phenolic oxygens, the triazole nitrogen atom, and a methoxy group are coordinated to the metal. An oxo group occupies one apical position, whereas in the other apical position one phenolic oxygen of the other ligand residu is coordinating. In this manner a V_2O_2 four-membered ring is formed in which one phenolic oxygen atom of each ligand is bridging between the two metals. Consequently, the other phenolic moietie of the ligand system is merely bound to one vanadium centre. This is clearly shown in Figure 6.7*a*. Bond distances are listed in Table 6.2 and bond angles in Table 6.3. From these tables it appears that the complex is nearly centrosymmetric. The V=O bonds are 1.594(4) Å for V(1)-O(3) and 1.597(4) Å for V(2)-O(7), respectively. These short distances are consistent with a strong trans effect,[19,5b] which is reflected in weak ligation trans to the oxo group, *i.e.* elongation of the V-O(phenolate) bonds [V(1)-O(5) is 2.352(3) Å and V(1)-O(1) is 2.314(3) Å]. Normally V-O(phenolate) bond lengths are within the range of 1.85-2.01 Å.[8,10,20] The intramolecular V-V distance is 3.46 Å. The ligands are oriented parallel to each other, but like in **6.1** the ligand is not completely planar. One phenol moiety is significantly twisted compared to the triazole unit and the other phenol unit. Remarkably, the triazole unit is not deprotonated unlike L^1 in **6.1**, but a methoxide originating from the solvent is bound to the metal centre. Vanadium is in its +5 oxidation state, which means that the complex is neutral.

In the literature there is only one example in which a similar structure is reported for vanadium(V).[21] Bis[2-(2'-hydroxyphenyl)-chinolin-8-olato]dimethoxo-dioxo-divanadium(V) **6.3** (Figure 6.8) was formed when oxovanadium(IV) sulfate was reacted with 2-(2'-hydroxyphenyl)-8-quinolinol under aerobic conditions in the presence of methanol. In this case also, the vanadium ions are surrounded by a methoxy group, an oxo unit, the tridentate ligand, and the bridging phenolate group of the other ligand residu.

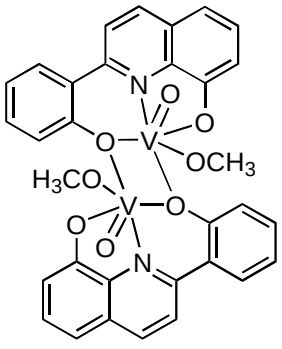

Figure 6.8 *Bis[2-(2'-hydroxyphenyl)-chinolin-8-olato]dimethoxo-dioxo-vanadium(V)* ***6.3****.*

It is known that vanadium(V) prefers hexacoordination rather than pentacoordination, which is a driving force towards the formation of the dimer,[22] but often an additional ligand, like mesityl,[23] a hydroxo unit[24] or an oxo group[5b,22a,25,26,27] serves as the bridge between the metal centres. Similar binding modes as in **6.2**, *i.e.* with a bridging phenolate moiety from

the ligand, have been proposed for V(IV) species[28,29] and recently, the crystal structure of a V(IV) complex with bridging phenol groups based on *N*,*N*-bis(2-hydroxybenzyl)aminoacetic acid was published.[30]

Table 6.2 *Selected bond distances (Å) of* ***6.2*** *with esd's in parentheses.*

V(1)-O(1)	1.944(3)	V(2)-O(5)	1.940(3)
V(1)-O(2)	1.855(4)	V(2)-O(6)	1.860(4)
V(1)-O(3)	1.594(4)	V(2)-N(4)	2.116(4)
V(1)-N(1)	2.109(4)	V(2)-O(1)	2.314(3)
V(1)-O(5)	2.352(3)	V(2)-O(7)	1.597(4)
V(1)-O(4)	1.799(4)	V(2)-O(8)	1.804(4)
N(1)-C(8)	1.349(7)	N(4)-C(22)	1.348(6)
N(1)-C(7)	1.364(6)	N(4)-C(23)	1.353(7)
N(3)-C(8)	1.325(7)	N(5)-C(22)	1.312(7)
N(2)-N(3)	1.368(6)	N(5)-N(6)	1.382(7)
N(2)-C(7)	1.317(6)	N(6)-C(23)	1.315(7)
O(2)-C(14)	1.364(7)	O(5)-C(16)	1.370(6)
O(1)-C(1)	1.376(6)	O(6)-C(29)	1.330(7)

Table 6.3 *Selected angles and torsion angles (°) of* ***6.2*** *with esd's in parentheses.*

O(1)-V(1)-O(2)	154.54(16)	O(5)-V(2)-O(6)	154.72(16)
O(1)-V(1)-N(1)	81.92(15)	O(5)-V(2)-N(4)	81.97(15)
O(2)-V(1)-N(1)	82.21(17)	O(6)-V(2)-N(4)	82.18(17)
O(1)-V(1)-O(3)	96.70(17)	O(5)-V(2)-O(7)	97.27(18)
O(2)-V(1)-O(2)	104.29(19)	O(7)-V(2)-N(4)	93.42(18)
O(4)-V(1)-O(5)	81.59(15)	O(1)-V(2)-O(8)	83.63(14)
V(1)-O(1)-V(2)	108.16(15)	V(1)-O(5)-V(2)	106.86(16)
O(5)-V(1)-O(1)-V(2)	1.62(12)	O(3)-V(1)-O(4)-C(15)	-22.3(5)

Complex **6.2** was further characterised using ES/MS, IR, and UV-Vis spectroscopy, and ^{1}H and ^{51}V NMR measurements. The IR spectrum of **6.2** in the solid state shows only one signal at 870 cm^{-1} for the ν(V=O) stretching mode, which indicates that the two V=O groups are indistinguishable. This value supports the conclusion that the vanadium centre is hexacoordinate, since it is known that ν(V=O) modes fall below 900 cm^{-1} for vanadium complexes having such coordination geometry.[31] A broad shoulder at 2900 cm^{-1} and a medium absorption at 1035 cm^{-1} are indicative for coordinated methoxides.[32]

The UV spectrum recorded in acetonitrile displays a band at 309 nm (ε = 8.9 x 10^3 M^{-1} cm^{-1}, assuming that the complex is monomeric, *vide infra*), and a small shoulder at 390 nm (ε = 2.6 x 10^3 M^{-1} cm^{-1}). Again, this spectrum is quite similar to that of the free ligand in DMF (310 nm, ε = 1.2 x 10^4 M^{-1} cm^{-1}). The absence of LMCT bands suggests that in acetonitrile the dimeric complex dissociates forming a mononuclear dioxovanadium species.[14] This conclusion is supported by the ^{1}H NMR spectrum recorded in acetonitrile, since only one set of aromatic signals is observed. In the case of the dimeric structure **6.2**, the bridging of one of the phenolic parts of the ligand between the two vanadium ions would make the ligand unsymmetrical and the aromatic proton absorption originating from the two phenol groups would, as a result, be clearly distinct. The presence of such a monomeric species in acetonitrile could not be established with ES/MS spectrometry. Possibly a neutral species like [L^2VO(OH)] is formed, which could not be detected. On the other hand, the negative ES/MS spectrum for **6.1** recorded in MeOH, shows several peaks, which could be assigned to corresponding monomeric and dimeric complexes with vanadium in +4 or +5 oxidation states. For example, the peak at *m/z* 317.0 is double charged and corresponds to {$V_2O_2(L^2)_2$ - $2H^+$}, which means that the vanadium(V) ions are reduced, providing the corresponding vanadium(IV) dimeric complex. More indications for the formation of vanadium(IV) species are found in the signals at *m/z* 634.9 {$(V^{IV})_2O_2(L^2)_2$ - $1H^+$}, *m/z* 652.0 {$(V^{IV}O)(V^{V}O)(L^2)_2$ + O^{2-}} and *m/z* 653.1 {$(V^{IV})_2O_2(L^2)_2$ + HO^-}. The same trends are displayed in the peaks at *m/z* 666.0, which can be assigned to the mixed-valence species {$(V^{IV}O)(V^{V}O)(L^2)_2$(OMe) - $1H^+$} and 667.1 which corresponds to {$(V^{IV}O)_2(L^2)_2$(OMe)}. The signal at *m/z* 347.9 can be assigned to {VOL^2(OMe) - H^+}, which is an indication that the dimer partly dissociates into monomers under these conditions.

The redox properties of complex **6.2** were examined too. The cyclic voltammogram recorded at –20 °C in butyronitrile is shown in Figure 6.9.

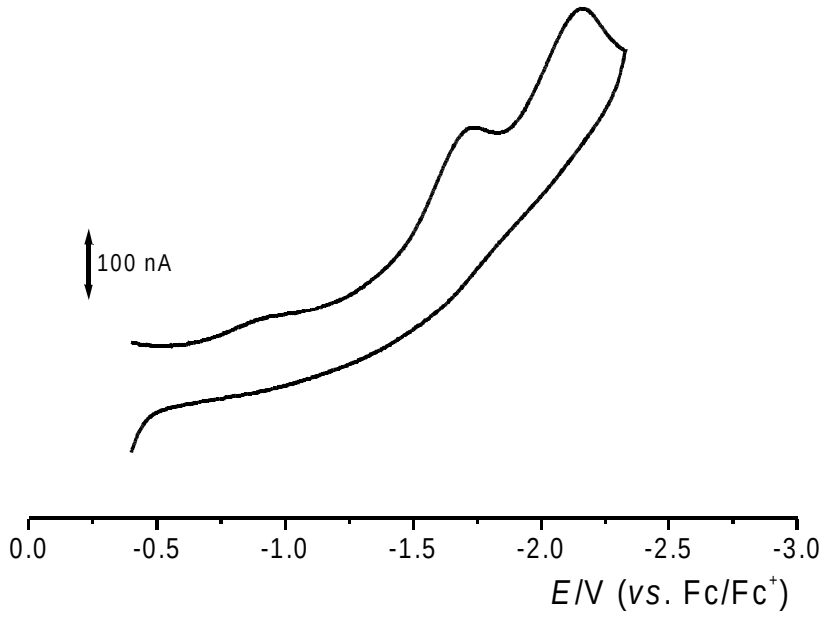

Figure 6.9 *Cyclic voltammogram of **6.2** in butyronitrile at -20°C. Scan rate 100 mV* s^{-1}.

The cyclic voltammogram shows two irreversible reduction peaks at $E_{1/2}$ = -1.72 V (relative to the Fc/Fc^+ couple) and $E_{1/2}$ = -2.16 V. Clearly, the reduced vanadium species is unstable.

The ^{51}V NMR spectrum of **6.2** was recorded in DMF solution and a single resonance was observed at -600 ppm (b.w. = 502 Hz), whereas addition of a small amount of H_2O_2 converts the vanadium complex into a species with a resonance at -604 ppm (b.w. = 1041 Hz), indicative for a peroxo species (*vide supra*).

6.5 Complexation studies using HL^3

Ligand HL^3, comprising of the 1,2,4-triazole unit and two pyridine groups, was also used for the synthesis of vanadium complexes (Scheme 6.4). A variety of vanadium containing reagents and reaction conditions were used to prepare well defined vanadium(IV) or vanadium(V) species. However, no well-defined complexes could be obtained. Scheme 6.4 shows a summary of these attempts. The reactions were performed under an argon atmosphere and $(VO_2Cl_2[PPh_4])$[33], $VO(O^iPr)_3$, $NaVO_3$, and NH_4VO_3 were used in acetonitrile, diethyl ether and methanol solutions of the ligand. Unfortunately, only starting materials were isolated after purification of the crude products, according to ^1H NMR analysis and EI and electrospray mass spectrometry measurements.

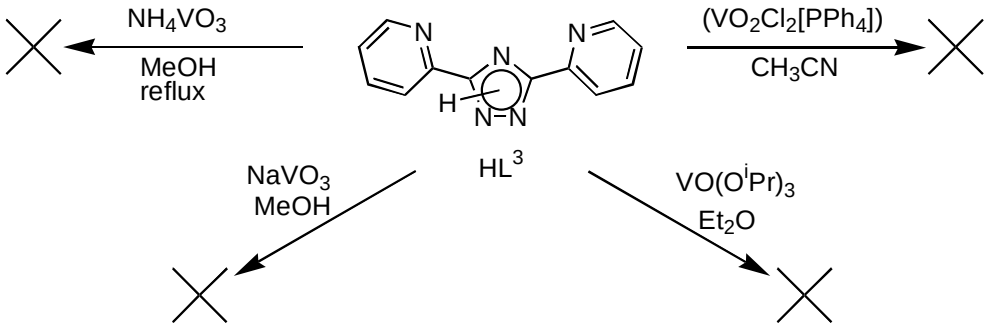

Scheme 6.4 *Attempts to prepare an oxovanadium complex of HL^3.*

A possible explanation for the apparently unstability of the well-defined vanadium complexes with HL^3 is that in this ligand only nitrogen donor atoms are present which makes the ligand less suitable for stabilisation of V(V). There are a few examples of oxovanadium(IV) or (V) complexes of all nitrogen ligand systems.[14,34] Deprotonation of the triazole unit would provide a negatively charged nitrogen atom, but perhaps this is still not sufficient for the formation of a stable complex. In comparison with **6.1** and **6.2**, vanadium(V) appears to need two negative donor sites, since a phenolate and a triazole unit are present in **6.1** and two phenolate groups in **6.2**. Another possibility is that the angle between the triazole nitrogen and the two pyridine nitrogens of this 'pincer'-type ligand[35] is too large, which makes it unsuitable for the incorporation of the small vanadium(V) ion.[36]

6.6 Catalytic oxidation reactions

The catalytic properties of the complexes **6.1** and **6.2** were examined in epoxidation reactions using cinnamyl alcohol and styrene as substrates.[37] Vanadium-catalysed epoxidations of allylic alcohols are often regioselective and high yields are usually obtained due to coordination of the alcohol functionality to the metal centre.[38] As a consequence, intramolecular oxygen transfer from a coordinated alkylperoxo moiety to the double bond of the coordinated allylic alcohol is easily accomplished.[39] $VO(acac)_2$ is often used for these type of reactions.[40] Therefore, the turnover numbers reached by **6.1** and **6.2** were compared with those found for $VO(acac)_2$ under the same reaction conditions. In each case 5 mol% of catalyst was used and the reaction was performed at 25 °C under an argon atmosphere. As oxidant was used either 2 equivalents of ^{t}BuOOH (~ 5 M solution in decane) or 5 equivalents of a 30% aqueous solution of H_2O_2. Toluene or acetonitrile were used as solvent, although **6.1** is only soluble in these solvents when a few drops of DMF are added. Table 6.4 summarises the results of the catalytic experiments.

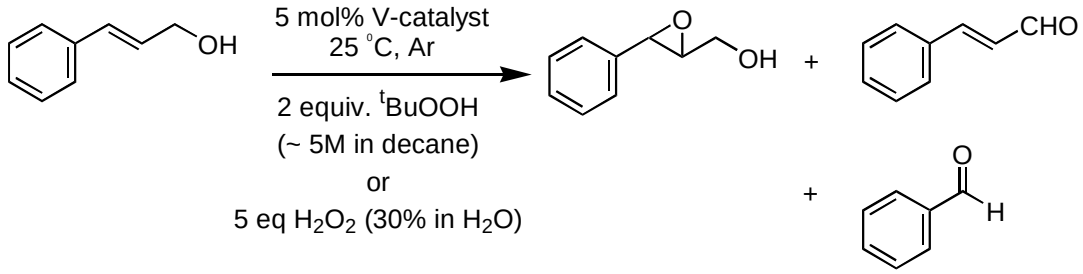

Scheme 6.5 *Catalytic oxidation of cinnamyl alcohol to the corresponding epoxide and cinnamaldehyde.*

Table 6.4 *Catalytic oxidation experiments using cinnamyl alcohol as substrate.*

Catalyst	Oxidant	Solvent	Time (h)	Epoxide (t.o.n.)[a]	Aldehyde (t.o.n.)[a]	Benzaldehyde (t.o.n.)[a]
6.1	^{t}BuOOH	CH_3CN[b]	3	1	1	<0.1
6.2	^{t}BuOOH	CH_3CN	3	2	2	<0.1
$VO(acac)_2$	^{t}BuOOH	CH_3CN	3	17	2	0.5
6.1	^{t}BuOOH	toluene[b]	4	7	1	<0.1
6.2	^{t}BuOOH	toluene	4	13	2	1
$VO(acac)_2$	^{t}BuOOH	toluene	4	22	0.5	0.5
6.1	H_2O_2	toluene[b]	4	2	1.5	<0.1
6.2	H_2O_2	CH_3CN	4	4	2	7
$VO(acac)_2$	H_2O_2	toluene	4	1	1	1
$VO(acac)_2$	H_2O_2	CH_3CN	4	5	1.5	8

(a) t.o.n. = mol product/mol catalyst. (b) A small amount of DMF is added to dissolve the catalyst.

When acetonitrile is used as solvent and ^{t}BuOOH as oxidant, $VO(acac)_2$ appears to be the most reactive catalyst. After 3 h, almost full conversion of the substrate is achieved and 17 turnovers towards the epoxide are obtained. The commonly accepted reaction mechanism for epoxidation of allylic alcohols using the $VO(acac)_2$ / ^{t}BuOOH system is shown in Scheme 6.6.[41]

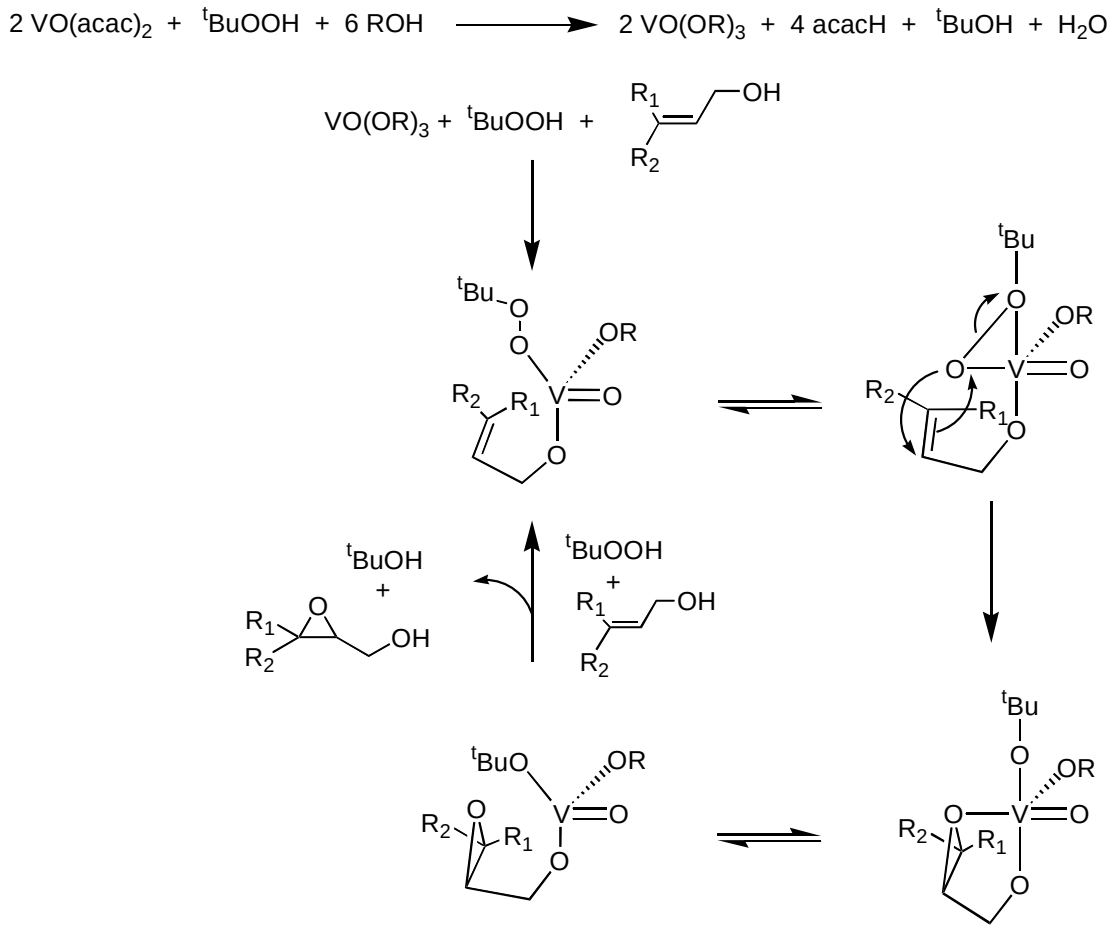

Scheme 6.6 *The commonly accepted mechanistic scheme for allylic epoxidations using $VO(acac)_2$ and ^{t}BuOOH.*[41a,42]

^{t}BuOOH rapidly oxidises $VO(acac)_2$ to a V(V) species in which the acetylacetonate ligand is completely dissociated from the metal. The V(V) complex then reacts with ^{t}BuOOH to yield an alkylperoxovanadium complex. In the presence of the allylic alcohol, an alkoxo-alkylperoxovanadium complex is formed in which an intramolecular oxygen transfer occurs, providing the epoxide. Accordingly, coordination of the hydroxy group of cinnamyl alcohol to vanadium results usually in high selectivity. However, in the presence of **6.1** and **6.2** equal amounts of epoxide and aldehyde are obtained, although both in low quantities. This may be an indication that the alcohol functionality experiences difficulties in binding to the vanadium ion, due to lack of appropriate free coordination sites on the metal centre. The

oxidising species in these cases may be a V(IV)← O^{t}Bu-O$^\bullet$ species, originating from a V(V)-OO^{t}Bu triangular peroxidic species by homolytic cleavage of the V(V)-O(peroxo)bond (Scheme 6.7).[43]

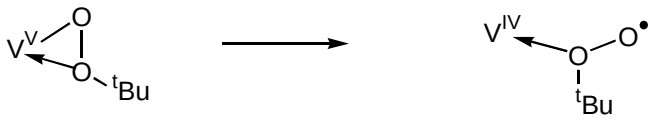

Scheme 6.7 *Proposed homolytic cleavage of the V(V)-peroxo bond of an alkylperoxovanadium(V) complex according to ref 43.*

The fact that the formation of scission products is not observed can be attributed to the presence of the ligands on vanadium. Basic ligands on the metal are known to increase the stability of the complex with concomitant decrease in their reactivity, but prevent the cleavage of epoxides to aldehydes.[44]

The stability of the peroxo intermediate depends on the nature of the solvent.[44] In the less polar solvent toluene, the catalytic activity of **6.1** and **6.2** is increased considerably. Complex **6.2** is again the most active one of these two, with 13 turnovers towards the epoxide and 2 towards cinnamaldehyde. However, 1 undesired turnover towards benzaldehyde also took place.

When H_2O_2 is used as the oxidant, hydroxyl radicals may be generated by decomposition of a peroxovanadium(V) complex (see Scheme 6.8).[45] Another possibility is the formation of a V(IV)-O-O$^\bullet$ species, which also can act as the oxidative species.[44] The radical nature of the reaction is reflected in diminished selectivity when H_2O_2 was used instead of ^{t}BuOOH. The use of **6.2** or $VO(acac)_2$ resulted in the large amounts of benzylaldehyde, which may be formed by oxidative cleavage of the epoxide. Although less active, **6.1** appears to be a more selective catalyst since no benzylaldehyde was produced.

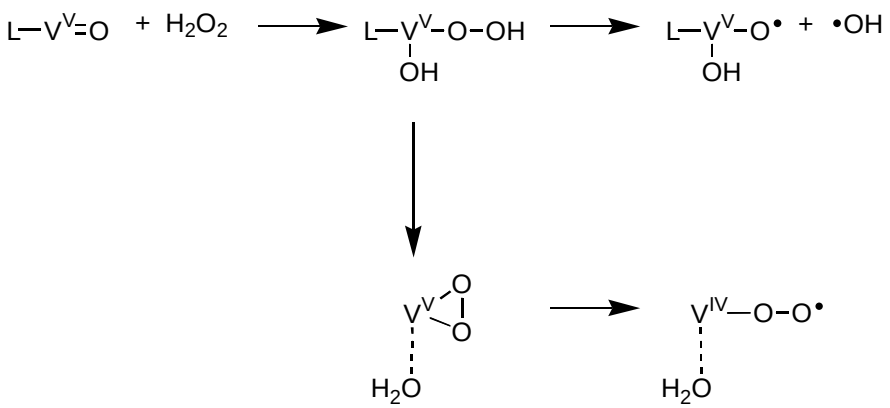

Scheme 6.8 *Possible mechanisms for activation of hydrogen peroxide by vanadium(V).*

When toluene is used as solvent in the presence of $VO(acac)_2$, maximally 3 turnovers were obtained. This observation can be explained when the catalysis mainly occurs *via* the formation of hydroxyl radicals, since toluene can serve as a $^{\bullet}OH$ trap more efficiently than acetonitrile.[46]

Vanadium(v) complexes are also capable of epoxidation of unfunctionalised alkenes with peroxides.[37,38] Usually, epoxidations in the presence of alkylhydroperoxides are more selective than those using H_2O_2.[41a] Furthermore, the reactions are often inhibited by water and alcohols.[47] Therefore, complexes **6.1** and **6.2** were tested as catalysts for the alkene epoxidation using ^{t}BuOOH (~ 5 M in decane, 2 equiv). Styrene was chosen as substrate (Scheme 6.9). It is known that in acetic acid solutions at 70 °C, styrene and styrene derivatives are oxidised to the corresponding aldehydes using $VO(acac)_2$ and hydrogen peroxide.[48] Yields ranging from 85 to 98% have been reported depending on the substituents on the aromatic rings. Since we aimed to make epoxides instead of aldehydes, the oxidation experiments were performed at 25 °C, using 5 mol% of catalyst in toluene or acetonitrile solutions. Under these conditions, epoxidation is expected to occur. The results are shown in Table 6.5**.**

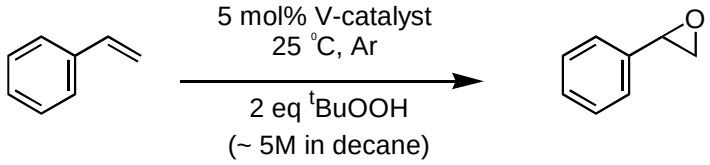

Scheme 6.9 *Catalytic oxidation of styrene.*

Table 6.5 *Catalytic oxidation experiments of styrene using 2 equiv. of ^{t}BuOOH (~ 5M in decane).*

Catalyst	Solvent	Time (h)	Styrene oxide (t.o.n.)	Benzaldehyde (t.o.n.)
6.1	toluene	4	1	<0.1
6.2	CH_3CN	4	1	<0.1
$VO(acac)_2$	toluene	4	2	1

Unfortunately, both complexes only gave stoichiometric amounts of styrene oxide. A detailed study by Mimoun, in 1986, of selective stoichiometric epoxidation of various alkenes with an oxo[*N*-(2-oxidophenyl)salicylideneaminato]vanadium(v) alkylperoxide gave insight in the possible reaction mechanism.[47] A mechanistic scheme was proposed in which first the substrate coordinates to the vanadium in the butylperoxo complex. Then, insertion

into one of the vanadium-peroxo bonds occurs, after which the peroxometallocycle collapses yielding the epoxide. The reaction becomes catalytic when the coordinated butoxy group is replaced by additional ^{t}BuOOH, providing the original vanadium(V) peroxide (Scheme 6.10). Possibly, in the case of **6.1** and **6.2** this final step does not occur due to high stability of the alkoxide species, resulting in a stoichiometric reaction.

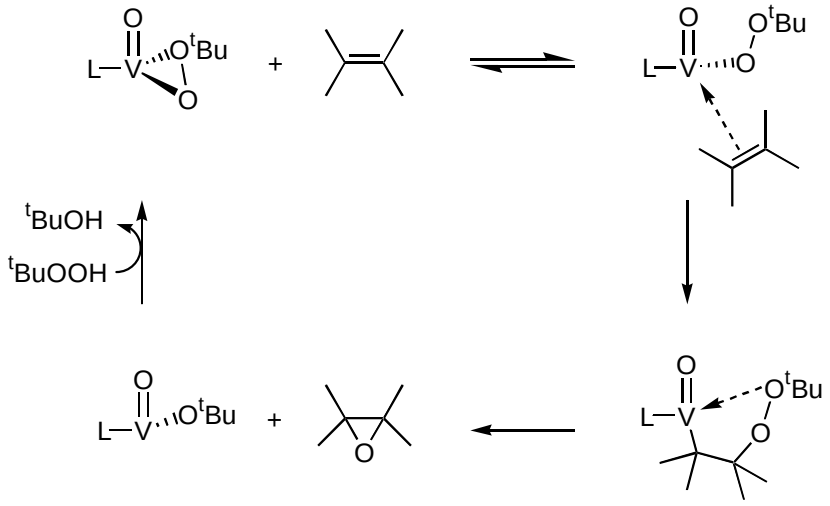

Scheme 6.10 *Proposed heterolytic mechanism for epoxidation of unfunctionalised alkenes by a vanadium(V) butylperoxide complex.* [37]

Another mechanism which also could be applicable to this system is depicted in Scheme 6.11. This mechanism is commonly proposed for hydroxylation reactions.[43]

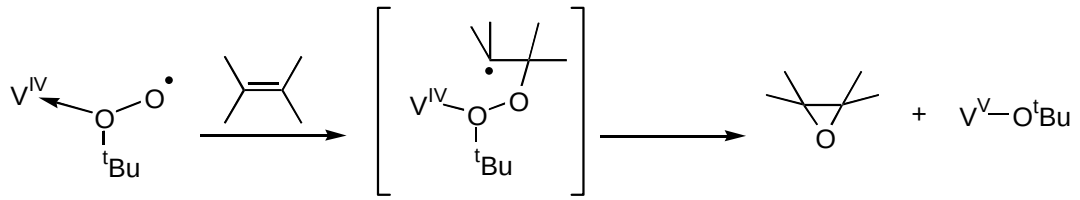

Scheme 6.11 *Proposed homolytic mechanism for epoxidation of unfunctionalised alkenes by a vanadium-tert-butylperoxide complex.*[43]

Here, a V(IV)←O^{t}Bu-O$^{\bullet}$ diradical species (*vide supra*) reacts which the alkene forming a free radical intermediate, which homolytically decomposes to provide the epoxide and the V(V) compound with a coordinated butoxy group (Scheme 6.11). In this case, when additional ^{t}BuOOH is able to replace the *tert*-butoxy group, the process becomes catalytic too.

Normally, oxidations which are homolytic in nature provide lower selectivity and lower yields of the epoxides. However, because of the low turnover numbers found using **6.1** and **6.2** as catalysts, it is impossible to distinguish between the discussed heterolytic and homolytic pathways. The results were compared with those found for $VO(acac)_2$ under the same conditions. In the latter case, almost no catalytic activity was observed as well, since two turnover numbers towards styrene oxide and one towards benzaldehyde were obtained after 4 h. Again, these low turnover numbers do not allow reliable mechanistic considerations.

6.7 Conclusions

In this chapter, the synthesis of two new vanadium(V) complexes **6.1** and **6.2** is described, based on 1,2,4-triazole ligands H_2L^1 and H_3L^2 which are air stable and easily obtainable. The complexes were examined as catalysts in epoxidation reactions of cinnamyl alcohol and styrene. The results were compared with those obtained for the often used commercially available vanadium(IV) reagent $VO(acac)_2$. For the allylic alcohol, the best results were obtained using toluene as the solvent and ^{t}BuOOH as the oxidant. Although $VO(acac)_2$ appeared to be the more active catalyst, reasonable turnover numbers are obtained especially for **6.2**. Because of different product selectivities for $VO(acac)_2$ compared to **6.1** and **6.2**, it was assumed that different reaction mechanisms are operating for these two classes of catalysts.

When using H_2O_2 as the oxidant, there is not only a significant drop in the catalytic activity of the complexes, but also more of the cleavage product benzaldehyde is produced. This may be caused by the formation of hydroxyl radicals.

The catalysts were also tested on their ability to oxidise styrene to styrene epoxide with ^{t}BuOOH. However, only stoichiometric amounts of the epoxide are formed using **6.1** and **6.2** and also in the presence of $VO(acac)_2$ only low oxidation activity was observed. Obviously, these complexes are not suitable for the epoxidation of unfunctionalised alkenes. Despite the fact that they are active in allylic alcohol epoxidation, they can not compete with $VO(acac)_2$ concerning activity and reaction rates.

6.8 Experimental section

6.8.1 General information

For general information, see Chapters 2 and 4. GC analyses were performed on a Hewlett Packard 6890 Gas Chromatograph using a HP-1 dimethylpolysiloxane column. Calibration was performed using authentic samples of the epoxide and alkene and authentic samples of

further byproducts. Conversions and yields were determined using bromobenzene as internal standard, and calculated using the Chemstation software. X-ray structures were determined by Dr. M. Lutz and Dr. A.L. Spek at the University of Utrecht.

6.8.2 Cyclic voltammetry

The cyclic voltammetry measurements were performed at the Department of Inorganic Chemistry of the University of Amsterdam with assistance of Dr. Frantisek Hartl and Taasje Mahabiersing. The solvents, butyronitrile (^{n}PrCN, Acros) and dimethylformamide were dried by distillation from CaH_2. The supporting electrolyte Bu_4NPF_6 (Aldrich) was re-crystallised twice from absolute ethanol and dried overnight under vacuum at 353 K for 12 h before use. Samples were prepared and carefully handled under a dry nitrogen atmosphere, using standard Schlenk techniques. Conventional cyclic voltammograms were recorded with a PAR Model 283 potentiostat, using an airtight, light-protected, single-compartment cell placed in a Faraday cage. A Pt disk (0.42 mm diameter) working electrode was polished with a 0.25 µm diamond paste between scans. Coiled Pt and Ag wires served as auxiliary and pseudoreference electrodes, respectively. Ferrocene was added as internal standard.[49] The concentration of the studied complexes was typically 10^{-3} M.

6.8.3 X-ray crystallography of 6.1

A yellow coloured plate-shaped crystal of **6.1** having approximate dimensions of 0.43 x 0.25 x 0.03 mm was used for the X-ray study.

Crystal data. $[C_{13}H_8N_4O_3V][NH_4] \cdot CH_3OH$, M_r = 369.26, triclinic, space group $P\bar{1}$ (no. 2) with a = 8.7959(8), b = 8.875(2), c = 10.636(2) Å, α = 87.155(17), β = 72.165(14), γ = 79.154(14)°, V = 776.2(2) Å^3, Z = 2, D_c = 1.580 g cm^{-3}, R(int) = 0.0638, T = 150(2) K.

Data collection, structure analysis and refinement. 5245 reflections up to a resolution of $(\sin\theta)/\lambda$ = 0.59 Å^{-1} were measured on an Enraf-Nonius CAD4T diffractometer with rotating anode (λ = 0.71073 Å). 2738 reflections were unique (R(int) = 0.0638). An absorption correction was performed with PLATON[50] (routine DELABS, μ = 0.67 mm^{-1}, 0.43-0.81 transmission). The structure was solved with automated Patterson methods (DIRDIF97[51]) and refined with SHELXL97[52] against F^2 of all reflections. Non-hydrogen atoms were refined freely with anisotropic displacement parameters. The hydrogen atoms of the ammonium ion were refined freely with isotropic displacement parameters. R-values [$I > 2\sigma(I)$]: $R1$ = 0.0519, $wR2$ = 0.0955. R-values (all refl.): $R1$ = 0.0976, $wR2$ = 0.1094. Goodness of fit = 1.03. Rest electron density between –0.38 and 0.32 e/Å^3. Structure checking and calculations were performed with the PLATON package.

6.8.4 X-ray crystal structure determination of 6.2

A red coloured plate-shaped crystal of **6.2** having approximate dimensions of 0.36 x 0.27 x 0.06 mm was used for the X-ray study.

Crystal data. $C_{30}H_{24}N_6O_8V_2 \cdot 2H_2O$, M_r = 734.46, monoclinic, space group *Pc* (no. 7) with a = 8.0989(8), b = 10.2358(16), c = 18.537(3) Å, β = 90.557(3)°, V = 1536.7(4) Å^3, Z = 2, D_c = 1.587 g cm^{-3}, R(int) = 0.0526, T = 150(2) K.

Data collection, structure analysis, and refinement. 20666 reflections up to a resolution of $(\sin\theta)/\lambda$ = 0.59 Å^{-1} were measured on an Nonius KappaCCD diffractometer with rotating anode (λ = 0.71073 Å). Intensities were obtained using the program EVAL14.[53] 5306 reflections were unique (R(int) = 0.0526). An absorption correction was performed with PLATON[50] (routine DELABS, μ = 0.68 mm^{-1}, 0.53-0.85 transmission). The structure was solved with direct methods (SHELXS97[54]) and refined with SHELXL97[52] against F^2 of all reflections. Non-hydrogen atoms were refined freely with anisotropic displacement parameters. Hydrogen atoms were located in the difference Fourier map. The hydrogen atoms of the water molecule were kept fixed at their located positions, the other hydrogens were refined as rigid groups. The crystal appeared to be an inversion twin. The Flack x parameter refined to 0.63(3). 436 refined parameters. R-values [$I > 2\sigma(I)$]: $R1$ = 0.0431, $wR2$ = 0.1027. R-values (all refl.): $R1$ = 0.0551, $wR2$ = 0.1111. Goodness of fit = 1.15. Rest electron density between –0.39 and 0.49 e/Å^3. Structure checking and calculations were performed with the PLATON package.

6.8.5 Catalytic oxidations

The oxidations were performed in toluene or acetonitrile as solvent, under an argon atmosphere in a water bath thermostated at 25 °C. In a typical reaction, 78 µmol of substrate was added to a 2 ml stock solution of 3.75 µmol of vanadium catalyst (*i.e.* 1.88 µmol in the case of **6.2**) and a known amount of the internal standard bromobenzene. The reaction was initiated by the addition of 17 µl of ^{t}BuOOH (~ 5 M solution in decane, 2 equiv.) or 38 µl of H_2O_2 (30% solution in water, 5 equiv) and monitored by GC.

6.8.6 Syntheses

3-(2-Hydroxyphenyl)-5-(pyridin-2-yl)-1,2,4-triazole (H_2L^1) The ligand[2] was kindly provided by Prof. J.G. Vos, Dublin City University, Ireland.[2]

3,5-Bis(2-hydroxyphenyl)-1,2,4-triazole (H_3L^2) The ligand was synthesised as described in the literature.[17]

3,5-Bis(pyridin-2-yl)-1,2,4-triazole (HL^3) The ligand was synthesised as described in the literature.[18]

$[VO_2L^1](NH_4) \cdot CH_3OH$ (6.1) Ligand H_2L^1 (80 mg, 0.34 mmol) was suspended in MeOH (5 ml). $NaVO_3$ (55 mg, 0.045 mmol, 1.3 equiv.) was added and the mixture was refluxed under an argon atmosphere for 18 h. After cooling to RT, unreacted $NaVO_3$ was removed by filtration. NH_4PF_6 (219 mg, 1.34 mmol, 4 equiv.) was added to the yellow solution. After the NH_4PF_6 was fully dissolved, the mixture was placed in a Et_2O bath. Complex **6.1** was obtained as yellow needles (50 mg, 0.15 mmol, 44%). ^{1}H NMR (DMF-d_7) 9.32 (d, 1H, *J* = 5.1 Hz), 8.52-8.44 (m, 2H), 8.26 (dd, 1H, *J* = 1.5, *J* = 7.7 Hz), 7.94 (dt, 1H, *J* = 1.8, *J* = 6.2 Hz), 7.54 (dt, 1H, *J* = 1.8, *J* = 7.9 Hz), 7.08 - 6.97 (m, 2H); ^{51}V NMR (DMF-d_7) -540 (b.w. = 849 Hz); ES/MS (MeOH) *m*/*z* 318.9 {VO_2L^1 - NH_4^+}; Anal. calcd. for $C_{13}H_{12}N_5O_3V$ x CH_3OH: C 45.54; H 4.37; N 18.97%, found: C 45.21; H 4.27; N 18.84%. λ_{max}(DMF) 296 nm (ε = 4.3 x 10^4 M^{-1} cm^{-1}), 370 nm (ε = 1.6 x 10^4 M^{-1} cm^{-1}).

$[(VOL^2)_2(OMe)_2] \cdot 2H_2O$ (6.2) Ligand H_3L^2 (200 mg, 0.79 mmol) was suspended in CH_3CN (10 ml). $VO(O^iPr)_3$ (201 mg, 0.82 mmol, 1.04 equiv.) was added and after 5 min MeOH (10 ml) was added. Stirring was continued until the solution became clear (15 min). Dark green crystals of **6.2** could be obtained by slow evaporation of the solvent (194 mg, 0.31 mmol, 77%). Crystals suitable for X-ray analysis were obtained after recrystallisation from MeOH-CH_3CN. ^{1}H NMR (acetonitrile-d_3/DMSO-d_6) 7.99 (d, 2H, *J* = 7.3 Hz), 7.39-7.34 (m, 2H), 6.95 (t, 2H, *J* = 7.3 Hz), 6.74 (d, 2H, *J* = 8.1 Hz); ^{51}V NMR (DMF-d_7) -600 (b.w. = 502 Hz); ^{51}V NMR (CD_3CN) -589 (b.w. = 1045 Hz); ES/MS (MeOH) *m*/*z* 317.0 {$V_2O_2(L^2)_2$ - $2H^+$}, *m*/*z* 634.9 {$(V^{IV})_2O_2(L^2)_2$ - $1H^+$}, *m*/*z* 652.0 {$(V^{IV}O)(V^{V}O)(L^2)_2$ + O^{2-}}, *m*/*z* 653.1 {$(V^{IV})_2O_2(L^2)_2$ + HO^-}, *m*/*z* 666.0 {$(V^{IV}O)(V^{V}O)(L^2)_2(OMe)$ - $1H^+$}, *m*/*z* 667.1 {$V^{IV}O)_2(L^2)_2(OMe)$}, *m*/*z* 347.9 {$VOL^2(OMe)$ - H^+}; Anal. calcd. for $C_{30}H_{24}N_6O_8V_2$ x $2H_2O$: C 49.06; H 3.84; N 11.44%, found: C 49.33; H 3.92; N 11.46%; λ_{max}(CH_3CN) 309 nm (ε = 8.9 x 10^3 M^{-1} cm^{-1}), 390 nm (ε = 2.6 x 10^3 M^{-1} cm^{-1}).

6.9 References

1 This ligand was kindly provided by Prof. Dr. J.G. Vos, Dublin City University, Ireland.

2 For the synthesis of H_2L^1, see (a) Hage, R.; Haasnoot, J.G.; Reedijk, J.; Wang, R.; Ryan, E.M.; Vos, J.G.; Spek, A.L.; Duisenberg, A.J.M. *Inorg. Chim. Acta* **1990**, *174*, 77. (b) Case, F.H. *J.Org. Chem.* **1965**, *30*, 931. (c) Browne, E.J.; Polka, J.B. *J. Chem. Soc. C*, **1968**, 824.

3 Haasnoot, J.G. *Coord. Chem. Rev.* **2000**, *200*, 131.

4 Hills, A.; Hughes, D.L.; Leigh, G.J.; Sanders, J.R. *J. Chem. Soc., Dalton Trans.* **1991**, 61.

5 Liu, H.X.; Wang, W.; Wang, X.; Tan, M.Y. *J. Coord. Chem.* **1994**, *33*, 347.

6 Giacomelli, A.; Floriani, C.; Ofir De Souza Duarte, A.; Chiesi-Villa, A.; Guastini, C. *Inorg. Chem.* **1982**, *21*, 3310.

7 Root, C.A.; Hoeschele, J.D.; Cornman, C.R.; Kampf, J.W.; Pecoraro, V.L. *Inorg. Chem.* **1993**, *32*, 3855.

8 Vergopoulos, V.; Priebsch, W.; Fritzche, M.; Rehder, D. *Inorg. Chem.* **1993**, *32*, 1844.

9 Li, X.-H.; Soo Lah, M.; Pecoraro, V.L. *Inorg. Chem.* **1988**, *27*, 4657.

10 Asgedom, G.; Sreedhara, A.; Kivikoski, J.; Valkonen, J.; Rao, C.P. *J. Chem. Soc., Dalton Trans.* **1995**, 2459.

11 Crans, D.C.; Shin, P.K. *J. Am. Chem. Soc.* **1994**, *116*, 1305.

12 See also Chapter 5.

13 (a) Conte, V.; Di Furia, F.; Moro, S. *J. Mol. Cat. A* **1995**, *104*, 159. (b) Howarth, O.W.; Hunt, J.R. *J. Chem. Soc., Dalton Trans.* **1979**, 1388.

14 Butler, A.; Carrano, C.J. *Coord. Chem. Rev.* **1991**, *109*, 61.

15 Bonadies, J.A.; Carrano, C.J. *J. Am. Chem. Soc.* **1986**, *108*, 4088.

16 Mabbott, G.A. *J. Chem. Ed.* **1983**, *60*, 697.

17 (a) Ryabukhin, Yu. I.; Faleeva, L.N.; Korobkova, V.G. *Chem. Heterocycl. Compd. (Engl. Transl.)* **1983**, *19*, 332. (b) McConnan, J. *J. Chem. Soc.* **1997**, *91*, 196.

18 (a) Geldard, J.F.; Lions, F. *J. Org. Chem.* **1965**, *30*, 318. (b) Hage, R. 'Ruthenium and Osmium Complexes Containing Triazole Ligands', PhD Thesis, Leiden, 1991, Chapter 6.

19 (a) Cornman, C.R.; Kampf, J.; Pecoraro, V.L. *Inorg. Chem.* **1992**, *31*, 1981. (b) Kabanos, T.A.; Keramidas, A.D.; Papaioannou, A.; Terzis, A. *Inorg. Chem.* **1994**, *33*, 845.

20 (a) Plass, W.; Pohlmann, A.; Yozgatli, H.-P. *J. Inorg. Biochem.* **2000**, *80*, 181. (b) Asgedom, G.; Sreedhara, A.; Kivikoski, J.; Valkonen, J.; Kolehmainen, E.; Rao, C.P. *Inorg. Chem.* **1996**, *35*, 5674. (c) Asgedom, G.; Sreedhara, A.; Kivikoski, J.; Valkonen, J.; Rao, C.P. *J. Chem. Soc., Dalton Trans.* **1995**, 2459. (d) Li, X.; Soo Lah, M.; Pecoraro, V.L. *Inorg. Chem.* **1988**, *27*, 4657.

21 Hefele, H.; Uhlemann, E.; Weller, F. *Z. Naturforsch.* **1997**, *52 b*, 693.

22 (a) Oyaizu, K.; Yamamoto, K.; Yoneda, K.; Tsuchida, E. *Inorg. Chem.* **1996**, *35*, 6634. (b) Asgedom, G.; Sreedhara, A.; Kivikoski, J.; Valkonen, J.; Kolehmainen, E.; Rao, C.P. *Inorg. Chem.* **1996**, *35*, 5674.

23 Thiele, K.; Görls, H.; Imhof, W.; Seidel, W. *Z. Anorg. Allg. Chem.* **1999**, *625*, 1927.

24 Mimoun, H.; Chaumette, P.; Mignard, M.; Saussine, L. *Nouv. J. Chim.* **1983**, *7*, 467.

25 Mahroof-Tahir, M.; Keramidas, A.D.; Goldfarb, R.B.; Anderson, O.P.; Miller, M.M.; Crans, D.C. *Inorg. Chem.* **1997**, *36*, 1657.

26 Duncan, C.A.; Copeland, E.P.; Kahwa, I.A.; Quick, A.; Williams, D.J. *J. Chem. Soc., Dalton Trans.* **1997**, 917.

27 Rajaiah Saneetha, N.M.; Pal., S. *Bull. Chem. Soc. Jpn.* **2000**, *73*, 357.

28 *Comprehensive Coordination Chemistry*, Wilkinson, G. Ed.; Pergamon Press, Oxford, 1987, *3*, 539-540.

29 Syamal, A.; Kale, K.S. *Inorg. Chem.* **1979**, *18*, 992.

30 Ceccato, A.S.; Neves, A.; De Brito, M.A.; Drechsel, S.M.; Mangrich, A.S.; Werner, R.; Haase, W.; Bortoluzzi, A.J. *J. Chem. Soc., Dalton Trans.* **2000**, 1573.

31 Micera, G.; Sanna, D. in *Vanadium in the Environment, Part One: Chemistry and Biochemistry*, Nriagu, J.O., Ed.; John Wiley & Sons, New York, **1998**, Chapter 7.
32 Syamal, A.; Theriot, L.J. *J. Coord. Chem.* **1973**, *2*, 193.
33 Alborn, E.; Diemann, E.; Müller, A. *Z. Anorg. Allg. Chem.* **1972**, *394*, 1.
34 (a) Døssing, A.; Hazell, A.; Toftlund, H. *Acta Chem. Scan.* **1996**, *50*, 95. (b) Kelm, H.; Krüger, H.-J. *Inorg. Chem.* **1996**, *35*, 3533. (c) Knopp, P.; Wieghardt, K.; Nuber, B.; Weiss, J.; Sheldrick, W.S. *Inorg. Chem.* **1990**, *29*, 363.
35 (a) Dani, P.; Karlen, T.; Gossage, R.A.; Gladiali, S.; Van Koten, G. *Angew. Chem. Int. Ed.* **2000**, *39*, 743. (b) Del Rio, J.; Back, S.; Hannu, M.S.; Rheinwald, G.; Lang, H.; Van Koten, G. *Inorg. Chim. Acta*, **2000**, *300*, 1094.
36 See Chapter 1.
37 Butler, A.; Clague, M.J.; Meister, G.E. *Chem. Rev.* **1994**, *94*, 625.
38 See also Chapter 1.
39 Sheng, M.N.; Zajacek, J.G. *J. Org. Chem.* **1970**, *35*, 1839.
40 (a) Lempers, H.E.B.; Ripollés i Garcia, A.; Sheldon, R.A. *J. Org. Chem.* **1998**, *63*, 1408. (b) Hiyama, T.; Obayashi, M. *Tetrahedron Lett.* **1983**, *24*, 395. (c) Mihelich, E.D. *Tetrahedron Lett.* **1979**, *49*, 4729. (d) Itoh, T.; Jitsukawa, K.; Kaneda, K.; Teranishi, S. *J. Am. Chem. Soc.* **1979**, *101*, 159. (e) Tanaka, S.; Yamamoto, H.; Nozaki, H.; Sharpless, K.B.; Michaelson, R.C.; Cutting, J.D. *J. Am. Chem. Soc.* **1974**, *96*, 5254. (f) Sharpless, K.B.; Michaelson, R.C. *J. Am. Chem. Soc.* **1973**, *95*, 6136.
41 (a) Conte, V.; Di Furia, F.; Licini, G. *Appl. Cat. A* **1997**, *157*, 335. (b) Chong, A.O.; Sharpless, K.B. *J. Org. Chem.*, **1977**, *42*, 1587. (c) Di Furia, F.; Modena, G. *Rec. Trav. Chim. Pays-Bas* **1979**, *98*, 181. (d) Cenci, S.; Di Furia, F.; Modena, G. *J. Chem. Soc., Perkin Trans. 2*, **1978**, 979. (e) Curci, R.; Di Furia, F.; Testi, R.; Modena, G. *J. Chem. Soc., Perkin Trans. 2*, **1974**, 752.
42 Chong, A.O.; Sharpless, K.B. *J. Org. Chem.* **1977**, *42*, 1587.
43 Mimoun, H. *Isr. J. Chem.* **1983**, *23*, 451.
44 Mimoun, H.; Saussine, L.; Daire, E.; Postel, M.; Fischer, J.; Weiss, R. *J. Am. Chem. Soc.* **1983**, *105*, 3101.
45 Shul'pin, G.B.; Attanasio, D.; Suber, L. *J. Cat.* **1993**, *142*, 147.
46 Roelfes, G.; Lubben, M.; Hage, R.; Que, L. Jr.; Feringa, B.L. *Chem. Eur. J.* **2000**, *6*, 2152.
47 Mimoun, H; Mignard, M.; Brechot, P.; Saussine, L. *J. Am. Chem. Soc.* **1986**, *108*, 3711.
48 Choudary, B.M.; Reddy, P.N. *J. Mol. Cat. A* **1995**, *103*, L1.
49 Gritzner, G.; Kuta, J. *Pure Appl. Chem.* **1984**, *56*, 461.
50 Spek, A.L. *PLATON. A multipurpose crystallographic tool*. Utrecht University, The Netherlands, **1998**.
51 Beurskens, P.T.; Admiraal, G. Beurskens, G.; Bosman, W.P.; Garcia-Granda, S.; Gould, R.O.; Smits, J.M.M.; Smykalla, C. *The DIRDIF97 program system*, Technical Report of the Crystallography Laboratory, University of Nijmegen, The Netherlands, **1997**.

52 Sheldrick, G.M. *SHELXL97. Program for crystal structure refinement*, University of Göttingen, Germany, **1997**.

53 Duisenberg, A.J.M. PhD Thesis, Utrecht University, The Netherlands, **1998**.

54 Sheldrick, G.M. *SHELXS97. Program for crystal structure solution*, University of Göttingen, Germany, **1997**.

Chapter 7

Chiral Ligands for Vanadium and Manganese

7.1 Introduction

In Chapters 3, 5, and 6 the syntheses of several oxovanadium complexes were described. These compounds were tested as catalysts in oxidation reactions like brominations and epoxidations. Unfortunately, it was found that these compounds often can not compete with commercially available $VO(acac)_2$ in reactivity and reaction rates. Therefore, we focussed on the design of chiral vanadium complexes for asymmetric epoxidations or sulfoxidations. In this chapter, the attempts to obtain such catalysts are described.

7.2 Asymmetric oxidation reactions

Epoxides are versatile building blocks in organic synthesis, since they are precursors for many functionalised products.[1] Carrying out epoxidations of olefins in an enantioselective way may lead to two stereogenic centres, which make these reactions even more important. The use of transition-metal complexes as catalysts for epoxidation reactions has received much attention during the past two decades.[2,3,4] For example, titanium-catalysed asymmetric epoxidation of allylic alcohols has been developed by Katsuki and Sharpless.[5] Enantiomerically pure tartrate esters are used as ligands for titanium and *tert*-butylhydroperoxide (TBHP) is used as the oxidant. Yields normally range from 70 – 90% and e.e.'s up to >95% can be achieved.[6,7]

Mn-salen complexes also have extensively been studied as catalysts in asymmetric epoxidation of olefins, especially by the groups of Jacobsen[8] and Katsuki.[9] In general, epoxides can be obtained with yields above 80% and e.e.'s usually exceed 90%. As oxidants *e.g.* hypochoride (bleach), iodosylbenzene, or *meta*-chloroperbenzoic acid (*m*-CPBA) are used.[10]

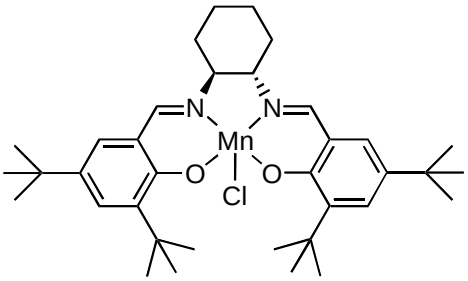

Figure 7.1 *Mn-salen complex used by Jacobsen et al. for asymmetric epoxidations.*[8]

7.2.1 Vanadium catalysed asymmetric epoxidations

Prior to the discovery of titanium-catalysed asymmetric epoxidation, Sharpless *et al.* put much effort into the development of vanadium complexes based on chiral hydroxamic acids for this purpose.[5b,11,12] These ligands themselves are very resistant towards oxidation and seem to bind well to vanadium ions. After exploring more than 20 chiral hydroxamate ligands and using a variety of allylic alcohols as substrate, an optimum case was reached as is depicted in Scheme 7.1. When using 2-phenylcinnamyl alcohol as substrate, 1 mol% of vanadium alkoxide, 2 equiv. of *tert*-butyl hydroperoxide (TBHP) and 3 mol% of a chiral hydroxamic acid, the epoxide was obtained in 90% yield with an enantiomeric excess of 80%.

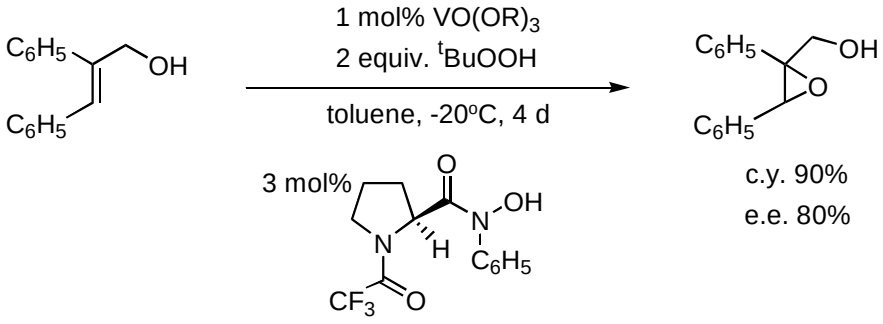

Scheme 7.1 *Vanadium-catalysed asymmetric epoxidation of an allylic alcohol developed by Sharpless et al.*[6,11]

Despite many modifications of both chiral ligand and substrate, the value of 80% e.e. was never surpassed. Furthermore, binding of the ligand to vanadium caused a significant deactivation of the catalyst. The vanadium-catalysed reaction in the absence of the hydroxamate ligand is completed in less than one day, whereas the enantioselective reaction described in Scheme 7.1 requires four days. But despite this strong ligand deceleration effect, 3 equiv. of the hydroxamic acid with respect to vanadium were needed to attain the highest e.e. values. This can be rationalised by considering the possible binding modes of the hydroxamic acid to vanadium alkoxides as described in Scheme 7.2.[6] The monodentate ethoxy ligand is replaced by a bidendate hydroxamate ligand to form a monohydroxamate complex (schematically indicated as B). This complex is active and responsible for the asymmetric induction. However, ligand exchange in vanadium(v) alkoxides is rapid.[13] Therefore, complex B will be in equilibrium with complexes A and C. The achiral compound A is a fast catalyst but will produce racemic epoxides. Obviously the formation of A must be prevented by adding an excess of the chiral ligand. However, as a consequence vanadium can take on even two or three hydroxamate ligands to form dihydroxamate (C) and trihydroxamate (D) species, respectively. Since at least two adjacent exchangeable ligand sites are required in order to epoxidise allylic alcohols,[14] these complexes are inactive. While the undesired formation of A is suppressed as much as possible by adding an excess of chiral ligand, the disadvantage is that essentially all the vanadium is bound in the inactive forms C and D. The increased ligand concentration does induce the enantiomeric excess to

rise to a plateau, but the reaction rate decreases steadily. An optimum was found for 3 equiv. of the chiral ligand. In that case, high e.e. values are found accompanied with still reasonable reaction times.

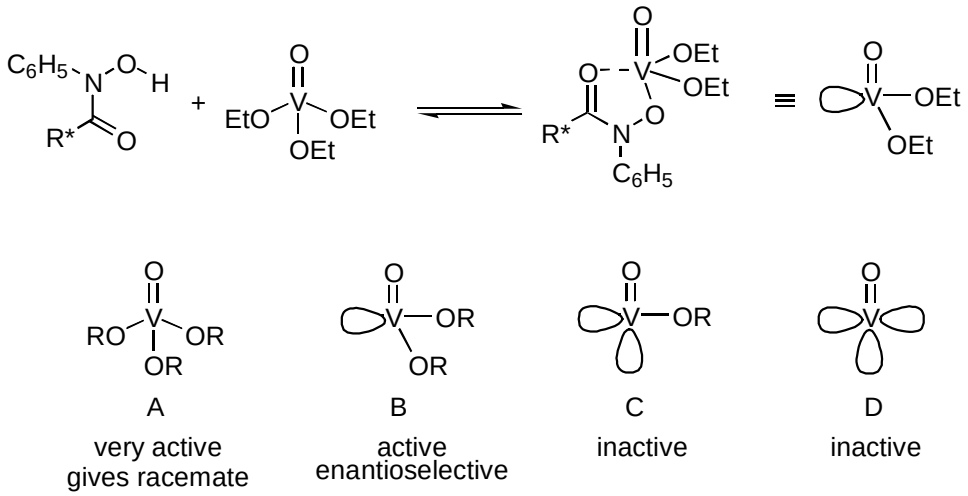

Scheme 7.2 *Binding modes of hydroxamate ligands to vanadium.*

Although the Sharpless system could not be developed to achieve e.e.'s higher than 80% due to ligand deceleration along with dynamic ligand exchange processes, in 1999 Yamamoto *et al.* reported much higher e.e.'s in vanadium mediated asymmetric epoxidation of allylic alcohols by using new chiral hydroxamic acids derived from 2,2'-binaphthol (Scheme 7.3).[15]

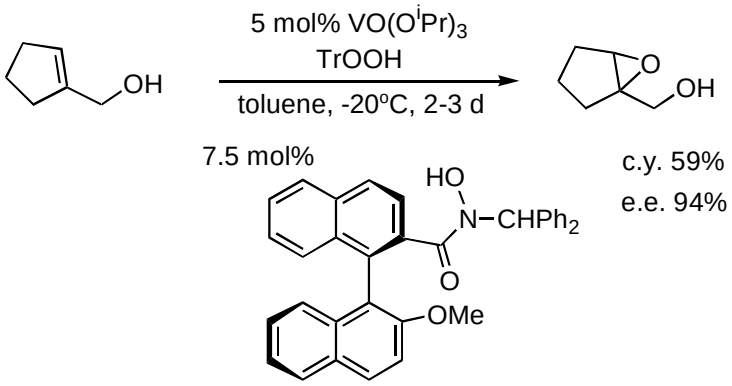

Scheme 7.3 *Vanadium-catalysed asymmetric epoxidation of an allylic alcohol according to Yamamoto et al.*[15]

It was found that increased steric bulk both on the nitrogen of the hydroxyl amine part and on the peroxidic oxidant led to a dramatic increase in enantioselectivity. The best result was obtained using 1-cyclopenten-1-ylmethanol as substrate, 5 mol% of $VO(O^iPr)_3$ (triisopropoxyvanadium(V) oxide), 7.5 mol% of the chiral ligand and trityl hydroperoxide

(triphenylmethyl hydroperoxide, TrOOH). After 2 - 3 days the epoxide was formed in 59% yield and an e.e. of 94% was reached. Only 1.5 equiv. of the chiral ligand based on vanadium was needed in order to obtain these high e.e. values. Probably 1:1 complexes between vanadium and the sterically demanding hydroxamic acid are formed, whereas in this case the formation of the inactive dihydroxamate and trihydroxamate species is impossible.

A possible intermediate was proposed[16] based on the X-ray structure of the ligand and the commonly accepted square bipyrimidal geometry of vanadium complexes containing hydroxamate or peroxo ligands[17] (Figure 7.2). The vanadium ion is surrounded by the bulky hydroxamate ligand and the trityl peroxide (OOR in Figure 7.2). The allylic alcohol is apically bound, which would lead to a favourable oxygen transfer to the *Si*-face of the carbon-carbon double bond.

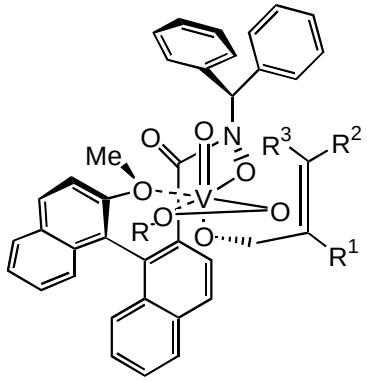

Figure 7.2 *Possible intermediate in the asymmetric epoxidation proposed by Yamamoto et al.[16]*

Recently, this catalytic system was improved even further by using an iterative positional optimisation approach on chiral *α*-amino acid-based hydroxamic acid ligands.[18] This approach involves screening one component of a ligand structure for selectivity, while holding the other units constant. Finally, the *N*-bis(1-naphthyl)methyl-substituted hydroxamic acid, as depicted in Figure 7.3, was found to be the most effective ligand for a range of disubstituted allylic alcohols in the presence of $VO(O^iPr)_3$. Moderate-to-high enantioselectivities and yields could be obtained using a ligand-to-metal ratio of 1.5. For instance, with *α*-phenylcinnamyl alcohol as the substrate, the corresponding epoxide could be obtained in 93% yield with an e.e. of 96% after 6 h, using TBHP as the oxidant.

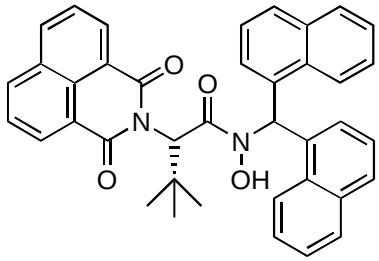

Figure 7.3 *Optimised hydroxamic acid ligand for vanadium-catalysed asymmetric allylic oxidation by Yamamoto et al.[18]*

Another hydroxamic acid based catalytic system was published by Bolm *et al.* in 2000. Vanadium complexes of *N*-hydroxy-[2.2]paracyclophane-4-carboxylic amides (Scheme 7.4) were found to be promising in asymmetric allylic epoxidations.[19] Also in this system a ligand-to-metal ratio of 1.5 gave the best results. When TBHP was used as the oxidant, the epoxide of (*E*)-2-methyl-3-phenyl-2-propen-1-ol was obtained in 85% yield and 71% e.e.

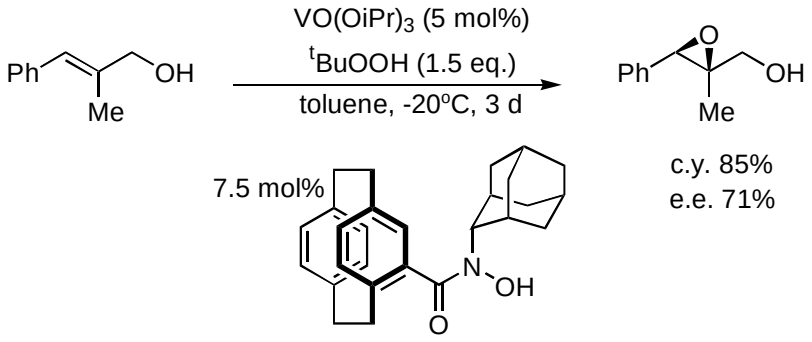

Scheme 7.4 *Vanadium-catalysed asymmetric oxidation of an allylic alcohol developed by Bolm and Kühn.*[19]

7.2.2 Sulfide oxidations

Sulfides are another class of useful substrates in asymmetric oxidation of organic compounds leading to optically active sulfoxides.[20] These products has been used for example as auxiliaries or intermediates. More recently, they have been introduced as ligands in enantioselective metal catalysis.[21] A number of methods for the synthesis of these sulfoxides are available,[22,23] but the most common ones are based on stereoselective transformations involving chiral auxiliaries[24] or a modified Sharpless reagent.[25]

Vanadium complexes are also known to be capable of oxidising sulfides selectively to their corresponding sulfoxide producing almost no sulfone.[26,27] Therefore, chiral analogues of these complexes appear promising catalysts for the asymmetric sulfide oxidations.[28]

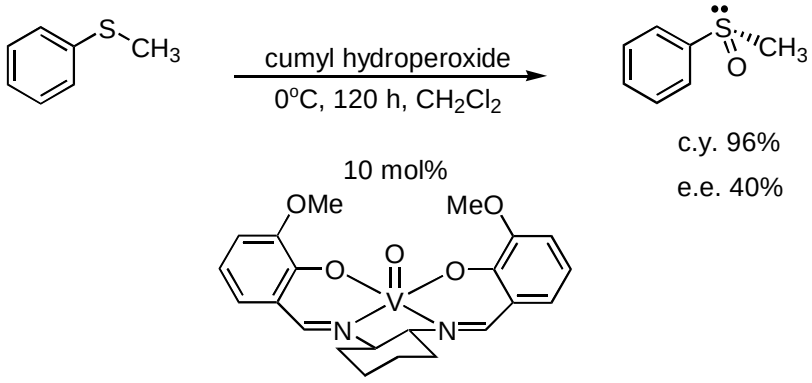

Scheme 7.5 *Vanadium-catalysed asymmetric sulfide oxidation described by Fujita et al.*[29]

Indeed Fujita *et al.* found that optically active tetradentate Schiff base-oxovanadium(IV) complexes catalyse asymmetric sulfoxidations.[29,30,31] When methyl phenyl sulfide was used as the substrate and cumyl hydroperoxide (*α,α*-dimethylbenzyl hydroperoxide) as the oxidant, the corresponding sulfoxide could be obtained in 96% yield with an e.e. of 40% (Scheme 7.5).[29]

Recently, Bolm *et al.* reported an elegant method for the asymmetric oxidation of sulfides which provides optically active sulfoxides with e.e.'s up to 85%.[32,33] The best results were obtained with a ligand derived from *tert*-leucinol (Scheme 7.6). Large substituents at C4 and C6 of the ligand aryl group afforded a higher asymmetric induction.[34] This simple method does not require complicated conditions, since the reaction can be performed in air at room temperature and exclusion of humidity is not necessary. However, H_2O_2 has to be added slowly, because otherwise the corresponding sulfone is obtained as well. In this case, the reaction is ligand-accelerated and the enantioselectivity is hardly effected by the presence of achiral vanadium species (*i.e.* $VO(acac)_2$).

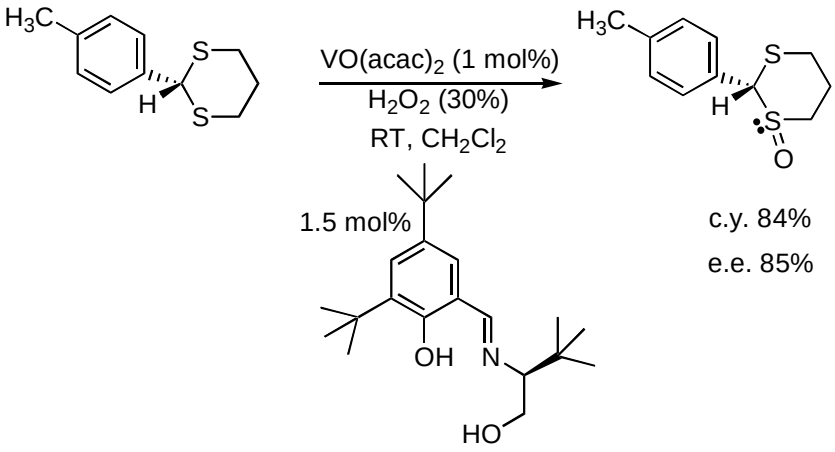

Scheme 7.6 *Vanadium-catalysed asymmetric sulfide oxidation described by Bolm et al.*[32]

Bolm's catalytic system has been adopted and optimised for different substrates by others.[28] For instance, Ellman *et al.* achieved 98% conversion and 91% e.e. in the asymmetric oxidation of *tert*-butyl disulfide and utilised the product as a precursor in the synthesis of enantiomerically pure *tert*-butanesulfinamides.[35]

Recently, it has been found that vanadium haloperoxidases are also capable of catalysing the oxidation of sulfides to the corresponding sulfoxides using H_2O_2.[36] For instance, vanadium bromoperoxidase (V-BrPO) from the brown seaweed *Ascophyllum nodosum*[37] converts methyl phenyl sulfide to the corresponding (*R*)-sulfoxide with up to 96% enantiomeric excess.[36a]

7.3 Synthesis of chiral ligands

Several promising vanadium-based asymmetric catalytic systems have been developed, especially in recent years.[38] It can be concluded from the overview given above that the successful catalysts for epoxidations of allylic alcohols are all based on hydroxamate ligands, whereas for the asymmetric sulfoxidation tri- or tetradentate Schiff base ligands are used. In order to explore vanadium-catalysed asymmetric oxidation reactions, chiral ligands based on pyridine *N*-oxides were designed. In this way, ligands can be obtained which closely resemble the Bolm system, but in which the phenol unit is replaced by the pyridine *N*-oxide. Furthermore, a few achiral complexes with vanadium including the pyridine *N*-oxide or quinoline *N*-oxide moiety are already known.[39] To be able to construct chiral *N*-oxides, we synthesised the *N*-oxide of 2-pyridinecarboxaldehyde (**7.3**) as a building block (Scheme 7.7). Although in the course of this research a method for the synthesis of these type of compounds was published using dimethyldioxirane[40], we found a convenient route using the hydrogen peroxide-urea adduct (UHP).

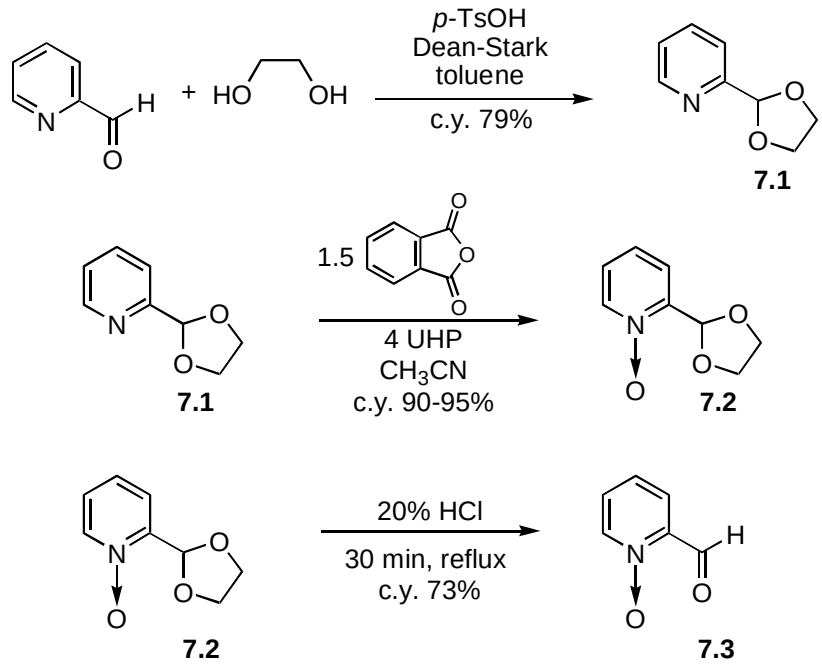

Scheme 7.7 *Three-step synthesis of the N-oxide of 2-pyridinecarboxaldehyde.*

First, the aldehyde of 2-pyridinecarboxaldehyde was protected as acetal **7.1** using ethylene glycol in toluene under Dean-Stark conditions. Then, analogously to a literature procedure[41] the protected *N*-oxide **7.2** was made with the use of UHP and phthalic anhydride in acetonitrile. The advantages of this method are that the reaction is simple, efficient, and safe[42] and that the product can be easily isolated by extraction. The best results (*i.e.* 90-95% yield) were obtained when 4 molar equiv. of the H_2O_2-urea complex and 1.5 molar equiv. of

the anhydride were used. To remove the acetal protection group, **7.2** dissolved in 20% aqueous HCl, was placed in an oil bath of 110 °C for 30 min to afford **7.3** in 73% yield. In order to prevent decomposition it turned out to be important that reaction times do not exceed 30 min. Compound **7.3** is stable for several months, when stored under an argon atmosphere at 4 °C.

In a first test reaction to see wether **7.3** could be used as a building block for the synthesis of Schiff base ligands, the *N*-oxide and 2-aminoethylpyridine were condensed in the presence of Na_2SO_4 to produce **7.4** (Scheme 7.8). This imine ligand was isolated as an orange-red oil in 99% yield after filtration and evaporation of the solvent. Further purification was not needed. However, it should be noted that the reaction must be performed under an argon atmosphere and that the product must be stored strictly under argon in order to prevent decomposition.

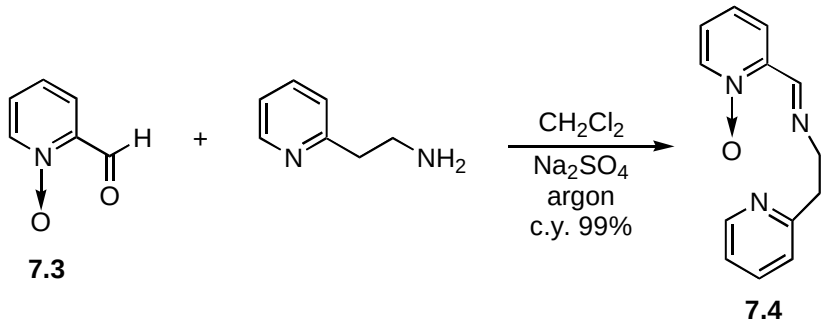

7.3 **7.4**

Scheme 7.8 *Synthesis of the achiral Schiff base ligand **7.4**.*

Analogously to the above described imine formation reaction, pyridine carboxaldehyde *N*-oxide **7.3** was allowed to react with (racemic) 1-aminoethylpyridine in dry dichloromethane under an argon atmosphere to produce the chiral ligand **7.5** (Figure 7.9). In this case also, the product was obtained quantitatively as a yellow oil which needed no further purification. Again, the product must be handled and stored under argon.

Unfortunately, attempts to synthesise other tridentate Schiff bases using 1-amino-2-propanol, (1*R*,2*S*)-(-)-norephedrine, glycine ethylester and 2-(1-aminoethyl)phenol resulted in mixtures of products, which could not be identified by ^{1}H NMR.

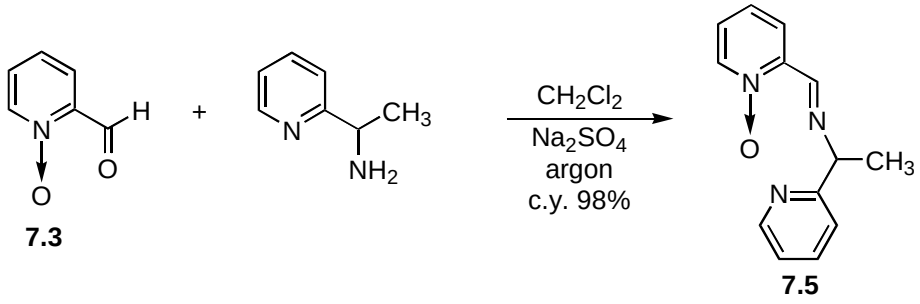

7.3 **7.5**

Scheme 7.9 *Synthesis of pyridine N-oxide based chiral ligand **7.5**.*

A tetradentate chiral ligand (L^1) based on **7.3** was prepared using (*R*,*R*)-diaminocyclohexane. This imine was obtained after reaction of the bisamine and two equivalents of the pyridine-*N*-oxide carboxaldehyde in dichloromethane under an argon atmosphere. Pale yellow crystals of L^1 were obtained upon crystallisation from a dichloromethane / pentane mixture in 72% yield.

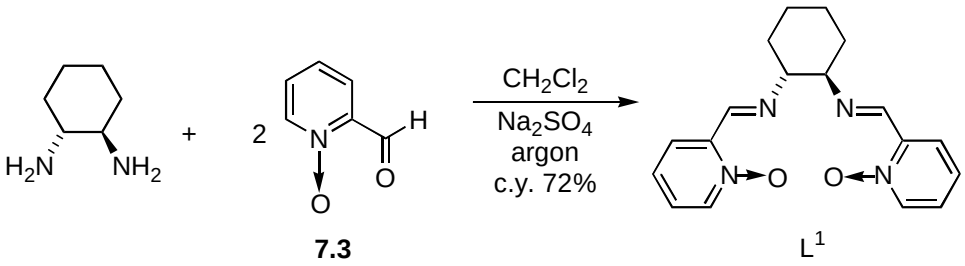

Scheme 7.10 *Synthesis of a tetradentate Schiff base ligand based on pyridine-N-oxides.*

7.4 Attempted syntheses of chiral vanadium complexes

The ligands described above were used for the complexation of vanadium. For example, **7.4** was allowed to react with *e.g.* $[VO_2Cl_2(PPh_4)]$[43], $VO(O^iPr)_3$ and $VO(acac)_2$ in the solvents acetonitrile, ethanol, and methanol, respectively. However, no well-defined products could be obtained according to ^1H NMR spectroscopy. This may be due to the sensitivity of the ligands.

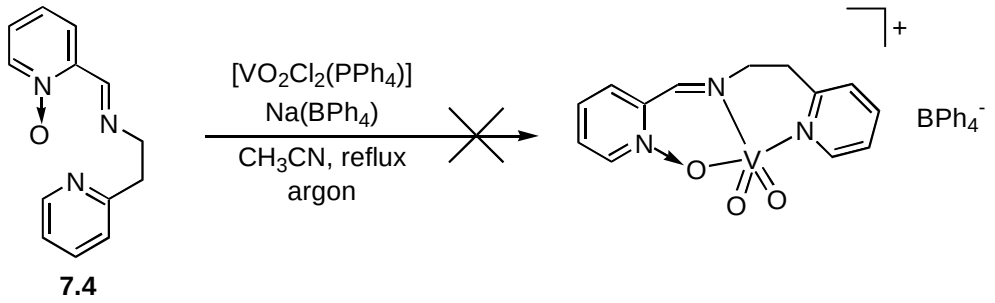

Scheme 7.11 *Attempted synthesis of a V(v) complex of pyridine-N-oxide based ligand **7.4**.*

Because of the resemblance of L^1 with the well-known salen systems (see also Figure 7.1) and the fact that several vanadium-salen complexes are already known,[29,30,31,44] it was anticipated that this ligand was suitable for the incorporation of vanadium. However, also with this pyridine-*N*-oxide based ligand, no well-defined complexes were obtained. According to ^1H NMR spectroscopy, a complex product mixture was formed. This may be due to the neutral character of the ligand, which probably can not provide enough stabilisation for the vanadium ion.

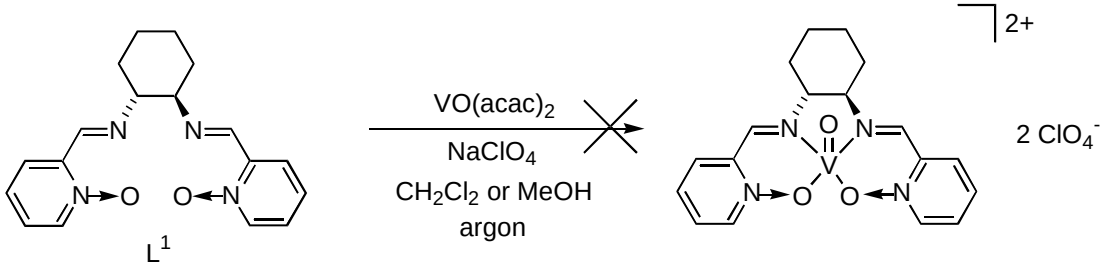

Scheme 7.12 *Attempted synthesis of a vanadium(IV) complex of tetradentate ligand L¹.*

7.5 Synthesis of a chiral manganese complex

Because of the close resemblance of L¹ with the salen-type ligands, it appeared of interest to examine the properties of a manganese complex of this ligand and compare these with the manganese-salen analogue. Furthermore, pyridine *N*-oxides (*e.g.* 4-phenylpyridine-*N*-oxide) have been used as additives in (salen)Mn-catalysed epoxidation.[45,46] They have a favourable effect on reaction rate, yield, *cis*/*trans* ratio and enantioselectivities. The *N*-oxide additives function as axial ligands as was for instance proven by a study of a catalyst strapped with pyridine *N*-oxide.[46] From the X-ray crystal structure of this manganese(III) complex, it became clear that the *N*-oxide group is axially coordinated, opposite to the chloride counterion.

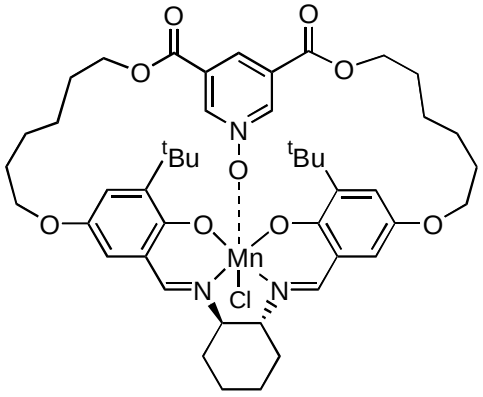

Figure 7.4 *Manganese(III) complex of a salen-derived ligand strapped with pyridine N-oxide.*[46]

In order to prepare a manganese complex of a pyridine *N*-oxide-based salen-derived ligand, $[Mn(II)(ClO_4)_2 \cdot 6H_2O]$ dissolved in acetonitrile was added to a solution of L¹. Complex **7.6** could be isolated in 67% yield as orange crystals after slow evaporation of dichloromethane into the red reaction mixture (Scheme 7.13).

Finally, after many attempts, crystals suitable for X-ray determination were obtained in this manner. They had to be rapidly covered with a thin layer of paraffin oil to avoid

deterioration in air. An ORTEP presentation of **7.6** is shown in Figure 7.5 and selected bond distances, angles and torsion angles are shown in Table 7.1.

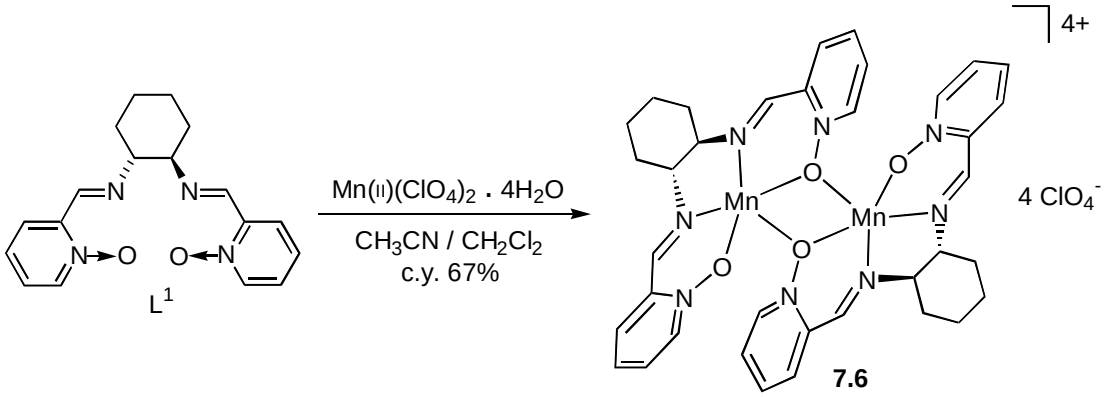

Scheme 7.13 *Synthesis of dinuclear manganese(II) complex **7.6** based on L[1].*

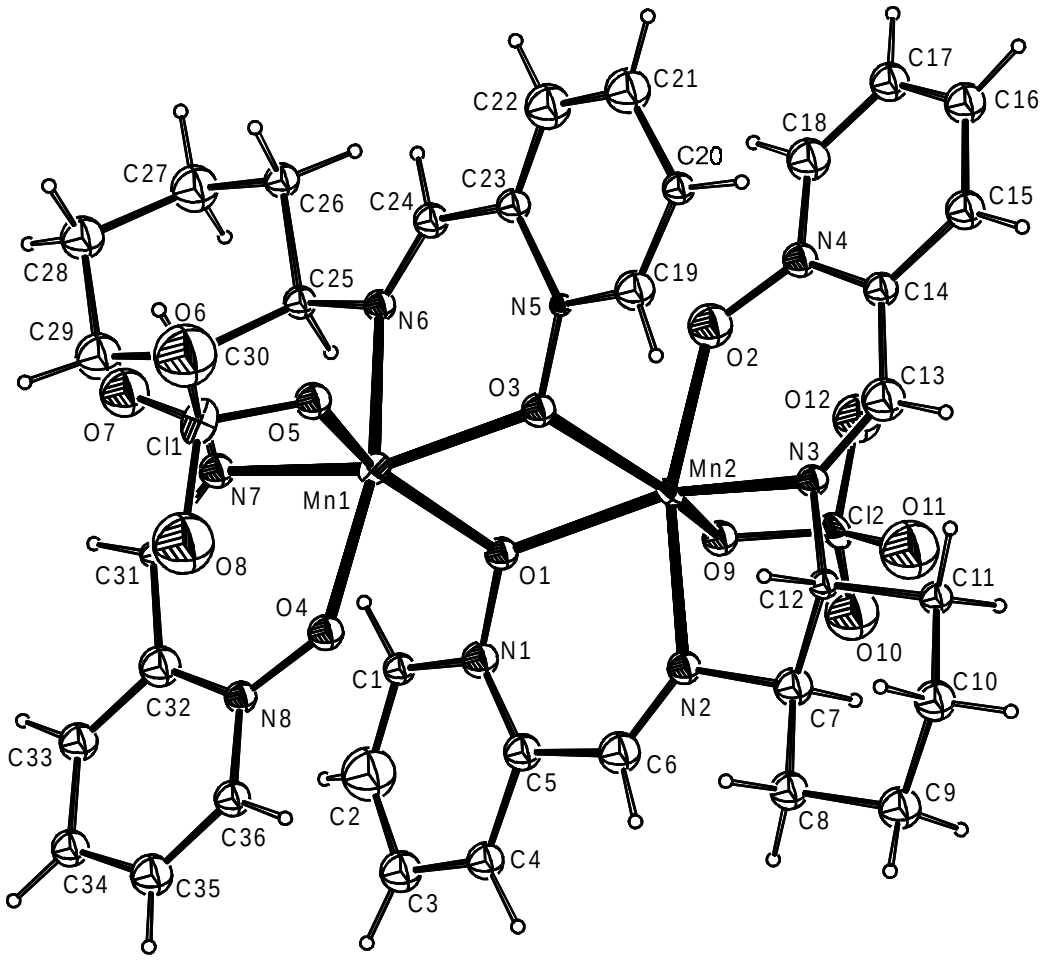

Figure 7.5 *An ORTEP plot of the cation of **7.6** with the two bound perchlorate anions (50% probability level).*

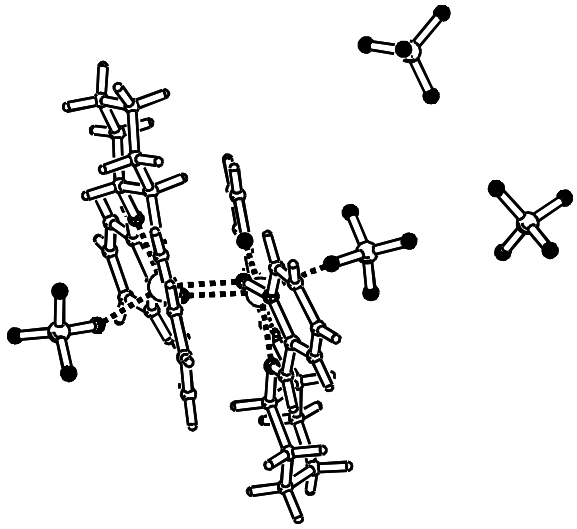

Figure 7.6 *Side-view of dinuclear **7.6** with two coordinating and two non-coordinating perchlorate anions (PLUTON representation).*

Table 7.1 *Selected bond distances (Å), angles and torsion angles (°) of **7.6** with estimated standard deviations (esd's) in parentheses.*

Bond distances			
Mn(1)-O(1)	2.229(17)	Mn(2)-O(1)	2.165(18)
Mn(1)-O(3)	2.129(18)	Mn(2)-O(2)	2.05(2)
Mn(1)-O(4)	2.051(19)	Mn(2)-O(3)	2.282(18)
Mn(1)-O(5)	2.193(17)	Mn(2)-O(9)	2.183(17)
Mn(1)-N(6)	2.224(19)	Mn(2)-N(2)	2.20(2)
Mn(1)-N(7)	2.23(2)	Mn(2)-N(3)	2.19(2)
Cl(1)-O(5)	1.456(17)	Cl(2)-O(9)	1.447(17)
O(3)-N(5)	1.34(3)	O(1)-N(1)	1.35(3)
O(4)-N(8)	1.30(3)	O(2)-N(4)	1.34(3)
N(6)-C(24)	1.22(3)	N(3)-C(13)	1.28(4)
N(7)-C(31)	1.26(3)	N(2)-C(6)	1.28(3)
Mn(1)-Mn(2)	3.57(2)	O(1)-O(3)	2.57(5)
Bond angles and torsion angles			
Mn(1)-O(1)-Mn(2)	108.7(7)	Mn(1)-O(3)-Mn(2)	108.1(8)
O(1)-Mn(1)-O(3)	72.4(7)	O(1)-Mn(2)-O(3)	70.7(6)
O(1)-Mn(1)-O(5)	154.0(7)	O(1)-Mn(2)-O(9)	86.7(6)
Mn(1)-O(3)-N(5)	124.6(14)	Mn(2)-O(1)-N(1)	123.9(14)
Mn(1)-O(4)-N(8)	136.0(17)	Mn(2)-O(2)-N(4)	134.3(17)
O(1)-Mn(1)-O(3)-Mn(2)	1.4(8)	O(1)-Mn(1)-O(3)-N(5)	145.5(19)

The X-ray analysis showed that a dinuclear Mn(II)-Mn(II) complex had been formed. The complex crystallises in the triclinic space group *P*1. Each asymmetric unit contains one formula unit, consisting of three moieties: a cationic dinuclear manganese complex with two bonded perchlorates (disordered) and two free ClO_4^- anions. This is clearly shown in a side-view of the complex (Figure 7.6). The complex has a pseudo inversion center. One pyridine-*N*-oxide moiety of the ligand bridges between the manganese centres, giving rise to a Mn_2O_2 four-membered ring. Each manganese ion is hexacoordinate in a distorted octahedral environment by to imine nitrogen atoms, three oxygens from pyridine-*N*-oxide units and one perchlorate anion.

The Mn-O bonds differ considerably in length ranging from 2.05 to 2.28 Å.[47,48] The Mn-N distances range from 2.19 to 2.23 Å.[49] These long manganese-donor distances supports the assignment that the manganese centres are in a +2 oxidation state.[50] One perchlorate ion is coordinated to each manganese ion with a Mn-O distance of respectively 2.19 and 2.18 Å for Mn(1) and Mn(2). The intramolecular Mn-Mn distance is 3.57(2) Å.

7.6 Spectro-electrochemical and EPR spectroscopy measurements[51]

Before the X-ray structure of **7.6** was elucidated, the oxidation state of the manganese ion was unclear. It also was unknown whether the complex existed as a monomer or as a dinuclear species. The orange colour of the compound could suggest the presence of a Mn(III) centre, because the majority of the Mn(II) compounds have forbidden *d-d* transitions according to both the LaPorte and the spin state selection rules.[52] As a result, the *d-d* electronic spectra are of low intensity and the complexes are colourless or very pale in colour. On the other hand, the electronic spectra of Mn(III) compounds do have spin allowed *d-d* transitions and accordingly they have more colour.[52]

The paramagnetic shifted signals in the range –16 to 23 ppm in the ^{1}H NMR spectrum of **7.6** (see Figure 7.7) in acetonitrile could also be an indication for a Mn(III) species, for these features are quite similar to those in the spectra reported for Mn(III) monomeric species.[53]

However, one other manganese complex of a Schiff base ligand containing pyridine *N*-oxide groups is known,[48] which also has an uncommon, brown-red colour. Here, the manganese is in the +2 oxidation state. Furthermore, in an early study of metal complexes of pyridine *N*-oxide, the unusual yellow colour of the manganese(II) complex was already noticed and ascribed to the presence of a low-lying metal-to-ligand charge-transfer ($e_g \rightarrow \pi^*$) band.[54] In a detailed study a few years later, evidence supporting this assignment was provided by calculations of the optical electronegativity of the metal ion and of the acceptor π^* orbitals of the pyridine *N*-oxide ligand.[55]

Magnetic susceptibility measurements clearly showed that **7.6** exists of two very weakly antiferromagnetically coupled $S = 5/2$ systems ($J = -0.2$ cm^{-1}). This means that two Mn(II) centres are present, as was confirmed by the X-ray structure.

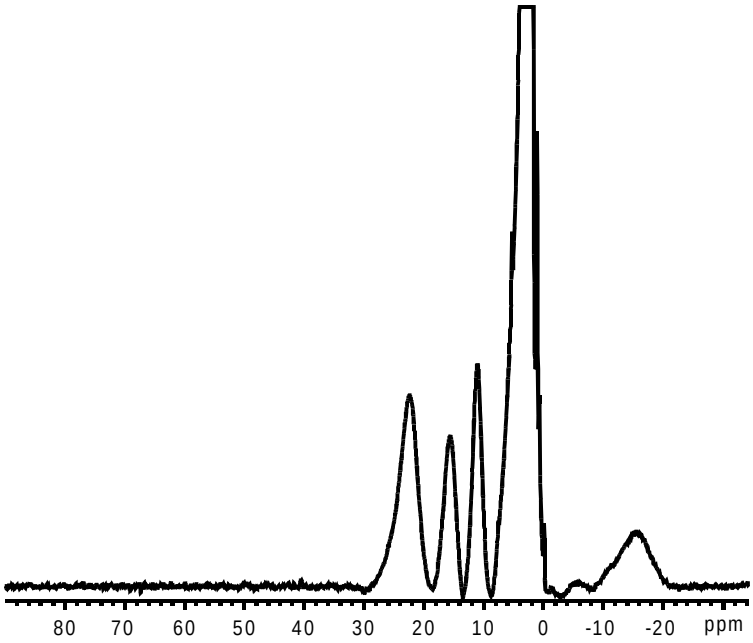

Figure 7.7 *^1H NMR spectrum of **7.6** recorded in CD_3CN.*

This result is also in agreement with the observed ES/MS spectrum of **7.6** in acetonitrile. Here, besides a large peak at m/z 325 attributable to the ligand $\{L^1 + 1H^+\}$, a peak at 478 was observed which corresponds to $\{\mathbf{7.6} - 2ClO_4^-\}$.

The redox properties of **7.6** were examined using cyclic voltammetry measurements in acetonitrile at room temperature (Figure 7.8). The cyclic voltammogram shows one reversible reduction peak at $E_{1/2}$ = 0.94 V relative to the saturated calomel electrode (SCE).

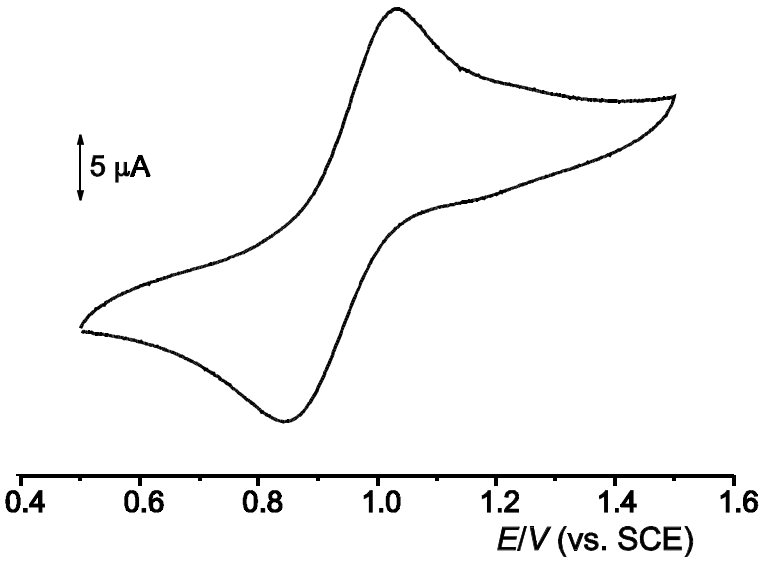

Figure 7.8 *Cyclic voltammogram of **7.6** in acetonitrile at RT. Scan rate 100 mVs^{-1}.*

Coulometric measurements showed that the reversible oxidation process involves two electrons.[56] The oxidation wave can therefore be assigned to the Mn(II)Mn(II) / Mn(III)Mn(III) couple. For these measurements, an argon-saturated acetonitrile solution (at -25 °C) containing **7.6** and 0.1 M $TBAPF_6$ was electrochemically oxidised at +1.35 V versus the reference (Ag / 0.01 M $AgNO_3$), (*i.e.* at +1.26 V vs Fc+ / Fc or at +1.66 V vs. NHE). When the current had dropped to background levels, 182 mC had passed (see coulometry curve I, Figure 7.9) which corresponds to 2.0 electrons per molecule. Subsequently the solution was re-reduced at -0.3 V versus the reference. A charge of 170 mC passed, *i.e.* 1.9 electrons per molecule (see coulometry curve II).

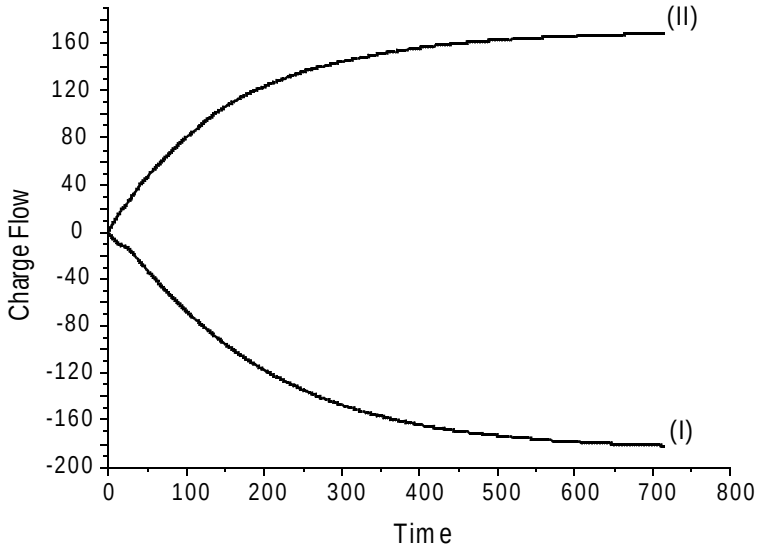

Figure 7.9 *Coulometry curves of **7.6** in acetonitrile at –25°C.*

The EPR spectrum of a solution of **7.6** in acetonitrile was recorded as well. Broad bands typical for weakly coupled d5 centres were observed.[57] A multiline signal at g = 2, which is present too, probably arises from a mononuclear Mn(II) impurity.[58,52] The impurity is presumably generated by decomposition of **7.6**. The broad signals disappear upon oxidation. This was expected, since due to fast spin relaxation, usually no EPR signals are observed for Mn(III)-Mn(III) complexes.[52] The mononuclear impurity, however, survives the two-electron oxidation.

From a solution of **7.6** in acetonitrile four UV-Vis spectra were taken. Spectrum 1 (Figure 7.10) was taken before the oxidation. It exhibits two bands at 272 nm ($\varepsilon = 2.5 \times 10^4$ $M^{-1}cm^{-1}$) and at 470 nm ($\varepsilon = 7.2 \times 10^2$ $M^{-1}cm^{-1}$). The second spectrum (spectrum 2) was recorded after completion of the two-electron oxidation yielding the Mn(III)-Mn(III) complex. As expected, the extinction coefficients increase upon formation of the Mn(III) species (*vide supra*). After about 15 min, the UV-Vis spectrum was again recorded (spectrum 3) in order to get an impression about the stability of the oxidised form. Finally after re-reduction to the Mn(II) dinuclear complex, spectrum 4 was taken. The similarity of, respectively, spectrum 1 and 4

and of spectrum 2 and 3 provides evidence that the complex can be chemically reversibly oxidised and that the oxidised form is stable at -25 °C for at least 15 min.

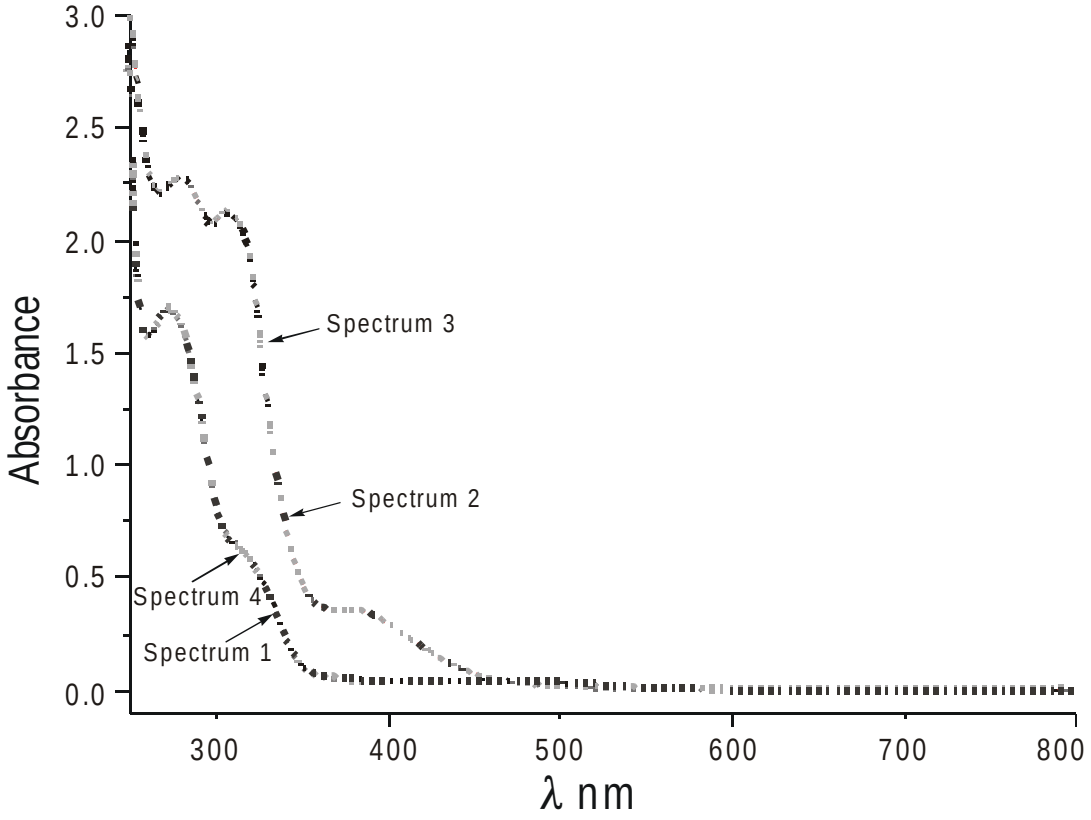

Figure 7.10 *Spectro-electrochemistry measurements: oxidation and re-reduction and again oxidation of* ***7.6*** *in acetonitrile at –25 °C.*

7.7 Oxidation experiments

Preliminary epoxidation experiments with complex **7.6** (1 mol% based on manganese) were performed using styrene as the substrate in acetone.[59] One equivalent of hydrogen peroxide (30% aqueous solution) was added and the reaction was followed by GC analysis. Unfortunately, the complex proved to be inactive, since neither the formation of styrene oxide nor the formation of side-products was observed. However, manganese-salen systems are only catalytically active in the presence of additives like Me-imidazole and carboxylates.[60] These additives function as an axial ligand. Manganese-salen complexes containing an additional 'arm' which can function as an axially coordinating group have been reported to catalyse epoxidation reactions using H_2O_2 as well (Figure 7.11).[61] In that case additives are unnecessary.

In the epoxidation reaction of styrene using complex **7.6**, *p*-cresol was added as an axial ligand. Nevertheless, under these reaction conditions the manganese complex proved to be completely inactive as well in styrene epoxidation, although some catalase activity was observed upon addition of hydrogen peroxide. In nature, some enzymes are known containing two manganese centres in their active site which catalyse the decomposition of H_2O_2. They are called catalases.[62,27] As was established by X-ray analysis of the active site of *Thermus thermophilus*, the manganese ions are separated from each other by a distance of 3.6 Å,[62] which is similar to the Mn-Mn distance found for **7.6** [3.57(2) Å]. Due to this close resemblance, the catalase activity of **7.6** is explicable.

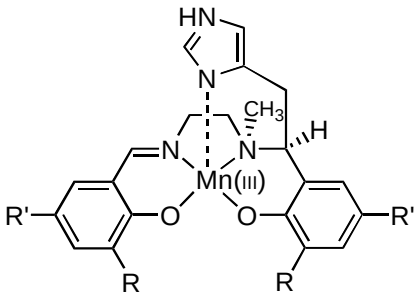

Figure 7.11 *Mn(III)-salen complexes with an internal axial ligand.*[61]

7.8 Conclusions

In this chapter, the synthesis of some new tri- and tetradentate ligands containing a pyridine *N*-oxide moiety was described. Unfortunately, no well-defined vanadium complexes could be isolated. This is probably due to the neutral character of the ligands, which results in poor coordination to vanadium. In addition, these ligands are sensitive towards decomposition. Attempts to synthesise Schiff base ligands, which would coordinate in an anionic manner to the metal centre (*e.g.* the Schiff base of **7.3** with 1-amino-2-propanol or 2-(1-aminoethyl)phenol), failed.

A novel strikingly orange-coloured manganese complex based on the pyridine *N*-oxide salen-derived ligand L^1 was synthesised and characterised using various spectroscopic techniques. The X-ray structure revealed that the complex is a dinuclear Mn(II) complex in which one of the pyridine *N*-oxide units of L^1 bridges between the metal centres and the other one coordinates to only one manganese ion. Surprisingly, one perchlorate ion is bound to each manganese centre and two perchlorates are non-coordinating. Unfortunately, preliminary experiments showed that the complex was inactive in the catalytic epoxidation reaction of styrene using H_2O_2 as the oxidant, even in the presence of *p*-cresol as an axial ligand.

7.9 Experimental section

7.9.1 General information

For general information, see Chapters 2 and 3. ***Caution***: perchlorate salts are potentially explosive and should be handled with care! Dichloromethane was distilled from P_2O_5, whereas benzene was distilled from Na-benzophenone. 2-(1-Aminoethyl)phenol and 1-aminoethylpyridine were kindly provided by Dr. René La Crois and Drs. Maartje Verdouw, respectively. Magnetic susceptibility, spectro-electrochemistry, EPR and coulometry measurements were performed by Dr. T. Weyhermüller, Dr. E. Bothe, and Dr. E. Bill from the Max-Planck Institut für Strahlenchemie in Mülheim (Ruhr), Germany. The epoxidation experiments with manganese complex **7.6** were performed by Dr. René La Crois. The X-ray structure was determined and solved by Drs. A. Meetsma. They are kindly acknowledged for their contributions described in this chapter.

7.9.2 X-ray crystallography of 7.6

An orange colourless thin needle-shaped crystal of **7.6** having approximate dimensions of 0.10 x 0.10 x 0.38 mm was picked from the mother liquor and covered with a thin layer of paraffin oil to avoid deterioration by air.

Crystal data. $C_{36}H_{40}Mn_2N_8O_4 \cdot 4\ ClO_4^-$, M = 1156.44, triclinic, space group $P\bar{1}$, T = 180 K, a = 9.917(5) Å, b = 9.99(1) Å, c = 12.11(1) Å, α = 87.25(9)°, β = 67.50(6)°, γ = 80.65(6)°, V = 1093.6(16) Å^3, Z = 1, D_x = 1.756 g cm^{-3}, μ(MoKα) = 1.0 cm^{-1}, F(000) = 1008, *GooF* = 1.126, $wR(F^2)$ = 0.2598 for 3696 reflections and 312 parameters, 28 restraints and $R(F)$ = 0.0938 for 2757 reflections obeying $F_o \geq 4.0\ \sigma(F_o)$ criterion of observability.

Data collection, structure analysis, and refinement. The crystal used for characterisation and data collection was glued on top of a glass fiber by using inert-atmosphere handling techniques and was transferred into the cold nitrogen stream of the low temperature unit[63] mounted on an Enraf-Nonius *CAD-4F*2[64] diffractometer, interfaced to a *INDY* (*Silicon Graphics*) *UNIX* computer (Mo tube, 50 kV, 40 mA, monochromated MoKα radiation, $\Delta\omega$ = 1.30 + 0.34 tg θ).

The scattering power of the studied crystal was weak and reflections' profiles showed anisotropic mosaicity; this mosaicity did not allow using a narrower scan angle.

Unit cell parameters[65] and orientation matrix were determined from a least-squares treatment of the *SET4*[66] setting angles of 22 reflections in the range 13.32° < θ < 20.38°. The unit cell was identified as triclinic, space group $P\bar{1}$: the *E*-statistics were indicative of a non-centrosymmetric space group.[67] Reduced cell calculations did not indicate any higher metric lattice symmetry[68] and examination of the final atomic coordinates of the structure did yield an inversion centre[69,70] , but is not fully compatible with the final structure. The synthesis is performed with an *R,R* configuration of the starting ligand; which gives by inversion an *S,S* configuration.

The intensities of three standard reflections, monitored every three hours of X-ray exposure time, showed no greater fluctuations during data collection than those expected

from Poisson statistics. Intensity data were corrected for Lorentz and polarisation effects, scale variation, for absorption[71] (correction: in the range 1.60 and 6.06) and reduced to F_o^2.[72]

The structure was solved by direct methods with *SIR-97*.[73] The positional and isotropic displacement parameters for the non-hydrogen atoms were refined. Ultimately the anisotropic displacement parameters of the Mn and Cl atoms were refined. Refinement was complicated (frustrated) by disorder problems: from the solution it was clear that the perchlorate anions were highly disordered and also some disorder in the ligand rings was observed. In the subsequent refinements bond restrains for the two non-bonded perchlorate anions (to Cl3 and to Cl4) Cl-O, O-O and for some C-C and C-N distances of the ligand were applied (in which the disorder is compensated by the large thermal displacement parameters). The hydrogen atoms were included in the final refinement riding on their carrier atoms with their positions calculated by using sp^2 or sp^3 hybridisation at the C-atom as appropriate with $U_{iso} = c \times U_{equiv}$ of their parent atom, where $c = 1.2$ and where values U_{equiv} are related to the atoms to which the H atoms are bonded.

Final refinement converged at $wR(F^2) = 0.2598$ for 3596 reflections and $R(F) = 0.0938$ for 2657 reflections with $F_o \geq 4.0\ \sigma(F_o)$ and 312 parameters and 28 restraints. The final difference Fourier map was essentially featureless with a few peaks of max. 1.3(2) e / Å^3 within 1.0 Å from the O-position of the highly disordered perchlorate anions.

The absolute structure of the molecule actually chosen was determined by Flack's[74]-refinement (**x** = 0.0(1)), these absolute exhibited configuration is in agreement with the predicted configuration as known by synthesis route. The positional and anisotropic displacement parameters for the non-hydrogen atoms and isotropic displacement parameters for hydrogen atoms were refined on F^2 with full-matrix least-squares procedures minimising the function $Q = \sum_h [w(\,|\,(F_o^2) - k(F_c^2)\,|\,)^2]$, where $w = 1/[\sigma^2(F_o^2) + (aP)^2 + bP]$, $P = [\max(F_o^2,0) + 2F_c^2] / 3$, F_0 and F_c are the observed and calculated structure factor amplitudes, respectively; a and b were refined.

Neutral atom scattering factors and anomalous dispersion corrections were taken from *International Tables for Crystallography*[75] All calculations were performed on a Pentium-III / Debian-Linux computer at the University of Groningen with the program packages *SHELXL*[76] (least-square refinements), *PLATON*[71] (calculation of geometric data and the *ORTEP* illustrations) and a locally modified version of the program *PLUTO*[77] (preparation of illustrations).

Each asymmetric unit contains one formula unit, consisting of three moieties: a cation di-nuclear Mn-complex with two bonded perchlorates and two (disordered) ClO_4^- anions, with no atom setting at special position. No missed symmetry (*MISSYM*) or solvent-accessible voids were detected by procedures implemented in *PLATON*.[78,79]

7.9.3 Spectro-electrochemistry measurements

A 7.5 ml argon-saturated acetonitrile solution (at -25 °C) containig 1.1 mg of **7.6** and 0.1 M $TBAPF_6$ were electrochemically oxidised at +1.35 V versus the reference (Ag / 0.01 M

$AgNO_3$), (*i.e.* at +1.26 V vs Fc+/Fc or at +1.66 V vs. NHE). When the current had dropped to background levels, 182 mC had passed (see coulometry curve I) which corresponds to 2.0 electrons per molecule. A sample of 0.2 ml of was taken out for EPR measurements, and subsequently the solution was re-reduced at -0.3 V versus the reference. A charge of 170 mC passed, *i.e.* 1.9 electrons per molecule, see coulometry curve II. The following four UV/VIS spectra were taken successively in the coulometric cell (d= 0.5 cm), see Figure 7.10:

1. Before oxidation.
2. After completion of oxidation.
3. About 15 min after completion of oxidation.
4. After completion of re-reduction.

7.9.4 Syntheses

2-(1,3-Dioxolan-2-yl)pyridine (7.1) 2-Pyridinecarboxaldehyde (40 g, 0.37 mol) and ethylene glycol (65 g, 1.05 mol, 2.8 equiv.) were dissolved in toluene (1 l). A spatula of *p*-toluenesulfonic acid was added and the reaction mixture was refluxed under Dean-Stark conditions for 18 h. Evaporation of the solvent yielded a dark brown oil which was purified by bulb to bulb destillation (15 mmHg, 150 °C). Yield as a yellow oil: 44.38 g (0.29 mol, 79%). ^{1}H NMR ($CDCl_3$) 8.58 (d, 1H, J = 4.8 Hz), 7.69 (dt, 1H, J = 1.8 Hz, J = 7.7 Hz), 7.48 (d, 1H, J = 8.1 Hz), 7.26-7.21 (m, 1H), 5.81 (s, 1H), 4.15-4.00 (m, 4H); ^{13}C-NMR ($CDCl_3$) 156.6 (C), 148.8 (CH), 136.3 (CH), 123.5 (CH), 120.3 (CH), 103.2 (CH), 65.1 (CH_2); CI/MS m/z 152 {M + 1H$^+$}, 168 {M + 1O^{2-} + 1H$^+$}.

2-(1,3-Dioxolan-2-yl)-pyridine-1-oxide (7.2) A suspension of UHP (H_2O_2-urea complex, 7.55 g, 80 mmol, 4 equiv.) and phthalic anhydride (4.44 g, 30 mmol, 1.5 equiv.) in CH_3CN (75 ml) was stirred for 15 min. Subsequently the protected pyridinecarboxaldehyde **7.1** was added and the reaction mixture was stirred for 18 h at RT. The reaction was followed by TLC (EtOAc-hexane, 2 : 1) until all the starting material had disappeared. About 50 ml of a saturated K_2CO_3 solution was added until the reaction mixture was alkaline (pH 8). Next, $CHCl_3$ (50 ml) was added. The water layer was extracted with $CHCl_3$ (3 x 50 ml). Water (25 ml) was added to the aqueous layer followed by extraction with another 50 ml of CH_3Cl. The combined organic layers were washed with brine (40 ml) and dried on Na_2SO_4. Evaporation of the solvent yielded **7.2** as a slightly yellow oil (3.10 g, 18.5 mmol, 93%). ^{1}H NMR ($CDCl_3$) 8.13-8.10 (m, 1H), 7.45-7.42 (m, 1H), 7.21-7.14 (m, 2H), 6.22 (s, 1H), 3.96 (m, 4H); ^{13}C-NMR ($CDCl_3$) 147.2 (C), 139.5 (CH), 125.7 (CH), 125.5 (CH), 123.3 (CH), 97.0 (CH), 65.1 (CH_2); HRMS calcd for $C_8H_9NO_3$: 167.058, found: 167.059.

2-Formyl-pyridine-1-oxide (7.3) The protected pyridine *N*-oxide (3.00 g, 17.9 mmol) was dissolved in 20% HCl (150 ml) and heated at 110 °C for 30 min. The reaction mixture was neutralised with solid $NaHCO_3$ and extracted with $CHCl_3$ (6 x 100 ml). The combined organic layers were dried on Na_2SO_4. After evaporation of the solvent, a yellow solid was

obtained (2.15 g, 17.5 mmol, 97%) which was purified by crystallisation from benzene (15 ml). The resulting yellow crystals were washed with pentane, dried *in vacuo* and stored under argon. Yield: 1.59 g (12.9 mmol, 72%). ^{1}H NMR ($CDCl_3$) 10.62 (s, 1H), 8.20 (d,1H, J = 6.2 Hz), 7.83-7.80 (m, 1H), 7.45 (dt, 1H, J = 2.2 Hz, J = 7.0 Hz), 7.31 (t, 1H, J = 7.7 Hz); ^{13}C-NMR (DMSO-d_6) 186.2 (CH), 143.2 (C), 140.2 (CH), 130.8 (CH), 125.3 (CH), 125.2 (CH); CI / MS m/z 124 {M + 1H$^+$}.

2-({[2-(2-Pyridinyl)ethyl]imino}methyl)-pyridine-1-oxide (7.4) To a solution of pyridine-carboxaldehyde *N*-oxide **7.3** (50 mg, 0.41 mmol) in dry CH_2Cl_2 (3 ml) was added 2-aminoethylpyridine (50 mg, 0.41 mmol, 1.0 equiv.) dissolved in CH_2Cl_2 (2 ml). A spatula of Na_2SO_4 was added and the reaction mixture was stirred under an argon atmosphere for 45 min. The mixture was filtered and concentrated *in vacuo* yielding a yellow oil which solidified upon standing (92 mg, 0.40 mmol, 99%). ^{1}H NMR ($CDCl_3$) 8.77 (1H, s), 8.37 (d, 1H, J = 4.4 Hz), 8.00 (d, 1H, J = 6.6 Hz), 7.77-7.34 (m, 1H), 7.41 (dt, 1H, J = 1.5 Hz, J = 7.7 Hz), 7.14-6.92 (m, 4H), 3.96 (t, 2H, J = 7.3 Hz), 3.03 (t, 2H, J = 7.3 Hz); ^{13}C-NMR ($CDCl_3$) 158.9 (C), 153.7 (CH), 148.9 (CH), 144.9 (C), 139.2 (CH), 135.8 (CH), 126.4 (CH), 125.0 (CH), 124.0 (CH), 123.0 (CH), 121.0 (CH), 60.1 (CH_2), 38.0 (CH_2); CI / MS m/z 128 {M + 1H$^+$}, 212 {M - 1O^{2-} + 1H$^+$}.

2-({[1-(2-Pyridinyl)ethyl]imino}methyl)-pyridine-1-oxide (7.5) Pyridine *N*-oxide **7.3** (50 mg, 0.41 mmol) was dissolved in dry CH_2Cl_2 (3 ml) and a solution of 1-aminoethylpyridine (rac) (50 mg, 0.41 mmol, 1.0 equiv.) in CH_2Cl_2 (2 ml) was added at once. Na_2SO_4 was added and the reaction mixture was stirred for 45 min under an argon atmosphere. After evaporation of the solvent, a yellow oil was obtained (90 mg, 0.40 mmol, 98%). ^{1}H NMR ($CDCl_3$) 9.18 (s, 1H), 8.59 (d, 1H, J = 4.0 Hz), 8.23-8.20 (m, 1H), 8.12-8.09 (m, 1H), 7.69 (dt, 1H, J = 1.8 Hz, J = 7.7 Hz), 7.47 (d, 1H, J = 8.1 Hz), 7.34-7.28 (m, 2H), 7.21-7.17 (m, 1H), 4.86 (q, 1H, J = 6.6 Hz), 1.66 (d, 1H, J = 6.6 Hz); ^{13}C NMR ($CDCl_3$) 162.7 (C), 153.1 (CH), 149.0 (C), 145.4 (C), 139.5 (CH), 136.5 (CH), 126.7 (CH), 125.2 (CH), 124.6 (CH), 122.0 (CH), 71.3 (CH), 23.2 (CH_3).

2-{[((*R*,*R*)-2-{[(2-picolyl-1-oxide)methylidene]amino}cyclohexyl)imino]-methyl}-pyridine-1-oxide (L^1) (*R*,*R*)-Diaminocyclohexane (250 mg, 2.19 mmol) was dissolved in dry CH_2Cl_2 (30 ml). Pyridine *N*-oxide **7.3** (539 mg, 4.38 mmol, 2.0 equiv.) was added and the reaction mixture was stirred for 30 min under an argon atmosphere. Na_2SO_4 was added and the mixture stirred for an additional 1 h. The solution was filtered and the reaction volume was reduced *in vacuo* to ~ 5 ml. The resulting bright yellow solution was syringed under a pentane layer (~ 25 ml). After diffusion of the two layers, yellow crystals were formed. Yield: 0.51 g (1.57 mmol, 72%). ^{1}H NMR ($CDCl_3$) 8.88 (s, 2H), 8.11-8.08 (m, 2H), 7.91-7.88 (m, 2H), 7.23-7.17 (m, 4H), 3.58-3.55 (m, 2H), 1.87-1.72 (m, 6H), 1.50-1.44 (m, 2H); ^{13}C NMR ($CDCl_3$) 153.1 (CH), 145.3 (C), 139.4 (CH), 126.5 (CH), 125.4 (CH), 124.6 (CH), 73.8 (CH), 32.5 (CH_2), 24.1 (CH_2); CI / MS m/z 325 {M + 1H$^+$}, 309 {M - 1O^{2-} + 1H$^+$}, 293 {M – 2O^{2-} + 1H$^+$}; Anal. calcd. for $C_{18}H_{20}N_4O_2 \cdot 0.25\ H_2O$: C 65.74; H 6.28; N 17.04%, found: C 65.85; H 6.28; N 16.95%.

$[Mn(L^1)(ClO_4)_2]_2$ (7.6) To a solution of ligand L^1 (50 mg, 0.154 mmol) dissolved in CH_3CN (4 ml) was added a solution of $Mn(II)(ClO_4)_2 \cdot 6\ H_2O$ (56 mg, 0.155 mmol) dissolved in CH_3CN (1 ml). The orange-red solution was stirred for 1 h. Orange crystals were obtained by slow diffusion of CH_2Cl_2 into the solution. Yield: 60 mg (0.104 mmol, 67%). ^1H NMR (CD_3CN) 22.4, 15.7, 11.1, 5.3, -5.4, -15.5; ES / MS *m* / *z* 325 $\{L^1 + 1H^+\}$, 478 $\{2M - 2ClO_4^-\}$; Anal. calcd. for $(C_{18}H_{20}N_4O_{10}Cl_2Mn)_2$: C 37.39; H 3.49; N 9.69; Mn 9.50%, found: C 37.30; H 3.20; N 9.54; Mn 9.34%; $\lambda_{max}(CH_3CN)$ 272 nm (ε = 2.5 x 10^4 $M^{-1}cm^{-1}$) and at 470 nm (ε = 7.2 x 10^2 $M^{-1}cm^{-1}$).

7.10 References

1 Gorzynski Smith, J. *Synthesis*, **1984**, 629.
2 Jørgensen, K. A. *Chem. Rev.* **1989**, *89*, 431.
3 *Comprehensive Asymmetric Catalysis*, Jacobsen, E.N.; Pfaltz, A.; Yamamoto, H., Eds., Springer, Berlin, 2000.
4 Jacobsen, E.N. in *Catalytic Asymmetric Synthesis*, Ojima, I., Ed., VCH, Weinheim, 1993, Chapter 4.2.
5 (a) Katsuki, T.; Sharpless, K.B. *J. Am. Chem. Soc.* **1980**, *102*, 5974. (b) Sharpless, K.B. *Chemtech* **1985**, 692.
6 Berrisford, D.J.; Bolm, C.; Sharpless, K.B. *Angew. Chem. Int. Ed. Engl.* **1995**, *34*, 1059.
7 Katsuki, T.; Martin, V.S. in *Organic Reactions*, Paquette, L.A. *et al.*, Eds., John Wiley & Sons, New York, 1996, Chapter 1.
8 Zhang, W.; Loebach, J.L.; Wilson, S.R.; Jacobsen, E.N. *J. Am. Chem. Soc.* **1990**, *112*, 2801.
9 Irie, R.; Nodda, K.; Ito, Y.; Katsuki, T. *Tetrahedron Lett.* **1990**, *31*, 7345.
10 See for an overview: (a) La Crois, R.M. 'Manganese Complexes as Catalysts in Epoxidation Reactions', PhD Thesis, Groningen, 2000, Chapter 1. (b) Hoogenraad, M. 'Manganese Complexes as Catalysts for Homogeneous Oxidation Reactions', PhD Thesis, Leiden, 2000, Chapter 1.
11 Michaelson, R.C.; Palermo, R.E.; Sharpless, K.B. *J. Am. Chem. Soc.* **1977**, *99*, 1990.
12 Sharpless, K.B.; Verhoeven, T.R. *Aldrichim. Acta* **1979**, *12*, 63.
13 Boyle, T.J.; Eilerts, N.W.; Heppert, J.A.; Takusagawa, F. *Organometallics* **1994**, *13*, 2218.
14 See Chapter 6.6.
15 Murase, N.; Hoshino, Y.; Oishi, M.; Yamamoto, H. *J. Org. Chem.* **1999**, *64*, 338.
16 Hoshino, Y.; Murase, N.; Oishi, M.; Yamamoto, H. *Bull. Chem. Soc. Jpn.* **2000**, *73*, 1653.
17 Fisher, D.C.; Barclay-Peet, S.J.; Balfe, C.A.; Raymond, K.N. *Inorg. Chem.* **1989**, *28*, 4399.
18 Hoshino, Y.; Yamamoto, H. *J. Am. Chem. Soc.* **2000**, *122*, 10452.
19 Bolm, C.; Kühn, T. *Synlett* **2000**, 899.
20 Carreño, M.C. *Chem. Rev.* **1995**, *95*, 1717.
21 Kagan, H.B.; Ronan, B. *Rev. Heteroatom. Chem.* **1992**, *7*, 92.
22 Kagan, H.B.; Rebiere, F. *Synlett* **1990**, 643.

23 Kagan, H.B. in *Catalytic Asymmetric Synthesis*, Ojima, I., Ed., VCH, Weinheim, 1993, Chapter 4.3.

24 (a) Guerrero-de la Rosa, V.; Ordoñez, M.; Llera, J.M.; Alcudia, F. *Synthesis* **1995**, 761. (b) Anderson, K.K. *Tetrahedron Lett.* **1962**, 93.

25 Brunel, J.M.; Kagan, H.B. *Synlett* **1996**, 404 and references therein.

26 Butler, A.; Clague, M.J.; Meister, G.E. *Chem. Rev.* **1994**, *94*, 625.

27 See also Chapter 1.

28 See for recent examples: (a) Skarżewski, J.; Ostrycharz, E.; Siedlecka, R. *Tetrahedron Asymmetry*, **1999**, *10*, 3457. (b) Vetter, A.H.; Berkessel, A. *Tetrahedron Lett.* **1998**, *39*, 1741.

29 Nakajima, K.; Kojima, M.; Fujita, J. *Chem. Lett.* **1986**, 1483.

30 Nakajima, K.; Kojima, M.; Toriumi, K.; Saito, K.; Fujita, J. *Bull. Chem. Soc. Jpn.* **1989**, *62*, 760.

31 Nakajima, K.; Kojima, K.; Kojima, M.; Fujita, J. *Bull. Chem. Soc. Jpn.* **1990**, *63*, 2620.

32 Bolm, C.; Bienewald, F. *Angew. Chem. Int. Ed. Engl.* **1995**, *34*, 2640.

33 Bolm, C.; Bienewald, F. *Synlett* **1998**, 1327.

34 Bolm, C.; Schlingloff, G.; Bienewald, F. *J. Mol. Cat. A* **1997**, *117*, 347.

35 (a) Cogan, D.A.; Liu, G.; Kim, K.; Backes, B.J.; Ellman, J.A. *J. Am. Chem. Soc.* **1998**, *120*, 8011. (b) Liu, G.; Cogan, D.A.; Ellman, J.A. *J. Am. Chem. Soc.* **1997**, *119*, 9913.

36 (a) Ten Brink, H.B.; Tuynman, A.; Dekker, H.L.; Hemrika, W.; Izumi, Y.; Oshiro, T.; Schoemaker, H.E.; Wever, R. *Inorg. Chem.* **1998**, *37*, 6780. (b) Andersson, M.A.; Willets, A.; Allenmark, S.G. *J. Org. Chem.* **1998**, *62*, 8455. (c) Andersson, M.A.; Allenmark, S.G. *Tetrahedron* **1998**, *54*, 15293.

37 See Chapter 3.

38 For a review see: Conte, V.; Di Furia, F.; Licini, G. *Appl. Cat. A* **1997**, *157*, 335.

39 (a) Gonzalez-Baro, A.C.; Baran, E.J. *J. Coord. Chem.* **1998**, *43*, 335. (b) Mimoun, H.; Saussine, L.; Daire, E.; Postel, M.; Fischer, J.; Weiss, R. *J. Am. Chem. Soc.* **1983**, *105*, 3101. (c) Durgaprasad, G.; Patel, C.C. *Indian J. Chem.* **1973**, *11*, 1300.

40 Dyker, G.; Hölzer, B. *Tetrahedron* **1999**, *55*, 12557.

41 Kaczmarek, Ł.; Balicki, R.; Nantka-Namirski, P. *Chem. Ber.* **1992**, *125*, 1965.

42 Cooper, M.S.; Heaney, H.; Newbold, A.J.; Sanderson, W.R. *Synlett* **1990**, 533.

43 Ahlborn, E.; Diemann, E.; Müller, A. *Z. Anorg. Allg. Chem.* **1972**, *394*, 1.

44 (a) Chang, C.J.; Labinger, J.A.; Gray, H.B. *Inorg. Chem.* **1997**, *36*, 5927. (b) Schmidt, H.; Bashirpoor, M.; Rehder, D. *J. Chem. Soc., Dalton Trans.* **1996**, 3865. (c) Oyaizu, K.; Yamamoto, K.; Yoneda, K.; Tsuchida, E. *Inorg. Chem.* **1996**, *35*, 6634. (d) Hughes, D.L.; Kleinkes, U.; Leigh, G.J.; Maiwald, M.; Sanders, J.R.; Sudbrake, C. *J. Chem. Soc., Dalton Trans.* **1994**, 2457.

45 Hughes, D.L.; Smith, G.B.; Liu, J.; Dezeny, G.C.; Senanayake, C.H.; Larsen, R.D.; Verhoeven, T.R.; Reider, P.J. *J. Org. Chem.* **1997**, *62*, 2222.

46 Finney, N.S.; Pospisil, P.J.; Chang, S.; Palucki, M.; Konsler, R.G.; Hansen, K.B.; Jacobsen, E.N. *Angew. Chem., Int. Ed. Engl.* **1997**, *36*, 1720, and references cited therein.

47 (a) Higuchi, C.; Sakiyama, H.; Ōkawa, H.; Fenton, D.E. *J. Chem. Soc., Dalton Trans.* **1995**, 4015. (b) Sakiyama, H.; Tamaki, H.; Kodera, M.; Matsumoto, N.; Ōkawa, H. *J. Chem. Soc., Dalton Trans.* **1993**, 591.

48 Gou, S.; You, X.; Yu, K.; Lu, J. *Inorg. Chem.* **1993**, *32*, 1883.

49 Pessiki, P.J.; Khangulov, S.V.; Ho, D.M.; Dismukes, G.C. *J. Am. Chem. Soc.* **1994**, *116*, 891.

50 La Crois, R.M. 'Manganese Complexes as Catalysts in Epoxidation Reactions', PhD Thesis, Groningen, 2000.

51 Magnetic susceptibility, spectro-electrochemistry, EPR and coulometry measurements were performed by Dr. T. Weyhermüller, Dr. E. Bothe and Dr. E. Bill from the Max-Planck Institut für Strahlenchemie in Mülheim (Ruhr), Germany.

52 *Comprehensive Coordination Chemistry*, Wilkinson, G. Ed.; Pergamon Press, Oxford, 1987, *4*, Chapter 41.

53 Hoogenraad, M. 'Manganese Complexes as Catalysts for Homogeneous Oxidation Reactions', PhD Thesis, Leiden, 2000, Chapter 5.

54 Carlin, R.L. *J. Am. Chem. Soc.* **1961**, *83*, 3773.

55 Byers, W.; Chou, B.F.-C.; Lever A.B.P.; Parish, R.V. *J. Am. Chem. Soc.* **1969**, *91*, 1329.

56 Mazurek, W.; Bond, A.M.; Murray, K.S.; O'Connor, M.J.; Wedd, A.G. *Inorg. Chem.* **1985**, *24*, 2484.

57 Schultz, B.E.; Ye, B.-H.; Li, X.; Chan, S.I. *Inorg. Chem.* **1997**, *36*, 2617.

58 Goodman, B.A.; Raynor, J.B. *Adv. in Inorg. Chem. and Radiochem.* **1970**, *13*, 135.

59 Measurements performed by Dr. R.M. La Crois, University of Groningen, The Netherlands.

60 (a) Krishnan, R.; Vancheesan, S. *J. Mol. Catal. A* **1999**, *142*, 377. (b) Pietikäinen, P. *Tetrahedron* **1998**, *54*, 4319. (c) Pietikäinen, P. *Tetrahedron Lett.* **1994**, *35*, 941. (d) Irie, R.; Hosoya, N.; Katsuki, T. *Synlett* **1994**, 255.

61 (a) Berkessel, A.; Frauenkorn, M.; Schwenkreis, T.; Steinmetz, A. *J. Mol. Catal. A* **1997**, *117*, 339. (b) Berkessel, A.; Frauenkorn, M.; Schwenkreis, T.; Steinmetz, A.; Baum, G.; Fenske, D. *J. Mol. Catal. A* **1996**, *113*, 321. (c) Schwenkreis, T.; Berkessel, A. *Tetrahedron Lett.* **1993**, *30*, 4785.

62 Hage, R. *Recl. Trav. Chim. Pays-Bas*, **1996**, *115*, 385.

63 Bolhuis, F. van, *J. Appl. Cryst.* **1971**, *4* ,263.

64 Enraf-Nonius *CAD*4-*UNIX* Version 5.1, Utrecht modified version October 1994. Enraf-Nonius Delft, Scientific Instruments Division, Delft, The Netherlands.

65 Duisenberg, A.J.M. *J. Appl. Cryst.* **1992**, *25*, 92.

66 Boer, J.L. de; Duisenberg, A.J.M. *Acta Cryst.* **1984**, *A40*, C-410.

67 Snow, M.R.; Tiekink, E.R.T. *Acta Cryst.* **1988**, *B44*, 676.

68 Spek, A.L. *J. Appl. Cryst.* **1988**, *21*, 578.

69 Le Page, Y. *J. Appl. Cryst.* **1987**, *20*, 264.

70 Le Page, Y. *J. Appl. Cryst.* **1988**, *21*, 983.

71 Spek, A.L. *PLATON*, Program for the automated analysis of molecular geometry, Version of March 2000, University of Utrecht, The Netherlands.

72 Spek, A.L. *HELENA*, Program for reduction of *CAD*4 Data, Utrecht University, 1993, The Netherlands.

73 Altomare, A.; Burla, M.C.; Camalli, M.; Cascarano, G.L.; Giacovazzo, C.; Guagliardi, A.; Moliterni, A.G.G.; Polidori, G.; Spagna, R. *J. Appl. Cryst.* **1999**, *32*, 115. *SIR-97*, A package for crystal structure solution by direct methods and refinement, University of Bari, University of Perugia, University of Roma, Italy.

74 Flack, H.D. *Acta Cryst.* **1983**, *A39*, 876.

75 International Tables for crystallography, 1992, Volume C; Wilson, A.J.C., Ed.; Kluwer Academic Publishers, Dordrecht, The Netherlands.

76 Sheldrick, G.M. *SHELXL-97*, Program for the refinement of crystal structures, University of Göttingen, Germany.

77 Meetsma, A. *PLUTO*, Molecular Graphics Program, University of Groningen, The Netherlands.

78 Spek, A.L. *Acta Cryst.* **1990**, *A46*, C-34.

79 Spek, A.L. *Am. Crystallogr. Assoc. Abstr.* **1994**, *22*, 66.

Chapter 8

Non-heme Iron Complexes for Catalytic Oxidation[1]

8.1 Introduction

In nature, a variety of non-heme metalloenzymes are present which are capable of oxidation of substrates with high turnover frequencies and / or excellent selectivity.[2] Examples include the diiron containing enzyme methane monooxygenase (MMO), which selectively oxidises methane to methanol[3] and iron bleomycin (Fe-BLM), a metalloglycopeptide capable of selective oxidative DNA cleavage using O_2.[4] Another example is the mononuclear copper enzyme galactose oxidase (GOase)[5] which catalyses the aerobic oxidation of benzylic and allylic alcohols to their corresponding aldehydes with concomitant formation of H_2O_2. In this enzyme, the copper ion is coordinated in the equatorial plane to two histidine residues (His_{496} and His_{581}), a tyrosinate residue (Tyr_{272}) and a water molecule and to another tyrosinate residue (Tyr_{495}) in the apical position.[6] The radical-based mechanism proposed for the oxidation of primary alcohols by GOase is shown in Scheme 8.1.[6,7]

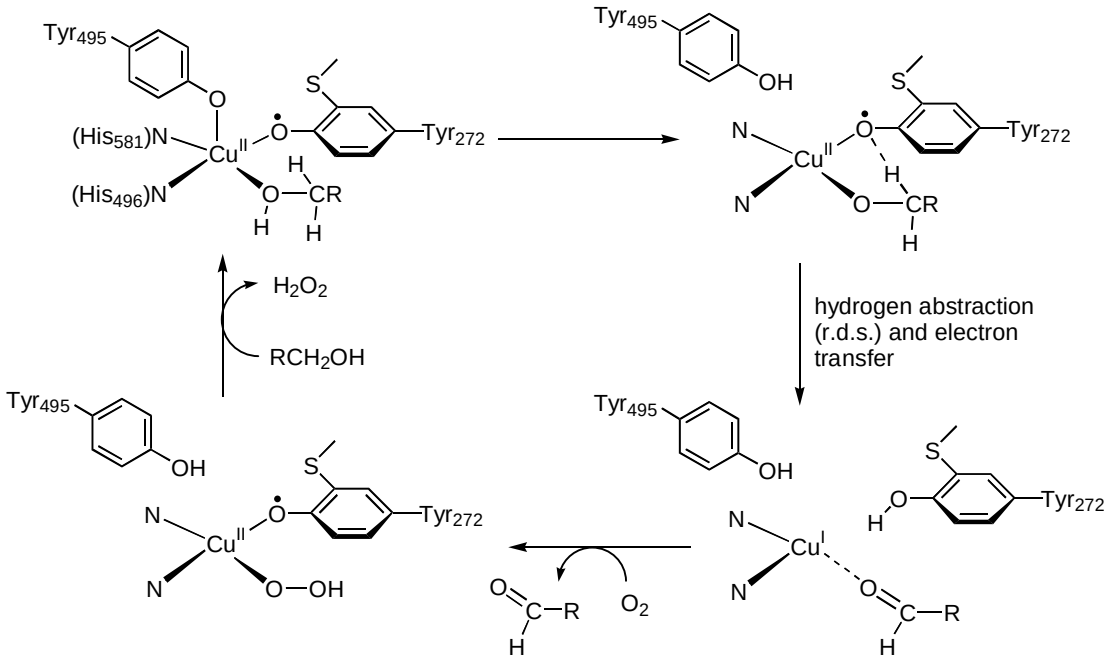

Scheme 8.1 *Proposed mechanism of catalytic alcohol oxidation by galactose oxidase.*[6]

In the first step of the catalytic cycle, the primary alcohol binds to an equatorial coordination site of the Cu(II) tyrosyl radical species replacing the water molecule. Then,

deprotonation occurs with the axial Tyr_{495} residue acting as the base. Subsequently, a hydrogen atom is abstracted in the rate-determining step from the carbon atom of the primary alcohol by the tyrosyl radical. The resulting ketyl radical is oxidised to the aldehyde by an intramolecular electron transfer to the Cu(II) ion. The original Cu(II) tyrosyl radical species is restored by the oxidation of the Cu(I) centre and the tyrosine residue with dioxygen, producing hydrogen peroxide.

To obtain more insight into the oxidation mechanism of these type of enzymes, many functional model systems were studied. These studies often not only provide invaluable information about metalloenzymes, but they may also result in the development of new generations of homogeneous oxidation catalysts.[8] Beautiful examples are the GOase models, developed by the groups of Wieghardt and Stack, which are capable of oxidising alcohols to the corresponding aldehydes with high yield and selectivity.[9]

Stack *et al.* synthesised copper complexes based on diimine-diphenolate ligands. A binaphthyl unit in the backbone was incorporated to enforce a distortion of the square-planar geometry coordination, preferred by Cu(II) ions, towards a tetrahedral geometry. In this manner, the stability of the Cu(I) intermediate is increased. The substituents on the phenolate rings are necessary in order to stabilise the Cu(II)-phenoxyl radical species.

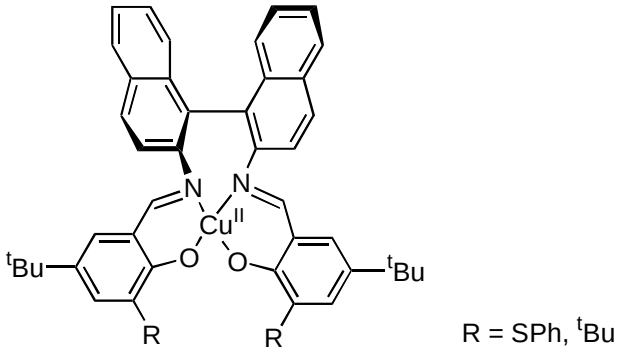

Figure 8.1 *GOase mimic developed by Stack et al.*[9a]

The Cu(II)-phenolate complex as shown in Figure 8.1 acts as a precursor of the catalytically active copper(II) phenoxyl-radical species. The catalytic oxidation seems to proceed by the same mechanism as the enzyme-catalysed reaction (*vide supra*). Benzylic and allylic alcohols can be converted to the corresponding aldehyde with concomitant formation of hydrogen peroxide using molecular oxygen at room temperature. Turnover numbers as high as 1300 have been reported.

The model system used by Wieghardt *et al.* is based on the ligand 2,2'-thiobis(2,4-di-*tert*-butylphenol) (Scheme 8.2). The catalytically active species was identified as the bis(phenolato)-bridged dicopper(II) complex. Each copper ion is coordinated to a phenoxyl radical. Using this catalyst in tetrahydrofuran under an atmosphere of air at 20 °C, ethanol is converted to acetaldehyde in 63% yield in 12 h. A turnover number of 630 was reached. When secondary alcohols were used as substrates, the formation of ketones was not

observed. However, the corresponding dimeric glycols were obtained in high yields. These results were explained by assuming that in this case two alkoxides instead of one bind to the two copper ions. Now, C-C bond formation can take place between the two coordinated ketyl radicals yielding the glycol products.

A catalytic cycle was postulated for the oxidation of primary alcohols as shown in Scheme 8.2. First an alkoxide binds to one of the Cu(II) ions at the axial position. Then, hydrogen abstraction takes place in a rate-determining step. The corresponding aldehyde is formed after an intramolecular electron transfer step. Finally, oxidation of the coordinated phenolate ligands to phenoxyl radicals by O_2 regenerates the original catalyst. In this case, the Cu(I) intermediate is not involved in the catalytic mechanism.

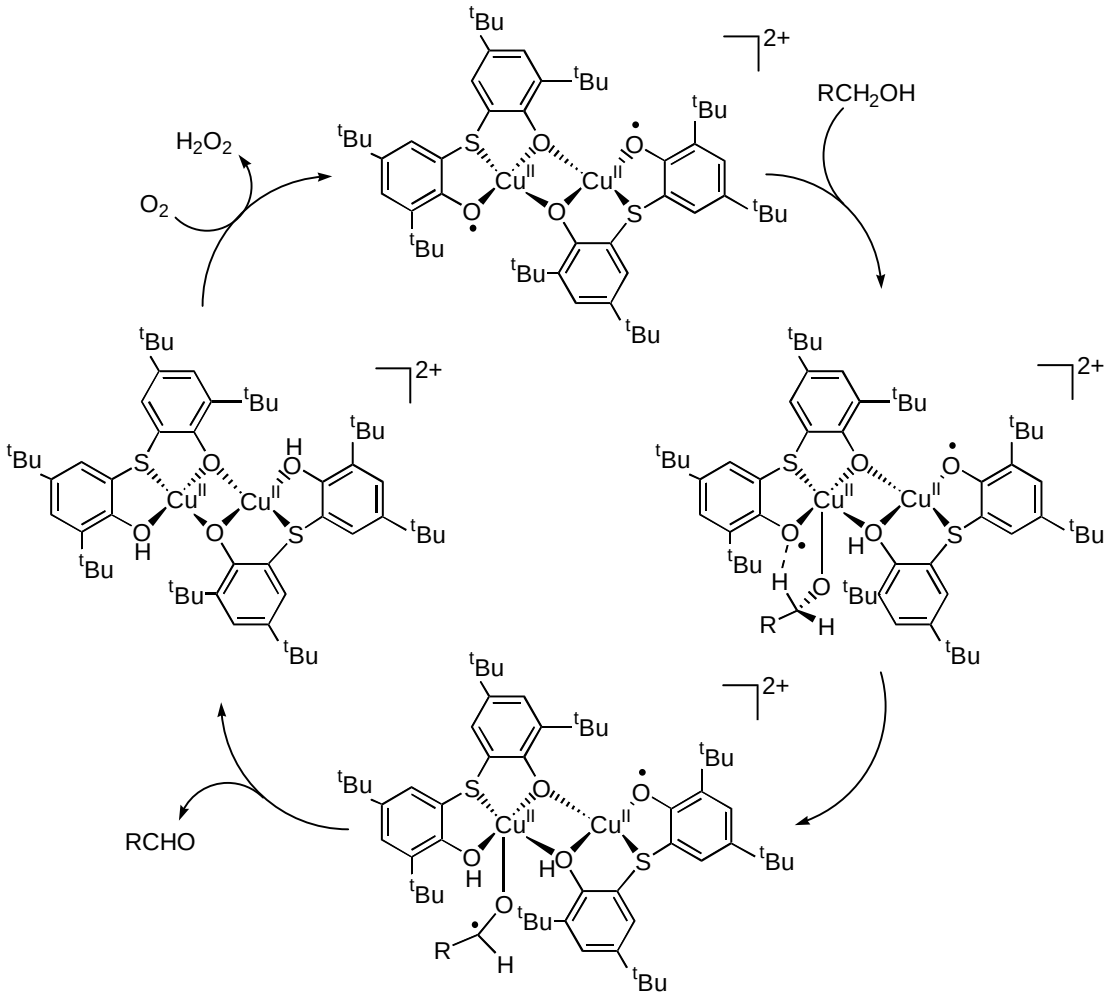

Scheme 8.2 *Proposed mechanism for the catalytic oxidation of primary alcohols by a bis(phenolato)-bridged dicopper(II) complex by Wieghardt et al.*[9b]

Other examples of selective metal-catalysed oxidations of alcohols to aldehydes include a system which uses a combination of $RuCl_2(PPh_3)_3$ and TEMPO,[10] a water-soluble palladium(II)-bathophenanthroline system,[11] a copper-phenanthroline system which uses hydrazines as additives,[12] and a manganese(IV) dinuclear system[13] based on trimethyl-

triazacyclononane.[14] The latter system is capable of oxidising benzyl alcohols to their corresponding benzaldehydes with high turnover numbers (up to 1000) using H_2O_2 or *tert*-butyl hydroperoxide (TBHP).[13]

In our group, an iron(II) complex **8.1** of the pentadentate ligand *N*,*N*-bis(2-pyridylmethyl)-*N*-bis(2-pyridyl)methylamine (N4Py) was developed as a model system for iron bleomycin (Fe-BLM).[15,16,17] This system is capable of oxidising alkanes using H_2O_2 *via* a radical type mechanism. To explore the effect of ligand variations on the oxidation behaviour of the complex, ligand HL^1 was prepared in which one of the pyridyl groups is replaced by a phenolate moiety.

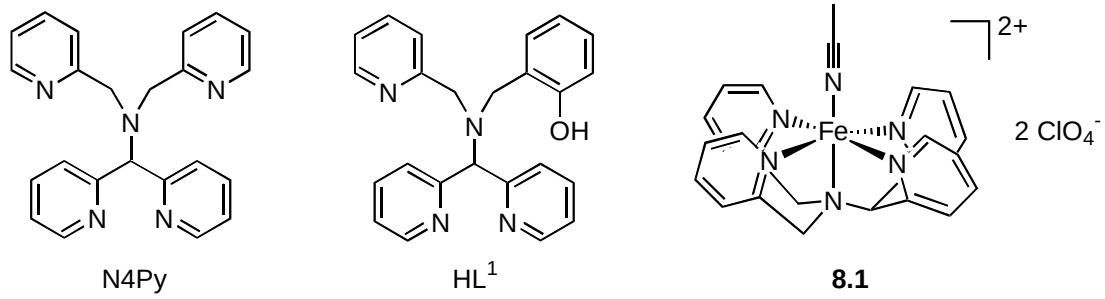

Figure 8.2 *N4Py, the corresponding Fe(II) complex $[Fe(N4Py)CH_3CN]^{2+}$ (**8.1**) and ligand HL^1.*

8.2 Synthesis and characterisation of an oxo diiron(III) complex of HL^1.

The synthesis of 2-{[[di(2-pyridyl)methyl](2-pyridylmethyl)amino]methyl}phenol (HL^1) is shown in Figure 8.3.[1,18]

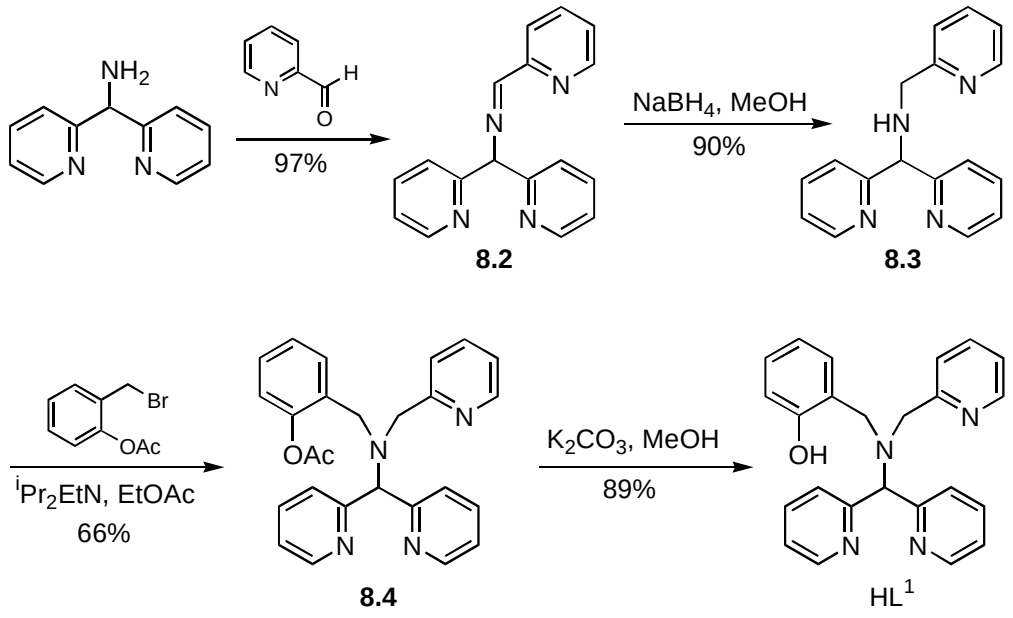

Figure 8.3 *Synthesis of ligand HL^1.*[1,18]

In a first step, bis(2-pyridyl)methylamine[19] is allowed to react neat with freshly distilled pyridine-2-carboxaldehyde. The generated imine **8.2** was reduced using $NaBH_4$ providing **8.3** in 90% yield. The phenol unit was introduced by reaction of this amine with acyl protected *o*-hydroxy-benzylbromide in the presence of diisopropylethylamine in ethyl acetate. After column chromatography **8.4** was obtained pure in 66% yield. Subsequently, the acetate group was removed by basic hydrolysis in methanol yielding HL^1 in 89%.

Complexation of the ligand HL^1 with $Fe(II)(ClO_4)_2 \cdot H_2O$ in MeOH, in the presence of 1 equiv. of Et_3N followed by slow diffusion of ethyl acetate into the methanolic solution yielded purple crystals of complex **8.5** (λ_{max} = 540 nm, ε = 5.6 x 10^3 $M^{-1}cm^{-1}$) in 50% yield (Scheme 8.3).[20]

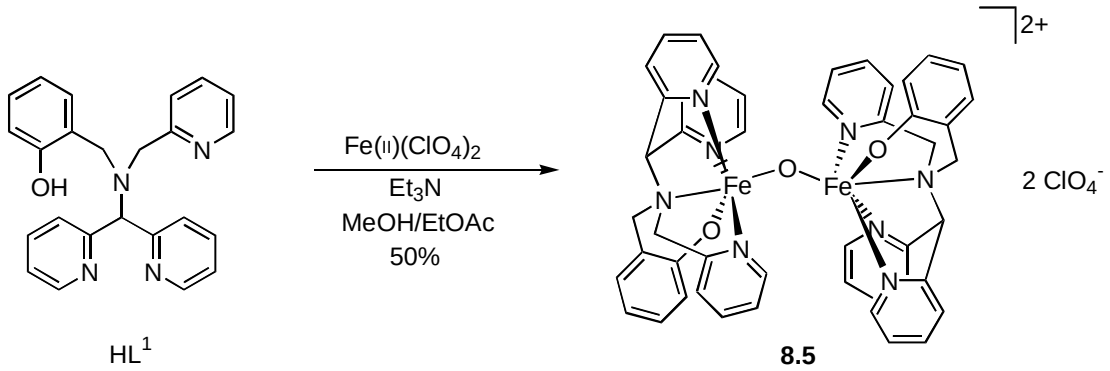

Scheme 8.3 *Synthesis of the μ-oxo Fe(III) dinuclear complex **8.5** of ligand HL^1.*

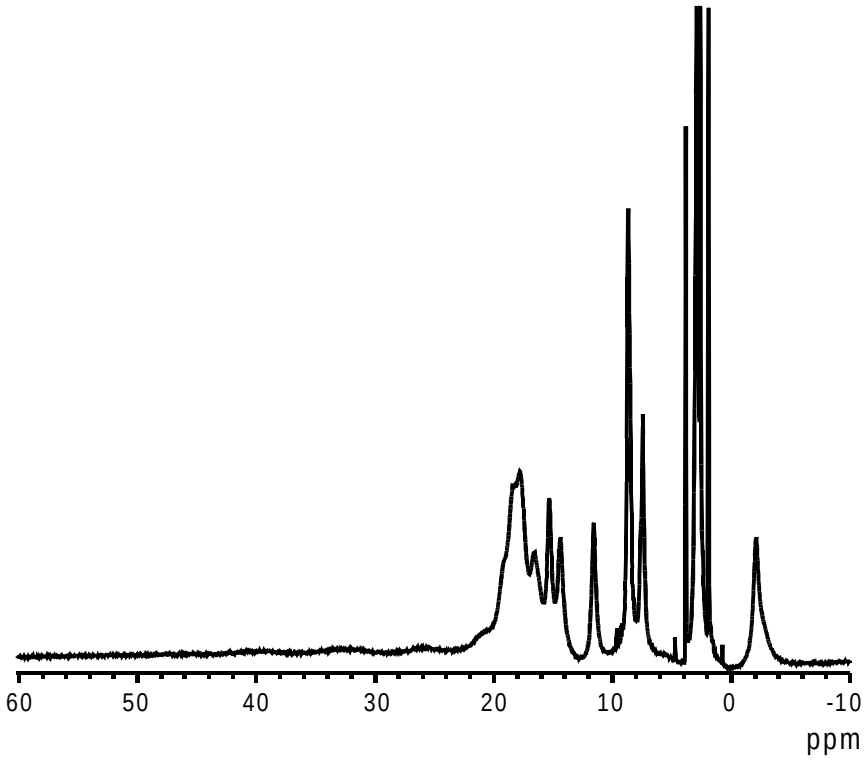

Figure 8.4 *^{1}H-NMR spectra of **8.5** recorded in CD_3CN.*

The complex was characterised as an antiferromagnetically coupled diiron(III) species based on its EPR-silent nature and its relatively narrow ^{1}H NMR spectrum, which exhibits paramagnetically shifted signals in the 0 - 40 ppm range.[21] The ES/MS spectrum shows a peak at m/z 445 ($[(L^1)Fe(\mu\text{-}O)Fe(L^1)]^{2+}$), which is consistent with the formulation of **8.5** as $\{[(L^1)Fe(\mu\text{-}O)Fe(L^1)](ClO_4)_2\}$. Unfortunately, the obtained crystals were of inferior quality, and the X-ray structure could not be determined. Therefore, the μ-oxo diiron(III) complex of HL^1 with BF_4^- counterions instead of perchlorates was prepared as well (**8.6**), by addition of $Fe(BF_4)_2{\cdot}6H_2O$ to a solution of the ligand in MeOH-CH_3CN (1 : 1) together with 1.5 equiv. of Et_3N. Fluffy purple needles were obtained after crystallisation from CH_3CN/EtOAc, but unfortunately these too were unsuitable for X-ray analysis. The ES/MS spectrum again showed a peak at m/z 445 ($[(L^1)Fe(\mu\text{-}O)Fe(L^1)]^{2+}$), corresponding to the formulation of **8.6** as $[(L^1)Fe(\mu\text{-}O)Fe(L^1)](BF_4)_2$. Furthermore, the ^{1}H NMR spectrum closely resembles the one recorded for **8.5**.

However, crystals of the corresponding PF_6-salt **8.7** $\{[(L^1)Fe(\mu\text{-}O)Fe(L^1)](PF_6)_2\}$ proved to be suitable for X-ray analysis (Figure 8.5). This compound was synthesised by adding $Fe(NO_3)_3{\cdot}9H_2O$ to a solution of the ligand HL^1 in methanol, followed by the addition of 1 equiv. of Et_3N and 2 equiv. of NH_4PF_6. Dark purple-blue crystals were obtained by slow diffusion of ether into the solution of **8.7**.

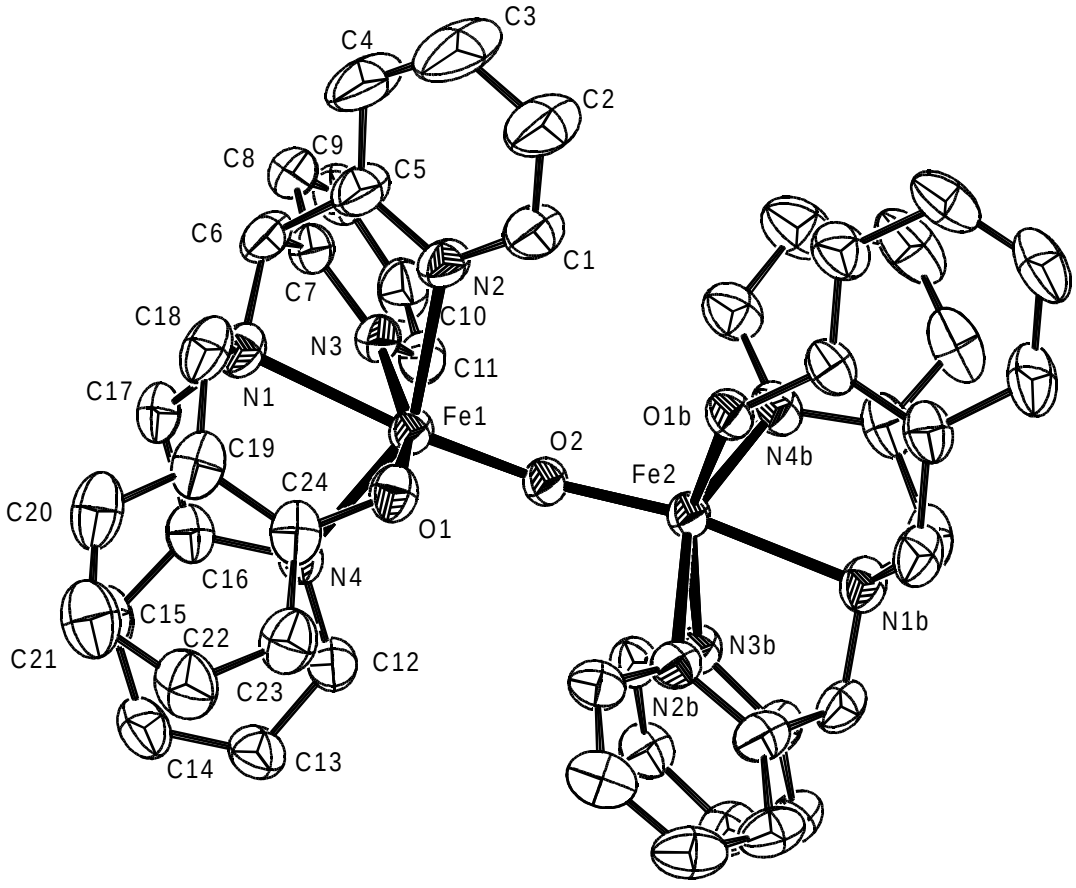

Figure 8.5 *ORTEP plot of **8.7** (50% probability level).*

Table 8.1 *Selected bond distances (Å) and angles (°) of* ***8.7*** *with estimated standard deviations (esd's) in parentheses.*

Bond distances			
Fe(1)-N(1)	2.258(2)	Fe(2)-N(1b)	2.250(2)
Fe(1)-N(2)	2.174(2)	Fe(2)-N(2b)	2.179(2)
Fe(1)-N(3)	2.217(2)	Fe(2)-N(3b)	2.241(2)
Fe(1)-N(4)	2.135(2)	Fe(2)-N(4b)	2.132(2)
Fe(1)-O(1)	1.9298(18)	Fe(2)-O(1b)	1.9285(17)
Fe(1)-O(2)	1.7899(17)	Fe(2)-O(1b)	1.7897(17)
O(1)-C(24)	1.344(4)	O(1b)-C(24b)	1.349(3)
Bond angles			
O(1)-Fe(1)-O(2)	103.73(8)	O(1b)-Fe(2)-O(2)	103.85(8)
N(1)-Fe(1)-O(2)	93.82(8)	N(1b)-Fe(2)-O(2)	167.94(8)
Fe(1)-O(1)-C(24)	123.00(17)	Fe(2)-O(1B)-C(24b)	124.97(16)
O(1)-Fe(1)-N(1)	89.04(8)	O(1b)-Fe(2)-N(1b)	88.20(8)
O(1)-Fe(1)-N(4)	88.67(8)	O(1b)-Fe(2)-N(4b)	88.10(8)
N(2)-Fe(1)-N(3)	81.49(8)	N(2b)-Fe(2)-N(3b)	79.15(8)
Fe(1)-O(2)-Fe(2)	151.22(1)		

Each iron(III) ion adopts a distorted octahedral coordination geometry involving a tertiary amine, three pyridine nitrogens, a phenolate oxygen atom and the bridging oxygen atom. The angle between the two iron centres and the bridging oxygen atom is 151.22(11)°. The crystal structure of **8.7** gave no indications that a proton is present at the phenolate moiety, which is consistent with the ES / MS results of **8.5** (*vide supra*).

The iron to O(2) bond lengths of 1.79 Å are as expected, since Fe(III)-O(oxo) distances are known in the literature to range from 1.73 - 1.82 Å.[22] The Fe-phenolate distances of 1.93 Å are also normal for these type of complexes.[23] The Fe-N distances are in the range of 2.13 – 2.26 Å. These values are comparable with Fe-N distances found for other μ-oxo Fe(III) dimeric complexes.[24] The intramolecular Fe-Fe distance is 3.47 Å, which is also comparable to other μ-oxo diiron(III) species (3.39-3.56 Å).[22,25] However, the Fe-O-Fe unit in a μ-oxo Fe(III) dimer based on N4Py[15a] (*vide infra*, complex **8.8**) is linear, resulting in a slightly longer Fe-Fe distance than for **8.7**, *i.e.* 3.60 Å.

8.3 Catalytic oxidation

Complex **8.5** was examined as a catalyst (0.1 mol%) in the oxidation of various substrates using H_2O_2 as the oxidant. The oxidation experiments were performed in acetone, under an argon atmosphere in a water bath thermostated at 25ºC. The substrate (1000 equiv.) was

added to a stock solution of the catalyst and a known amount of the internal standard bromobenzene. The reaction was initiated by addition of H_2O_2 (30% solution in water, 100 equiv.) and monitored by GC.

It was found that both primary and secondary alcohols are oxidised rapidly (Table 8.2). For instance, when benzylalcohol is used as the substrate, already after 75 min all H_2O_2 is consumed and a turnover number of 50 is reached. The best substrate turned out to be cyclohexenol. In that case, 65 turnovers towards cyclohexenone are obtained after 1 h.

Table 8.2 *Catalytic oxidation of primary and secondary alcohols with **8.5** using H_2O_2.*

Entry	Substrate	Product	Time (h)	t.o.n.[a]
1	benzylalcohol	benzaldehyde	75	50
2[b]	benzylalcohol	benzaldehyde	15	50
3[c]	benzylalcohol	benzaldehyde	180	96
4	cyclohexanol	cyclohexanone	60	28
5	cyclohexenol	cyclohexenone	60	65
6	cyclooctanol	cyclooctanone	90	35
7	1-octanol	octanal[d]	180	11
8	*sec*-phenylethyl alcohol	acetophenone	60	50

(a) t.o.n. = mol product / mol catalyst. (b) in the presence of 1 equiv. of CF_3SO_3H. (c) addition of another aliquot of H_2O_2 after 90 min. (d) a small amount of octanoic acid was formed as side product.

Alkenes and alkanes were investigated as well. As substrates cyclohexene, styrene, adamantane, and benzene were used. However, these reactions turned out to proceed much slower than the oxidation of primary and secondary alcohols, since 6 to 18 h are needed before all H_2O_2 was consumed, instead of 60-180 min. Moreover, selectivity is less and the turnover numbers are lower. Typically, values of 10-20 turnovers are found (Table 8.3).

Table 8.3 *Catalytic oxidation of alkenes and alkanes using **8.5** and H_2O_2.*

Entry	Substrate	Product	Time (min)	t.o.n.[a]
1	cyclohexene	2-cyclohexenone	18	14
		2-cyclohexenol		18
		cyclohexene oxide		2
2	styrene	benzaldehyde	6	28
		styrene oxide		16
3	adamantane	1-adamantanol	18	8
		2-adamantanol		3
		2-adamantanone		2
4	benzene	phenol	18	0

(a) t.o.n. = mol product / mol catalyst.

The oxidation of benzylalcohol was monitored in time by GC. In Figure 8.6 the turnover numbers per iron centre are plotted against time (indicated with ◆). Surprisingly, already 30 sec after the reaction is started by adding H_2O_2, 4 equiv. of benzaldehyde are formed in a reproducable manner. The origin of the initial burst of activity is unclear. After the initial oxidation, a lag phase was observed. A significant increase in catalytic activity occurred after approximately 40 min and after 75 min the catalytic activity ceased because all the H_2O_2 was consumed. A total of 50 turnovers towards benzaldehyde was reached. Although a trace of benzoic acid was obtained, no other side products were produced according to GC. Because 50% conversion based on the amount of H_2O_2 was obtained instead of quantitative yields, we concluded that part of the H_2O_2 had decomposed during the reaction, probably *via* catalase processes.

In the absence of complex **8.5**, a negligible amount of 0.004 mmol of benzaldehyde was formed under the standard reaction conditions. When $Fe(II)(ClO_4)_2$ was applied as the catalyst, only 8 turnovers towards benzaldehyde were reached.

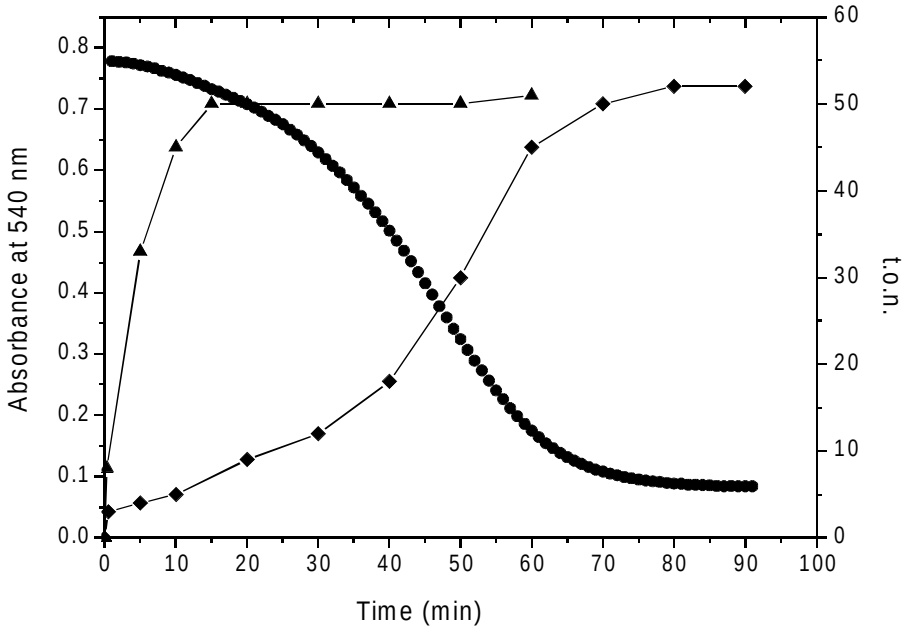

Figure 8.6 *Catalytic oxidation of benzylalcohol to benzaldehyde using* ***8.5*** *and H_2O_2: (◆) time course of the turnover numbers, (●) time dependent decay of the UV band at λ = 540 nm and (▲) catalytic oxidation in the presence of 1 equiv. of CF_3SO_3H.*

When another aliquot of H_2O_2 was added after 90 min, the catalyst became immediately active again. In this case no lag phase was observed. A value of 96 turnovers per iron centre was obtained after 180 min. This could be repeated at least 3 times without significant loss of activity, showing a good stability of the system during catalytic turnover.

The reaction was also carried out in acetonitrile. However, the reaction turned out to be much slower: only 26 turnover numbers were obtained after 3 h.

8.4 Further characterisation

The UV/Vis absorption of **8.5** at 540 nm was monitored concomitantly with the oxidation of benzylalcohol to benzaldehyde as shown in Figure 8.6 (●). During the lag phase the solution remains purple, but after 45 min the colour changed to yellow. This colour change coincides with the end of the lag phase, implying that the yellow species is responsible for the oxidation activity.

Several observations suggest that the active oxidising complex is a mononuclear species. First, the μ-oxo Fe(III) complex **8.5** is EPR-silent, whereas upon addition of benzylalcohol and H_2O_2, when the solution becomes yellow, a strong EPR signal was observed at g = 4.3 which is characteristic for a mononuclear high-spin iron(III) complex.[26] Secondly, it was found that alcohols, which are known to be capable of breaking up the oxo-bridge of some dinuclear iron μ-oxo complexes to form monomeric structures by coordination to the metal centre,[26] are oxidised rapidly. In contrast, the active yellow species is formed very slowly in the absence of substrate or with a non-coordinating substrate like cyclohexene. Finally, we envisaged that protonation of the oxo-bridge in **8.5** would facilitate the formation of the mononuclear species and hence would speed up the reaction. Upon addition of triflic acid (CF_3SO_3H) to **8.5** in acetone a blue colour (λ_{max} = 683 nm, ε = 5.5 10^3 $M^{-1}cm^{-1}$) appears (see Figure 8.7). The ^{1}H NMR spectrum of the blue solution shows broad signals in the -10 to 120 ppm range consistent with the presence of mononuclear high-spin Fe(III) species. The ES/MS spectrum shows prominent peaks at m/z 581 and 472, which corresponds to $[L^1Fe(III)OTf]^+$ and $[(HL^1)Fe(III)(OH)_2]^+$, respectively. Indeed when CF_3SO_3H (1 equiv.) was used, the reaction rate increased dramatically (see Figure 8.6, indicated by ▲). The yellow species was formed immediately upon addition of H_2O_2 and after 15 min already 50 turnovers are reached in the oxidation of benzylalcohol. The addition of more equivalents of acid does not improve the reaction rate, whereas the turnover numbers decrease. Also in the case of oxidation of alkenes and alkanes, the reaction can be dramatically accelerated by the addition of CF_3SO_3H, although the turnover numbers are lower. For example, when cyclohexene is used as the substrate, already 10 turnovers towards 2-cyclohexenol, 5 towards 2-cyclohexenone and 2 towards cyclohexene oxide were obtained after 30 min in the presence of 1 equiv. of CF_3SO_3H, whereas 6 h reaction time are required in the absence of acid.

In order to get more insight in the reaction mechanism, the kinetic deuterium isotope effect (KIE) was determined *via* a competition experiment between benzylalcohol and benzylalcohol-d_7. A value of k_H/k_D = 4.0 was obtained, which strongly indicates that cleavage of the benzylic C^α-H bond is involved in the rate-determining step.[9a] Comparable values are found for the Cu-based GOase mimics developed by Stack *et al.* (k_H/k_D = 5.3)[9a] and Itoh *et al.* (k_H/k_D = 6.8).[27] Furthermore, a KIE of 7.7 is found for GOase itself.[28]

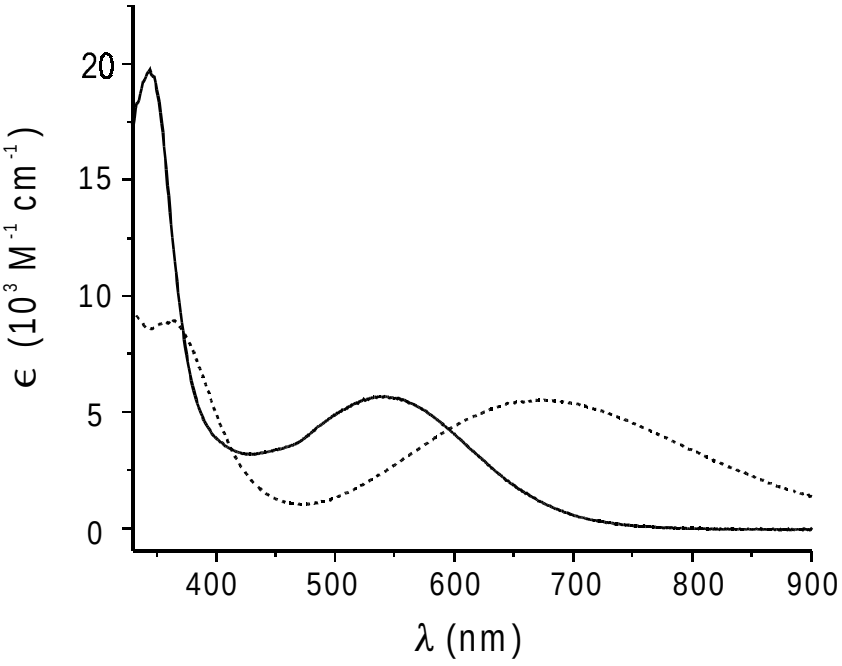

Figure 8.7 *UV-Vis spectra of **8.5** (solid line) and after addition of a drop of CF_3SO_3H (dashed line).*

Although the exact reaction mechanism of the alcohol oxidation using complex **8.5** as the catalyst is not known yet, some tentative conclusions can be drawn. From the fact that benzene, which can act as a hydroxyl radical trap,[17] is not oxidised by this system (see Table 8.3), combined with the large observed KIE, we conclude that oxidising species more selective than hydroxyl radicals are involved. When the KIE was determined 30 sec after starting the reaction by addition of H_2O_2, *i.e.* after the initial burst of activity, a value of 1.8 was obtained indicating the presence of a highly reactive oxidising species in the initial stage of the reaction. Finally, since the purple colour of **8.5** is indicative of a LMCT charge-transfer transition between the phenolic part of the ligand and the iron(III) centre,[29,30] it is most likely that the phenolic moiety is no longer coordinated to the iron centre in this yellow species, which is thought to be responsible for oxidation activity. This assumption is supported by the presence of the mononuclear species $[(HL^1)Fe(III)(OH)_2]^+$ in the electrospray mass spectrum of **8.5** with a trace of CF_3SO_3H (*vide supra*). Here, the phenol moiety is protonated and does not coordinate to the iron.

8.5 Cyclic voltammetry

The redox properties of **8.5** were examined in butyronitrile using cyclic voltammetry. The cyclic voltammogram was recorded at low temperature, since at room temperature the process was not fully reversible. However, at –42 °C, a reversible[31] reduction wave was

observed at $E_{1/2}$ = -1.08 V *vs* Fc/Fc$^+$, with a peak-to-peak separation (ΔE_P) of 80 mV (Figure 8.8).

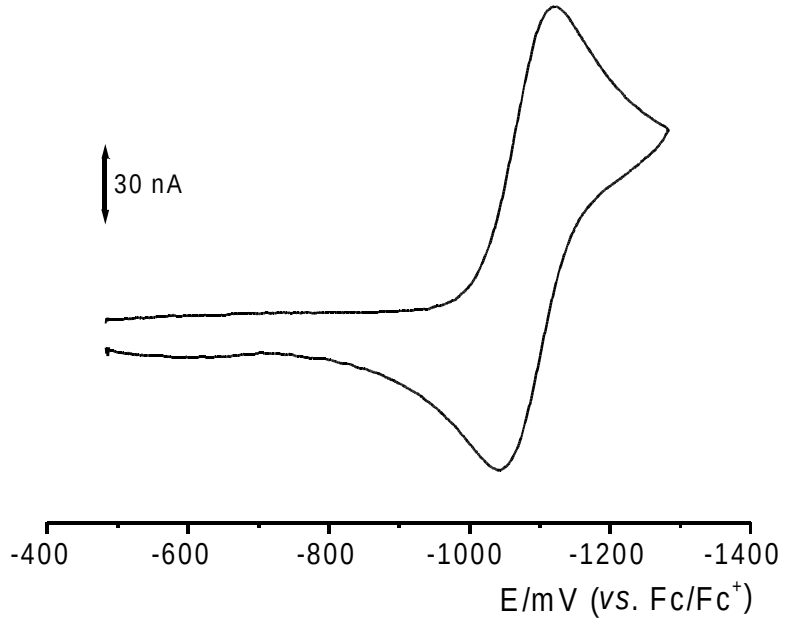

Figure 8.8 *Cyclic voltammogram of **8.5** in butyronitrile at –42 °C. Scan rate 100 mV s^{-1}.*

This cathodic process is ascribed to the one-electron reduction of the Fe(III)Fe(III) complex to the mixed-valence species Fe(II)Fe(III) by comparison with literature data.[32] An additional, irreversible, reduction wave was observed at –1.70 V. This transition step can probably be assigned to the reduction of the formed mixed-valence Fe(II)Fe(III) species into the thermally unstable two-electron reduced Fe(II)Fe(II) complex.[32]

The redox properties of **8.5** have been compared with those of two related μ-oxo diiron(III) complexes **8.8**[33] and **8.9**[34] (Scheme 8.4). Compound **8.8** was prepared starting from N4Py. Reaction of this ligand with Fe(III)$(ClO_4)_3 \cdot 10H_2O$ in MeOH, followed by crystallisation of the product from a CH_3CN-EtOAc mixture yielded [(N4Py)Fe(μ-O)Fe(N4Py)]$(ClO_4)_4$ **8.8**.[33]

Complex **8.9** was synthesised by reaction of the sodium salt of L^2 with Fe(III)$(ClO_4)_3 \cdot 10H_2O$ in an acetone/H_2O mixture. Slow evaporation of acetone from the reaction mixture afforded [(L^2)Fe(μ-O)Fe(L^2)]$(ClO_4)_2$ (**8.9**).[34] The cyclic voltammogram of **8.8** recorded at room temperature in CH_3CN showed a reversible reduction wave at $E_{1/2}$ = 0.37 V (ΔE_P = 80 mV) *vs* SCE, which corresponds to $E_{1/2}$ = -0.055 V relative to the Fc/Fc$^+$ couple. This process is again followed by an irreversible reduction wave: at –0.49 V corresponding to –0.91 V *vs* Fc/Fc$^+$. In the CV spectrum of **8.9** in butyronitrile, a quasi-reversible[31] wave was observed at room temperature at $E_{1/2}$ = -0.70 V (ΔE_P = 110 mV) *vs* Fc/Fc$^+$. In this case too, an irreversible wave was detected at –1.34 V.

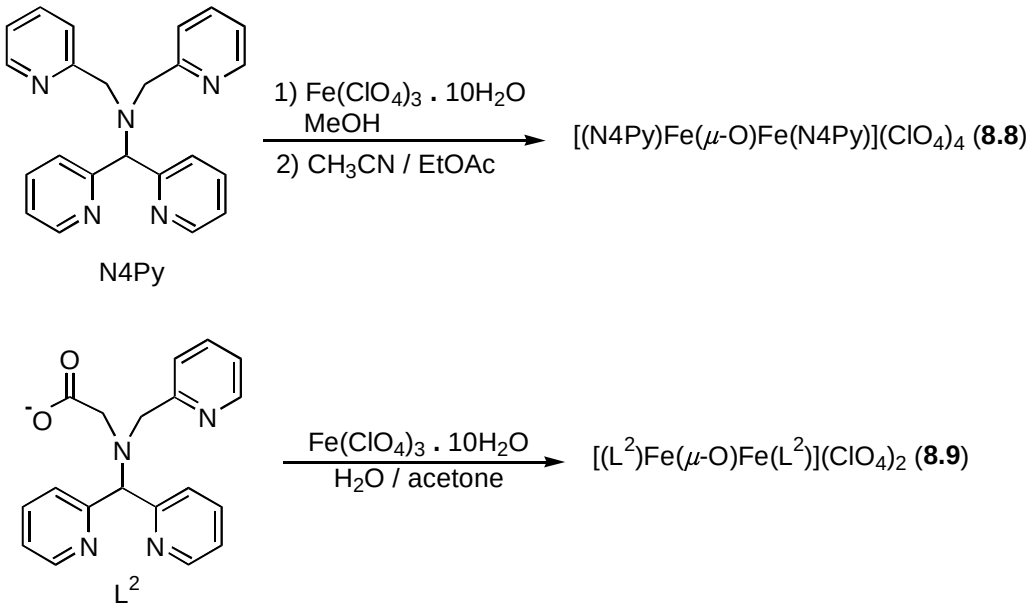

Scheme 8.4 *Synthesis of μ-oxo diiron(III) complexes **8.8** and **8.9** from N4Py and L², respectively.*

In accordance with **8.5** and literature data,[32,35] the first reduction waves of **8.8** and **8.9** are attributed to the Fe(III)Fe(III)/Fe(II)Fe(III) couple. The Fe(II)Fe(III) product is reduced at the second reduction wave to the unstable Fe(II)Fe(II) dimer. In our attempts to further confirm these assignments, PM3 calculations were performed.[36] Unfortunately, these calculations proved to be unsuccessful. Calculated geometries of the diiron(III) complexes did not match the ones known from the crystal structures and the geometries of the reduced species were therefore also unreliable.

8.6 Spectro-electrochemical measurements

In order to characterise the thermally unstable mixed-valence diiron [(L)Fe(II)(μ-O)Fe(III)(L)]$^{n+}$(*n* ClO_4^-) species by UV-Vis spectroscopy, the diiron(III) complexes were reduced *in situ* in butyronitrile at –70 °C. This low temperature was chosen in order to be certain that thermal decomposition of the mixed-valence species does not take place.

The UV-Vis spectra recorded during the reduction of **8.5** at –1.1 V are shown in Figure 8.9. Curve *a* (Figure 8.9) represents the spectrum of compound **8.5**. As discussed above, an absorption maximum at 540 nm (ε = 5.6 x 10^3 $M^{-1}cm^{-1}$) was found corresponding to the purple colour of the complex.[37] During the reduction process, this absorption decreases and a new band arises at 655 nm (with $\varepsilon \approx 3.7 \times 10^3$ $M^{-1}cm^{-1}$). Isosbestic points are observed at 370 nm, 485 nm, and 599 nm, indicating that the new species is formed quantitatively. Curve *k* (Figure 8.9) represents the one-electron reduced, mixed-valence Fe(II)Fe(III) species.

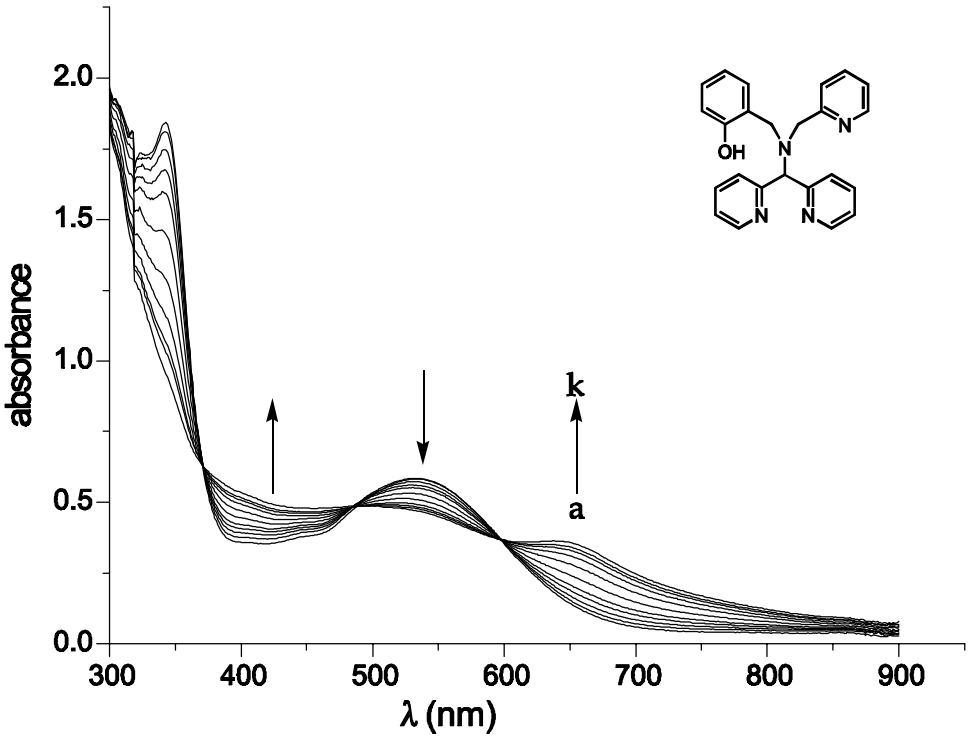

Figure 8.9 *UV-Vis spectra recorded in butyronitrile at –70 °C during the gradual electrochemical reduction of the diiron(III) complex* ***8.5*** *(a) to the mixed-valence Fe(II)Fe(III) species (k).*

Figure 8.10 shows the spectral response to the one-electron reduction of **8.8** at -0.055 V at –70 °C in butyronitrile. The original brown complex does not exhibit any distinct absorption maximum (curve *a*, Figure 8.10). During the reduction process three new bands appear at 370 ($\varepsilon \approx 4.5 \times 10^3$ $M^{-1}cm^{-1}$), 441 ($\varepsilon \approx 4 \times 10^3$ $M^{-1}cm^{-1}$), and 527 nm ($\varepsilon \approx 2.5 \times 10^3$ $M^{-1}cm^{-1}$) (curve *j*, Figure 8.10). An isosbestic point is observed at 359 nm.

Table 8.4 *Spectro-electrochemical properties of* $[(L)Fe(\mu\text{-}O)Fe(L)]^{n+}(n\ ClO_4^-)$.

Entry	Ligand	Complex	$E_{1/2}$ (V)[a] *vs* Fc/Fc$^+$	λ_{max} (nm)[b]
1	$(L^1)^-$	**8.5**	-1.08	655
2	$(L^2)^-$	**8.9**	-0.70	588
3	N4Py	**8.8**	-0.055[c]	527

(a) Cyclic voltammetry measurements in butyronitrile, assigned to the Fe(III)Fe(III)/Fe(II)Fe(III) couple. (b) UV-Vis spectroscopy in butyronitrile, λ_{max} *(nm) values assigned to the mixed-valence Fe(II)Fe(III) species at –70 °C. (c) Cyclic voltammetry performed in acetonitrile.*

The results of the spectro-electrochemical measurements performed with **8.9** are shown in Figure 8.11. Curve *a* (Figure 8.11) is the UV-Vis spectrum of the brown diiron(III) complex before reduction. A small shoulder is observed at 394 nm ($\varepsilon = 1.0 \times 10^3$ $M^{-1}cm^{-1}$). Upon stepwise reduction at –0.7 V again two bands arise (at 474 ($\varepsilon \approx 1.5 \times 10^3$ $M^{-1}cm^{-1}$) and 588 nm ($\varepsilon \approx 1.3 \times 10^3$ $M^{-1}cm^{-1}$)). An isosbestic point is observed at 350 nm.

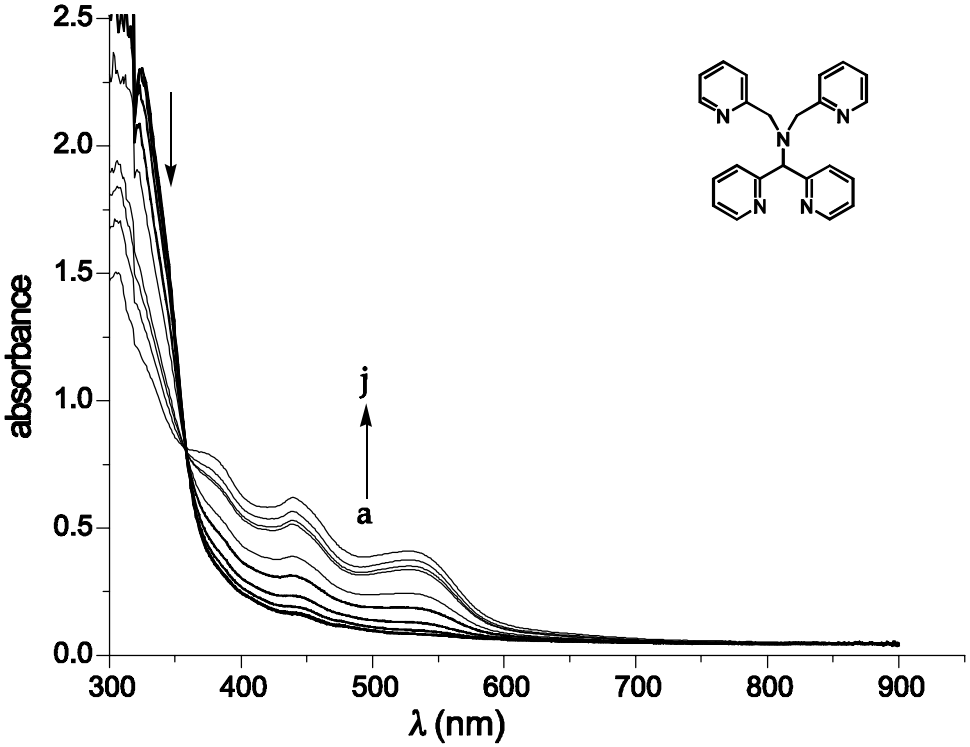

Figure 8.10 *UV-Vis spectra recorded in butyronitrile –70 °C during the gradual electrochemical reduction of the diiron(III) complex* ***8.8*** *(a) to the mixed-valence Fe(II)Fe(III) species (j).*

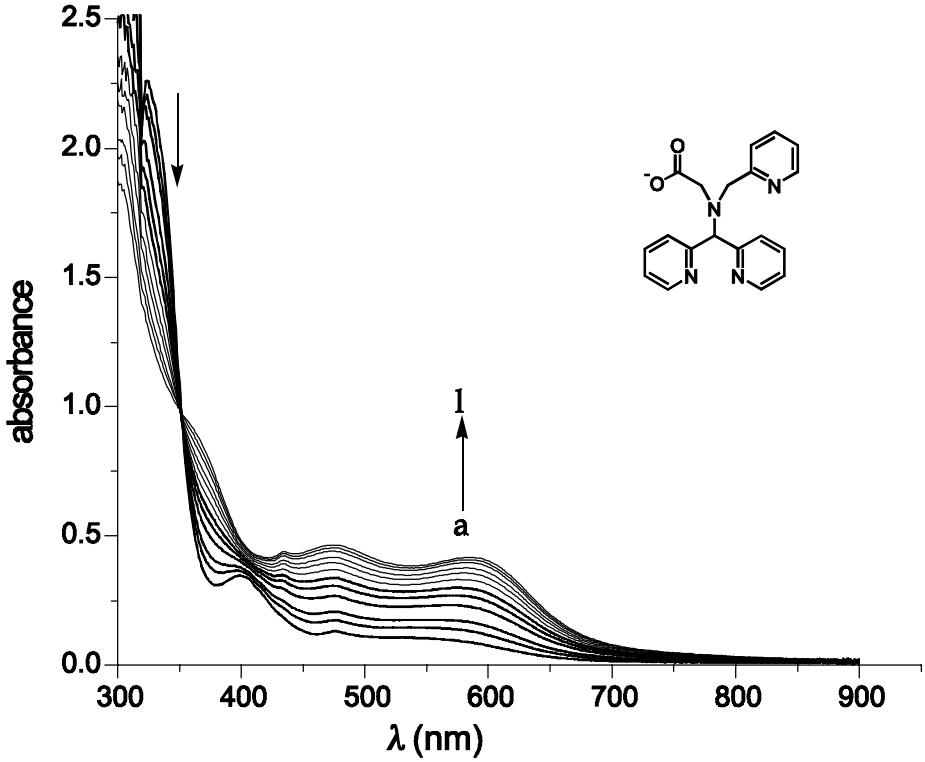

Figure 8.11 *UV-Vis spectra recorded in butyronitrile –69 °C during the gradual electrochemical reduction of the diiron(III) complex* ***8.9*** *(a) to the mixed-valence Fe(II)Fe(III) species (l).*

The data in Table 8.4 testify that the presence of negatively charged carboxylate and phenolate moieties in the ligand results in a decrease of the reduction potentials due to increased electron density on the metal centres. Apparently, the phenol group is even a stronger donor than the carboxylate unit. On the other hand, formation of the Fe(II)Fe(III) species of complex **8.8** is easily accomplished. The neutral character of the ligand N4Py results in a +4 charged diiron(III) complex, which readily takes up an electron.

Mixed-valence Fe(II)Fe(III) complexes generally exhibit a broad absorption band in the near-infrared region (900-1300 nm), due to electron transfer from the reduced Fe(II) centre to the Fe(III) centre[38,39,40] (metal-to-metal charge-transfer transitions or intervalence transfer (IT)[41]). The optical intervalence transfer is defined as an optical transition, which involves transfer of an electron from one nearly localised site to an adjacent one and Hush developed the theoretical basis for these type of mixed-valence systems.[42] The extent of electron delocalisation α^2 can be calculated[40] from the properties of the intervalence band according to equation 1:

$$\alpha^2 = \frac{(4.2 \times 10^{-4}) \cdot \varepsilon_{max} \cdot \Delta\nu_{1/2}}{(d^2 \cdot E_{op})} \qquad \text{(eq 1)}$$

with ε_{max} = extinction coefficient of the IT band, $\Delta\nu_{1/2}$ = bandwidth at half height of the IT band, d = distance between the metal centres and E_{op} = the energy of IT band (ν_{max}).

The value for $\Delta\nu_{1/2}$ can also be calculated by using equation 2:[42]

$$\Delta\nu_{1/2} = (2.31 \times 10^3 E_{op})^{1/2} \qquad \text{(eq 2)}$$

If the measured bandwidth is in agreement with the calculated bandwidth the system is most likely valence trapped (localised). However, often a ratio of $\Delta\nu_{1/2}$(observed)/$\Delta\nu_{1/2}$(calculated) ≈ 1.3 is found,[40,43] which corresponds to weakly or moderately coupled dinuclear mixed-valence complexes.[42] Also, a few valence trapped Fe(II)Fe(III) complexes have been structurally characterised.[32,38,44] Fully delocalised ($Fe^{2.5+}$, $Fe^{2.5+}$) complexes, however, are rare.[39,45]

The absorption spectra in the near-infrared region could not be recorded for complexes **8.5**, **8.8**, and **8.9** because no suitable equipment was available. Therefore the extent of electron delocalisation in these systems could not be determined. The observed λ_{max} values as summarised in Table 8.4 for the Fe(II)Fe(III) species are most likely LMCT absorptions and the recorded UV-Vis spectra closely resemble those reported in the literature for other Fe(II)Fe(III) complexes.[38,40,41]

Mixed-valence complexes can also be characterised by EPR spectroscopy. Antiferromagnetic coupling of the (high)-spin systems in the Fe(II)Fe(III) complexes gives rise to EPR signals with *g* values slightly less than 2.[38,41] These values are comparable with those

observed for mixed-valence forms of diiron sites in proteins such as hemerythrin and the hydroxylase of methane monooxygenase (*vide infra*).[22] However, the signals are usually only observed at nearly liquid-helium temperatures,[38,39,46] and as no suitable equipment was available, these experiments were not performed.

8.7 Other ligands

To explore ligand effects on the electronic and catalytic properties of the corresponding iron complexes even further, three more ligands were synthesised. In ligand HL^3, for example, the pyridyl group of HL^1 is replaced by a methyl group.[18] This ligand was easily prepared by reaction of bis(2-pyridyl)methylamine with salicylaldehyde, followed by reduction of the imine using $NaBH_4$ and subsequent reductive methylation using $NaBH(OAc)_3$ and formaldehyde in dichloroethane.[18] Unfortunately, no well-defined complexes could be synthesised from HL^3 using *e.g.* $Fe(ClO_4)_2{\cdot}6H_2O$, $Fe(BF_4)_2{\cdot}6H_2O$, or $Fe(NO_3)_3{\cdot}9H_2O$ and NH_4PF_6. However, several stable carboxylate bridged diiron(III) complexes could be isolated after addition of sodium acetate or sodium benzoate (Scheme 8.5).
The complexes were characterised by ^1H NMR spectroscopy. In all cases, paramagnetic shifted signals in the 0 to 40 ppm range were observed, consistent with the assignment of **8.10**, **8.11** and **8.12** as antiferromagnetically coupled (μ-oxo)(μ-carboxylato)diiron(III) complexes. These results were confirmed by ES / MS data and elemental analyses.

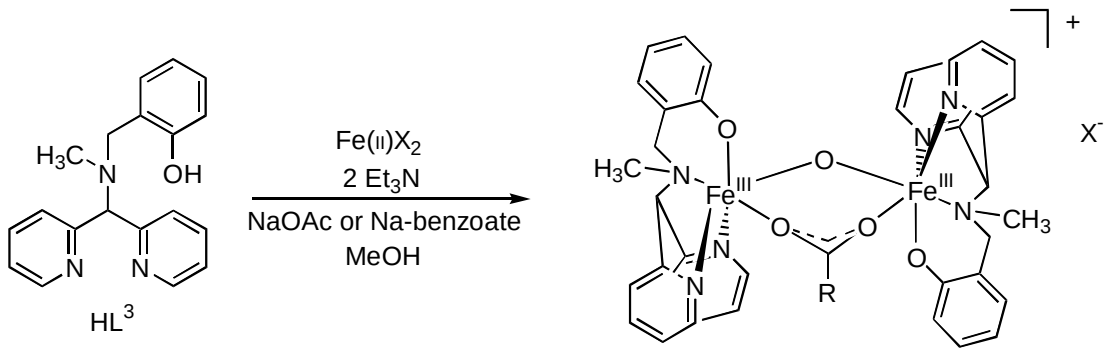

R = CH_3; X = ClO_4^- **8.10**
R = phenyl; X = ClO_4^- **8.11**
R = phenyl; X = BF_4^- **8.12**

Scheme 8.5 *Synthesis of carboxylate bridged diiron(III) complexes of HL^3.*

Complex **8.12** was tested as a catalyst in the oxidation of benzylalcohol towards benzaldehyde under the same reaction conditions as described in Chapter 8.3. The reaction

was much slower than in the case of **8.5**, since 27 turnovers were obtained in 18 h. When the acetate-bridged complex **8.10** was used, 47 turnovers towards benzaldehyde were observed after 18 h. Presumably, analogously to the **8.5** system, the diiron complexes first have to dissociate into monomeric species to achieve catalytic turnover. This is much more difficult to accomplish with carboxylate-bridged complexes than with the μ-oxo species, because of the presence of an additional bridging ligand between the iron centres which keeps the complex in an even more stable dimeric form. Most likely, analogously to the acid effect in the catalytic oxidations using **8.5**, addition of CF_3SO_3H might speed up this dissociation process and hence shorter reaction times could be reached.

In nature, many carboxylate bridged non-heme diiron containing metalloproteins are known that bind and/or activate dioxygen.[2c,d] Well-known examples of this class include methane monooxygenase (MMO), which selectively oxidises methane to methanol and fatty acid desaturases, which convert saturated fatty acids into their unsaturated derivatives. Probably the best studied example is hemerythrin (Hr), a protein responsible for oxygen transport in marine invertebrates.[47] It consists of a triply bridged diiron(II) cluster, whereas MMO and fatty acid desaturases have a bis(μ-carboxylato)diiron(II) core (Scheme 8.6).[48]

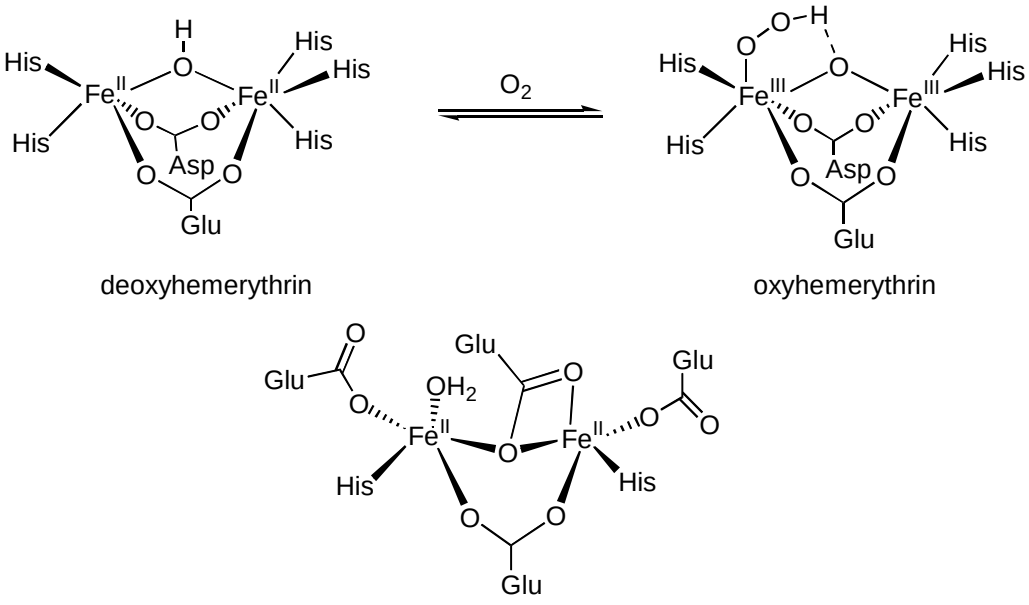

Scheme 8.6 *Diiron active sites of hemerythrin (Hr) and methane monooxygenase (MMO).*

The reaction mechanisms of diiron metalloenzymes as MMO and fatty acid desaturases are believed to proceed in the following way: (i) O_2 reacts with the diiron(II) centre (Enz_{red}) affording a diiron(III) peroxide species (*P*). (ii) cleavage of the peroxide O-O bond results in the formation of a diiron(IV) species (Q), and (iii) reduction of this high-valence species *via* a mixed-valence diiron(III,IV) intermediate (*R* or *X*) yield the diiron(III) state (Enz_{ox}). In recent

years many complexes have been developed which mimic the active sites of these enzymes.[22, 48, 49]

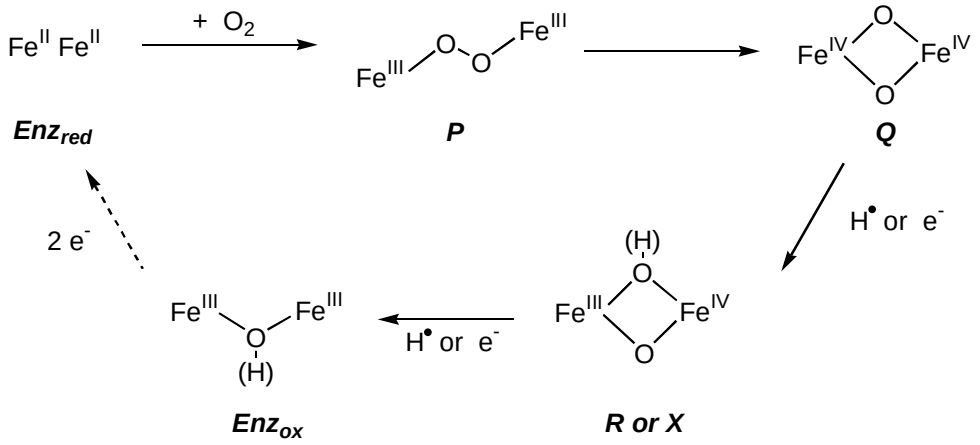

Scheme 8.7 *Proposed common mechanism for dioxygen activation by non-heme diiron enzymes.*[48]

Because without the addition of carboxylates no well-defined complexes of HL^3 could be isolated, we designed ligand HL^4. In this ligand, the methyl group is replaced by a benzyl group. It was expected that the corresponding iron complex would crystallise more easily than the methyl analogue.[50] HL^4 was synthesised starting from bis(2-pyridyl)methylamine (Scheme 8.8).

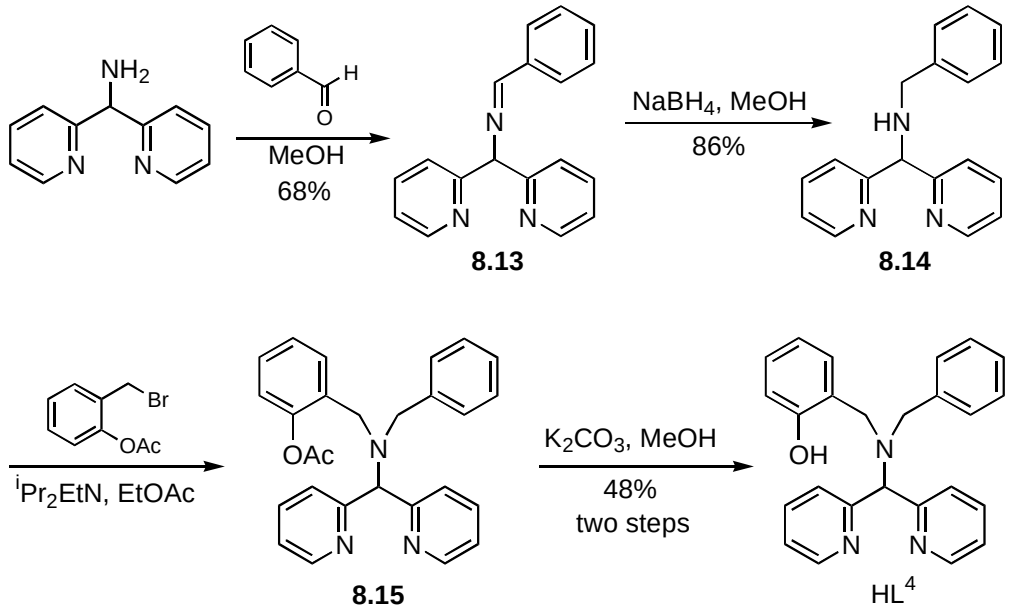

Scheme 8.8 *Synthesis of ligand HL^4.*

An imine formation reaction with benzaldehyde in methanol afforded **8.13** in 68% yield. Reduction using $NaBH_4$ gave **8.14** in 86% yield. The phenolic moiety again was introduced by reaction of amine **8.14** with acyl protected *o*-hydroxy-benzylbromide in the presence of diisopropylethylamine in ethyl acetate. After column chromatography, basic hydrolysis using K_2CO_3 in methanol provided HL^4. However, in this case too, treatment of the ligand with $Fe(ClO_4)_2{\cdot}6H_2O$ or $Fe(NO_3)_3{\cdot}9H_2O$ and NH_4PF_6 did not result in the formation of well-defined complexes.

In ligand H_2L^5, two pyridyl groups of N4Py have been replaced by phenolate moieties (Scheme 8.9).[18] Again, the synthesis started with an imine formation reaction using bis(2-pyridyl)methylamine and salicylaldehyde.[51] Subsequent reduction by $NaBH_4$ afforded **8.16**. The phenol unit was introduced as described above for the synthesis of HL^5.

Complexation of H_2L^5 with iron was accomplished by reaction with $Fe(III)(ClO_4)_3{\cdot}10H_2O$ in the presence of Et_3N in acetone. After slow evaporation of EtOAc into the solution, a very dark purple solid was obtained. The ^1H NMR spectrum of the solid recorded in CD_3CN indicated the presence of two paramagnetic compounds. The signals in the 0 to 40 ppm region appertain to an antiferromagnetically coupled μ-oxo-diiron(III) complex (**8.17**), whereas the signals between –20 and 0 ppm and 60 to 100 ppm are indicative for a mononuclear species. These assignments were confirmed by ES/MS spectra recorded in CH_3CN. A peak at m/z 919 was found, which corresponds to $[(L^5)Fe(\mu\text{-}O)Fe(L^5) + 1H^+]$ together with a peak at m/z 451, attributable to $[(L^5)Fe]^+$.

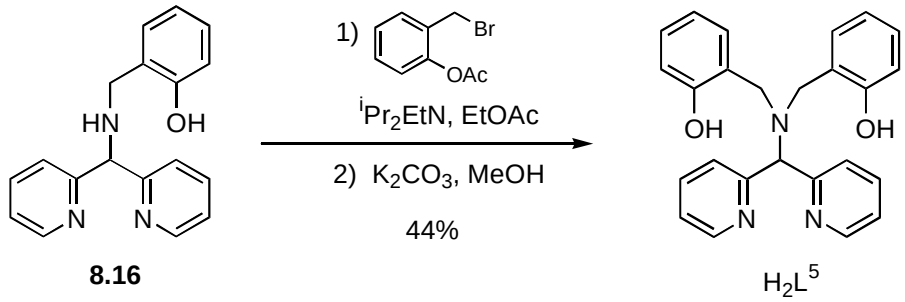

Scheme 8.9 *Synthesis of H_2L^5.*[18]

When H_2L^5 was allowed to react with $Fe(III)(ClO_4)_3{\cdot}10H_2O$ in nitromethane in the presence of Et_3N, nearly black crystals were obtained after slow evaporation of Et_2O into the solution. Unfortunately, the X-ray structure could not be determined because the crystals probably existed of microcrystals grown together. Elemental analysis was consistent with a formulation of the mononuclear complex as $[(L^5)Fe\text{-}OH_2]$ (**8.18**). Presumably, the complex easily dimerises in solution, since the ^1H NMR spectrum recorded in CD_3CN again showed the existence of a mixture of the mono- and dinuclear species, although in this case, the mononuclear compound was present in a large excess. No catalysis experiments were performed using this system.

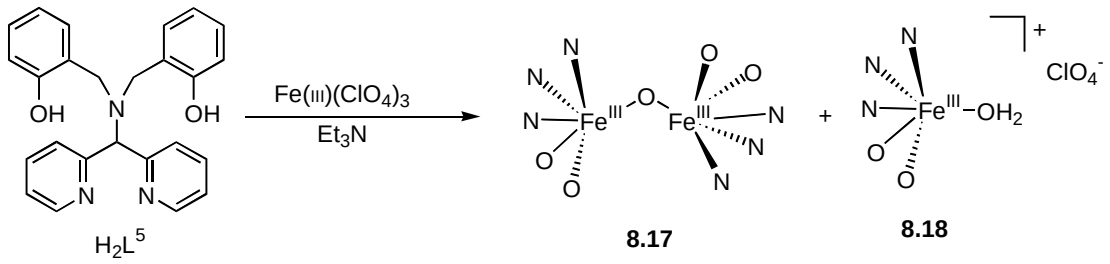

Scheme 8.10 *Synthesis of a mono- and a dinuclear iron(III) complex based on H_2L^5.*

8.8 Conclusions

A new Fe(III) containing catalyst (**8.5**) based on the pentadentate ligand HL^1 has been developed for selective and efficient oxidation of primary and secondary alcohols using H_2O_2. Yields up to 65% based on H_2O_2 can be reached. A dramatic enhancement in the reaction rate upon addition of acid has been observed, which is attributed to accelerated formation of the active mononuclear catalyst. The applied ligand, HL^1, consists of three pyridine groups and one phenolate moiety. In order to explore the influence of ligand variation on the properties of the iron complexes, several derivatives of this ligand were synthesised and their complexation behaviour with iron were studied. For instance, the ligand HL^3 with one of the pyridine units replaced by a methyl group, afforded stable carboxylate bridged μ-oxo-diiron(III) complexes which proved to be active in the catalytic oxidation of benzylalcohol to benzaldehyde. Moderate to high turnover numbers were obtained, although the reactions were much slower than observed for **8.5**. When two phenolate groups are present in the ligand (H_2L^5), a mixture of mono- and dinuclear Fe(III) complexes was obtained.

The electronic properties of **8.5** were compared with those of two related complexes **8.8** and **8.9**. As was shown by spectro-electrochemical measurements, the corresponding Fe(II)Fe(III) complexes are formed quantitatively and are stable at low temperature. The spectral responses of **8.8** and **8.9** to the one-electron reduction are very similar, although the λ_{max} values of **8.9** shifted to lower energy compared to **8.8**. This is probably due to stronger σ-donation from the negatively charged ligand L^2, which results in a more negative reduction potential. Due to increased electron density on the metal centres in **8.5**, even a further decrease in reduction potential was observed for this complex.

When comparing the catalytic oxidation properties of **8.5** with those of complexes **8.8** and **8.9**, it can be concluded that **8.5** is a more selective catalyst than **8.8** and **8.9**, which exhibit a radical type oxidation mechanism.[33b,50] Probably, because of the non-coordinating phenolate moiety in the active Fe(III) monomeric species originating from **8.5**, an additional free coordination site is created, which makes more selective two-electron oxidation pathways

possible. However, to reveal the exact reaction mechanism of oxidation reactions catalysed by **8.5**, more mechanistic studies should be performed.

8.9 Experimental section

8.9.1 General information

For general information, see Chapter 2. GC analyses were performed on a Hewlett Packard 6890 Gas Chromatograph using a HP-1 dimethyl polysiloxane column, a HP-5 5%-phenylmethylsiloxane column (benzene) or a HP5890A column (benzylalcohol-d_7). ***Caution***: perchlorate salts are potentially explosive and should be handled with care! Complexes **8.8** and **8.9**[34a] were prepared by Dr. Gerard Roelfes. Mrs. C.M. Jeronimus-Stratingh is gratefully acknowledged for performing the ES/MS measurements. The X-ray structure was determined by Dr. M. Lutz at the University of Utrecht. Drs. Peter Oosting, Dr. Gerard Roelfes and Dr. René La Crois are kindly acknowledged for their contributions to this chapter.

8.9.2 Catalytic oxidations

The oxidation experiments were performed in acetone, under an argon atmosphere in a waterbath thermostatted at 25ºC. In a typical reaction, 3.5 mmol of substrate (1000 equiv.) was added to 4 ml of a stock solution of 1.75 µmol of the catalyst (*i.e.* 3.5 µmol of iron) and a known amount of the internal standard bromobenzene. The reaction was initiated by addition of 35 µl of H_2O_2 (30% solution in water, 100 equiv.). An aliquot (0.5 ml) was taken from the reaction mixture and filtered over a small silica column. The silica was thoroughly washed with Et_2O. The sample was concentrated to a volume of 2 ml by passing an Ar stream over the solution and subsequently analysed by GC.

8.9.3 Cyclic voltammetry

The cyclic voltammetry measurements (for **8.5** and **8.9**) were performed in the Molecular Photonic Materials group at the University of Amsterdam with assistence of Dr. Frantisek Hartl and Taasje Mahabiersing. They are kindly acknowledged for their contributions to the results described in this chapter. Butyronitrile (^{n}PrCN) was dried by distillation from CaH_2. The supporting electrolyte Bu_4NPF_6 (Aldrich) was recrystallised twice from absolute ethanol and dried overnight under vacuum at 353 K for 12 h before use. All (spectro)electrochemical samples were prepared and carefully handled under a dry nitrogen atmosphere, using standard Schlenk techniques. Conventional cyclic voltammograms were recorded with a PAR Model 283 potentiostat, using an airtight, light-protected, single-compartment cell

placed in a Faraday cage. A Pt disk (0.42 mm diameter) working electrode was polished with a 0.25 µm diamond paste between the scans. Coiled Pt and Ag wires served as auxiliary and pseudoreference electrodes, respectively. Ferrocene was added as internal standard.[52] The concentration of the studied complexes was typically 10^{-3} M.

The electrochemical measurements of **8.8** were performed by Dr. Gerard Roelfes on a PAR 273A potentiostat in acetonitrile using 0.1 M Bu_4NClO_4 as the supporting electrolyte. The cyclic voltammogram was obtained by using a three-component system consisting of a glassy carbon working electrode, a platinum wire auxiliary electrode and a saturated calomel reference electrode.

8.9.4 Spectro-electrochemical measurements and instrumentation

UV-Vis spectra were recorded on a software-updated Perkin-Elmer Lambda 5 spectrophotometer. UV-Vis spectro-electrochemical experiments at room and low temperatures were carried out with previously described OTTLE cells[53,54], equipped with a Pt minigrid working electrode (32 wires/cm) and with CaF_2 or quartz windows. Potential control during electrolyses was achieved with a PA4 potentiostat (EKOM, Czech Republic). The solutions were 10^{-3} M in the iron complexes and contained 3.10^{-1} M Bu_4NPF_6. A thin-layer cyclic voltammogram was recorded in the course of each spectroelectrochemical experiment to localise the investigated redox process.

8.9.5 X-ray crystallography of 8.7

A dark blue coloured crystal of **8.7** having approximate dimensions of 0.45 x 0.24 x 0.15 mm was used for the X-ray study.

Crystal data. $[C_{48}H_{42}Fe_2N_8O_3](PF_6)_2$, M_r = 1180.54,[55] monoclinic, space group C2/c (No. 15), a = 31.0660(6), b = 11.1832(2), c = 33.8507(7) Å, β = 100.6240(7)°, V = 11558.7(4) Å^3, Z = 8, D_c = 1.357 g/cm^3,[55] 83260 reflections were measured, 10198 reflections were unique, R(int) = 0.043, T = 150(2) K.

Data collection, structure analysis, and refinement. The intensity data were collected on a Nonius KappaCCD diffractometer with rotating anode (λ=0.71073 Å). The theta range was 1.94-25.00° with indices hkl –36/36, -13/13, -40/40. The absorption correction was based on multiple measured reflections (program PLATON,[56] routine MULABS, μ = 0.64 mm^{-1},[55] 0.85-0.90 transmission). The structure was solved with Patterson methods (DIRDIF97[57]) and refined with SHELXL97[58] against F^2 of all reflections. Non-hydrogen atoms were refined freely with anisotropic displacement parameters. Hydrogen atoms were refined as rigid groups. The crystal structure contains large voids (2593 Å^3/unit cell) filled with disordered methanol and diethylether molecules. Their contribution to the structure factors was secured by back-Fourier transformation (program PLATON, CALC SQUEEZE, 129 e$^-$/unit cell). 676 refined parameters, no restraints. R-values [I > 2σ(I)]: R1= 0.0416, wR2 = 0.1173. R-values [all

refl.]: R1= 0.0520, wR2 = 0.1224. GoF = 1.049. Rest electron density between –0.45 and 0.77 e / Å^3. Molecular illustration, structure checking, and calculations were performed with the PLATON package.[56]

8.9.6 Syntheses

[(L^1)Fe(μ-O)Fe(L^1)](ClO$_4$)$_2$ (8.5) To 2-{[[di(2-pyridyl)methyl](2-pyridylmethyl)amino]-methyl}phenol (HL^1) (142 mg, 0.371 mmol) dissolved in MeOH (5 ml) was added Fe(ClO$_4$)$_2$·6H$_2$O (160 mg, 0.441 mmol) in MeOH (1 ml). Subsequently, Et$_3$N (52 µl, 0.374 mmol, 1.0 equiv.) was added dropwise. After stirring for 15 min, the reaction mixture was filtered over cotton wool and placed in an EtOAc bath. After a few days a resulting dark micro-crystalline solid was collected. The solid was washed with EtOAc and recrystallised from MeOH, yielding complex **8.5** as purple crystals in 51% yield (102 mg). ^{1}H NMR (acetonitrile-d$_3$) 40 (br), 32 (br), 26, 17.4, 16.9, 15.7, 14.4, 13.5, 10.7, 7.8, 6.5, 2.9, 1.7, -3.0; ES / MS (acetone) *m* / *z* 445 {*M* – 2ClO$_4^-$}; Anal. calcd. for C$_{48}$H$_{42}$N$_8$O$_{11}$Fe$_2$Cl$_2$·H$_2$O: C 52.07; H 4.01; N 10.13%, found: C 52.17; H 3.80; N 10.03%; λ_{max}(CH$_3$CN) 540 (ε = 5.6 x 10^3 M^{-1} cm^{-1}).

[(L^1)Fe(μ-O)Fe(L^1)](BF$_4$)$_2$ (8.7) Ligand HL^1 (50 mg, 0.131 mmol) was dissolved in a mixture of MeOH (2 ml) and CH$_3$CN (2 ml). Fe(BF$_4$)$_2$·6H$_2$O (44 mg, 0.130 mmol) and Et$_3$N (27 µl, 0.0194 mmol, 1.5 equiv.) were added. The reaction mixture was stirred for 10 min and the purple solution was placed in a Et$_2$O bath. The resulting purple microcrystalline solid was collected, dissolved in CH$_3$CN, and placed in an EtOAc bath. Complex **8.7** was isolated as fluffy purple needles after a few days. Yield: 35 mg (50%). ^{1}H NMR (acetonitrile-d$_3$) 39 (br), 33 (br), 25, 16.9, 15.7, 14.4, 13.5, 10.7, 7.8, 7.3, 7.1, 6.5, 1.7, -3.0; ES / MS (acetone) *m* / *z* 445 {*M* – 2BF$_4^-$}; Anal. calcd. for C$_{48}$H$_{42}$N$_8$O$_3$B$_2$F$_8$Fe$_2$·4H$_2$O: C 50.73; H 4.44; N 9.86%, found: C 50.30; H 4.46; N 9.70%.

[(L^1)Fe(μ-O)Fe(L^1)](PF$_6$)$_2$ (8.7) To a solution of ligand HL^1 (51 mg, 0.133 mmol) in MeOH (3 ml) was added Fe(NO$_3$)$_3$·9H$_2$O (54 mg, 1.34 mmol), Et$_3$N (18.5 µl, 0.133 mmol, 1.0 equiv.), and NH$_4$PF$_6$ (54 mg, 0.331 mmol, 2.5 equiv.). The resulting dark blue solution was stirred under an argon atmosphere for 15 min. Slow evaporation of diethyl ether into the solution resulted in the formation of dark blue crystals, which were suitable for X-ray analysis. Yield: 22 mg (29%). ^{1}H NMR (acetonitrile-d$_3$) 16.9, 15.7, 14.4, 13.4, 10.7, 7.8, 7.3, 7.2, 6.5, 2.9, 2.1, 1.7, -3.0; ES / MS (acetone) *m* / *z* 445 {*M* – 2PF$_6^-$}, 1035 {*M* – PF$_6^-$}.

[(L^3)Fe(μ-O)(μ-OAc)Fe(L^3)](ClO$_4$) (8.10) Ligand 2-{[[di(2-pyridyl)methyl](methyl)amino]-methyl}phenol (HL^3) (50 mg, 0.164 mmol) was dissolved in MeOH (3 ml). Subsequently, Fe(ClO$_4$)$_2$·6H$_2$O (59 mg, 0.164 mmol), Et$_3$N (34 µl, 0.245 mmol, 1.5 equiv.), and NaOAc (11.5 mg, 0.085 mmol) were added. After stirring for 15 min, the resulting red solution was filtered over cotton wool and placed in a Et$_2$O bath. After one week, complex **8.9** was obtained as red needles in 33% yield (0.024 g). ^{1}H NMR (acetonitrile-d$_3$) 28.8, 16.5, 14.4, 13.9,

10.8, 4.1, 3.8, 3.5, 2.6, 0.2; ES / MS (acetone) *m* / *z* 795 {*M* – ClO_4^-}; Anal. calcd. for $C_{40}H_{41}N_6O_9Fe_2Cl \cdot H_2O$: C 52.51; H 4.74; N 9.19%, found: C 52.68; H 4.47; N 9.28%.

[(L^3)Fe(*μ*-O)(*μ*-$O_2CC_6H_5$)Fe(L^3)](ClO_4) (8.11) Ligand HL^3 (70 mg, 0.229 mmol) was dissolved in MeOH (5 ml). Subsequently, $Fe(ClO_4)_3 \cdot 10H_2O$ (122 mg, 0.228 mmol) and Et_3N (64 µl, 0.460 mmol, 2.0 equiv.) were added and the reaction mixture was stirred for 15 min. The solvent was partially removed by slow evaporation through cotton wool at room temperature until purple-red crystals appeared. Yield: 75% yield (0.082 g). ^{1}H NMR (acetonitrile-d_3) 27.2, 15.7, 14.1, 13.4, 10.1, 8.4, 8.1, 7.9, 7.5, 73, 6.7, 4.0, 2.2, 1.2, -0.5; ES / MS (acetone) *m* / *z* 857 {*M* – ClO_4^-}, 795 {*M* – ($^-O_2CC_6H_5$) + ($^-$OAc)}; Anal. calcd. for $C_{45}H_{41}N_6O_9Fe_2Cl$: C 56.48; H 4.32; N 8.78%, found: C 56.16; H 4.72; N 8.11%.

[(L^3)Fe(*μ*-O)(*μ*-$O_2CC_6H_5$)Fe(L^3)](BF_4) (8.12) Ligand HL^3 (150 mg, 0.491 mmol) was dissolved in MeOH (5 ml). Subsequently, $Fe(BF_4)_2 \cdot 6H_2O$ (166 mg, 0.492 mmol), Et_3N (99 mg, 0.978 mmol, 2.0 equiv.), and sodium benzoate (35 mg, 0.243 mmol) were added and the reaction mixture was stirred for 15 min. After partial evaporation of the solvent at room temperature through cotton wool, dark purple-red crystals were obtained (0.280 g) which were dissolved in acetone and placed in an EtOAc bath. After one week, dark red crystals of **8.10** were isolated in 47% yield (0.108 g). ^{1}H NMR (acetonitrile-d_3) 26.5, 15.7, 14.1, 13.4, 10.1, 8.1, 6.7, 3.3, 2.2, 1.3, -0.6; Anal. calcd. for $C_{45}H_{41}N_6O_5Fe_2BF_4 \cdot H_2O$: C 56.16; H 4.50; N 8.73%, found: C 56.61; H 4.65; N 8.32%.

***N*-[Phenylmethylidene][di(2-pyridinyl)]methanamine (8.13)** Bis(2-pyridyl)methylamine (3.00 g, 16.2 mmol) and freshly distilled benzaldehyde (1.72 g, 16.2 mmol) were stirred in MeOH (30 ml) for 4 h. After removal of the solvent the resulting yellow solid was crystallised from CH_2Cl_2 / pentane. Yield as large yellow needles: 3.01 g (11.0 mmol, 68%). ^{1}H NMR ($CDCl_3$) 8.51 (s, 2H), 8.49 (s, 1H), 7.81-7.78 (m, 2H), 7.58-7.48 (m, 4H), 7.32-7.30 (m, 3H), 7.05-7.00 (m, 2H), 5.88 (s, 1H); ^{13}C NMR ($CDCl_3$) 162.35 (CH), 161.32 (C), 148.98 (CH), 136.31 (CH), 135.75 (C), 130.65 (CH), 128.22 (CH, 2x), 122.09 (CH), 121.88 (CH), 81.24 (CH).

***N*-Benzyl-*N*-[di(2-pyridinyl)methyl]amine (8.14)** To imine **8.13** (3.01 g, 11.0 mmol) dissolved in MeOH (40 ml), cooled in an ice-bath, was added in portions $NaBH_4$ (0.42 g, 1 equiv.). The light yellow solution was stirred for 1.5 h at room temperature. HCl (2 M) was added until pH = 2 was reached. Stirring was continued for 10 min, NaOH (4 M) was added until pH = 8. After removal of the solvent, the resulting reaction mixture was extracted with EtOAc (1 x 70 ml, 2 x 50 ml). The organic layers were washed with brine and dried (Na_2SO_4). Yield as a yellow oil which solidified upon extensive drying under reduced pressure 2.60 g (9.44 mmol, 86%). ^{1}H NMR ($CDCl_3$) 8.55 (d, 2H, *J* = 4.4 Hz), 7.62 (dt, 2H, *J* = 7.7 Hz, *J* = 1.5 Hz), 7.43 (d, 2H, *J* = 7.7 Hz), 7.36-7.22 (m, 5H), 7.16-7.11 (m, 2H), 5.15 (s, 1H), 3.79 (s, 2H); ^{13}C NMR ($CDCl_3$) 161.33 (C), 149.16 (CH), 139.99 (C), 136.52 (CH), 128.27 (CH, 2x), 126.86 (CH), 122.33 (CH), 122.10 (CH), 68.44 (CH), 51.69 (CH_2).

2-({Benzyl[di(2-pyridinyl)methyl]amino}methyl)phenol (HL^4) To a mixture of amine **8.14** (1.69 g, 6.14 mmol) and acyl protected *o*-hydroxybenzyl bromide (1.48 g, 6.44 mmol, 1.05 equiv.) in EtOAc (30 ml) was added diisopropylethylamine (0.87 g, 6.75 mmol, 1.1 equiv.). The reaction mixture was refluxed for 5 d. The solvent was removed under reduced pressure and the residu was purified by column chromatography on silica (ethyl acetate : Et_3N : hexane = 2 : 8 : 1). Yield as a mixture of acylated (**8.15**) and deacylated amine: 1.46 g. Subsequently, 1.46 g of the mixture was dissolved in MeOH (15 ml). K_2CO_3 (0.48 g, 3.47 mmol) was added and the reaction mixture was stirred for 1 h. Water (15 ml) was added and the mixture was extracted with CH_2Cl_2 (3 x 30 ml) The combined organic layers were washed with brine (20 ml) and dried on Na_2SO_4. Evaporation of the solvents under reduced pressure afforded HL^4 as a yellow foam. Yield: 1.12 g (2.94 mmol), 48%. ^{1}H NMR ($CDCl_3$) 11.90 (s, 1H), 8.67-8.66 (m, 2H), 7.60-7.54 (dt, 2H, J = 7.7 Hz, J = 1.8 Hz), 7.34-7.32 (m, 2H), 7.24-7.10 (m, 6H), 7.05-7.02 (m, 2H), 6.94-6.88 (m, 2H), 6.69-6.66 (m, 1H), 5.22 (s, 1H), 3.71 (s, 2H), 3.65 (s, 2H); ^{13}C NMR ($CDCl_3$) 158.52 (C), 157.88 (C), 148.78 (CH), 138.49 (C), 136.35 (CH), 130.72 (CH), 129.15 (CH), 128.79 (CH), 128.21 (CH), 126.84 (CH), 124.51 (CH), 123.21 (C), 122.35 (CH), 118.31 (CH), 116.54 (CH), 69.11 (CH), 53.77 (CH_2), 51.69 (CH_2); CI/MS m/z 382 {M + $1H^+$}.

[(L^5)Fe(OH_2)](ClO_4) (8.18) To a solution of H_2L^5 (150 mg, 0.377 mmol) in nitromethane (8 ml) was added $Fe(ClO_4)_3 \cdot 10H_2O$ (202 mg, 0.378 mmol) and Et_3N (105 µl, 0.755 mmol, 2.0 equiv.). The dark purple solution was stirred for 1 h, filtered over cotton wool and placed in a EtOAc bath. Nearly black crystals were isolated after one week. Yield: 0.120 g (0.211 mmol, 56%). ^{1}H NMR (acetonitrile-d_3) 98.5, 85.3, 66.4, 47.1, 37.0, 29.5, 15.4, 8.6, 7.3, -12.8 (mixture of **8.17** and **8.18**); ES/MS (CH_3CN) m/z 919 {(L^5)Fe(μ-O)Fe(L^5) + $1H^+$}, 451 {(L^5)Fe-OH_2 – ClO_4^-}; Anal. calcd. for $C_{25}H_{25}N_3O_7FeCl$: C 52.61; H 4.41; N 7.36%, found: C 52.83; H 4.09; N 7.51%.

8.10 References and notes

1 Part of this chapter has been described in: Ligtenbarg, A.G.J.; Oosting, P.; Roelfes, G.; La Crois, R.M.; Lutz, M.; Spek, A.L.; Hage, R.; Feringa, B.L. *Chem. Commun.* **2001**, 385.

2 For reviews on iron based enzymes, see: (a) Solomon, E.I.; Brunold, T.C.; Davis, M.I.; Kemsley, J.N.; Lee, S.-K.; Lehnert, N.; Neese, F.; Skulan, A.J.; Yang, Y.-S.; Zhou, J. *Chem. Rev.* **2000**, *100*, 235. (b) Que, L., Jr.; Ho, R.Y.N. *Chem. Rev.* **1996**, *96*, 2607. (c) Wallar, B.J.; Lipscomb, J.D. *Chem. Rev.* **1996**, *96*, 2625. (d) Feig, A.L.; Lippard, S.J. *Chem. Rev.* **1994**, *94*, 759.

3 (a) DeWitt, J.G.; Bentsen, J.G.; Rosenzweig, A.C.; Hedman, B.; Green, J.; Pilkington, S.; Papaefthymiou, G.C.; Dalton, H.; Hodgson, K.O.; Lippard, S.J. *J. Am. Chem. Soc.* **1991**, *113*, 9219. (b) Fox, B.G.; Froland, W.A.; Dege, J.E.; Lipscomb, J.D. *J. Biol. Chem.* **1989**, *264*, 10023.

4 Roelfes, G. 'Models for Non-Heme Iron Containing Oxidation Enzymes', PhD Thesis, Groningen, 2000, Chapter 1.

5 (a) Stubbe, J.; Van der Donk, W.A. *Chem. Rev.* **1998**, *98*, 705. (b) Klinman, J.P. *Chem. Rev.* **1996**, *96*, 2541. (c) Borman, C.D.; Saysell, C.G.; Sokolowski, A.; Twitchett, M.B.; Wright, C.; Sykes, A.G. *Coord. Chem. Rev.* **1999**, *190-192*, 771.

6 Krüger, H.-J. *Angew. Chem. Int. Ed.* **1999**, *38*, 627.

7 Whittaker, J.W. in *Metal Ions in Biological Systems*, Sigel, H.; Sigel, A., Eds.; Marcel Dekker, New York, 1994, *Vol. 30*, 315.

8 (a) Krüger, H.J. *Angew. Chem. Int. Ed.* **1999**, *38*, 627. (b) Que, L., Jr.; *J. Chem. Soc., Dalton Trans.* **1997**, 3933. (c) Que, L., Jr.; Dong, Y. *Acc. Chem. Res.* **1996**, *29*, 190.

9 (a) Wang, Y.; DuBois, J.L.; Hedman, B.; Hodgson, K.O.; Stack, T.D.P. *Science* **1998**, *279*, 537. (b) Chaudhuri, P.; Hess, M.; Flörke, U.; Wieghardt, K. *Angew. Chem. Int. Ed.* **1998**, *37*, 2217.

10 Dijksman, A.; Arends, I.W.C.E.; Sheldon, R.A. *Chem. Commun.* **1999**, 1591.

11 Brink, G.J. ten; Arends, I.W.C.E.; Sheldon, R.A. *Science* **2000**, *287*, 1636.

12 Markó, I.E.; Giles, P.R.; Tsukazaki, M.; Brown, S.M.; Urch, C.J. *Science* **1996**, *274*, 2044.

13 Zondervan, C.; Hage, R.; Feringa, B.L. *Chem. Commun.* **1997**, 419.

14 (a) Wieghardt, K.; Bossek, U.; Nuber, B.; Weiss, J.; Bonvoisin, J.; Corbella, M.; Vitols, S.E.; Girerd, J.J. *J. Am. Chem. Soc.* **1988**, *110*, 7398. (b) Hage, R.; Gunnewegh, E.A.; Niël, J.; Tjan, F.S.B.; Weyhermüller, T.; Wieghardt, K. *Inorg. Chem. Acta* **1998**, *268*, 43. (c) Hage, R.; Iburg, J.E.; Kershner, J.; Koek, J.H.; Lempers, E.L.M.; Martens, R.J.; Racheria, U.S.; Russel, S.W.; Swarthoff, T.; Vliet, M.R.P. van; Warnaar, J.B.; Wolf, L. van der; Krijnen, B. *Nature* **1994**, *369*, 637.

15 (a) Roelfes, G. 'Non-heme iron containing oxidation enzymes', PhD Thesis, Groningen, 2000. (b) Lubben, M. 'Model systems for iron and copper containing oxygenases', PhD Thesis, Groningen, 1994.

16 (a) Lubben, M.; Meetsma, A.; Wilkinson, E.C.; Feringa, B.; Que, L., Jr. *Angew. Chem. Int. Ed. Engl.* **1995**, *34*, 1512. (b) Roelfes, G.; Lubben, M.; Chen, K.; Ho, R.Y.N.; Meetsma, A.; Genseberger, S.; Hermant, R.M.; Hage, R.; Mandal, S.K.; Young, V.G., Jr.; Zang, Y.; Kooijman, H.; Spek, A.L.; Que, L., Jr.; Feringa, B.L. *Inorg. Chem.* **1999**, *38*, 1929. (c) Ho, R.Y.N.; Roelfes, G.; Feringa, B.L.; Que, L., Jr. *J. Am. Chem. Soc.* **1999**, *121*, 264.

17 Roelfes, G.; Lubben, M.; Hage, R.; Que, L., Jr.; Feringa, B.L. *Chem. Eur. J.* **2000**, *6*, 2152.

18 La Crois, R.M. 'Manganese complexes as catalysts in epoxidation reactions', PhD Thesis, Groningen, 2000, Chapter 2.

19 Niemers, E.; Hiltmann, R. *Synthesis* **1976**, 593.

20 Complex **8.5** was first synthesised by Drs. P. Oosting, University of Groningen.

21 Morman, R.E.; Holz, R.C.; Ménage, S.; O'Connor, C.J.; Zhang, J.H.; Que, L., Jr. *Inorg. Chem.* **1990**, *29*, 4629.

22 Kurtz, D.M., Jr. *Chem. Rev.* **1990**, *90*, 585.

23 Aneetha, H.; Panneerselvam, K.; Liao, T.-F.; Lu, T.-H.; Chung, C.-S. *J. Chem. Soc., Dalton Trans.* **1999**, 2689.

24 Norman, R.E.; Holz, R.C.; Ménage, S.; O'Connor, C.J.; Zhang, J.H.; Que, L., Jr. *Inorg. Chem.* **1990**, *29*, 4629.

25 Gorun, S.M.; Lippard, S.J. *Inorg. Chem.* **1991**, *30*, 1630.

26 Kim, J.; Larka, E.; Wilkinson, E.C.; Que, L., Jr. *Angew. Chem. Int. Ed. Engl.* **1995**, *34*, 2048.

27 Itoh, S.; Taki, M.; Takayama, S.; Nagatomo, S.; Kitagawa, T.; Sakurada, N.; Arakawa, R.; Fukuzumi, S. *Angew. Chem. Int. Ed.* **1999**, *38*, 2774.

28 Maradufu, A.; Cree, G.M.; Perlin, A.S. *Can. J. Chem.* **1971**, *49*, 3429.

29 Ito, S.; Suzuki, M.; Kobayashi, T.; Itoh, H.; Harada, A.; Ohba, S.; Nishida, Y. *J. Chem. Soc., Dalton Trans.* **1996**, 2579.

30 Yan, S.; Que, L., Jr.; Taylor, L.F.; Anderson, O.P. *J. Am. Chem. Soc.* **1988**, *110*, 5222.

31 (a) Evans, D.H.; O'Connell, K.M.; Petersen, R.A.; Kelly, M.J. *J. Chem. Educ.* **1983**, *60*, 290. (b) Mabbott, G.A. *J. Chem. Ed.* **1983**, *9*, 697.

32 (a) Aneetha, H.; Panneerselvam, K.; Liao, T.-F.; Lu, T.-H.; Chung, C.-S. *J. Chem. Soc., Dalton Trans.* **1999**, 2689. (b) Bernard, E.; Moneta, W.; Laugier, J.; Chardon-Noblat, S.; Deronzier, A.; Tuchagues, J.-P.; Latour, J.-M. *Angew. Chem., Int. Ed. Engl.* **1994**, *33*, 887. (c) Schepers, K.; Bremer, B.; Krebs, B.; Henkel, G.; Althaus, E.; Mosel, B.; Müller-Warmuth, W. *Angew. Chem., Int. Ed. Engl.* **1990**, *29*, 531. (d) Snyder, B.S.; Patterson, G.S.; Abrahamson, A.J.; Holm, R.H. *J. Am. Chem. Soc.* **1989**, *111*, 5214.

33 (a) Roelfes, G. 'Models for non-heme iron containing oxidation enzymes', PhD Thesis, 2000, Chapter 2. (b) Lubben, M. 'Model systems for iron and copper containing oxygenases', PhD Thesis, Groningen, 1994, Chapter 3.

34 (a) Complex **8.9** was first synthesised by Drs. Peter Oosting, University of Groningen. (b) Roelfes, G. 'Models for non-heme iron containing oxidation enzymes', PhD Thesis, 2000, Chapter 5.

35 Dutta, S.K.; Ensling, J.; Werner, R.; Flörke, U.; Haase, W.; Gütlich, P.; Nag, K. *Angew. Chem., Int. Ed. Engl.* **1997**, *36*, 152.

36 PM3 calculations were performed by Dr. Peter Budzelaar, University of Nijmegen.

37 Pyrz, J.W.; Roe, A.L.; Stern, L.J.; Que, L., Jr. *J. Am. Chem. Soc.* **1985**, *107*, 614.

38 Mashuta, M.S.; Webb, R.J.; McCusker, J.K.; Schmitt, E.A.; Oberhausen, K.J.; Richardson, J.F.; Buchanan, R.M.; Hendrickson, D.N. *J. Am. Chem. Soc.* **1992**, *114*, 3815.

39 Spreer, L.O.; Li, A.; MacQueen, D.B.; Allan, C.B.; Otvos, J.W.; Calvin, M.; Frankel, R.B.; Papaefthymiou, G.C. *Inorg. Chem.* **1994**, *33*, 1753.

40 Borovik, A.S.; Papaefthymiou, V.; Taylor, L.F.; Anderson, O.P.; Que, L., Jr. *J. Am. Chem. Soc.* **1989**, *111*, 6183.

41 Borovik, A.S.; Murch, B.P.; Que, L., Jr.; Papaefthymiou, V.; Münck, E. *J. Am. Chem. Soc.* **1987**, *109*, 7190.

42 Hush, N.S. *Prog. Inorg. Chem.* **1967**, *8*, 391.

43 Powers, M.J.; Meyer, T.J. *J. Am. Chem. Soc.* **1979**, *100*, 6284.

44 (a) Bossek, U.; Hummel, H.; Weyhermüller, T.; Bill, E.; Wieghardt, K. *Angew. Chem., Int. Ed. Engl.* **1995**, *34*, 2642. (b) Arena, F.; Floriani, C.; Chiesi-Villa, A.; Guastini, C. *J. Chem. Soc., Chem. Commun.* **1986**, 1369.

45 Drüeke, S.; Chaudhuri, P.; Pohl, K.; Wieghardt, K.; Ding, X.-Q.; Bill, E.; Sawaryn, A.; Trautwein, A.X.; Winkler, H.; Gurman, S.J. *J. Chem. Soc., Chem. Commun.* **1989**, 59.

46 Hartman, J.R.; Rardin, R.L.; Chaudhuri, P.; Pohl, K.; Wieghardt, K.; Nuber, B.; Weiss, J.; Papaefthymiou, G.C.; Frankel, R.B.; Lippard, S.J. *J. Am. Chem. Soc.* **1987**, *109*, 7387.

47 Que, L., Jr. in *Bioinorganic Catalysis*, Second Edition, Reedijk, J.; Bouwman, E., Eds.; Marcel Dekker, New York, 1999, Chapter 10.

48 Que, L., Jr. *J. Chem. Soc., Dalton Trans.* **1997**, 3933.

49 (a) Herold, H.; Lippard, S.J. *J. Am. Chem. Soc.* **1997**, *119*, 144. (b) Ménage, S.; Vincent, J.-M.; Lambeaux, C; Fontecave, M. *J. Mol. Cat. A* **1996**, *113*, 61. (c) Que, L., Jr.; Dong, Y. *Acc. Chem. Res.* **1996**, *29*, 190.

50 Roelfes, G. 'Non-heme iron containing oxidation enzymes', PhD Thesis, Groningen, 2000, Chapter 6.

51 Ligtenbarg, A.G.J.; Spek, A.L.; Hage, R.; Feringa, B.L. *J. Chem. Soc., Dalton Trans.* **1999**, 659.

52 Gritzner, G.; Kuta, J. *Pure Appl. Chem.* **1984**, *56*, 461.

53 Krejcik, M.; Danek, M.; Hartl, F. *J. Electroanal. Chem. Interfacial Electrochem.* **1991**, *317*, 179.

54 Hartl, F.; Luyten, H.; Nieuwenhuis, H.A.; Schoemaker, G.C. *Appl. Spectros.* **1994**, *48*, 1522.

55 Derived values do not contain the contribution of the distorted solvent.

56 Spek, A.L. 'PLATON. A multipurpose crystallographic tool', Utrecht University, The Netherlands, **2000**.

57 Beurskens, P.T.; Admiraal, G.; Beurskens, G.; Bosman, W.P.; Garcia-Granda, S.; Gould, R.O.; Smits, J.M.M.; Smykalla, C. 'The DIRDIF97 program system, Technical Report of the Crystallography Laboratory', University of Nijmegen, The Netherlands, 1997.

58 Sheldrick, G.M. 'SHELXL-97. Program for crystal structure refinement', University of Göttingen, Germany, 1997.

Chapter 9

Conclusions and Future Prospects

9.1 Introduction

The oxidation chemistry of vanadium(V) peroxide complexes has attracted renewed attention with the discovery in 1983 of a naturally occurring vanadium containing enzyme, vanadium bromoperoxidase.[1,2] To get a better understanding of the working mechanism of the enzyme, many vanadium(V) complexes have been prepared and studied as functional enzyme mimics. Furthermore, the coordination chemistry of vanadium related to its biological functions has been extensively explored.[3]

The tendency of vanadium(V) to coordinate peroxides was already known for decades. A classic spot test for vanadate, for instance, is the formation of the red oxoperoxovanadium(V) ion.[1] However, since only a limited number of vanadium complexes have been investigated as oxidation catalysts so far, it was our intention to develop and study a number of different types of vanadium complexes. To gain insight in the catalytic properties of these compounds, we envisioned to study the biomimetic properties of our novel complexes (*i.e.* to examine their catalytic properties in bromination reactions) and to use them as catalysts in a variety of other oxidation reactions, like epoxidations and hydroxylation reactions.

In this chapter, the results on the vanadium and iron oxidation chemistry are summarised. General conclusions will be drawn on the use of vanadium complexes as oxidation catalysts and recommendations for future research will be given.

9.2 Oxidation catalysis with high-valent vanadium complexes

As described in Chapters 3, 5, and 6, several ligands proved to be successful to incorporate vanadium.[4] The resulting complexes (Figure 9.1) were structurally characterised in detail and their oxidising properties were studied in bromination and epoxidation reactions. However, also several new ligands were synthesised (see Chapters 4 and 7), that turned out to be unsuitable for vanadium coordination, since no well-defined complexes could be isolated.

Complex **3.1** was tested whether it could serve as a functional mimic for vanadium bromoperoxidase in a reaction where trimethoxybenzene (TMB) was used as substrate and hydrogen peroxide as the oxidant. Bromination activity was indeed observed. The best result was obtained using 10 mM of TMB, 50 mM of Bu_4NBr, 10 mM of H_2O_2, and 8 mM HCl. A conversion of 62% towards TMBBr was reached in one hour (with a blank reaction of

18%). However, it was shown that the applied acidic conditions caused the dissociation of the ligand from the vanadium centre. As a result, the observed catalysis was actually accomplished by a bare vanadium(V) species. Furthermore, it was shown that simple vanadium reagents, like *e.g.* $VO(acac)_2$ are often almost as active or even more active than ligated complexes.

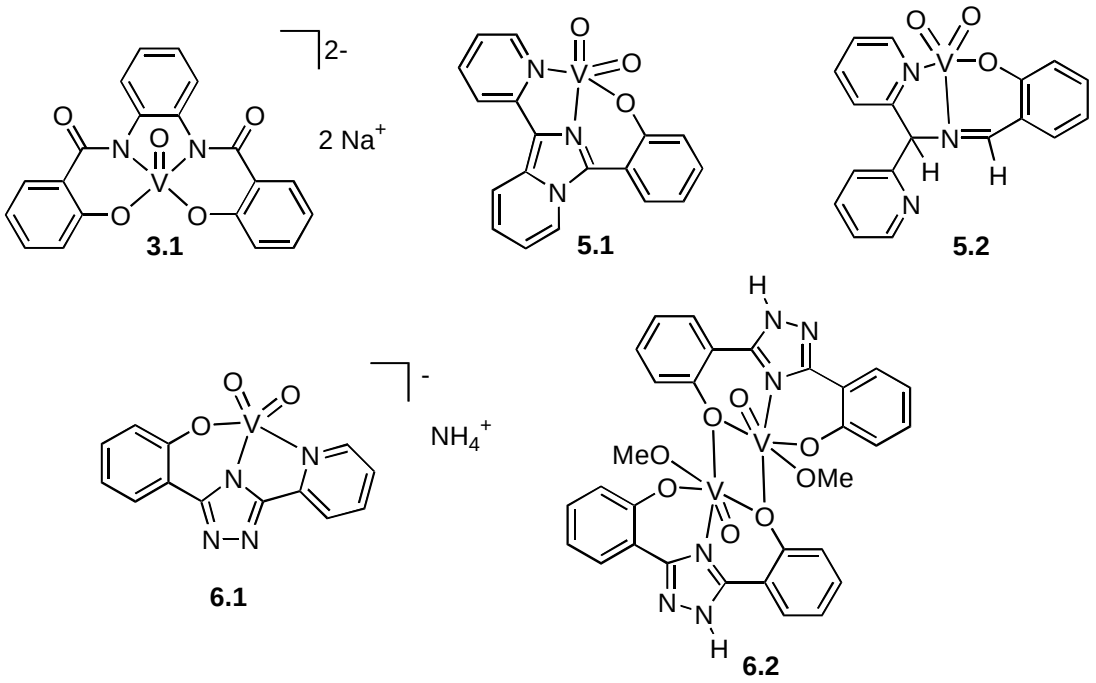

Figure 9.1 *Summary of the vanadium complexes tested as catalysts in oxidation reactions.*

The biomimetic properties of complexes **5.1** and **5.2** were also investigated. However, both complexes were catalytically inactive, since no bromination activity was observed. Complexes **6.1** and **6.2** were used as catalysts in the epoxidation reaction of cinnamyl alcohol. Although, especially for **6.2**, reasonable turnover numbers towards the epoxide were obtained, the commercially available $VO(acac)_2$ turned out to be even more active.

In Chapter 7 we focussed on the design and synthesis of new chiral ligands. Attempts were made to synthesise new chiral vanadium complexes which could subsequently be applied as catalysts in asymmetric oxidation reactions. Unfortunately, no well-defined vanadium species could be isolated. However, we were able to obtain a novel manganese complex based on a pyridine *N*-oxide salen-derived ligand, but preliminary experiments showed that this complex was inactive in the catalytic epoxidation of styrene.

9.3 Future prospects

Although predictions regarding the applicability of ligands for coordination of vanadium(IV) or vanadium(V) appear difficult to make, it seems that at least one oxygen donor atom is required for the formation of well-defined vanadium species. In general, tridentate ligands readily afford dioxovanadium(V) complexes. Tetradentate ligands are suitable for the synthesis of stable oxovanadium(IV) or -(V) complexes. The stability and robustness of the complexes is particularly put to the test in functional models for vanadium bromoperoxidase, since these complexes have to be resistant to the harsh, acidic conditions necessary for the reaction to proceed. These conditions easily cause dissociation of the ligand from the vanadium centre and therefore often two or three oxygen donor sites are needed to afford the required stability.

Bare vanadium(V) species already display high activity in bromination reactions. For example, *cis*-dioxovanadium(V) (VO_2^+) catalyses the bromination of TMB with a turnover rate of 15 mol TMBBr / mol vanadium h^{-1}.[5] Furthermore, most ligated functional model systems known in the literature only equal this activity, whereas V-BrPO functions with a turnover rate of 4.7 x 10^5 mol Br-product / mol enzyme h^{-1}. Even the best mimic known until now, developed by Butler *et al.*, appears to be only a slightly better catalyst than $VO(acac)_2$.[6] Therefore, the search for a ligand system that provides a catalyst capable of approaching the enzyme in reaction rate and selectivity remains a difficult task. Obviously, the structural environment of the vanadate in the enzyme plays an important role in the catalytic process, so the fact that the structure of the active site is now known in detail may facilitate the design of a catalyst which indeed resembles the reaction rates of the enzyme.

Vanadium-catalysed epoxidations of allylic alcohols using *tert*-butylhydroperoxide (TBHP) are well-known, since high yields are obtained and the reactions often proceed regioselective.[7] Especially commercially available $VO(acac)_2$ is very appropriate for this purpose and is therefore often recommended as the catalyst.[8] High regioselectivities are a result of coordination of the allylic alcohol to the vanadium centre. Only vanadium complexes of bidentate ligands have the required vacant coordination sites for binding of the allylic alcohol and the peroxide in an η^2 manner. To achieve different product selectivities, other ligated vanadium species could be applied as shown in Chapter 6.

A thriving topic in vanadium chemistry is the search for chiral vanadium catalysts for the asymmetric epoxidation of allylic alcohols. Many effective systems have already been developed.[9] Moderate-to-high enantioselectivities and yields were reached in the allylic epoxidation of a range of disubstituted allylic alcohols using a *N*-bis(1-naphthyl)methyl-substituted hydroxamic acid.[10] Until now, the ligands used for asymmetric allylic epoxidations are mainly bulky hydroxamic acids, which are not easily accessible. In the near future the research will therefore certainly be focussed on the development of other, more simple, bulky bidentate ligands for the synthesis of vanadium epoxidation catalysts.

In recent years many promising results have been reported in the field of vanadium catalysed asymmetric sulfide oxidations also, especially by Bolm and Ellman.[9d-f] High yields and enantioselectivities were reached with a limited number of substrates. The best results

were reported by Ellman *et al.* using a Schiff base ligand derived from *tert*-leucinol.[9d] In the asymmetric oxidation of *tert*-butyl disulfide, 98% conversion and 91% e.e. were reached. However, e.e's above 80% with simple sulfides like methyl phenyl sulfide have never been achieved. Future research in asymmetric vanadium-catalysed sulfoxidation chemistry should therefore be concentrated on the development of chiral vanadium complexes capable of oxidising a broader range of sulfide substrates.

A real challenge remains the development of a vanadium catalyst capable of epoxidation of unfunctionalised olefins, since only low turnovers can be achieved with $VO(acac)_2$. Furthermore, research regarding vanadium-catalysed oxidation of alcohols to their corresponding aldehydes and ketones as well as hydroxylation reactions has remained highly underexposed.

9.4 Oxidation catalysis with iron complexes

As described in Chapter 8, a new non-heme diiron(III) complex $[(L^1)Fe\text{-}O\text{-}Fe(L^1)](ClO_4^-)_2$ (**8.5**) (for HL^1, Figure 9.2) has been synthesised and characterised. The ligand is closely related to the well-known all-nitrogen pentadentate ligand N4Py.[11] The complex proved to be an excellent catalyst for the selective oxidation of primary and secondary alcohols using hydrogen peroxide.[12] Yields up to 65% based on H_2O_2 were reached. A remarkable increase in reaction rate was achieved by the addition of 1 equiv. of triflic acid (CF_3SO_3H).

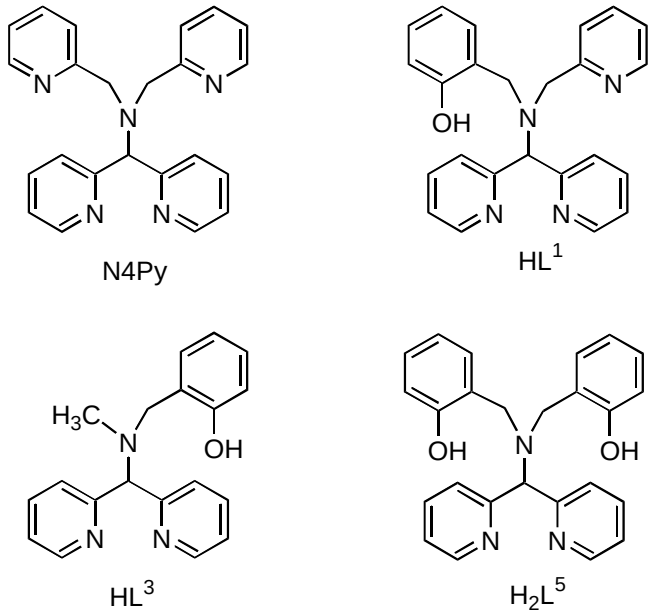

Figure 9.2 *N4Py and related ligands for iron.*

In the literature, only a few examples of iron mediated alcohol oxidations are known. For instance, the oxidation of alcohols by Fenton's reagent (Fe^{2+}-H_2O_2) has been investigated[13] as well as oxidations using potassium ferrate(VI) (K_2FeO_4),[14] but these are stoichiometric oxidation reactions.

For the N4Py-Fe system comparable turnover numbers in the catalytic oxidation of benzyl alcohol were found as for **8.5**.[11a] However, in contrast to the non-selective radical type of oxidation chemistry observed for the N4Py system, complex **8.5** turned out to be a selective oxidation catalyst. To gain insight in the reaction mechanism of oxidations catalysed by the HL^1 derived iron(III) species (**8.5**), the oxidation of benzylalcohol was monitored in time by GC and UV measurements and the kinetic deuterium isotope effect was determined. Several observations suggest that the active oxidising complex is a mononuclear species in which the phenolic moiety is no longer coordinated to the iron centre. Nevertheless, in order to reveal the exact mechanism, additional experiments with model substrates need to be done. Furthermore, spectroscopic techniques like resonance Raman, UV-Vis, or EPR spectroscopy, as well as kinetic measurements may give deeper insight in the nature of reactive intermediates and reaction pathways.

To study the effect of ligand variations on the properties of the corresponding iron species even further, additional pentadentate and tetradentate ligands related to N4Py were synthesised (HL^3, H_2L^5 in Figure 9.2). The complexation chemistry of these ligands with iron was investigated and a few complexes were isolated and characterised. On account of the promising results obtained with **8.5**, the oxidising properties of these new iron complexes deserve to be explored in detail as well.

9.5 References

1 Butler, A.; Clague, M.J.; Meister, G.E. *Chem. Rev.* **1994**, *94*, 625.

2 Vilter, H. *Phytochemistry* **1984**, *23*, 1387.

3 Rehder, D. *Coord. Chem. Rev.* **1999**, *182*, 297.

4 Ligtenbarg, A.G.J.; Spek, A.L.; Hage, R.; Feringa, B.L. *J. Chem. Soc., Dalton Trans.* **1999**, 659.

5 Butler, A. in *Bioinorganic Catalysis*, Reedijk, J.; Marcel Dekker, New York, 1993, Chapter 13.

6 (a) Clague, M.J.; Keder, N.L.; Butler, A. *Inorg. Chem.* **1993**, *32*, 4754. (b) Chapter 3.

7 (a) Lempers, H.E.B.; Ripollés i Garcia, A.; Sheldon, R.A. *J. Org. Chem.* **1998**, *63*, 1408. (b) Tanaka, S.; Yamamoto, H.; Nozaki, H.; Sharpless, K.B.; Michaelson, R.C.; Cutting, J.D. *J. Am. Chem. Soc.* **1974**, *96*, 5254. (c) Sharpless, K.B.; Michaelson, R.C. *J. Am. Chem. Soc.* **1973**, *95*, 6136.

8 (a) *Encyclopedia of Reagents for Organic Synthesis*, Paquette, L.A., Ed., John Wiley & Sons, Chichester, 1995, *8*. (b) Nicolaou, K.C.; Sorensen, E.J. *Classics in Total Synthesis*, VCH, Weinheim, 1996, Chapter 34.

9 (a) Hoshino, Y.; Yamamoto, H. *J. Am. Chem. Soc.* **2000**, *122*, 10452. (b) Hoshino, Y.; Murase, N.; Oishi, M.; Yamamoto, H. *Bull. Chem. Soc. Jpn.* **2000**, *73*, 1653. (c) Murase, N.; Hoshino, Y.; Oishi, M.; Yamamoto, H. *J. Org. Chem.* **1999**, *64*, 338. (d) Cogan, D.A.; Liu, G.; Kim, K.; Backes, B.J.; Ellman, J. A. *J. Am. Chem. Soc.* **1998**, *120*, 8011. (e) Bolm, C.; Bienewald, F. *Synlett* **1998**, 1327. (f) Bolm, C.; Bienewald, F. *Angew. Chem. Int. Ed. Engl.* **1995**, *34*, 2640.

10 Hoshino, Y.; Yamamoto, H. *J. Am. Chem. Soc.* **2000**, *122*, 10452.

11 (a) Roelfes, G.; Lubben, M.; Hage, R.; Que, L., Jr.; Feringa, B.L. *Chem. Eur. J.* **2000**, *6*, 2152. (b) Roelfes, G. 'Non-heme iron containing oxidation enzymes', PhD Thesis, Groningen, 2000. (c) Lubben, M. 'Model systems for iron and copper containing oxygenases', PhD Thesis, Groningen, 1994.

12 Ligtenbarg, A.G.J.; Oosting, P.; Roelfes, G.; La Crois, R.M.; Lutz, M.; Spek, A.L.; Hage, R.; Feringa, B.L. *Chem. Commun.* **2001**, 385.

13 Walling, C; Kato, S. *J. Am. Chem. Soc.* **1971**, *93*, 4275.

14 (a) Rao, K.V.; Rao, M.P.; Sethuram, B.; Rao, T.N. *Indian J. Chem.* **1988**, *27A*, 1035. (b) Audette, R.J.; Quail, J.W.; Smith, P.J. *J. Chem. Soc., Chem. Commun.* **1972**, 38.

Samenvatting

Vanadium- en ijzercomplexen voor katalytische oxidatie

Algemene achtergrond: vanadium

Vanadium werd in 1802 in Mexico ontdekt door Andres Manuel del Rio als bestanddeel van een mineraal. Een Frans chemicus was echter van mening dat het hier ging om onzuiver chroom, en de ontdekking werd daarom weer ingetrokken. Het element werd herontdekt in 1831 door de Zweedse chemicus Nils Gabriel Sefström in de overblijfselen van ijzererts uit Småland. Hij vernoemde het element naar de Noorse schoonheidsgodin Vanadis, omdat hij onder de indruk was van de prachtige kleuren van de vanadiumbevattende verbindingen. Vanadis is een andere naam voor Freyja, de Germaanse godin van schoonheid, jeugd en liefde. Vanadium komt voor in oxidatietoestanden variërend van –3 tot +5, uitgezonderd –2. De toestanden +4 en +5 zijn over het algemeen de meest stabiele vormen. Veel van deze verbindingen bevatten een of twee oxogroepen (zie figuur 1). Vanwege de d^1-configuratie van vanadium(IV)ionen, kunnen vanadium(IV)complexen gemakkelijk worden gekarakteriseerd met behulp van ESR-spectroscopie. Vanadium(V)complexen daarentegen hebben geen ESR-signaal, omdat de complexen door de d^0-toestand van het ion diamagnetisch zijn. Dat maakt ze uitermate geschikt voor analyse met behulp van NMR. Vooral ^{51}V-NMR wordt vaak gebruikt voor de karakterisering, omdat de chemische verschuivingen erg beïnvloed worden door de coördinatieomgeving van het ion.

V(IV) : d^1

Vaak oxocomplexen, bijv. $VO(acac)_2$

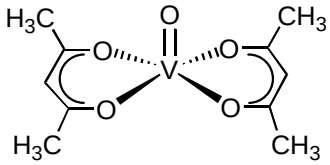

oxovanadium(IV)

V(V) : d^0

Vaak oxo- of dioxocomplexen

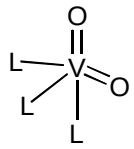

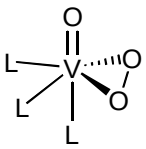

dioxovanadium(V) oxoperoxovanadium(V)

Figuur 1 *Oxovanadium(IV)- en -(V)verbindingen (acac = acetylacetonaat; L = ligand).*

Vanadium maakt 0,014% uit van de aardkorst en is het op een na meest voorkomende overgangsmetaal in de oceanen (50 nM). In 1983 is een enzym ontdekt in bruine zeealgen dat vanadium bevat in zijn actieve centrum: vanadiumbroomperoxidase (V-BrPO). Haloperoxidasen zijn enzymen die de oxidatie van haliden naar hun overeenkomstige hypohalide zuren of naar andere twee-elektron geoxideerde intermediairen zoals OX^-, X_3^-

of X^+ katalyseren. In aanwezigheid van nucleofiele acceptoren worden gehalogeneerde verbindingen geproduceerd:

$$H_2O_2 + X^- + H^+ \longrightarrow H_2O + HOX$$

$$HOX + Org\text{-}H \longrightarrow Org\text{-}X + H_2O$$

De naamgeving van deze enzymen is gebaseerd op het meest elektronegatieve halide dat door het enzym geoxideerd kan worden.

In 1996 is door Messerschmidt en Wever de kristalstructuur opgehelderd van een vanadiumchloorperoxidase (V-ClPO) dat werd geïsoleerd uit de schimmel *Curvularia inaequalis*. Hieruit bleek dat het enzym vanadaat (VO_3^-) bevat in zijn actieve centrum. De zuurstofatomen vormen waterstofbruggen met verschillende aminozuurresiduen van de eiwitketen (zie figuur 2). De kristalstructuur van de peroxidevorm werd gepubliceerd in 1997. Om het mechanisme van de halogeneringsreacties beter te kunnen begrijpen zijn er met name veel functionele enzymmodellen voor V-BrPO ontwikkeld en bestudeerd.

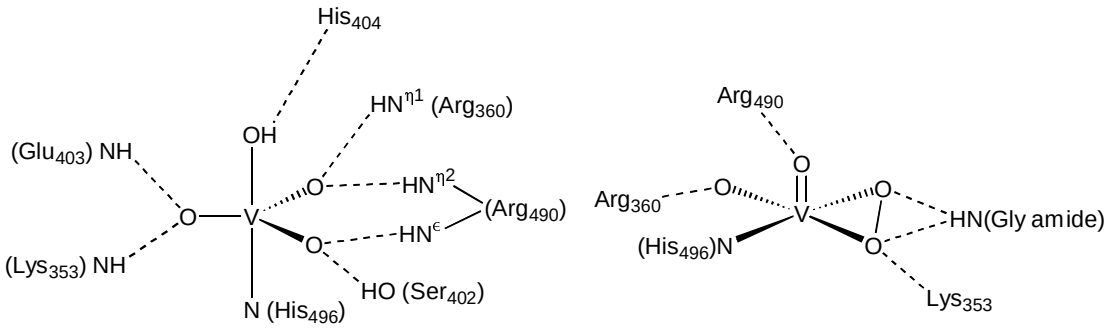

Figuur 2 *Het actieve centrum van V-ClPO en de overeenkomstige peroxovorm.*

Vanadium(V)ionen zijn in het algemeen erg geschikt voor het activeren van peroxiden en daarom worden vanadium(V)complexen ook gebruikt als katalysator in andere oxidatiereacties. Enkele voorbeelden hiervan zijn sulfoxidaties, epoxidaties van alkenen en allylische alcoholen, hydroxyleringen van aromaten en alkanen en oxidaties van primaire of secundaire alcoholen tot hun overeenkomstige aldehyden en ketonen.

Algemene achtergrond: ijzer

IJzer is het meest voorkomende metaal na aluminium en maakt 6,2% uit van de aardkorst. De naam 'ijzer' is afgeleid van het Keltisch-Illyrische woord *isarno* (via het Gotische *eisarn* en het Middenduitse *isen*) en het symbool 'Fe' komt van het Latijnse *ferrum*. De meest voorkomende vormen van ijzer zijn de oxidatietoestanden +2 en +3. Veel ijzer(III)verbindingen hebben een sterke neiging om structuren met een zuurstofbrug erin

[(L)Fe-O-Fe(L)] te vormen. In de natuur zijn vele ijzerbevattende enzymen te vinden die zorgen voor bijvoorbeeld zuurstoftransport of zuurstofactivering.

Doel van het onderzoek

Het hoofddoel van het onderzoek dat beschreven is in dit proefschrift was het synthetiseren van nieuwe oxo- en dioxovanadiumverbindingen en het onderzoeken van hun katalytische eigenschappen in verschillende oxidatiereacties. Want hoewel in de literatuur vele syntheses van vanadium(IV)- en -(V)verbindingen worden beschreven, zijn maar weinig complexen getest als oxidatiekatalysatoren. Een tweede doelstelling van het onderzoek was het bestuderen van de oxidatiechemie van ijzercomplexen die gebaseerd zijn op liganden afgeleid van N4Py (figuur 3). Het ijzer(II)complex van N4Py is een uitstekend enzymmodel gebleken en is al uitgebreid bestudeerd in onze groep. In dit proefschrift wordt o.a. een dinucleair ijzer(III)complex van een ligand waarbij een pyridinegroep is vervangen door een fenolgroep (HL^1) uitgebreid beschreven.

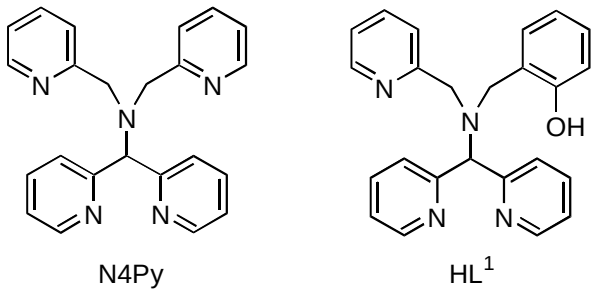

Figuur 3 *Het N4Py-ligand en een derivaat hiervan (HL^1).*

Vanadiumcomplexen en katalytische oxidatie

Veel aandacht is besteed aan het ontwikkelen van functionele modelsystemen voor vanadiumbroomperoxidase. Om deze goed te kunnen vergelijken met de beste, tot dusver uit de literatuur bekende, modelsystemen, werden de desbetreffende liganden, waaronder ook L^2 (zie figuur 4) en de vanadiumcomplexen gesynthetiseerd. Hierbij werd ontdekt dat L^2 in de vaste toestand voorkomt als een dimeer met een onverwachte structuur. De twee monomeren worden bijeengehouden door sterke waterstofbruggen. In hoofdstuk 2 wordt de uitgebreide karakterisering van deze verbinding vermeld. Er werd met behulp van ^{1}H-NMR-studies, IR- en UV-spectroscopie aangetoond dat dimerisatie alleen optreedt in de vaste fase en niet in oplossing. Kristallografische studies bij 130 K en 298 K toonden aan dat de structuur in de vaste toestand het best omschreven kan worden als een intermediair tussen een fenolimine en een quinoïd-tautomere vorm.

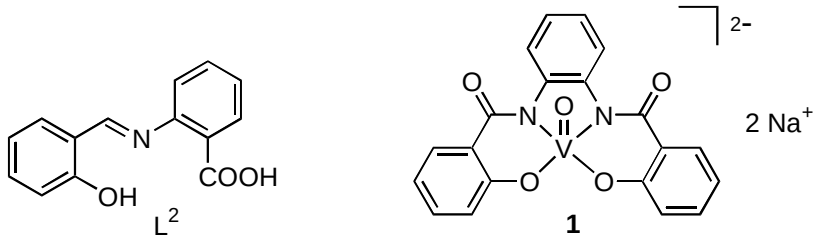

Figuur 4 *Imineligand L² en vanadium(IV)complex **1**.*

In hoofdstuk 3 worden de resultaten van de biomimetische bromeringsreactie, uitgevoerd met complex **1** (figuur 4) als katalysator, vermeld. De synthese van deze oxovanadium(IV)-diamidaatverbinding is bekend in de literatuur, maar complex **1** werd nooit toegepast als oxidatiekatalysator. Waterstofperoxide werd gebruikt als oxidator, trimethoxybenzeen (TMB) als substraat, en tetrabutylammoniumbromide als halidebron. Toevoeging van zuur was nodig om de reactie te laten verlopen. Het beste resultaat werd verkregen door 10 mM TMB, 10 mM H_2O_2 en 8 mM HCl te gebruiken bij een katalysatorconcentratie van 0,25 mM. Na één uur was er 62% conversie naar het monogebromeerde product (TMBBr) bereikt. Zonder katalysator was dit slechts 18%. Hieruit bleek dat deze katalysator qua activiteit vergelijkbaar was met andere modelsystemen bekend uit de literatuur. Grondige NMR- en UV-Vis-studies toonden echter aan dat het ligand onder de zure condities snel dissocieert van het vanadiumion. De waargenomen katalyse wordt daarom hoogstwaarschijnlijk verzorgd door een niet-ligand-gebonden vanadiumreagens. Bovendien werd bewezen dat bijvoorbeeld het commercieel verkrijgbare $VO(acac)_2$ bijna net zo actief is als de in de literatuur bestudeerde modelsystemen.

Zoals al eerder is aangegeven, zijn vanadiumcomplexen niet alleen geschikt als katalysatoren voor bromeringsreacties, maar ook voor een aantal andere oxidatiereacties, zoals epoxidaties, hydroxyleringen en sulfoxidaties. Omdat de coördinatieomgeving van het metaal in grote mate van invloed is op de eigenschappen ervan, wordt de keuze van het ligand erg belangrijk. In hoofdstuk 4 wordt daarom aandacht besteed aan het ontwerp en de synthese van nieuwe ligandsystemen voor vanadium. Enkele van de besproken liganden zijn weergegeven in figuur 5.

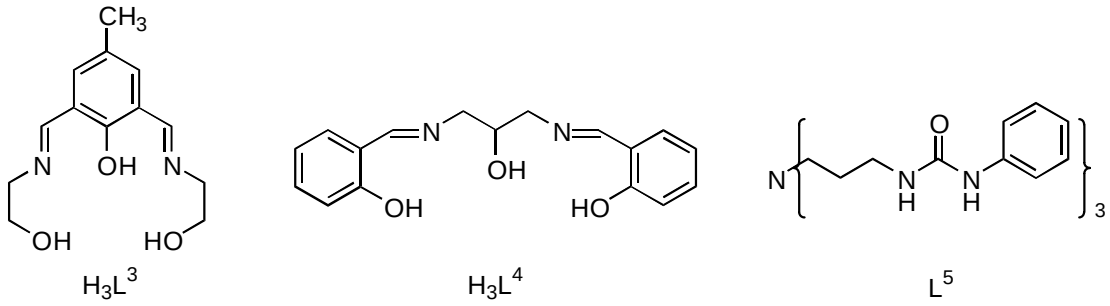

Figuur 5 *Enkele, voor complexatiestudies met vanadium gebruikte, liganden.*

Een aantal liganden, waaronder H_3L^3 en H_3L^4, werd ontworpen voor de complexatie van twee vanadiumionen. Uitgebreide complexatiestudies, waarbij oplosmiddelen, vanadiumreagentia en reactiecondities gevarieerd werden, leverden echter geen goed gedefinieerde complexen op. Het tweede deel van hoofdstuk 4 behandelt de pogingen om een structureel modelsysteem voor vanadiumbroomperoxidase (V-BrPO) te maken. Hiervoor werden liganden zoals L^5 gebruikt (figuur 5). Binding van vanadaat (VO_3^-) via waterstofbruggen aan de aanwezige ureumgroepen zou het actieve centrum van V-BrPO precies nabootsen, maar helaas kon complexatie niet worden aangetoond.

In hoofdstuk 5 wordt beschreven hoe een bis(pyridine)imine-ligand (HL^6 in figuur 6) werd gebruikt voor de complexatie van vanadium. Een onverwachte oxidatieve ligandcylisatie leidde tot de vorming van complex **2**. Dit dioxovanadium(V)complex, waarvan de röntgenstructuur werd bepaald, werd uitgebreid gekarakteriseerd met behulp van UV-Vis-spectroscopie, ^{1}H- en ^{51}V-NMR en elektrospray-massaspectrometrie. Er wordt een mechanisme voor de ligandcyclisatie voorgesteld. Complex **2** werd getest als katalysator in the bromeringsreactie van TMB, maar er werd geen katalytische activiteit waargenomen.

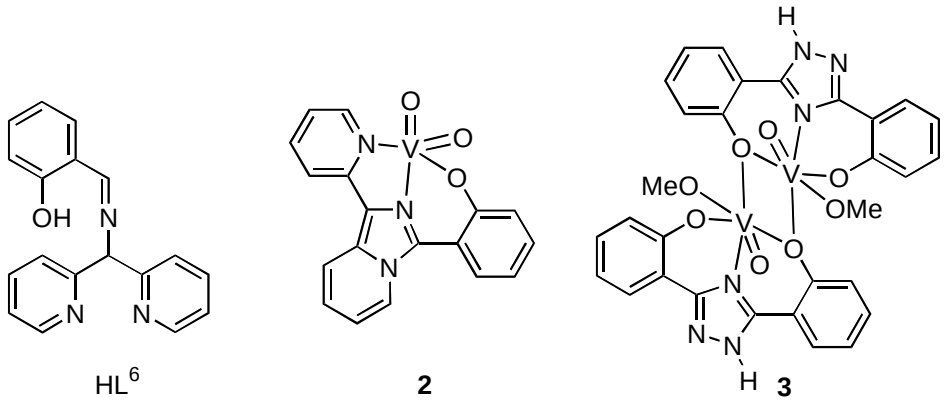

Figuur 6 *Bis(pyridine)imine-ligand HL^6, het door ligandcyclisatie gevormde vanadium(V)complex **2** en het op een triazoolligand gebaseerde dinucleaire vanadium(V)complex **3**.*

Hoofdstuk 6 beschrijft de synthese en karakterisering van vanadiumtriazoolverbindingen. Een voorbeeld van een dergelijk complex is weergegeven in figuur 6 (**3**). Deze complexen werden getest als katalysator in de epoxidatie van kaneelalcohol en styreen. *Tert*-butylhydroperoxide (TBHP) of H_2O_2 werd gebruikt als oxidator. De resultaten werden vergeleken met de gevonden data voor $VO(acac)_2$-gekatalyseerde reacties. Vooral voor **3** werden redelijke turnovergetallen gevonden in de epoxidatie van kaneelalcohol met TBHP, maar $VO(acac)_2$ bleek een actievere katalysator.

In hoofdstuk 7 wordt de synthese van een aantal chirale liganden op basis van pyridine-*N*-oxide beschreven (zie bijvoorbeeld L^7 in figuur 7). Het doel was om de overeenkomstige vanadiumcomplexen te gebruiken als katalysatoren bij de asymmetrische sulfoxidatie of epoxidatie van allylische alcoholen. Helaas leidden de vele pogingen tot complexatie met vanadium niet tot goed gedefinieerde complexen. Daarentegen is er wel een bijzonder,

oranjegekleurd, chiraal dinucleair mangaan(II)complex gemaakt op basis van het 'salen'-verwante pyridine-*N*-oxide ligand L^7. In de röntgenstructuur van **4** is te zien dat een van de pyridine-*N*-oxide-groepen van het ligand een brug vormt tussen de twee mangaanionen. Verder zijn twee perchloraationen gebonden aan mangaan, terwijl de andere twee niet-coördinerend zijn. Spectro-elektrochemische metingen, uitgevoerd met **4**, worden uitvoerig beschreven. Bovendien werd het complex getest in de epoxidatiereactie van styreen met H_2O_2. Helaas werd er geen epoxide gevormd.

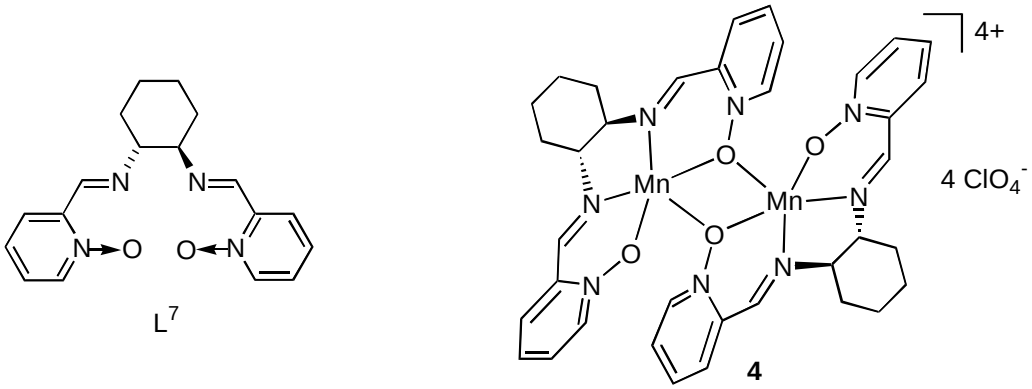

Figuur 7 *Een chiraal 'salen'-verwant pyridine-N-oxide-ligand en het overeenkomstige mangaan(II)complex **4**.*

IJzercomplexen en katalytische oxidatie

In hoofdstuk 8 wordt het gebruik van het pentadentaatligand HL^1 (zie figuur 3) voor de complexatie van ijzer beschreven. Met dit ligand werd een μ-oxo-dinucleair ijzer(III)complex gevormd (zie **5** in figuur 8).

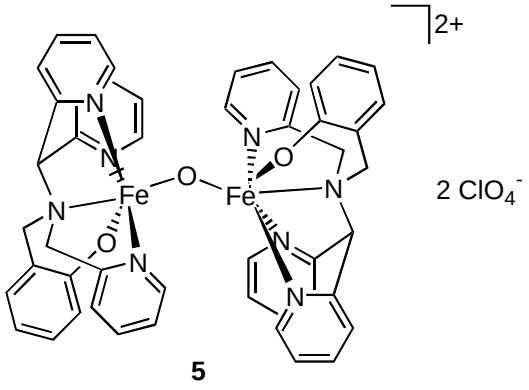

Figuur 8 *Het op HL^1 gebaseerde μ-oxo-di-ijzer(III)complex.*

Dit complex bleek in staat om snel en selectief primaire en secundaire alcoholen te oxideren tot de overeenkomstige aldehyden en ketonen met behulp van H_2O_2. Er werd gevonden dat toevoeging van één equivalent trifluorsulfonzuur (CF_3SO_3H) een dramatische reactieversnelling tot gevolg had. Bij de oxidatie van benzylalcohol bijvoorbeeld, werden

onder normale condities 50 turnovers naar benzaldehyde verkregen na 75 minuten. Ditzelfde aantal werd daarentegen bij toevoeging van 1 equivalent CF_3SO_3H al na 15 minuten verkregen. Overoxidatie van benzaldehyde naar benzoëzuur werd in beide gevallen nauwelijks waargenomen.

Met verbinding **5** werden spectro-elektrochemische metingen uitgevoerd. De resultaten werden vergeleken met die van andere, aan N4Py (figuur 3) gerelateerde, verbindingen.

Conclusies

Zoals hierboven is aangegeven, was het doel van dit onderzoek de synthese van nieuwe vanadiumcomplexen en het onderzoeken van hun katalytische eigenschappen. De conclusie luidt dat er inderdaad een aantal interessante, nieuwe oxo- en dioxovanadiumverbindingen gesynthetiseerd en uitgebreid gekarakteriseerd zijn. Deze complexen werden getest als katalysator in biomimetische bromeringsreacties en in epoxidaties met TBHP of H_2O_2 als oxidator. Vaak werden redelijke turnovergetallen gevonden, maar er is gebleken dat het commercieel verkrijgbare $VO(acac)_2$ vaak een even goede en soms zelfs betere katalysator is.

Het tweede deel van dit proefschrift beschrijft de synthese en karakterisering van verschillende nieuwe ijzer(III)complexen. Vooral de katalytische eigenschappen van een dinucleair μ-oxo-ijzer(III)complex werden uitgebreid onderzocht. Hieruit bleek dat dit complex een prima katalysator is voor de snelle en selectieve oxidatie van primaire en secundaire alcoholen met behulp van H_2O_2.